VOLUME: 17 NO: 6 YEAR: 2020

Indexed in PMC and Web of Science
ULAKBİM / TR Dizin, Scopus

ISSN: 1304-530X

TURKISH JOURNAL OF PHARMACEUTICAL SCIENCES

An Official Journal of the Turkish Pharmacists' Association, Academy of Pharmacy

TURKISH
JOURNAL OF PHARMACEUTICAL SCIENCES

TURKISH
JOURNAL OF PHARMACEUTICAL SCIENCES

TURKISH JOURNAL OF PHARMACEUTICAL SCIENCES

AIMS AND SCOPE

The Turkish Journal of Pharmaceutical Sciences is the only scientific periodical publication of the Turkish Pharmacists' Association and has been published since April 2004.
Turkish Journal of Pharmaceutical Sciences journal is regularly published 6 times in a year (February, April, June, August, October, December). The issuing body of the journal is Galenos Yayinevi/Publishing House level.
The aim of Turkish Journal of Pharmaceutical Sciences is to publish original research papers of the highest scientific and clinical value at an international level. The target audience includes specialists and professionals in all fields of pharmaceutical sciences.
The editorial policies are based on the "Recommendations for the Conduct, Reporting, Editing, and Publication of Scholarly Work in Medical Journals (ICMJE Recommendations)" by the International Committee of Medical Journal Editors (2013, archived at http://www.icmje.org/) rules.

Editorial Independence

Turkish Journal of Pharmaceutical Sciences is an independent journal with independent editors and principles and has no commerical relationship with the commercial product, drug or pharmaceutical company regarding decisions and review processes upon articles.

ABSTRACTED/INDEXED IN

PubMed Central
Web of Science-Emerging Sources Citation Index (ESCI)
SCOPUS SJR
TÜBİTAK/ULAKBİM TR Dizin
Directory of Open Access Journals (DOAJ)
ProQuest
Chemical Abstracts Service (CAS)
EBSCO
EMBASE
GALE
Index Copernicus
Analytical Abstracts
International Pharmaceutical Abstracts (IPA)
Medicinal & Aromatic Plants Abstracts (MAPA)
British Library
CSIR INDIA
GOALI
Hinari
OARE
ARDI
AGORA
Türkiye Atıf Dizini
Türk Medline
UDL-EDGE
J- Gate
Idealonline
ROOTINDEXING
CABI

OPEN ACCESS POLICY

This journal provides immediate open access to its content on the principle that making research freely available to the public supports a greater global exchange of knowledge.
Open Access Policy is based on the rules of the Budapest Open Access Initiative (BOAI) http://www.budapestopenaccessinitiative.org/. By "open access" to peer-reviewed research literature, we mean its free availability on the public internet, permitting any users to read, download, copy, distribute, print, search, or link to the full texts of these articles, crawl them for indexing, pass them as data to software, or use them for any other lawful purpose, without financial, legal, or technical barriers other than those inseparable from gaining access to the internet itself. The only constraint on reproduction and distribution, and the only role for copyright in this domain, should be to give authors control over the integrity of their work and the right to be properly acknowledged and cited.

CORRESPONDENCE ADDRESS

All correspondence should be directed to the Turkish Journal of Pharmaceutical Sciences editorial board;

Post Address: Turkish Pharmacists' Association, Mustafa Kemal Mah 2147.Sok No:3 06510 Çankaya/Ankara, TURKEY
Phone: +90 (312) 409 81 00
Fax: +90 (312) 409 81 09
Web Page: http://turkjps.org
E-mail: teb@teb.org.tr

PERMISSIONS

Requests for permission to reproduce published material should be sent to the publisher.
Publisher: Erkan Mor
Adress: Molla Gürani Mah. Kaçamak Sok. 21/1 Fındıkzade, Fatih, Istanbul, Turkey
Telephone: +90 212 621 99 25
Fax: +90 212 621 99 27
Web page: http://www.galenos.com.tr/en
E-mail: info@galenos.com.tr

ISSUING BODY CORRESPONDING ADDRESS

Issuing Body : Galenos Yayınevi
Address: Molla Gürani Mah. Kaçamak Sk. No: 21/1, 34093 İstanbul, Turkey
Phone: +90 212 621 99 25 Fax: +90 212 621 99 27
E-mail: info@galenos.com.tr

MATERIAL DISCLAIMER

The author(s) is (are) responsible for the articles published in the JOURNAL.
The editor, editorial board and publisher do not accept any responsibility for the articles.

galenos yayınevi

Galenos Publishing House
Owner and Publisher
Derya Mor
Erkan Mor
Publication Coordinator
Burak Sever
Web Coordinators
Fuat Hocalar
Turgay Akpınar
Graphics Department
Ayda Alaca
Çiğdem Birinci
Gülşah Özgül
Finance Coordinator
Sevinç Çakmak

Project Coordinators
Duygu Yıldırm
Gamze Aksoy
Gülay Akın
Hatice Sever
Melike Eren
Özlem Çelik Çekil
Pınar Akpınar
Rabia Palazoğlu
Research & Development
Mert Köse
Özlem Akgüney Küççük
Digital Marketing Specialist
Seher Altundemir

Publisher Contact
Address: Molla Gürani Mah. Kaçamak Sk. No: 21/1
34093 İstanbul, Turkey
Phone: +90 (212) 621 99 25 **Fax:** +90 (212) 621 99 27
E-mail: info@galenos.com.tr/yayin@galenos.com.tr
Web: www.galenos.com.tr | Publisher Certificate Number: 14521
Printing at: Özgün Basım Tanıtım San. Tic. Ltd. Şti.
Yeşilce Mah. Aytekin Sok. Oto Sanayi Sitesi No: 21 Kat: 2
Seyrantepe Sanayi, Kağıthane, İstanbul, Türkiye
Telefon/Phone: +90 (212) 280 00 09 Sertifika No: 48150
Printing Date: December 2020
ISSN: 1304-530X
International scientific journal published quarterly.

TURKISH
JOURNAL OF PHARMACEUTICAL SCIENCES

INSTRUCTIONS TO AUTHORS

Turkish Journal of Pharmaceutical Sciences journal is published 6 times (February, April, June, August, October, December) per year and publishes the following articles:

• Research articles

• Reviews (only upon the request or consent of the Editorial Board)

• Preliminary results/Short communications/Technical notes/Letters to the Editor in every field of pharmaceutical sciences.

The publication language of the journal is English.

The Turkish Journal of Pharmaceutical Sciences does not charge any article submission or processing charges.

A manuscript will be considered only with the understanding that it is an original contribution that has not been published elsewhere.

The Journal should be abbreviated as "Turk J Pharm Sci" when referenced.

The scientific and ethical liability of the manuscripts belongs to the authors and the copyright of the manuscripts belongs to the Journal. Authors are responsible for the contents of the manuscript and accuracy of the references. All manuscripts submitted for publication must be accompanied by the Copyright Transfer Form [copyright transfer]. Once this form, signed by all the authors, has been submitted, it is understood that neither the manuscript nor the data it contains have been submitted elsewhere or previously published and authors declare the statement of scientific contributions and responsibilities of all authors.

Experimental, clinical and drug studies requiring approval by an ethics committee must be submitted to the JOURNAL with an ethics committee approval report including approval number confirming that the study was conducted in accordance with international agreements and the Declaration of Helsinki (revised 2013) (http://www.wma.net/en/30publications/10policies/b3/). The approval of the ethics committee and the fact that informed consent was given by the patients should be indicated in the Materials and Methods section. In experimental animal studies, the authors should indicate that the procedures followed were in accordance with animal rights as per the Guide for the Care and Use of Laboratory Animals (http://oacu.od.nih.gov/regs/guide/guide.pdf) and they should obtain animal ethics committee approval.

Authors must provide disclosure/acknowledgment of financial or material support, if any was received, for the current study.

If the article includes any direct or indirect commercial links or if any institution provided material support to the study, authors must state in the cover letter that they have no relationship with the commercial product, drug, pharmaceutical company, etc. concerned; or specify the type of relationship (consultant, other agreements), if any.

Authors must provide a statement on the absence of conflicts of interest among the authors and provide authorship contributions.

All manuscripts submitted to the journal are screened for plagiarism using the 'iThenticate' software. Results indicating plagiarism may result in manuscripts being returned or rejected.

The Review Process

This is an independent international journal based on double-blind peer-review principles. The manuscript is assigned to the Editor-in-Chief, who reviews the manuscript and makes an initial decision based on manuscript quality and editorial priorities. Manuscripts that pass initial evaluation are sent for external peer review, and the Editor-in-Chief assigns an Associate Editor. The Associate Editor sends the manuscript to at least two reviewers (internal and/or external reviewers). The Associate Editor recommends a decision based on the reviewers' recommendations and returns the manuscript to the Editor-in-Chief. The Editor-in-Chief makes a final decision based on editorial priorities, manuscript quality, and reviewer recommendations. If there are any conflicting recommendations from reviewers, the Editor-in-Chief can assign a new reviewer.

The scientific board guiding the selection of the papers to be published in the Journal consists of elected experts of the Journal and if necessary, selected from national and international authorities. The Editor-in-Chief, Associate Editors may make minor corrections to accepted manuscripts that do not change the main text of the paper.

In case of any suspicion or claim regarding scientific shortcomings or ethical infringement, the Journal reserves the right to submit the manuscript to the supporting institutions or other authorities for investigation. The Journal accepts the responsibility of initiating action but does not undertake any responsibility for an actual investigation or any power of decision.

The Editorial Policies and General Guidelines for manuscript preparation specified below are based on "Recommendations for the Conduct, Reporting, Editing, and Publication of Scholarly Work in Medical Journals (ICMJE Recommendations)" by the International Committee of Medical Journal Editors (2013, archived at http://www.icmje.org/).

Preparation of research articles, systematic reviews and meta-analyses must comply with study design guidelines:

CONSORT statement for randomized controlled trials (Moher D, Schultz KF, Altman D, for the CONSORT Group. The CONSORT statement revised recommendations for improving the quality of reports of parallel group randomized trials. JAMA 2001; 285: 1987-91) (http://www.consort-statement.org/);

PRISMA statement of preferred reporting items for systematic reviews and meta-analyses (Moher D, Liberati A, Tetzlaff J, Altman DG, The PRISMA Group. Preferred Reporting Items for Systematic Reviews and Meta-Analyses: The PRISMA Statement. PLoS Med 2009; 6(7): e1000097.) (http://www.prisma-statement.org/);

STARD checklist for the reporting of studies of diagnostic accuracy (Bossuyt PM, Reitsma JB, Bruns DE, Gatsonis CA, Glasziou PP, Irwig LM, et al., for the STARD Group. Towards complete and accurate reporting of studies of diagnostic accuracy: the STARD initiative. Ann Intern Med 2003;138:40-4.) (http://www.stard-statement.org/);

STROBE statement, a checklist of items that should be included in reports of observational studies (http://www.strobe-statement.org/);

MOOSE guidelines for meta-analysis and systemic reviews of observational studies (Stroup DF, Berlin JA, Morton SC, et al. Meta-analysis of observational studies in epidemiology: a proposal for reporting Meta-analysis of observational Studies in Epidemiology (MOOSE) group. JAMA 2000; 283: 2008-12).

GENERAL GUIDELINES

Manuscripts can only be submitted electronically through the Journal Agent website (http://journalagent.com/tjps/) after creating an account. This system allows online submission and review.

TURKISH
JOURNAL OF PHARMACEUTICAL SCIENCES

INSTRUCTIONS TO AUTHORS

Format: Manuscripts should be prepared using Microsoft Word, size A4 with 2.5 cm margins on all sides, 12 pt Arial font and 1.5 line spacing.

Abbreviations: Abbreviations should be defined at first mention and used consistently thereafter. Internationally accepted abbreviations should be used; refer to scientific writing guides as necessary.

Cover letter: The cover letter should include statements about manuscript type, single-Journal submission affirmation, conflict of interest statement, sources of outside funding, equipment (if applicable), for original research articles.

ETHICS COMMITTEE APPROVAL

The editorial board and our reviewers systematically ask for ethics committee approval from every research manuscript submitted to the Turkish Journal of Pharmaceutical Sciences. If a submitted manuscript does not have ethical approval, which is necessary for every human or animal experiment as stated in international ethical guidelines, it must be rejected on the first evaluation.

Research involving animals should be conducted with the same rigor as research in humans; the Turkish Journal of Pharmaceutical Sciences asks original approval document to show implements the 3Rs principles. If a study does not have ethics committee approval or authors claim that their study does not need approval, the study is consulted to and evaluated by the editorial board for approval.

SIMILARITY

The Turkish Journal of Pharmaceutical Sciences is routinely looking for similarity index score from every manuscript submitted before evaluation by the editorial board and reviewers. The journal uses iThenticate plagiarism checker software to verify the originality of written work. There is no acceptable similarity index; but, exceptions are made for similarities less than 15 %.

REFERENCES

Authors are solely responsible for the accuracy of all references.

In-text citations: References should be indicated as a superscript immediately after the period/full stop of the relevant sentence. If the author(s) of a reference is/are indicated at the beginning of the sentence, this reference should be written as a superscript immediately after the author's name. If relevant research has been conducted in Turkey or by Turkish investigators, these studies should be given priority while citing the literature.

Presentations presented in congresses, unpublished manuscripts, theses, Internet addresses, and personal interviews or experiences should not be indicated as references. If such references are used, they should be indicated in parentheses at the end of the relevant sentence in the text, without reference number and written in full, in order to clarify their nature.

References section: References should be numbered consecutively in the order in which they are first mentioned in the text. All authors should be listed regardless of number. The titles of Journals should be abbreviated according to the style used in the Index Medicus.

Reference Format

Journal: Last name(s) of the author(s) and initials, article title, publication title and its original abbreviation, publication date, volume, the inclusive page numbers. Example: Collin JR, Rathbun JE. Involutional entropion: a review with evaluation of a procedure. Arch Ophthalmol. 1978;96:1058-1064.

Book: Last name(s) of the author(s) and initials, book title, edition, place of publication, date of publication and inclusive page numbers of the extract cited.

Example: Herbert L. The Infectious Diseases (1st ed). Philadelphia; Mosby Harcourt; 1999:11;1-8.

Book Chapter: Last name(s) of the author(s) and initials, chapter title, book editors, book title, edition, place of publication, date of publication and inclusive page numbers of the cited piece.

Example: O'Brien TP, Green WR. Periocular Infections. In: Feigin RD, Cherry JD, eds. Textbook of Pediatric Infectious Diseases (4th ed). Philadelphia; W.B. Saunders Company;1998:1273-1278.

Books in which the editor and author are the same person: Last name(s) of the author(s) and initials, chapter title, book editors, book title, edition, place of publication, date of publication and inclusive page numbers of the cited piece. Example: Solcia E, Capella C, Kloppel G. Tumors of the exocrine pancreas. In: Solcia E, Capella C, Kloppel G, eds. Tumors of the Pancreas. 2nd ed. Washington: Armed Forces Institute of Pathology; 1997:145-210.

TABLES, GRAPHICS, FIGURES, AND IMAGES

All visual materials together with their legends should be located on separate pages that follow the main text.

Images: Images (pictures) should be numbered and include a brief title. Permission to reproduce pictures that were published elsewhere must be included. All pictures should be of the highest quality possible, in

JPEG format, and at a minimum resolution of 300 dpi.

Tables, Graphics, Figures: All tables, graphics or figures should be enumerated according to their sequence within the text and a brief descriptive caption should be written. Any abbreviations used should be defined in the accompanying legend. Tables in particular should be explanatory and facilitate readers' understanding of the manuscript, and should not repeat data presented in the main text.

MANUSCRIPT TYPES

Original Articles

Clinical research should comprise clinical observation, new techniques or laboratories studies. Original research articles should include title, structured abstract, key words relevant to the content of the article, introduction, materials and methods, results, discussion, study limitations, conclusion references, tables/figures/images and acknowledgement sections. Title, abstract and key words should be written in both Turkish and English. The manuscript should be formatted in accordance with the above-mentioned guidelines and should not exceed 16 A4 pages.

Title Page: This page should include the title of the manuscript, short title, name(s) of the authors and author information. The following descriptions should be stated in the given order:

TURKISH
JOURNAL OF PHARMACEUTICAL SCIENCES

INSTRUCTIONS TO AUTHORS

1. Title of the manuscript (Turkish and English), as concise and explanatory as possible, including no abbreviations, up to 135 characters

2. Short title (Turkish and English), up to 60 characters

3. Name(s) and surname(s) of the author(s) (without abbreviations and academic titles) and affiliations

4. Name, address, e-mail, phone and fax number of the corresponding author

5. The place and date of scientific meeting in which the manuscript was presented and its abstract published in the abstract book, if applicable

Abstract: A summary of the manuscript should be written in both Turkish and English. References should not be cited in the abstract. Use of abbreviations should be avoided as much as possible; if any abbreviations are used, they must be taken into consideration independently of the abbreviations used in the text. For original articles, the structured abstract should include the following sub-headings:

Objectives: The aim of the study should be clearly stated.

Materials and Methods: The study and standard criteria used should be defined; it should also be indicated whether the study is randomized or not, whether it is retrospective or prospective, and the statistical methods applied should be indicated, if applicable.

Results: The detailed results of the study should be given and the statistical significance level should be indicated.

Conclusion: Should summarize the results of the study, the clinical applicability of the results should be defined, and the favorable and unfavorable aspects should be declared.

Keywords: A list of minimum 3, but no more than 5 key words must follow the abstract. Key words in English should be consistent with "Medical Subject Headings (MESH)" (www.nlm.nih.gov/mesh/MBrowser.html). Turkish key words should be direct translations of the terms in MESH.

Original research articles should have the following sections:

Introduction: Should consist of a brief explanation of the topic and indicate the objective of the study, supported by information from the literature.

Materials and Methods: The study plan should be clearly described, indicating whether the study is randomized or not, whether it is retrospective or prospective, the number of trials, the characteristics, and the statistical methods used.

Results: The results of the study should be stated, with tables/figures given in numerical order; the results should be evaluated according to the statistical analysis methods applied. See General Guidelines for details about the preparation of visual material.

Discussion: The study results should be discussed in terms of their favorable and unfavorable aspects and they should be compared with the literature. The conclusion of the study should be highlighted.

Study Limitations: Limitations of the study should be discussed. In addition, an evaluation of the implications of the obtained findings/results for future research should be outlined.

Conclusion: The conclusion of the study should be highlighted.

Acknowledgements: Any technical or financial support or editorial contributions (statistical analysis, English/Turkish evaluation) towards the study should appear at the end of the article.

References: Authors are responsible for the accuracy of the references. See General Guidelines for details about the usage and formatting required.

Review Articles

Review articles can address any aspect of clinical or laboratory pharmaceuticals. Review articles must provide critical analyses of contemporary evidence and provide directions of or future research. Most review articles are commissioned, but other review submissions are also welcome. Before sending a review, discussion with the editor is recommended.

Reviews articles analyze topics in depth, independently and objectively. The first chapter should include the title in Turkish and English, an unstructured summary and key words. Source of all citations should be indicated. The entire text should not exceed 25 pages (A4, formatted as specified above).

TURKISH
JOURNAL OF PHARMACEUTICAL SCIENCES

CONTENTS

TURKISH
JOURNAL OF PHARMACEUTICAL SCIENCES

CONTENTS

PUBLICATION NAME	Turkish Journal of Pharmaceutical Sciences
TYPE OF PUBLICATION	Vernacular Publication
PERIOD AND LANGUAGE	Bimonthly-English
OWNER	Erdoğan ÇOLAK on behalf of the Turkish Pharmacists' Association
EDITOR-IN-CHIEF	Prof.Terken BAYDAR, Ph.D.
ADDRESS OF PUBLICATION	Turkish Pharmacists' Association, Mustafa Kemal Mah 2147.Sok No:3 06510 Çankaya/ Ankara, TURKEY

TURKISH
JOURNAL OF PHARMACEUTICAL
SCIENCES

Volume: 17, No: 6, Year: 2020

CONTENTS

Turk J Pharm Sci 2020;17(6):576-577
DOI: 10.4274/tjps.galenos.2020.20727

LETTER TO EDITOR

Can Alpha-1 Antitrypsin Levels be Used to Predict the Prognosis of COVID-19 Therapy?

Alfa-1 Antitripsin Düzeyleri COVID-19 Tedavisinin Prognozunu Öngörmek için Kullanılabilir mi?

Elif ARAS ATİK*, Nesligül ÖZDEMİR, Kutay DEMİRKAN

Hacettepe University Faculty of Pharmacy, Department of Clinical Pharmacy, Ankara, Turkey

Key words: COVID-19, alpha-1 antitrypsin, treatment

Anahtar kelimeler: COVID-19, alfa-1 antitripsin, tedavi

Dear Editor,

The Coronavirus Disease-2019 (COVID-19) outbreak began to spread in China in December 2019 and was recognized as a pandemic by the World Health Organization in March 2020. The COVID-19 outbreak causes acute respiratory distress in patients and increases the need for intensive care. Smoking, advanced age, and comorbid diseases can be risk factors for COVID-19. In smokers, a 1.4-fold higher risk of serious symptoms and a 2.4-fold higher risk of mechanical ventilation and intensive care needs were determined.[1]

No parameter has yet been discovered that could predict the exact prognosis of COVID-19.

Alpha-1 antitrypsin (AAT) is a very common serine protease inhibitor that exists in plasma. Its main function is to protect lung cells from proteolytic damage by neutrophil elastase.[2] AAT is constantly present in the serum of healthy individuals (20-52 μmol/L) and the concentration may increase several times during inflammation.[2,3] AAT is an acute phase reactant as well as an anti-inflammatory, immunomodulatory, anti-infective, and tissue repair molecule.[4]

AAT deficiency is an inherited disorder that can cause liver and lung diseases. Due to insufficient function of AAT, neutrophil elastase destroys alveoli and causes lung disease. AAT deficiency is seen (1 in every 1,500-3,500 people) worldwide, but its frequency varies according to populations.[4] AAT deficiency has not yet been diagnosed in many individuals. Environmental factors such as smoking, chemicals, and exposure to dust affect the severity of AAT deficiency. People who have AAT deficiency usually develop symptoms of lung disease between the ages of 20 and 50. The risk of lung disease seems to be most clinically important when serum levels of AAT are less than 11 μmol/L.[5] Generally, the first symptoms are shortness of breath during exercise, decreased exercise ability, and wheezing. Unintended weight loss, recurrent respiratory infections, emphysema, weakness, and tachycardia can be seen in this group of patients. Smoking and exposure to tobacco products accelerate lung damage and emphysema symptoms.[6]

There are studies in the literature showing that AAT levels can be associated with different situations. ATT has significant anti-inflammatory and immunoregulatory effects that may be associated with human immunodeficiency virus (HIV) in addition to its effects on the lungs.[2] Functional deficiency of AAT may contribute to the development of emphysema in HIV-positive patients.[7]

In COVID-19 patients it is found that there is a hyperinflammatory response that affects disease severity and mortality. In particular, chronic obstructive pulmonary disease patients and smokers are more vulnerable to the effects of COVID-19.[8]

*Correspondence: E-mail: eczelifaras@gmail.com, Phone: +90 537 789 31 89 ORCID-ID: orcid.org/0000-0001-8667-6623
Received: 31.08.2020, Accepted: 13.09.2020

In conclusion, we would like to state that AAT levels, which are accepted as an acute phase reactant, should be evaluated in patients with COVID-19 to determine whether deficiency of AAT is the underlying reason for the poor course of COVID-19 in smokers and in patients with lung diseases. There has been no established study evaluating AAT levels in COVID-19 patients. The bad prognosis of the disease and increased need for mechanical ventilation in COVID-19 patients may be related to AAT levels. This specific protein should be considered a predictive factor in COVID-19 patients with a bad prognosis. In addition, intravenous augmentation therapy with purified human AAT is available for AAT deficiency to prevent lung destruction and stabilize the disease[9] and this treatment may be beneficial in COVID-19 patients as well.

Conflicts of interest: No conflict of interest was declared by the authors. The authors alone are responsible for the content and writing of the paper.

REFERENCES

1. Vardavas CI, Nikitara K. COVID-19 and smoking: A systematic review of the evidence. Tob Induc Dis. 2020;18:20.
2. Thudium RF, Lundgren J, Benfield T, Nordestgaard BG, Borges AH, Gerstoft J, Nielsen SD, Ronit A. HIV infection is independently associated with a higher concentration of alpha-1 antitrypsin. HIV Med. 2018;19:745-750.
3. Brantly M, Nukiwa T, Crystal RG. Molecular basis of alpha-1-antitrypsin deficiency. Am J Med. 1988;84:13-31.
4. de Serres F, Blanco I. Role of alpha-1 antitrypsin in human health and disease. J Intern Med. 2014;276:311-335.
5. Crystal RG. Alpha 1-antitrypsin deficiency, emphysema, and liver disease. Genetic basis and strategies for therapy. J Clin Invest. 1990;85:1343-1352.
6. Salvi S. Tobacco smoking and environmental risk factors for chronic obstructive pulmonary disease. Clin Chest Med. 2014;35:17-27.
7. Stephenson SE, Wilson CL, Crothers K, Attia EF, Wongtrakool C, Petrache I, Schnapp LM. Impact of HIV infection on α1-antitrypsin in the lung. Am J Physiol Lung Cell Mol Physiol. 2018;314:L583-L592.
8. Leung JM, Yang CX, Tam A, Shaipanich T, Hackett TL, Singhera GK, Dorscheid DR, Sin DD. ACE-2 expression in the small airway epithelia of smokers and COPD patients: implications for COVID-19. Eur Respir J. 2020;55:2000688.
9. Brode SK, Ling SC, Chapman KR. Alpha-1 antitrypsin deficiency: a commonly overlooked cause of lung disease. CMAJ. 2012;184:1365-1371.

Turk J Pharm Sci 2020;17(6):578-585
DOI: 10.4274/tjps.galenos.2019.69335

ORIGINAL ARTICLE

Combined Effects of Protocatechuic Acid and 5-Fluorouracil on p53 Gene Expression and Apoptosis in Gastric Adenocarcinoma Cells

Gastrik Adenokarsinoma Hücrelerinde Protokateşuik Asit ve 5-Florourasilin p53 Gen Ekspresyonu ve Apoptoz Üzerine Kombine Etkileri

Zahra MOTAMEDI[1], Sayed Asadollah AMINI[2], Elham RAEISI[3], Yves LEMOIGNE[4], Esfandiar HEIDARIAN[1]*

[1]Shahrekord University of Medical Sciences, Basic Health Sciences Institute, Clinical Biochemistry Research Center, Shahrekord, Iran
[2]Shahrekord University of Medical Sciences, Basic Health Sciences Institute, Cellular and Molecular Research Center, Shahrekord, Iran
[3]Shahrekord University of Medical Sciences, Department of Medical Physics and Radiology, School of Allied Medical Sciences, Shahrekord, Iran
[4]Institute for Medical Physics, Ambilly, France

ABSTRACT

Objectives: This study evaluated the combined effects of protocatechuic acid (PCA) and 5-fluorouracil (5-FU) on gastric adenocarcinoma (AGS) cells.

Materials and Methods: The 3-(4,5-dimethylthiazol-2-yl)-2,5-diphenyltetrazolium bromide assay, colony formation assay, flow cytometry technique, real-time quantitative polymerase chain reaction, and Western blotting were used to investigate cytotoxic effects, colony formation, apoptosis, *p53* gene expression, and Bcl-2 protein level in AGS cells treated with 5-FU and PCA.

Results: Our results demonstrated that PCA (500 μM) alone or in combination with 5-FU (10 μM) inhibited AGS cell proliferation, inhibited a colony formation, and increased apoptosis compared with untreated control cells. Moreover, the combined 5-FU/PCA exposure led to upregulation of p53 and downregulation of Bcl-2 protein when compared to the untreated control cells.

Conclusion: The results demonstrate that the combined 5-FU/PCA may promote antiproliferative and pro-apoptotic effects with the inhibition of colony formation in AGS cells. The mechanisms by which the combined 5-FU/PCA exposure exerts its effects are associated with upregulation of *p53* gene expression and downregulation of *Bcl-2* level. Therefore, the combination of 5-FU with PCA not only could be a promising approach to potentially reduce the dose requirements of 5-FU but also could promote apoptosis via p53 and Bcl-2 signaling pathways.

Key words: Apoptosis, 5-fluorouracil, protocatechuic acid, gastric cancer, combination, colony formation

ÖZ

Amaç: Bu çalışma protokateşuik asit (PCA) ve 5-florourasilin (5-FU) gastrik adenokarsinoma (AGS) hücreleri üzerine kombine etkisini değerlendirmiştir.

Gereç ve Yöntemler: 3-(4,5-dimetiltiazol-2-il)-2,5-difeniltetrazolium bromid yöntemi, koloni oluşturma yöntemi, akış sitometrisi tekniği, gerçek zamanlı kantitatif polimeraz zincir reaksiyonu ve Western blot yöntemleri 5-FU ve PCA'ya maruz kalan AGS hücrelerinde sitotoksisite, koloni oluşumu, apoptoz, *p53* gen ekspresyonu ve Bcl-2 düzeylerini belirlemek için kullanılmıştır.

Bulgular: Sonuçlarımız PCA'nın tek başına (500 μM) veya 5-FU (10 μM) ile kombinasyonunun uygulama yapılmamış kontrol hücrelerine göre AGS hücre proliferasyonunu ve koloni oluşturmunu inhibe ettiğini ve apoptozu artırdığını göstermiştir. Ek olarak, uygulama yapılmamış kontrol hücrelerine göre kombine 5-FU/PCA maruziyeti p53 düzeylerini artırmış ve Bcl-2 düzeylerini artırmıştır.

Sonuç: Sonuçlar göstermiştir ki AGS hücrelerinde kombine 5-FU/PCA maruziyeti koloni oluşumunu inhibe ederek antiproliferatif ve pro-apoptotik etkiler başlatabilir. Kombine 5-FU/PCA maruziyetinin etki gösterme mekanizması *p53* geninin artması ve *Bcl-2* geninin azalması ile ilişkili olabilir.

*Correspondence: E-mail: heidarian46@yahoo.com, heidarian_e@skums.ac.ir, Phone: +98-383-3346721 ORCID-ID: orcid.org/0000-0002-4701-144X
Received: 26.01.2019, Accepted: 14.03.2019

Bu nedenle, 5-FU'nun PCA ile birlikte kombinasyonu 5-FU'nun doz rejimlerinin azaltılmasında potansiyel olarak umut verici bir yaklaşım olurken, aynı zamanda p53 ve Bcl-2 sinyalleşme yolaklarıyla apoptozu başlatabilir.

Anahtar kelimeler: Apoptoz, 5-florourasil, protokateşuik asit, mide kanseri, kombinasyon, koloni oluşumu

INTRODUCTION

Gastric cancer figures worldwide among the major issues faced by health systems due to its incidence and mortality rate. The 5-year survival rate for this disease is only about 20%.[1] Gastric cancer's prevalence varies in different geographic regions.[2] Gastric cancer can be affected by predisposing factors to gastric carcinoma encompassing familial genetic background, smoking, inadequate intake of antioxidants, disproportionate salt intake, and infection by *H. pylori*. Furthermore, disorders such as gastritis, intestinal metaplasia, dysplasia, paraneoplastic lesions, and chronic atrophic gastritis are among the underlying causes of gastric cancer.[2]

The therapeutic options for gastric carcinoma are primarily surgery, radiotherapy, and chemotherapy.[3] 5-fluorouracil (5-FU) is a heterocyclic aromatic anticancer chemical agent that is widely used to handle various cancers by inhibiting the enzyme thymidylate synthase, preventing DNA replication.[4,5] However, 5-FU has many side effects (diarrhea, stomatitis, emesis, neutropenia, inflammation of the mouth, loss of appetite, low blood cell counts, hair loss, and skin inflammation).[6] Moreover, administration of 5-FU is frequently limited by dose-limiting toxicities. Interaction of chemotherapy with natural compounds may present a new perspective and an innovative strategy in cancer therapy. Interestingly, herbal compounds in tandem with 5-FU amplify the synergistic effects of administered therapeutics and exert cytotoxic effects specifically in tumor cells. Combined therapy with synergistic effects not only reduces the drug doses and resistance in chemotherapy but also decreases metastasis, raises the efficacy of 5-FU, and induces apoptosis.[7] Apoptosis in cells is a type of programmed cell death under the control of factors such as *p53* gene expression, which is mutated in most cancer cells. This gene plays a crucial role in genome stability, tumor suppression, induction of apoptosis, cell cycle stopping, and aging.[8] In addition, p53 acts as a transcription factor for pre-apoptotic proteins.[9]

Various experiments have been conducted to discover and use natural compounds for induction of apoptosis in cancer cells. Epidemiological studies have shown that a diet rich in phytochemical compounds is effective in inducing apoptosis in some cancers.[1,10] Phytochemicals with antioxidant activity can inhibit carcinogenic processes in several models due to the expression of key proteins in signal transduction pathways and induction of apoptosis.[11] It is also reported that many polyphenols can reduce the adverse effects of chemical therapies.[1] Protocatechuic acid (PCA), also known as 3,4-dihydroxybenzoic acid, is a herbal phenolic acid mainly present in fruits, vegetables, and nuts and has anti-inflammatory, antibacterial, antihyperglycemic, anticancer, antiulcer, and antispasmodic properties.[12-14] Therefore, the aim of the present study was to assess the combined effects of 5-FU and PCA on *p53* gene expression, colony formation, apoptosis, and Bcl-2 signaling protein level in the gastric adenocarcinoma (AGS) cell line.

MATERIALS AND METHODS

Chemicals and antibodies

The investigated human AGS cells were procured from the Pasteur Institute (Tehran, Iran). RPMI 1640 medium, trypsin 0.25%, penicillin/streptomycin (pen/strep), and fetal bovine serum (FBS) were supplied by Gibco (Rockville, MD, USA). Bcl-2 and β-actin primary antibodies were purchased from Elabscience Biotechnology Co. (Wuhan, China). PCA and 3-(4,5-dimethylthiazol-2-yl)-2,5-diphenyltetrazolium bromide (MTT) were obtained from Sigma-Aldrich (St. Louis, MO, USA). 5-FU was purchased from Haupt Pharma (Wolfratshausen GmbH Co, Germany). The Roti®ZOL total RNA extraction kit was obtained from Carl Roth GmbH, Germany. The Annexin V-PI staining kit was purchased from BD Bioscience (California, USA). Glyceraldehyde-3-phosphate dehydrogenase (GAPDH) and p53 primers were purchased from Macrogen Company (South Korea). The other reagents used were of analytical grade.

Cell viability assay

AGS cells were cultured in 96-well plates (5000 cells per well) overnight in RPMI 1640 medium that contained 10% FBS and 1% pen/strep at 37°C in 98% humidity with 5% CO_2. Subsequently, the cells were treated with 5-FU (0-55 µM), PCA (0-1100 µM, solution in dimethyl sulfoxide (DMSO) with 0.1% final concentration), and the combination of 5-FU with PCA (10 µM and 500 µM, respectively) for 24 h. Then the medium was removed and the cells were incubated with MTT solution (5 mg/mL) for 4 h at 37°C. Afterwards, DMSO was added to each well of 96-well plates. The absorbance of each well was measured with a microplate reader (Stat Fax-2100, USA) at 490-570 nm. The percentage of cell viability was assessed as follows: viability=A (sample)/A (control)x100.[15] At least three independent experiments were carried out.

Assessing the synergistic effects of 5-FU and PCA

The IC_{50} values of 5-FU and PCA were used to determine synergistic effects between 5-FU and PCA through the combination index (CI) using the CI equation:[16] $CI=A/A_{50}+B/B_{50}$, where A related to 5-FU concentration in combination with B, and B depicting PCA concentration in combination with A. A_{50} is the IC_{50} of 5-FU and the B_{50} is the IC_{50} of PCA. A CI value of 1 represents an additive effect, CI <1 indicates synergism, and CI >1 represents antagonism.[17] Therefore, a combination of 5-FU (10 µM, IC_{20}) and PCA (500 µM, IC_{30}) was used based on the results of the MTT assay.

Colony formation assay

For the colony formation assay, AGS cells were cultured in 6-well plates (3x10^5 cells per well) overnight. The cells were then treated with 5-FU alone (10 µM), PCA alone (500 µM), and the combination of 5-FU and PCA (10 µM and 500 µM, respectively) and incubated at 37˚C in an atmosphere of 5% CO_2 for 24 h. Then the medium was removed, while the cell culture medium was changed every 2 days for 14 days. Subsequently, the cells were washed with PBS and fixed with 70% ethanol and colonies were stained with 0.5% crystal violet. The number of colonies was counted and plating efficiency (PE) was calculated by the following formula: PE=(number of colonies/number of seeded cells) x100 and surviving fraction (SF) was determined by SF=(number of colonies/number of seeded cells x PE control) x100.[18]

Apoptosis detection assay

The percentage of apoptosis and necrosis of cells were determined through flow cytometry using the AnnexinV-FITC Apoptosis Detection Kit (BD Bioscience, Franklin Lakes, NJ, USA). Briefly, AGS cells (2x10^5 per well) were cultured in 6-well plates and incubated overnight. The cells were treated with 5-FU (10 µM) and PCA (500 µM) or a combination of 5-FU and PCA (10 µM and 500 µM, respectively) for 24 h. Then the cells were harvested by trypsinization, washed with PBS, and stained with Annexin V for 20 min according to the manufacture's protocol at room temperature in the dark.[19] The cells were analyzed using a FACScan system (Becton-Dickinson and Company, San Jose, CA, USA).

Reverse transcription-quantitative polymerase chain reaction (RT-qPCR)

RT-qPCR was then applied so as to assess the *p53* gene expression in AGS cells. In summary, total RNA from each of the untreated control cells, 5-FU (10 µM), and PCA (500 µM) or the combination of 5-FU and PCA (10 µM and 500 µM, respectively) was extracted after 24 h of treatment using Roti®ZOL solution according to the manufacturer's instructions. The total mRNA concentration and quality of RNA were evaluated by OD measurements at 260/280 ratio using a Nanodrop 2000 spectrophotometer (Thermo-USA). For cDNA synthesis 1 µg of RNA was used with a synthesis kit (Takara Bio Inc., Japan) according to the manufacturer's instructions and stored at -20˚C for subsequent use. The procedure of cDNA RT was applied using a Prime Script™ Reagent Kit (Takara Bio Inc., Japan) according to the manufacturer's instructions. Then cDNA was expanded by RT-qPCR using SYBR® Green PCR Master Mix (Takara Bio Inc., Japan) in the presence of specific primers. The sequences of the primers for the reaction were as follows: H-*p53*-F, forward 5'-CCCATCCTCACCATCATCACAC-3' and reverse 5'-GCACAAACACGCACCTCAAAG3' and H-*GAPDH*-F, forward 5'ACACCCACTCCTCCACCCTTTG3', and reverse 5'GTCCACCACCCTGTTGCTGTA-3'. The primers were prepared with Oligo 6.0 software (Molecular Biology Insights, Cascade, CO, USA) and confirmed by BLAST (NCBI). The *GAPDH* gene was used as a reference gene for normalization. Enzyme activation was conducted for 10 min at 95˚C, followed by 40 cycles of initial denaturation at 95˚C for 10 s and annealing/extension at 62˚C for 15 s and melting at 72˚C for 20 s in a 3000 Rotor Gene (Corbett, Australia) real-time PCR system.[20]

Western blotting

The AGS cells were grown in 6-cm dishes at the density of 6x10^5. After 24 h of treatment, protein extraction were performed for the control, 5-FU (10 µM), PCA (500 µM), and the combination of 5-FU and PCA (10 µM and 500 µM, respectively) using RIPA lysis buffer (50 mM Tris-HCl, pH 8, 150 mM NaCl, 1% Triton X-100, 1 mmol/L sodium orthovanadate, 0.5% sodium deoxycholate, 50 mmol/L NaF, 0.1% SDS, 1 mM EDTA, 0.1% sodium azide, 1 mmol/L phenylmethylsulfonyl fluoride, 50 µL of protease, and 250 µL of phosphatase inhibitor).[21] The supernatants were collected and protein concentrations were determined using Bradford's procedure.[22] The Western blot procedure was described previously[21] and primary antibodies Bcl-2 and β-actin were used according to the manufacturer's protocols. β-actin was determined as an internal control. Then the blots were washed with TBS-Tween buffer 3 times for 10 min and they were incubated with horseradish peroxidase-conjugated secondary antibody at room temperature for 2 h and washed again as described above. Band intensity was evaluated using chemiluminescent reagents (ECL; Thermo Fisher Scientific, USA) and analyzed using ImageJ software.[20]

Statistical analysis

The results of all experiments were expressed as mean ± standard deviation and the experiments were performed at least three times. SPSS (Version 20, SPSS Inc., Chicago, IL, USA) or GraphPad Prism 6 (Graphpad Software, San Diego, CA, USA) was used to perform the statistical analysis. Kruskal-Wallis analyses were used to assess between-group differences for the MTT assay, clonogenic assay, Annexin V assay, and RT-PCR. For expression analysis, the relative levels of quantitative gene expression were calculated by the $2^{-\Delta\Delta Ct}$ method and the data were expressed as fold change. Melting curve analysis was performed after amplification to verify product identity. Western blotting was repeated 3 times. P values less than 0.05 were considered statistically significant for the differences between the groups. The CI was calculated using experimental CompuSyn software (ComboSyn Inc, Paramus, NJ, USA), and CI <1, =1, and >1 indicated synergism, additive effect, and antagonism, respectively.

RESULTS

Effects of 5-FU, PCA, and their combination on AGS cell viability

The result of the MTT assay demonstrated that 5-FU, PCA, and their combination can reduce the proliferation of AGS cells after 24 h (Figure 1). The IC_{50} values of 5-FU and PCA alone were 40 µM and 700 µM, respectively (Figures 1A and 1B). The combination of 5-FU and PCA (10 µM and 500 µM, respectively) led to a synergistic CI equal to 0.6 with strong effects on AGS cell proliferation (Table 1). Moreover, the number of living cells decreased in the combination of 5-FU with PCA (10 µM and 500 µM, respectively) relative to untreated control cells and each agent alone (Figure 1C).

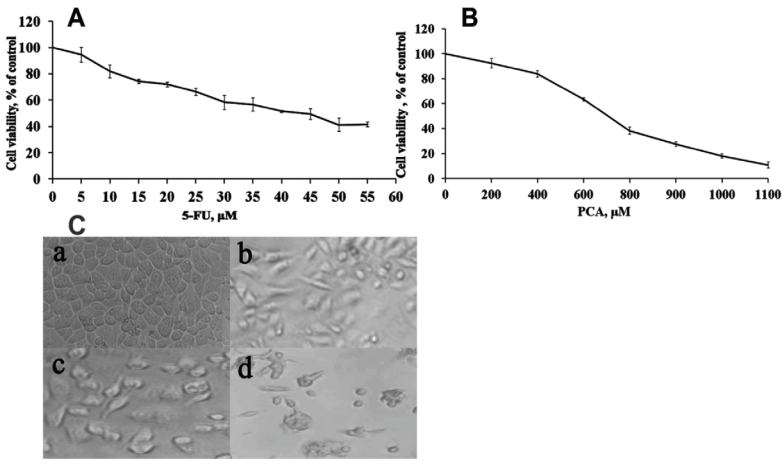

Figure 1. Inhibition of cell proliferation by 5-FU (A) and PCA (B) for 24 h. The cells were cultured at the density of $5x10^3$ cells per well for 24 h. At the end of treatment time, cell viability was measured by MTT assay. Data are expressed as mean ± SD of 3 independent experiments. Also Figure 1C demonstrates cell morphological changes in AGS cells after treatment with 5-FU, PCA, and their combination. 1C-a: control, 1C-b: 5-FU, 1C-c: PCA, 1C-d: 5-FU plus PCA

5-FU: 5-fluorouracil, PCA: Protocatechuic acid, MTT: 3-(4,5-dimethylthiazol-2-yl)-2,5-diphenyltetrazolium bromide, SD: Standard deviation, AGS: Gastric adenocarcinoma

Table 1. The viability percentage of the AGS cell line treated with combination of PCA and 5-FU after 24 h

Combination number	Dose combination, micromolar		Cell viability, %	CI
	5-FU (IC value)	PCA (IC value)		
1	5 (IC_{10})	600 (IC_{40})	39±4.4	0.72
2	10 (IC_{20})	500 (IC_{30})	20±2.7	0.60
3	20 (IC_{30})	400 (IC_{20})	45±4.1	0.81
4	30 (IC_{40})	200 (IC_{10})	45±2.9	0.79

AGS: Gastric adenocarcinoma, 5-FU: 5-fluorouracil, IC: Inhibitory concentration, PCA: Protocatechuic acid, CI: Combination index

Clonogenic assay of AGS cells

The results of the colony formation assay demonstrated that the combination of 5-FU with PCA (10 µM and 500 µM, respectively) significantly decreased the colony numbers of AGS cells and the proliferation rate compared with those of the untreated control cells and 5-FU treated cells (Figure 2). After 14 days of cell culture, the number of colonies consisted of 63, 46, 30, and 22 for the control, 5-FU, PCA, and 5-FU/PCA combinations, respectively (Figure 2B). The SF for 5-FU, PCA, and 5-FU/PCA combination were 71%, 49%, and 34%, respectively. The results also showed PE in the control and treated experimental cells (Figure 2A).

Effects of 5-FU and PCA on apoptosis

The results of the flow cytometry showed the percentage of apoptosis and necrosis of 5-FU and PCA in AGS cells (Figure 3). Apoptosis in AGS cells was induced 17% by 10 µM 5-FU, 23% by 500 µM PCA, and 27% by the combination of 5-FU and PCA (10 µM and 500 µM, respectively). Apoptosis significantly increased ($p<0.05$) in the combination of 5-FU and

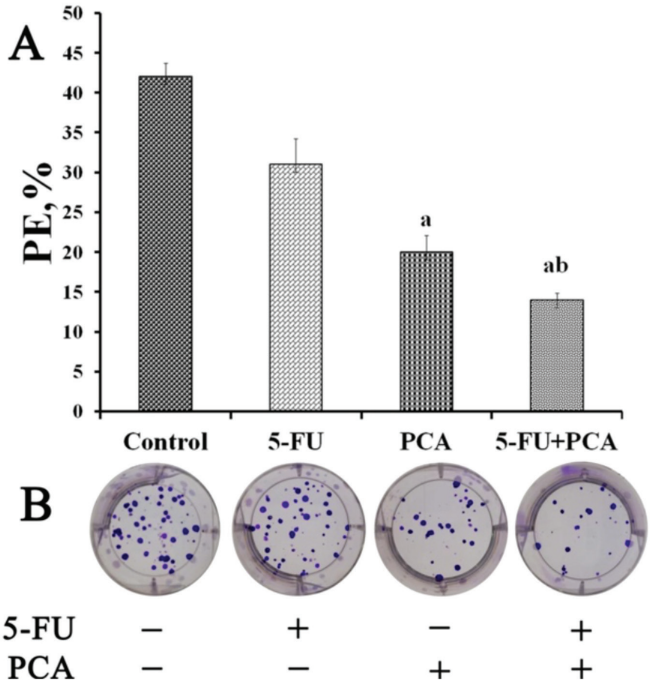

Figure 2. Colonies produced by the AGS cell line in the absence or presence of 5-FU, PCA, and 5-FU/PCA combination. (A): Histogram plot demonstrates plating efficiency (PE) in the control and treated experimental groups. (B): Colony formation in the control, 5-FU, PCA, and combination of 5-FU with PCA

[a]$p<0.05$ vs. control cells, [b]$p<0.05$ vs. 5-FU treated cells, PE: Plating efficiency, 5-FU: 5-fluorouracil, PCA: Protocatechuic acid, AGS: Gastric adenocarcinoma

PCA treatment when compared to that of the control and 5-FU treated cells (Figure 3).

Expression of p53 in AGS cells

The results of RT-qPCR showed *p53* gene expression in the combination of 5-FU and PCA (10 µM and 500 µM, respectively). PCA and the 5-FU/PCA combination led to a significant increase ($p<0.05$) in *p53* gene expression by almost 5.5- and 11.6- fold, respectively, in comparison with the control cells (Figure 4). No significant change was observed between 5-FU and untreated control cells.

Effects of 5-FU, PCA, and 5-FU/PCA combination on Bcl-2 signaling protein in AGS cells

The result of Western blotting demonstrated that the protein expression level of Bcl-2 markedly decreased after treatment with the 5-FU/PCA combination in AGS cells when compared to that of the untreated control cells and 5-FU treated cells (Figure 5).

DISCUSSION

The prevalence of cancer is increasing worldwide and the growing rate of mortality is quite alarming. Nowadays, 5-FU-based chemotherapy is a widespread procedure in the treatment of a wide range of cancers, including gastric, colorectal, and breast cancers, due to its effect in the inhibition of thymidylate synthase.[23,24] Combination therapy not only

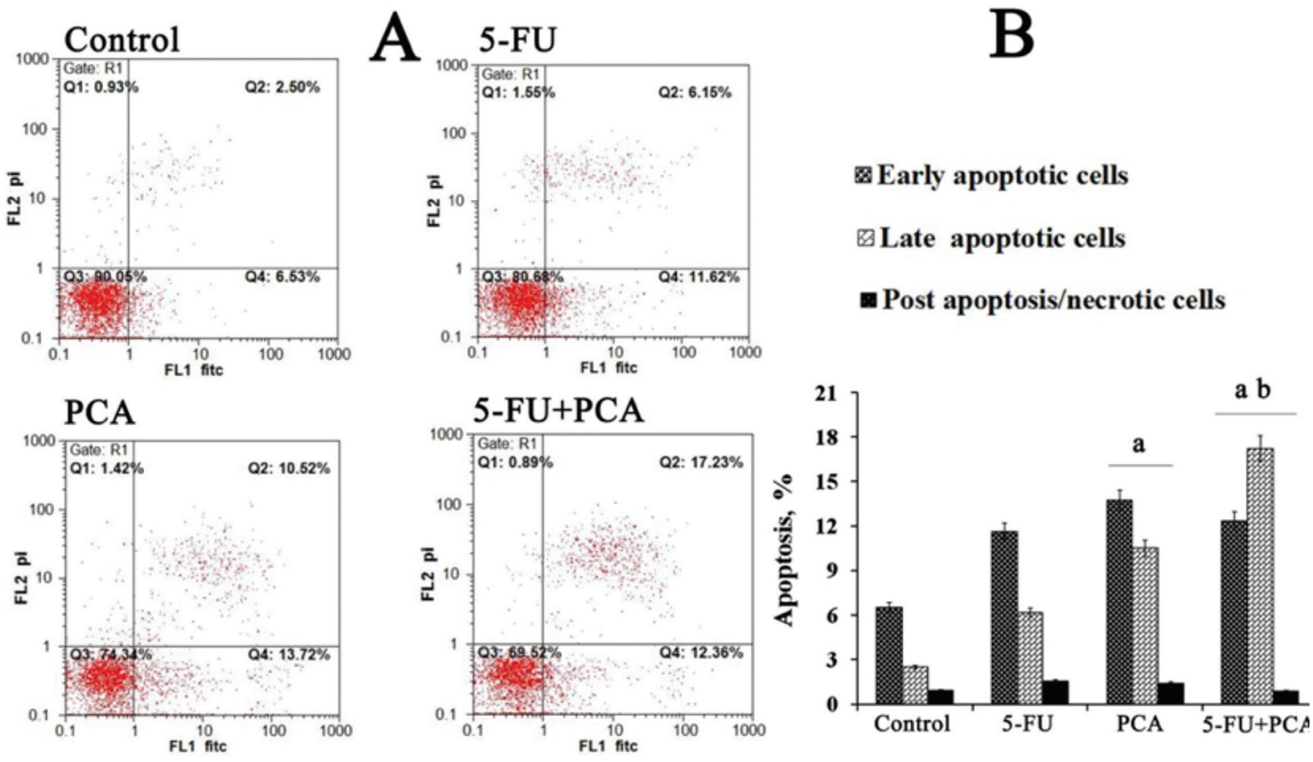

Figure 3. Induction of apoptosis after 24 h exposure to 5-FU (10 µM), PCA (500 µM), and combination of 5-FU and PCA (10 µM and 500 µM, respectively). Data were analyzed by FACScan and represent the mean of duplicate determinations. (A): Flow cytometry charts of Annexin V-FITC/PI staining in untreated (control) AGS cells and cells treated with 5-FU, PCA, and combination of 5-FU and PCA. (B): The percentage of apoptotic AGS cells. The results are expressed as mean ± SD of three separate experiments

[a]p<0.05 vs. control cells, [b]p<0.05 vs. 5-FU treated cells 5-FU: 5-fluorouracil, PCA: Protocatechuic acid, AGS: Gastric adenocarcinoma, SD: Standard deviation

amplifies chemotherapy's effects on tumor cells at lower concentrations but also it causes little toxicity to normal cells.[25] In the present study, the combined treatment of 5-FU with PCA had stronger antiproliferation effects than either agent alone (Figure 1). Several previous studies have shown that PCA alone can decrease cell proliferation and viability in some cancer cell lines such as breast, lung, liver, cervix, and prostate cancer cells,[26,27] which is in line with the findings in the present study. On the other hand, many studies have demonstrated that the combination of natural compounds with chemotherapeutic drugs enhanced their antitumor efficacy through various mechanisms, including cell sensitization, induction of apoptosis, inhibition of cell proliferation, invasion, metastasis, and angiogenesis,[28] which is in agreement with the findings of our study. It has been reported that natural compounds can disperse vimentin, an epithelial-mesenchymal transition factor, and cause loss of cytoplasmic integrity. These compounds can make changes in cellular morphology through destabilization of the nucleus, cytoskeleton, mitotic spindle, and cell flexibility.[7,29] Moreover, previous studies have shown that some antioxidants such as curcumin, resveratrol, and epigallocatechin-3-gallate not only have chemopreventive or chemotherapeutic effects but also they act as chemosensitizers on tumor cells.[7,30-32] Therefore, in the present study it seems that PCA, at least partly, sensitized the AGS tumor cells to 5-FU, which led to increased antiproliferation and cytotoxic efficiency of 5-FU.

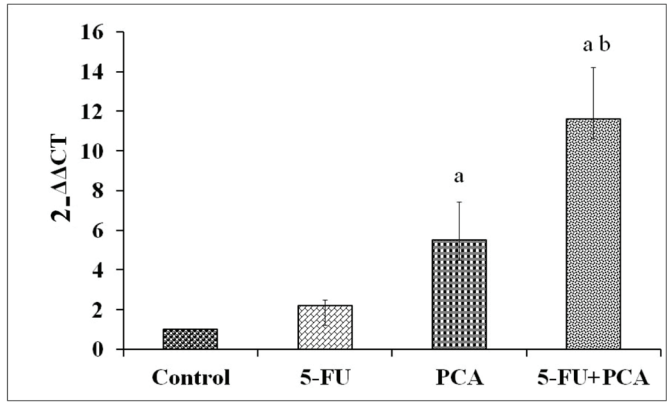

Figure 4. The gene expression of p53 in the presence or absence of 5-FU, PCA, and 5-FU/PCA combination on the AGS cells. Cells were exposed to a combination of 5-FU and PCA (10 µM and 500 µM, respectively). The expression of p53 was normalized with GAPDH as an internal standard

[a]p<0.05 vs. control cells, [b]p<0.05 vs. 5-FU treated cells

5-FU: 5-fluorouracil, PCA: Protocatechuic acid, AGS: Gastric adenocarcinoma, GAPDH: Glyceraldehyde-3-phosphate dehydrogenase

Our data demonstrated that the combined 5-FU and PCA resulted in a decrease in the number of colonies when compared to untreated control cells and each agent alone (Figure 2), which was in agreement with previous studies results.[33,34] A previous study showed that combined 5-FU, cisplatin, and curcumin enhanced the anticancer effects of 5-FU in human

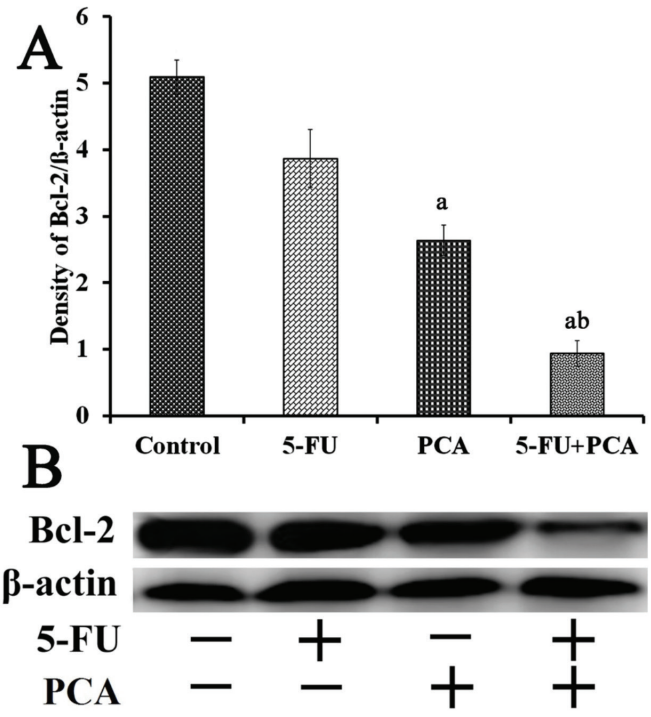

Figure 5. The Bcl-2 level of signaling pathway proteins in the AGS cell line. Cells were treated with 5-FU (10 µM), PCA (500 µM), and 5-FU/PCA combination (10 µM and 500 µM, respectively) for 24 h. (A): Density chart of Bcl-2/β-actin and (B): Western blots bands

[a]p<0.05 vs. control cells, [b]p<0.05 vs. 5-FU treated cells

Bcl-2: Bcl-2 protein 2, AGS: Gastric adenocarcinoma, 5-FU: 5-fluorouracil, PCA: Protocatechuic acid

gastric cancer MGC-803 cells by decreasing cell viability, inhibiting colony formation, and inducing apoptosis, which is in line with the present study findings.[33] It has also been reported that glabridin, the major isoflavane in licorice root, may inhibit the malignant proliferation of the human gastric cancer MKN-45 cell line and enhance the efficiency of 5-FU.[34] The reduction in the number of colonies in the present study through combined 5-FU and PCA, at least partly, may have resulted from synergistic effects due to loss of sensitized cytoplasmic integrity and cellular changes such as Bcl-2 reduction, p53 elevation, and cell morphology.

Our flow cytometry results demonstrated that treatment with PCA and 5-FU combined resulted in increasing apoptosis in AGS cells compared to the untreated control cells (Figure 3). Antioxidants are used as anticancer compounds and can lead to cell death by activating the internal or external pathways of apoptosis.[1] It has been demonstrated in several studies that PCA can induce apoptosis in cancer cells, which is in line with the results of the present study.[35-37] In addition, PCA-induced apoptosis was found to be associated with the inhibition of Bcl-2, the mitochondrial translocation of Bax and Bid, and the cytosolic release of cytochrome C, which is in agreement with our study findings.[38] On the other hand, it has been found that 5-FU induces apoptosis in cancer cells though p53.[24,39-41] It has also been reported that administration of 5-FU with troxerutin, a flavonoid, results in a dose-dependent suppression of cell proliferation and induces apoptosis, which is in line with our findings (Figures 1 and 3).[42] In addition, it is reported that antioxidants can reduce the side effects and potential harmful impact of medications,[43] influence multidrug resistance genes, which are responsible for resistance to different cytotoxic drugs, and enhance the residence time of chemotherapeutic drugs in cancer cells.[7] Therefore, in the present study, the elevated efficacy of 5-FU for AGS apoptosis in the presence of PCA, at least partly, is due to PCA antioxidant capacity through sensitized cytoplasmic integrity and cellular changes such as Bcl-2 reduction and p53 elevation, and can trigger other internal or external signaling pathways of apoptosis.

p53 acts as a transcription factor for a series of pro-apoptotic proteins (such as Bad, Bax, and Bid) and anti-apoptotic Bcl-2 signaling protein and induces apoptosis by releasing cytochrome C.[44] Natural antioxidants can cause cell death by controlling members of the Bcl-2 family and promoting DNA damage.[45] In addition, it has been demonstrated that Bcl-2, which encodes an inner mitochondrial protein, can antagonize apoptosis in many tumor cells.[38] Our results showed that the combined 5-FU/PCA increased *p53* gene expression and decreased cellular Bcl-2 signaling protein (Figures 4 and 5). In many previous studies, it was found that PCA has the potential to induce apoptosis, increase *p53* gene expression, and cause a decline in Bcl-2 protein, which is in agreement with our findings.[38,46] Nevertheless, in the present study, it seems that the combination of PCA with 5-FU can strongly increase *p53* gene expression (Figure 4). In another study, it was demonstrated that PCA acted as an apoptotic inducer of leukemia by decreasing the phosphorylation of retinoblastoma and decreasing the expression of Bcl-2, which is in line with the present study.[38] On the other hand, researchers determined that *Hibiscus* polyphenol-rich extract containing PCA caused apoptosis in human gastric carcinoma cells via p53 phosphorylation and the p38 MAPK/FasL cascade pathway.[46] In addition, it has been demonstrated that natural antioxidants such as forbesione, lupeol, luteolin, and myricetin can induce synergistic, apoptotic, and antiproliferative effects with 5-FU through the elevation of *p53* gene expression and decreasing of the cellular Bcl-2 signaling protein in some cancer cells, which is in line with our findings.[47-50] Therefore, in the present study, the elevation in *p53* gene expression and the reduction in Bcl-2 protein level in the presence of PCA, at least partly, may have resulted from the potential of PCA in cell sensitization to 5-FU by activating intracellular signaling pathways.

In the present study, we did not investigate the effects of the combined 5-FU/PCA treatment on other cellular signaling pathways such as FAK, MAPK, MMP, COX, JNK, Akt, ERK, Nf-κb, or caspases modulating factors, which influence invasion, metastasis, and apoptosis. We also did not study cell survival factors such as Bcl-xL or cFLIP. Thus, we suggest that prospective researchers investigate the above factors in combined 5-FU/PCA in future studies.

CONCLUSION

Our data indicate that the combined 5-FU/PCA treatment may promote antiproliferative and pro-apoptotic effects plus inhibition of colony formation in AGS cells. Some mechanisms by which the combined 5-FU/PCA treatment exerts its effects are associated with the upregulation of p53 and downregulation of Bcl-2 expression. Therefore, the combination of 5-FU with PCA not only could be a promising approach for potential reduction of dose requirements of 5-FU treatment but also could promote apoptosis via p53 and Bcl-2 signaling pathways.

ACKNOWLEDGEMENTS

We would like to express our gratitude to those who helped us in Clinical Biochemistry Research Center of Shahrekord University of Medical Sciences, Shahrekord, Iran. The results described in this paper were the MS dissertation of Ms. Zahra Motamedi. This study was funded by Shahrekord University of Medical Sciences, Shahrekord, Iran.

Conflicts of interest: No conflict of interest was declared by the authors. The authors alone are responsible for the content and writing of the paper.

REFERENCES

1. Teng H, Huang Q, Chen L. Inhibition of cell proliferation and triggering of apoptosis by agrimonolide through MAP kinase (ERK and p38) pathways in human gastric cancer AGS cells. Food Funct. 2016;7:4605-4613.
2. Mohammadi M, Zarghami N, Hedayati M, Ghaemmaghami S. Synergistic effects of resistin and visfatin as adipocyte derived hormones on telomerase gene expression in AGS gastric cancer cell line. Acta Med Iran. 2017;55:621-627.
3. Zheng LC, Yang MD, Kuo CL, Lin CH, Fan MJ, Chou YC, Lu HF, Huang WW, Peng SF, Chung JG. Norcantharidin-induced apoptosis of AGS human gastric cancer cells through reactive oxygen species production, and caspase- and mitochondria-dependent signaling pathways. Anticancer Res. 2016;36:6031-6042.
4. Noordhuis P, Holwerda U, Van der Wilt C, Van Groeningen C, Smid K, Meijer S, Pinedo HM. 5-Fluorouracil incorporation into RNA and DNA in relation to thymidylate synthase inhibition of human colorectal cancers. Ann Oncol. 2004;15:1025-1032.
5. Wagner AD, Grothe W, Haerting J, Kleber G, Grothey A, Fleig WE. Chemotherapy in advanced gastric cancer: a systematic review and meta-analysis based on aggregate data. J Clin Oncol. 2006;24:2903-2909.
6. Hauner K, Maisch P, Retz M. Nebenwirkungen der Chemotherapie. Der Urologe. 2017;56:472-479.
7. de Oliveira Júnior RG, Ferraz CAA, da Silva Almeida JRG, Grougnet R, Thiéry V, Picot L. Sensitization of tumor cells to chemotherapy by natural products: a systematic review of preclinical data and molecular mechanisms. Fitoterapia. 2018;21.
8. Sato Y, Tsurumi T. Genome guardian p53 and viral infections. Rev Med Virol. 2013;23:213-220.
9. Jiang L, Sheikh MS, Huang Y. Decision making by p53: life versus death. Mol Cell Pharmacol. 2010;2:69-77.
10. Fresco P, Borges F, Diniz C, Marques M. New insights on the anticancer properties of dietary polyphenols. Med Res Rev. 2006;26:747-766.
11. Sak K. Cytotoxicity of dietary flavonoids on different human cancer types. Pharmacogn Rev. 2014;8:122-146.
12. Tanaka T, Kojima T, Kawamori T, Mori H. Chemoprevention of digestive organs carcinogenesis by natural product protocatechuic acid. Cancer. 1995;75:1433-1439.
13. Khan AK, Rashid R, Fatima N, Mahmood S, Mir S, Khan S, Jabeen N, Murtaza G. Pharmacological activities of protocatechuic acid. Acta Pol Pharm. 2015;72:643-650.
14. Masella R, Santangelo C, D'archivio M, LiVolti G, Giovannini C, Galvano F. Protocatechuic acid and human disease prevention: biological activities and molecular mechanisms. Curr Med Chem. 2012;19:2901-2917.
15. Yoshimizu N, Otani Y, Saikawa Y, Kubota T, Yoshida M, Furukawa T, Kumai K, Kameyama K, Fujii M, Yano M, Sato T, Ito A, Kitajima M. Anti-tumour effects of nobiletin, a citrus flavonoid, on gastric cancer include: antiproliferative effects, induction of apoptosis and cell cycle deregulation. Aliment Pharmacol Ther. 2004;1:95-101.
16. Kapp N, Stander XX, Stander BA. Synergistic *in vitro* effects of combining an antiglycolytic, 3-bromopyruvate, and a bromodomain-4 inhibitor on U937 myeloid leukemia cells. Anticancer Drugs. 2018;29:429-439.
17. Koraneekit A, Limpaiboon T, Sangka A, Boonsiri P, Daduang S, Daduang J. Synergistic effects of cisplatin-caffeic acid induces apoptosis in human cervical cancer cells via the mitochondrial pathways. Oncol Lett. 2018;15:7397-7402.
18. Franken NA, Rodermond HM, Stap J, Haveman J, Van Bree C. Clonogenic assay of cells *in vitro*. Nat Protoc. 2006;1:2315-2319.
19. Pauzi AZM, Yeap SK, Abu N, Lim KL, Omar AR, Aziz SA, Chow ALT, Subramani T, Tan SG, Alitheen NB. Combination of cisplatin and bromelain exerts synergistic cytotoxic effects against breast cancer cell line MDA-MB-231 *in vitro*. Chin Med. 2016;11:46.
20. Sun Y, Zhang D, Mao M, Lu Y, Jiao N. Roles of p38 and JNK protein kinase pathways activated by compound cantharidin capsules containing serum on proliferation inhibition and apoptosis of human gastric cancer cell line. Exp Ther Med. 2017;14:1809-1817.
21. Heidarian E, Keloushadi M, Ghatreh-Samani K, Jafari-Dehkordi E. Gallic acid inhibits invasion and reduces *IL-6* gene expression, pSTAT3, pERK1/2, and pAKT cellular signaling proteins in human prostate cancer DU-145 cells. Int J Cancer Manag. 2017;10:e9163.
22. Bradford MM. A rapid and sensitive method for the quantitation of microgram quantities of protein utilizing the principle of protein-dye binding. Anal Biochem. 1976;72:248-254.
23. Mahlberg R, Lorenzen S, Thuss-Patience P, Heinemann V, Pfeiffer P, Mohler M. New perspectives in the treatment of advanced gastric cancer: S-1 as a novel oral 5-FU therapy in combination with cisplatin. Chemotherapy. 2017;62:62-70.
24. Longley DB, Harkin DP, Johnston PG. 5-fluorouracil: mechanisms of action and clinical strategies. Nat Rev Cancer. 2003;3:330-338.
25. Sun W, Sanderson PE, Zheng W. Drug combination therapy increases successful drug repositioning. Drug Discov Today. 2016;21:1189-1195.
26. Yin MC, Lin CC, Wu HC, Tsao SM, Hsu CK. Apoptotic effects of protocatechuic acid in human breast, lung, liver, cervix, and prostate cancer cells: potential mechanisms of action. J Agric Food Chem. 2009;57:6468-6473.

27. Tsao SM, Hsia TC, Yin MC. Protocatechuic acid inhibits lung cancer cells by modulating FAK, MAPK, and NF-kappaB pathways. Nutr Cancer. 2014;66:1331-1341.

28. Shukla S, Mehta A. Anticancer potential of medicinal plants and their phytochemicals: a review. Braz J Bot. 2015;38:199-210.

29. Satelli A, Li S. Vimentin in cancer and its potential as a molecular target for cancer therapy. Cell Mol Life Sci. 2011;68:3033-3046.

30. Hour TC, Chen J, Huang CY, Guan JY, Lu SH, Pu YS. Curcumin enhances cytotoxicity of chemotherapeutic agents in prostate cancer cells by inducing p21WAF1/CIP1 and C/EBPβ expressions and suppressing NF-kappaB activation. Prostate. 2002;51:211-218.

31. Fulda S, Debatin KM. Sensitization for anticancer drug-induced apoptosis by the chemopreventive agent resveratrol. Oncogene. 2004;23:6702-6711.

32. Braicu C, Gherman CD, Irimie A, Berindan-Neagoe I. Epigallocatechin-3-Gallate (EGCG) inhibits cell proliferation and migratory behaviour of triple negative breast cancer cells. J Nanosci Nanotechnol. 2013;13:632-637.

33. He B, Wei W, Liu J, Xu Y, Zhao G. Synergistic anticancer effect of curcumin and chemotherapy regimen FP in human gastric cancer MGC-803 cells. Oncol Lett. 2017;14:3387-3394.

34. Zhang L, Chen H, Wang M, Song X, Ding F, Zhu J, Liu X. Effects of glabridin combined with 5-fluorouracil on the proliferation and apoptosis of gastric cancer cells. Oncol Lett. 2018;15:7037-7045.

35. Guan S, Jiang B, Bao Y, An L. Protocatechuic acid suppresses MPP+-induced mitochondrial dysfunction and apoptotic cell death in PC12 cells. Food Chem Toxicol. 2006;44:1659-1666.

36. Liu YM, Jiang B, Bao YM, An LJ. Protocatechuic acid inhibits apoptosis by mitochondrial dysfunction in rotenone-induced PC12 cells. Toxicol In Vitro. 2008;22:430-437.

37. Lin HH, Chen JH, Huang CC, Wang CJ. Apoptotic effect of 3, 4-dihydroxybenzoic acid on human gastric carcinoma cells involving JNK/p38 MAPK signaling activation. Int J Cancer. 2007;120:2306-2316.

38. Tseng TH, Kao TW, Chu CY, Chou FP, Lin WL, Wang CJ. Induction of apoptosis by hibiscus protocatechuic acid in human leukemia cells via reduction of retinoblastoma (RB) phosphorylation and Bcl-2 expression. Biochem Pharmacol. 2000;60:307-315.

39. Petak I, Tillman DM, Houghton JA. p53 dependence of Fas induction and acute apoptosis in response to 5-fluorouracil-leucovorin in human colon carcinoma cell lines. Clin Cancer Res. 2000;6:4432-5541.

40. Bunz F, Hwang PM, Torrance C, Waldman T, Zhang Y, Dillehay L, Williams J, Lengauer C, Kinzler KW, Vogelstein B. Disruption of p53 in human cancer cells alters the responses to therapeutic agents. J Clin Invest. 1999;104:263-269.

41. Zhang L, Yu J, Park BH, Kinzler KW, Vogelstein B. Role of BAX in the apoptotic response to anticancer agents. Science. 2000;290:989-992.

42. Xu GY, Tang XJ. Troxerutin (TXN) potentiated 5-Fluorouracil (5-Fu) treatment of human gastric cancer through suppressing STAT3/NF-kappaB and Bcl-2 signaling pathways. Biomed Pharmacother. 2017;92:95-107.

43. Wagner H, Ulrich-Merzenich G. Synergy research: approaching a new generation of phytopharmaceuticals. Phytomedicine. 2009;16:97-110.

44. Tiwari M. Apoptosis, angiogenesis and cancer therapies. J Can Res Ther. 2012;1:3.

45. Hussain SA, Sulaiman AA, Balch C, Chauhan H, Alhadidi QM, Tiwari AK. Natural polyphenols in cancer chemoresistance. Nutr Cancer. 2016;68:879-891.

46. Lin HH, Huang HP, Huang CC, Chen JH, Wang CJ. Hibiscus polyphenol-rich extract induces apoptosis in human gastric carcinoma cells via p53 phosphorylation and p38 MAPK/FasL cascade pathway. Mol Carcinog. 2005;43:86-99.

47. Boueroy P, Hahnvajanawong C, Boonmars T, Saensa-ard S, Wattanawongdon W, Kongsanthia C, Salao K, Wongwajana S, Anantachoke N, Reutrakul V. Synergistic effect of forbesione from Garcinia hanburyi in combination with 5-Fluorouracil on cholangiocarcinoma. Asian Pac J Cancer Prev. 2017;18:3343-3351.

48. Liu Y, Bi T, Dai W, Wang G, Qian L, Shen G, Gao Q. Lupeol enhances inhibitory effect of 5-fluorouracil on human gastric carcinoma cells. Naunyn Schmiedebergs Arch Pharmacol. 2016;389:477-484.

49. Xu H, Yang T, Liu X, Tian Y, Chen X, Yuan R, Su S, Lin X, Du G. Luteolin synergizes the antitumor effects of 5-fluorouracil against human hepatocellular carcinoma cells through apoptosis induction and metabolism. Life Sci. 2016;144:138-147.

50. Wang L, Feng J, Chen X, Guo W, Du Y, Wang Y, Zang W, Zhang S, Zhao G. Myricetin enhance chemosensitivity of 5-fluorouracil on esophageal carcinoma *in vitro* and *in vivo*. Cancer Cell Int. 2014;14:71.

Turk J Pharm Sci 2020;17(6):586-592
DOI: 10.4274/tjps.galenos.2019.77992

ORIGINAL ARTICLE

The *In Vivo* Antinociceptive and Antiinflammatory Effects of *Verbascum exuberans* Hub.-Mor.

Verbascum exuberans Hub.-Mor.'ın *İn Vivo* Antinosiseptif ve Antiinflamatuvar Etkileri

Esra EYİİŞ[1]*, Bilgin KAYGISIZ[2], Fatma Sultan KILIÇ[2], Adnan AYHANCI[1]

[1]Eskişehir Osmangazi University Faculty of Science and Letters, Department of Biology, Eskişehir, Turkey
[2]Eskişehir Osmangazi University Faculty of Medicine, Department of Medical Pharmacology, Eskişehir, Turkey

ABSTRACT

Objectives: Safe and effective drugs are still lacking for many pain therapies. In recent years, growing interest has been devoted thus on herbal drugs as an option to identify new pain killers. Based on this, extensive researches are carried out on *Verbascum* L. genus due to its therapeutic potency on pain and inflammation therapy. In this study, among *Verbascum* species, the antinociceptive effect of *Verbascum exuberans* Hub.-Mor., and its contributions to nitrergic, serotonergic, or opioidergic pathways as well as its antiinflammatory acitivity were investigated.

Materials and Methods: Tail clip, tail flick, and hot plate tests were used to determine the central (spinal and supraspinal) antinociceptive effect, while an acetic acid-induced writhing test was used to measure the peripheral antinociceptive effect of the extract (250 and 500 mg/kg). The extract (250 mg/kg) was then combined with nω-nitro-L-arginine methyl ester, cyproheptadine, and naloxone to evaluate its involvement in nitrergic, serotonergic, or opioidergic pathways, respectively. Carrageenan-induced hind paw edema model was used to determine the antiinflammatory effect of the extract (250 mg/kg).

Results: The extract shows central spinal but not central supraspinal antinociceptive effect, and presents peripheral antinociceptive effect. The antinociceptive actions of the extract is largely regulated via targeting the nitrergic pathway, while the opioidergic pathway is partly involved. Further, the extract shows antiinflammatory effect due to the significant inhibitions on the time dependent edema progression and the cytokine (tumor necrosis factor-alfa and interleukin-1beta) productions.

Conclusion: *V. exuberans* could be stated as a new source with a high beneficial potential in alleviating pain and inflammation.

Key words: *Verbascum exuberans* Hub.-Mor., *Scrophulariaceae*, antinociceptive effect, antiinflammatory effect, tramadol

ÖZ

Amaç: Birçok ağrı tedavisi için güvenli ve etkili ilaçların arayışı hala devam etmektedir. Nitekim, son yıllarda, yeni ağrı kesicilerin keşfine bir seçenek olarak bitkisel ilaçlara ilginin arttığı görülmektedir. Bu bilgiye dayanarak, ağrı ve enflamasyon tedavisinde, tedavi edici potansiyeli nedeniyle *Verbascum* L. cinsine yönelik kapsamlı araştırmalar yürütülmektedir. Bu çalışmada, *Verbascum* türleri arasından, *Verbascum exuberans* Hub.-Mor.'ın antinosiseptif etkinliğini, bu etkide nitrerjik, serotonerjik ve opioiderjik yolaklar üzerindeki rolünü ve antiinflamatuvar aktivitesini araştırılmıştır.

Gereç ve Yöntemler: Ekstrenin (250 ve 500 mg/kg) santral (spinal ve supraspinal) antinosiseptif aktivitesi tail clip, tail flick ve hot plate testleri ile, periferal antinosiseptif etkisi ise asetik asit ile oluşturulmuş kıvranma testi ile ölçülmüştür. Daha sonra, ekstre (250 mg/kg) nω-nitro-L-arginin metil ester, siproheptadin ve nalokson ile kombine edilerek, sırasıyla, ekstrenin nitrerjik, serotonerjik ve opioiderjik yolaklardaki rolü belirlenmiştir. Karragenan ile oluşturulmuş arka ayak pençe ödem modeli ise ekstrenin (250 mg/kg) antiinflamatuvar aktivitesinin belirlenmesinde kullanılmıştır.

Bulgular: Ekstrenin santral spinal düzeyde etkili olduğu; ancak santral supraspinal düzeyde etkili olmadığı ve periferal antinosiseptif etkili olduğu görülmüştür. Ekstrenin antinosiseptif etkinliği büyük ölçüde nitrerjik yolağın üzerinden düzenlenirken, opioiderjik yolağın ise kısmen aracılık ettiği belirlenmiştir. Ayrıca, ekstrenin, zamana bağımlı ödem ilerlemesini ve sitokin (tümör nekroz faktörü alfa ve interlökin 1beta) birikimlerini önemli ölçüde engellemesi nedeni ile antiinflamatuvar etkili olduğu bulunmuştur.

Sonuç: *V. exuberans*'ın ağrı ve enflamasyonun giderilmesinde yüksek yararlı potansiyeli ile yeni bir kaynak olduğu ifade edilebilir.

Anahtar kelimeler: *Verbascum exuberans* Hub.-Mor., *Scrophulariaceae*, antinosiseptif aktivite, antiinflamatuvar etki, tramadol

*Correspondence: **E-mail:** esra.eyiis@yahoo.com, **Phone:** +90 222 239 37 50 **ORCID-ID:** orcid.org/0000-0001-5386-8143
Received: 08.01.2019, **Accepted:** 28.03.2019

INTRODUCTION

Pain is a major global health problem and its treatment is challenging.[1] Despite the present scientific advancements in pain therapies, potent, safe, and effective drugs are still lacking for many pain conditions.[2] Furthermore, many of the currently available treatments for pain are accompanied by adverse effects.[3] Therefore, optimization of the current pain relievers and identification of new ones are still a major focus of both the pharmaceutical industry and academics.[4] In recent years, increasing interest has been devoted to herbal remedies as potential therapeutic agents in the management of pain and inflammation. Among them, the genus *Verbascum* L. (Scrophulariaceae), also commonly known as mullein, has a long tradition in classical medicine and it has been used around the globe for diverse purposes.[5,6] In particular, the leaves and flowers of *Verbascum densiflorum* Bertol., *V. phlomoides* L., and *V. thapsus* L. have expectorant, mucolytic, and sedative properties that in Turkish folk medicine are used to treat respiratory disorders such as bronchitis, dry coughs, tuberculosis, and asthma. These species are also applied for the treatment of hemorrhoids, rheumatic pain, superficial fungal infections, wounds, and diarrhea. The oil prepared from the flowers is used to treat otitis media and is applied externally for eczema and other types of inflammatory skin conditions. These species are reported to be mildly diuretic and are applied for pruritic conditions of the urinary tract. Furthermore, they are traditionally consumed as a tea to relieve abdominal pain.[6-8] Additionally, the roots, leaves, flowers, and/or aerial parts of *Verbascum* species including *V. pumilum* Boiss. and Heldr., *V. orientale* (L). All., *V. cheiranthifolium* Boiss. var. *cheiranthifolium* Boiss., *V. chrysochaete* Stapff, *V. lasianthum* Boiss. ex Bentham, *V. symes* Murb. et Rech.f., and *V. pyramidatum* M. Bieb. are also used to treat painful symptoms in a wide range of diseases.[9-11]

Besides the folkloric uses, in general, pharmacological studies have shown that *Verbascum* species possess unique biological properties that can be beneficial for medical purposes. More importantly, *V. chionophyllum* Hub.-Mor., *V. pycnostachyum* Boiss. and Heldr., *V. latisepalum* Hub.-Mor., *V. salviifolium* Boiss.,[12] *V. lasianthum* Boiss. ex Benth., *V. pterocalycinum* var. *mutense* Hub.-Mor.,[13,14] *V. mucronatum* Lam.,[15] *V. mallophorum* Boiss. and Heldr.,[16] *V. xanthophoeniceum* Griseb.,[17] and *V. phlomoides* L.[18] as well as their isolated active compounds played significant roles as safe and efficient pain-killers. Altogether, this highlights the potency of the species from the genus *Verbascum* in pain and inflammation therapy. Considering thus the biological potential and the limited scientific information of this plant, in the present study, we for the first time investigated the antinociceptive and the antiinflammatory effects of the methanol extract prepared from *V. exuberans* Hub.-Mor. aerial parts, in experimental animal models.

MATERIALS AND METHODS

Plant material and extraction

V. exuberans (Scrophulariaceae), which in Turkish is named zibil sığırkuyruğu,[19] was collected from Manisa, Turkey. The endemic voucher specimen (KA 1243) is deposited at the Herbarium of the Faculty of Science and Arts of Celal Bayar University in Manisa, Turkey. The air-dried and powdered aerial parts of the plant material (20.354 g) was extracted with methanol (Sigma 34860) using a Soxhlet apparatus for 48 hours at 55°C. The obtained methanolic extract was filtered and evaporated in a rotator evaporator to give crude extract (2.534 g, 12.45% w/w). Subsequently, the crude methanolic extract was dissolved in distilled water and partitioned with an equal volume of petroleum ether (0.496 g, 2.43% w/w) (Sigma 270709) (to remove chlorophyll and other lipophilic constituents) at least four times. Finally, the remaining methanolic extract was lyophilized.

Animals and housing

Forty-nine adult, healthy, male Swiss albino mice (each group, n=7; *W*, 32±4 g) and 32 adult, healthy, male Sprague Dawley rats (each group, n=8; *W*, 240±20 g) were purchased from the animal breeding laboratories of Eskisehir Osmangazi University, Medical and Surgical Experimental Animals Implementation and Research Center. The animals were left for a week to acclimatize to animal room conditions and maintained on a standard pellet diet and water (*ad libitum*). All animals were kept at 22±2°C, with 45-50% relative humidity, a light/dark cycle of 12 h, and 10-15 changes of fresh air per hour in each cycle. The study was approved by the Animal Care and Use Committee at Eskisehir Osmangazi University (protocol no: 333-1/2013) and is in accordance with the National Institutes of Health Guide for the Care and Use of Laboratory Animals.

Study designs and experimental groups

Nω-nitro-L-arginine methyl ester (L-NAME) hydrochloride (N5751), cyproheptadine hydrochloride (C6022), tramadol hydrochloride (42965), λ-carrageenan (C1013), and indomethacin (I7378) were purchased from Sigma, while naloxone hydrochloride was purchased from Inresa. All of the drugs including *V. exuberans* and carrageenan were dissolved in sterile physiological saline. The drugs were administered intraperitoneally (ip) except for carrageenan. Carrageenan was given subcutanously (sc). For the experimental antinociceptive study design, the mice were randomly divided into 7 groups and received ip injections of (1) sterile physiological saline (0.1 mL/10 g) as a negative control, (2) a low dose of *V. exuberans* (250 mg/kg), (3) a high dose of *V. exuberans* (500 mg/kg), (4) *V. exuberans* 250 mg/kg+L-NAME 100 mg/kg, (5) *V. exuberans* 250 mg/kg + cyproheptadine 50 µg/kg, (6) *V. exuberans* 250 mg/kg + naloxone 1 mg/kg, and (7) tramadol (10 mg/kg) as a positive control, respectively. The animals of groups (4)-(6) were also given L-NAME, cyproheptadine, and naloxone, respectively, 30 min prior to the extract administration, while groups (1)-(3) and (7) received empty injections. Additionally, *V. exuberans* or tramadol was administered 60 min before the postdrug experiments. For the experimental antiinflammatory model design, the rats were randomly divided into 4 groups, which received injections of (1) sterile physiological saline 0.1 mL/100 g as a negative control, (2) sterile physiological saline 0.1 mL/100 g, (3) indomethacin 10 mg/kg as a positive control, and (4) a low

dose of *V. exuberans* (250 mg/kg), respectively. The animals of groups (2)-(4) were also given sterile physiological saline, indomethacin, and *V. exuberans*, respectively, 30 min prior to the carrageenan (100 μL, 1% w/v in saline) administration, while group (1) received only sterile physiological saline.

Experimental antinociceptive activity tests

Tail clip[20] and tail flick[21] tests were used to investigate central spinal antinociception. For the tail clip test an artery clip that exerts standardized pressure on the tail was positioned 2-2.5 cm from the base of the tail. The biting and turning response to the tail clip was recorded. The tail flick test was applied using a focused beam of high intensity light to the tail. The latency time to "flick" or withdraw the tail from the heat stimulus apparatus was noted (MAY, 9604-A Tail Flick Unit Commat, Ankara, Turkey). The hot plate test[22] was used to investigate central supraspinal antinociception. The animals were put on a hot plate surface unit (Ugo Basile Hot/Cold Plate 35100) that was stabilized at 55±0.1°C. The latency time of paw licking or jumping was recorded for the hot plate test.

The acetic acid-induced writhing test[23] was used to assess peripheral antinociception. After 5 min of 0.6% acetic acid (60 mg/kg, i.p.) administration, stretching movements of the animals (arching of back, development of tension in abdominal muscles, elongation of body, or extension of forelimbs) were counted for 10 min.

The cut-off time for the tail clip, tail flick, and hot plate tests was set at 30 seconds and they were performed consecutively and executed twice with the same animal for predrug and postdrug latency times. The results were calculated via the formula of maximal possible effect %=[(postdrug latency-predrug latency)/(cut-off time-predrug latency] x100. Furthermore, the acetic acid-induced writhing test was performed last.

Experimental antiinflammatory activity test

The carrageenan-induced hind paw edema model[24] was used to investigate the antiinflammatory potential. The inflammation was induced by a sc injection of 100 μL of 1% freshly prepared solution of carrageenan into the right hind paws of the rats. The increases in paw thicknesses were considered to be edema and were measured by a micrometric compass (Ozaki, Co, Tokyo, Japan). The measurements of the rat paws were performed just before the carrageenan injection, that is, at "0 h (time 0)" and then every 60 min over 6 h after the carrageenan injection. Meanwhile, blood samples were drawn from each rat via cardiac puncture under anesthesia pre- and postcarrageenan (solely at 6 h) injection. Within the blood collection, the blood samples were precipitated by centrifugation at 10,000 rpm for 3 min at 4˚C. The extracted serum samples were aliquoted and were kept at -20˚C until use. The tumor necrosis factor (TNF)-α (eBioscience BMS630) and the interleukin (IL)-1β (invitrogen KRC3011) assays were measured using ELISA. The proinflammatory cytokine production was calculated after plotting the standard curves and is expressed as pg/mL.

Statistical analysis

Statistical significance was assessed using One-Way or Two-Way analysis (one factor repeated) of variance followed by the Tamhane or Tukey test for multiple comparisons, respectively. Significance between the mean values is defined as $p<0.05$ or $p<0.001$.

RESULTS AND DISCUSSION

V. exuberans has a profound central antinociceptive effect via the spinal system

Sensory neurons encode mechanical, thermal (heat or cold), and chemical stimuli into nerve fibers that travel via the spinal cord to the brain to stimulate painful sensations, a process known as nociception.[25] In the present study, we used tail clip, tail flick, and hot plate tests to assess central nociception. The tail flick and hot plate tests are thermal nociceptive tests, whereas the tail clip test is mechanical.[26] Furthermore, the nociceptive threshold response is supraspinally organized in the hot plate test, while the tail clip and tail flick tests are spinally mediated.[27] In our experiments, we used a high (500 mg/kg) dose and a low (250 mg/kg) dose of *V. exuberans* (Figure 1). Treatment with the high dose of the extract significantly decreased the behavioral nociceptive responses of the mice to the mechanical noxious stimuli compared to the control in the tail clip test ($p<0.05$) (Figure 1A), but did not affect the behavioral nociceptive responses to the thermal noxious stimuli in the tail flick test or the hot plate test ($p>0.05$) (Figure 1B and 1C). Interestingly, the low dose of the extract showed a higher potency to relieve pain. *V. exuberans* at 250 mg/kg dose alone decreased the behavioral nociceptive responses compared to the control in the tail clip and tail flick tests ($p<0.05$) (Figure 1A and 1B), but not in the hot plate test ($p>0.05$) (Figure 1C). Moreover, in the tail clip test, the antinociception of the extract showed an effect similar to that of tramadol ($p>0.05$). Finally, the significant alterations in both the mechanical and thermal nociceptive threshold latencies of mice at 250 mg/kg dose indicate that *V. exuberans* has a profound central antinociceptive effect. Additionally, the central antinociceptive action of the extract affects the spinal but not the supraspinal system.

V. exuberans shows a peripheral antinociceptive effect

The abdominal constriction response induced by acetic acid was used to evaluate the potential of *V. exuberans* as a peripherally acting pain reliever. Acetic acid stimulates the pain nerve endings and induces contraction of abdominal muscles *via* sensitization of the nociceptive receptor to the peripherally released endogenous prostaglandins (PGs), in particular $PGE_{2\alpha}$ and $PGF_{2\alpha}$ as well as lipoxygenase products and cytokines.[28] In the present study, the behavioral nociceptive response of mice to the chemical noxious stimuli was greatly inhibited by *V. exuberans* at both doses compared to the control ($p<0.001$), thus clearly indicating a peripheral antinociceptive effect. Furthermore, the effect was stronger at the higher dose of the extract than at the lower dose ($p<0.05$) (Figure 1D). In our experiments, we used the well characterized drug tramadol as a positive control.[29,30] As expected, 10 mg/kg tramadol showed both central (spinal and supraspinal) and peripheral antinociceptive effects compared to the control in all the experimental nociceptive tests ($p<0.001$) (Figure 1). Strikingly,

when compared to tramadol, the inhibition of peripheral pain by the extract has greater benefit than the inhibition of central pain, suggesting that *V. exuberans* might be a new alternative for pain therapy.

V. exuberans mediates its central spinal and peripheral antinociception by targeting the nitrergic pathway

Activation of the L-arginine (arg)-nitric oxide (NO)- cyclic guanosine monophosphate (cGMP)-ATP sensitive K^+ channel pathway results in antinociception. NO mediates the antinociceptive effect via phosphorylation of the K_{ATP} channel and thereby activation of the guanylate cyclase-cGMP system.[31] To explore the role of the nitrergic pathway in the antinociceptive effect of *V. exuberans*, we combined the plant extract with L-NAME, a competitive L-arg-based nonselective NO synthase inhibitor (Figure 2). Addition of L-NAME to the mice pretreated with the extract ameliorated the behavioral nociceptive responses to the mechanical and the chemical noxious stimuli compared to the control ($p<0.001$) and 250 mg/kg extract alone ($p<0.05$) in both the tail clip and writhing tests (Figure 2A and 2D). Moreover, the enhanced antinociceptive responses of the extract exhibited a higher effect than tramadol in the tail clip test ($p<0.05$) (Figure 2A), while in the writhing test they showed similar potential ($p>0.05$) (Figure 2D). In addition, the extract nonsignificantly affected the behavioral nociceptive latencies of mice to the thermal noxious stimuli compared to the control and 250 mg/kg extract alone in both the tail flick and hot plate tests ($p>0.05$) (Figure 2B and 2C). However, in the presence of L-NAME the extract retained its antinociception properties rather than showing increased activity in the tail

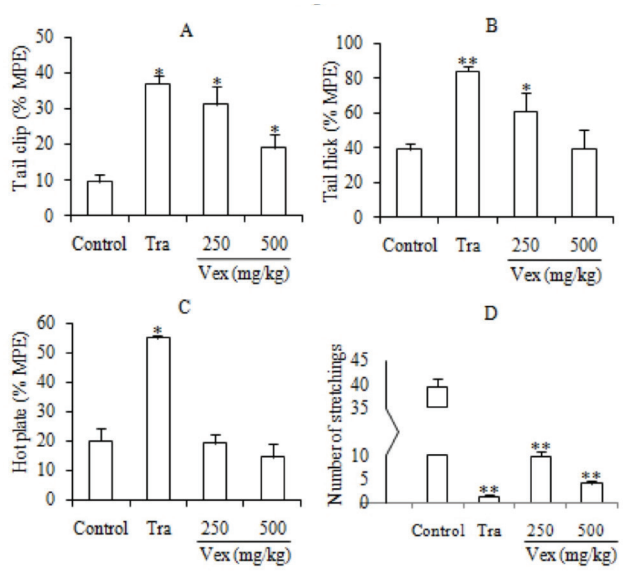

Figure 1. The effects of *V. exuberans* on central and peripheral nociception (Swiss albino mice; each group, n=7; *W*, 32±4 g). The central spinal antinociceptive effect was determined by the tail clip (A) and the tail flick (B) tests, while the central supraspinal antinociceptive activity was assessed by the hot plate test (C). The peripheral antinociceptive activity was determined by the acetic acid-induced writhing test (D). The latency time responses were defined as % MPE for the central antinociceptive tests, while for the peripheral antinociceptive test the movement responses were defined as the number of stretchings. All the test results were expressed as mean ± SEM. *$p<0.05$ compared to control, **$p<0.001$ compared to control, as determined by one way analysis of variance followed by the Tamhane test.

Tra: Tramadol, Vex: *V. exuberans*, MEP: Maximal possible effect, SEM: Standard error mean

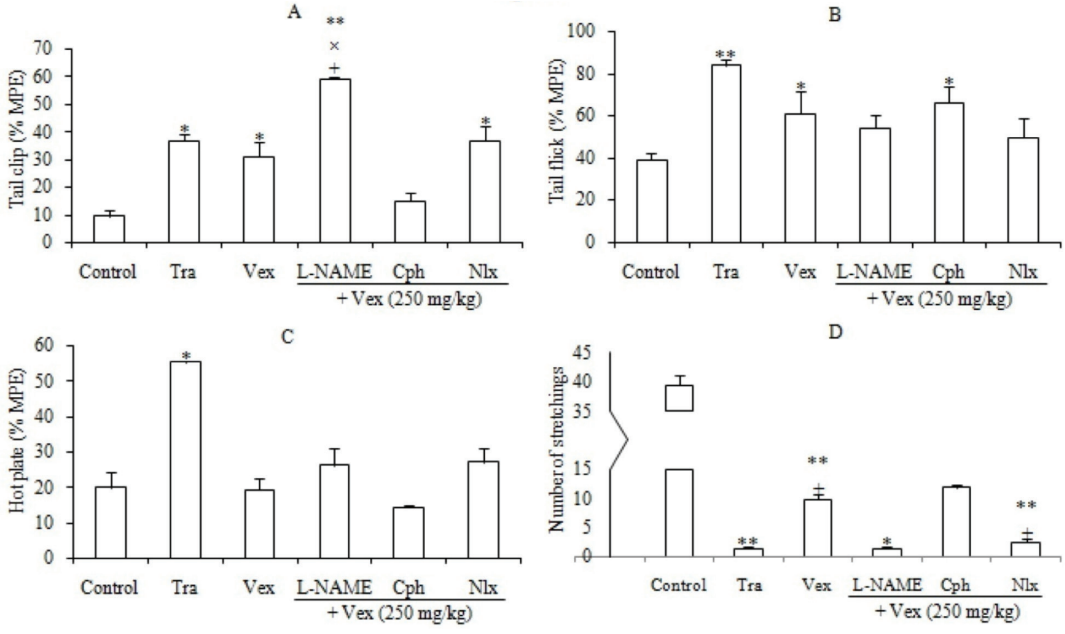

Figure 2. The effects of *V. exuberans* and its combinations on central and peripheral nociception (Swiss albino mice; each group, n=7; *W*, 32±4 g). The central spinal antinociceptive effect was determined by the tail clip (A) and the tail flick tests (B), while the central supraspinal antinociceptive activity was assessed by the hot plate test (C). The peripheral antinociceptive activity was determined by the acetic acid-induced writhing test (D). The latency time responses were defined as % MPE for the central antinociceptive tests, while for the peripheral antinociceptive test the movement responses were defined as the number of stretchings. All the test results were expressed as mean ± SEM. *$p<0.05$ compared to control; **$p<0.001$ compared to control, ×$p<0.05$ compared to 10 mg/kg tramadol, +$p<0.05$ compared to the single dose of 250 mg/kg *V. exuberans*, as determined by One-Way analysis of variance followed by the Tamhane test.

Tra: Tramadol, Vex: *V. exuberans* 250 mg/kg, Cph: Cyproheptadine, Nlx: Naloxone, MEP: Maximal possible effect, SEM: Standard error mean

flick test. This could be related to the concurrent effect of NO, which depends on dosage levels and the rate and timing of its release.[32,33] In conclusion, our results indicate that *V. exuberans* showed its antinociceptive effect in a L-NAME reversible manner, suggesting a central spinal and peripheral nitrergic mechanism. The results imply that the composition of the plant extract might have a specific effect on the nitrergic pathway.

Cyproheptadine does not affect the antinociceptive properties of V. exuberans

Involvement of the serotonergic pathway mediated antinociceptive effect of *V. exuberans* was tested using cyproheptadine, a serotonin (5-HT) receptor antagonist (Figure 2). Addition of cyproheptadine to mice pretreated with the plant extract did not significantly change the mechanical or thermal nociceptive threshold latencies compared to the controls in the tail clip test or the hot plate test ($p>0.05$) (Figure 2A and 2C). The supplementation of cyproheptadine let the extract decrease the behavioral nociceptive responses of mice compared to the controls in both the tail flick and writhing tests ($p<0.05$), while the nociceptive latencies showed nonsignificant alterations compared to 250 mg/kg extract alone ($p>0.05$) (Figure 2B and 2D). Together these results indicate that cyproheptadine does not evoke the obvious antinociceptive properties of *V. exuberans*. Animal studies report that 5-HT and 5-HT receptors have a complex role in modulating nociceptive reflexes. The complexity of effects produced by the 5-HT receptor in nociceptive transmission is due to the type of nociceptive stimuli, subtype of receptor, and dose of agonists or antagonists.[34] Since cyproheptadine is a high-affinity $5\text{-HT}_{1C,2}$ receptor antagonist, our data suggest that at least these receptors do not directly activate the antinociceptive effect of *V. exuberans*.

Naloxone partly inhibits V. exuberans-induced antinociception

The opioid system is very important in regulating pain. This system participates in both the perception and modulation of the pain process via central and peripheral mechanisms.[35] To explore the contribution of the opioidergic pathway to the antinociceptive effect of *V. exuberans* we used naloxone, a relatively nonselective opioid receptor antagonist (Figure 2). Supplementation of naloxone to mice pretreated with the plant extract caused nonsignificant behavioral nociceptive responses compared to the control and 250 mg/kg extract alone in both the tail flick and hot plate tests ($p>0.05$) (Figure 2B and 2C). The addition of naloxone enabled the extract to enhance the nociceptive latencies compared to the control in the tail clip test ($p<0.05$), whereas the latencies showed non-significant changes compared to both tramadol and 250 mg/kg extract alone ($p>0.05$) (Figure 2A). Our results indicate that the antinociceptive effect of the extract on both the mechanical and thermal nociceptive thresholds of mice was unaltered by naloxone, indicating that the spinally mediated actions of the extract are independent of the central opioidergic system. The therapeutic utility of opioids in pain therapy is limited due to their specific affinity to centrally mediated opioid receptors.[36] Therefore, targeting of peripheral opioid receptors may provide pain relief, while reducing many of the adverse effects.[37] In fact, addition of naloxone allowed the extract to suppress the acetic acid nociceptive stimuli by decreasing the stretching responses compared to both the control ($p<0.001$) and 250 mg/kg extract alone ($p<0.05$) in the writhing test (Figure 2D). Naloxone has a high affinity to μ-opioid receptors and a lower affinity to κ- and δ-opioid receptors. Importantly, our results extend this observation by showing that the antinociception produced by the extract activates these opioid receptors in the periphery. Reinforcing this, most of the opioid antinociceptive effects are mediated via activation of opioid receptors,[38] and these receptors have been identified on the peripheral terminals of afferent nerves, which can be the sites of intrinsic modulation of nociception.[39] In conclusion, *V. exuberans* might be safe with high potency as a pain reliever since the extract acts as a peripheral opioid agonist by decreasing the excitability of sensory nerves and/or inhibiting proinflammatory neuropeptides based on the chemogenic pain model.

V. exuberans inhibits edema progression via reduced proinflammatory cytokines

The antiinflammatory role of *V. exuberans* was tested using the carrageenan-induced model of acute peripheral inflammation and hyperalgesia. The mechanism of carrageenan induces biphasic inflammation. The initial phase (0-2 h) is primarily mediated via the release of histamine, serotonin, and bradykinin, while the late phase (2.5-6 h) is sustained by infiltration of leukocytes and is mainly attributed to the overproduction of PGs.[40] In our study, the paw edema size showed a rapid increase over the first hour of carrageenan injection ($p<0.05$), presented a small peak at 3 h ($p<0.05$), and progressively persisted until at least 6 h compared to the saline controls (2 h, $p<0.05$; 4-6 h, $p<0.001$) (Figure 3A). Following the carrageenan-induced inflammation, at 6 h, IL-1β and TNF-α, which are important peripheral and spinal hyperalgesic proinflammatory mediators,[41] were significantly increased compared to both the precarrageenan (time 0) ($p<0.05$) and the saline controls ($p<0.05$) (Figure 3B and 3C). In contrast, the low dose of *V. exuberans* did not affect edema size during 0-2 h ($p>0.05$), but significantly weakened the peaked edema at 3 h ($p<0.05$) and showed inhibition in the inflamed paw swellings up to 6 h ($p<0.001$) when compared to those of the rats that received carrageenan (Figure 3A). Furthermore, the extract showed a similar potency in both paw size and cytokine production at 6 h compared to the well-described drug indomethacin at 10 mg/kg[42] ($p>0.05$) (Figure 3B and 3C), whereas the extract had a much stronger effect on paw edema size during 3-5 h ($p<0.05$) (Figure 3A). Finally, at 6 h, *V. exuberans* accelerated recovery in the rat paw size as well as the cytokine productions to near normal levels compared to those of the saline and the precarrageenan controls ($p>0.05$), suggesting thus an antiinflammatory effect.

CONCLUSION

Importantly, our data show for the first time the potential of methanol extract from the aerial parts of *V. exuberans* to relieve pain and inflammation in experimental animals. The plant extract showed a central spinal and a peripheral antinociceptive

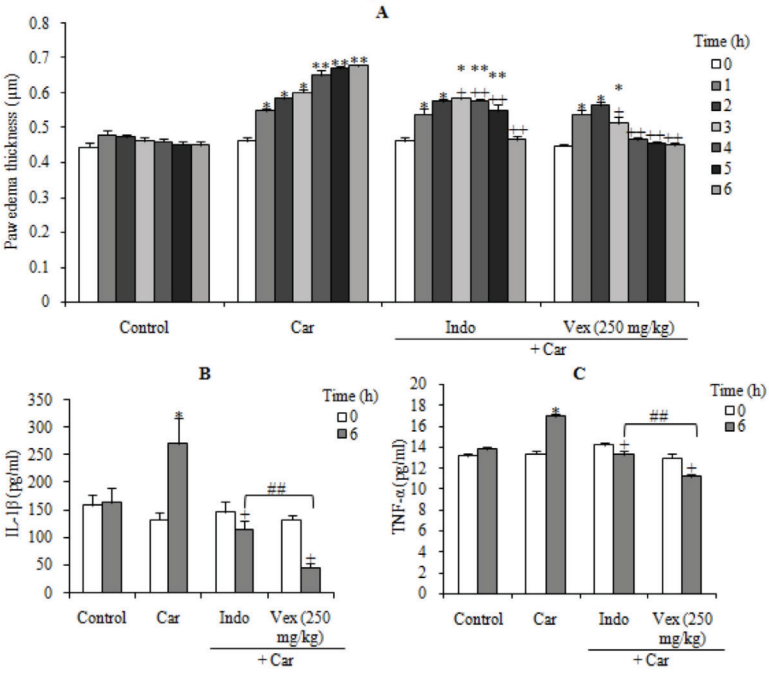

Figure 3. The effects of *V. exuberans* on inflammation (Sprague Dawley rats; each group, n=8; *W*, 240±20 g). The inflammation was induced by carrageenan (100 µL, 1% w/v in saline) into the subplantar surface of right hind paws. The increases in paw thicknesses were considered to be edema and were measured at different time intervals (0-6 h) (A). The proinflammatory cytokine production including IL-1β (B) and TNF-α (C) was measured immediately before the carrageenan injection (0 h) and then after the carrageenan injection solely at 6 h. The values were given as mean ± SEM. *p<0.05 compared to control, **p<0.001 compared to control, +p<0.05 compared to carrageenan, ++p<0.001 compared to carrageenan, ##p<0.001 compared to indomethacin, as determined by two way analysis of variance (one factor repeated) followed by the Tukey test

Car: Carrageenan, Vex: V. exuberans 250 mg/kg, Indo: Indomethacin 10 mg/kg, IL: Interleukin, TNF: Tumor necrosis factor, SEM: Standard error mean

effect as well as antiinflammatory activity. The antinociception induced by the extract is mainly organized via targeting of the nitrergic pathway, while the opioidergic pathway is only peripherally involved. Additionally, the bioactive compounds present in the extract might have a specific effect on the nitrergic pathway. To further understand the mechanism by which *V. exuberans* relieves pain and inflammation, it will be key to isolate and characterize the active agents responsible for the observed pharmacological activities.

ACKNOWLEDGEMENTS

The authors thank Dr. Kamuran Aktaş for collection and authentication of the plant material and Hülya Özen for assistance with the statistical analysis. This work was supported by the Scientific Research Fund of Eskisehir Osmangazi University (grant no: 2013-190), Eskisehir, Turkey.

Conflicts of interest: No conflict of interest was declared by the authors. The authors alone are responsible for the content and writing of the paper.

REFERENCES

1. Goldberg DS, McGee SJ. Pain as a global public health priority. BMC Public Health. 2011;11:770.
2. Pires JM, Mendes FR, Negri G, Duarte-Almeida JM, Carlini EA. Antinociceptive peripheral effect of Achillea millefolium L. and Artemisia vulgaris L.: both plants known popularly by brand names of analgesic drugs. Phytother Res. 2009;23:212-219.
3. Carter GT, Duong V, Ho S, Ngo KC, Greer CL, Weeks DL. Side effects of commonly prescribed analgesic medications. Phys Med Rehabil Clin N Am. 2014;25:457-470.
4. Zulfiker AHM, Mahbubur Rahman MM, Kamal Hossain M, Hamid K, Mazumder MEH, Sohel Rana M. *In vivo* analgesic activity of ethanolic extracts of two medicinal plants-*Scoparia dulcis* L. and *Ficus racemosa* Linn. Biol Med. 2010;2:42-48.
5. Hubert-Morath A. *Verbascum* L. In: Davis PH (ed). Flora of Turkey and the East Aegean Islands 6. Edinburgh; Edinburgh University Press; 1978:461-603.
6. Baytop T. Therapy with Medicinal Plants in Turkey (Past and Present). 2nd ed. İstanbul; Nobel Tip Kitapevleri Ltd; 1999:334.
7. Turker AU, Camper ND. Biological activity of common mullein, a medicinal plant. J Ethnopharmacol. 2002;82:117-125.
8. Turker AU, Gurel E. Common mullein (Verbascum thapsus L.): recent advances in research. Phytother Res. 2005;19:733-739.
9. Tuzlacı E, Erol MK. Turkish folk medicinal plants. Part II: Egirdir (Isparta). Fitoterapia. 1999;70:593-610.
10. Sezik E, Yeşilada E, Honda G, Takaishi Y, Takeda Y, Tanaka T. Traditional medicine in Turkey X. Folk medicine in Central Anatolia. J Ethnopharmacol. 2001;75:95-115.
11. Mükemre M, Behçet L, Çakilcioglu U. Ethnobotanical study on medicinal plants in villages of Çatak (Van-Turkey). J Ethnopharmacol. 2015;166:361-374.
12. Tatli II, Akkol EK, Yesilada E, Akdemir ZS. Antinociceptive and anti-inflammatory activities of seven endemic *Verbascum* species growing in Turkey. Pharm Biol. 2008;46:781-788.
13. Kupeli E, Tatli II, Akdemir ZS, Yesilada E. Bioassay-guided isolation of anti-inflammatory and antinociceptive glycoterpenoids from the flowers of Verbascum lasianthum Boiss. ex Bentham. J Ethnopharmacol. 2007;110:444-450 .
14. Akkol EK, Tatli II, Akdemir ZS. Antinociceptive and anti-inflammatory effects of saponin and iridoid glycosides from Verbascum pterocalycinum var. mutense Hub.-Mor. Z Naturforsch C J Biosci. 2007;62:813-820.
15. Akdemir Z, Kahraman C, Tatlı II, Küpeli Akkol E, Süntar I, Keles H. Bioassay-guided isolation of anti-inflammatory, antinociceptive and wound healer glycosides from the flowers of Verbascum mucronatum Lam. J Ethnopharmacol. 2011;136:436-443.
16. Speranza L, Franceschelli S, Pesce M, Menghini L, Patruno A, Vinciguerra I, De Lutiis MA, Felaco M, Felaco P, Grilli A. Anti-inflammatory properties of the plant *Verbascum mallophorum*. J Biol Regul Homeost Agents. 2009;23:189-195.
17. Dimitrova P, Kostadinova E, Milanova V, Alipieva K, Georgiev M, Ivanovska N. Antiinflammatory properties of extracts and compounds isolated from *Verbascum xanthophoeniceum* Griseb. Phytother Res. 2012;26:1681-1687.

18. Grigore A, Colceru-Mihul S, Litescu S, Panteli M, Rasit I. Correlation between polyphenol content and anti-inflammatory activity of *Verbascum phlomoides* (mullein). Pharm Biol. 2013;51:925-929.

19. Karaveliogullari FA. *Verbascum* L. In: Guner A, Aslan S, Ekim T, Vural M, Babac MT (eds). Turkiye Bitkileri Listesi (Damarli Bitkiler). İstanbul: Nezahat Gökyiğit Botanik Bahçesi ve Flora Araştırmaları Derneği Yayını. 2012;850-870.

20. Bianchi C, Franceschini J. Experimental observations on Haffner's method for testing analgesic drugs. Br J Pharmacol Chemother. 1954;9:280-284.

21. D'Amour FE, Smith DL. A method for determining loss of pain sensation. J Pharmacol Exp Ther. 1941;72:74-79.

22. Eddy NB, Leimbach D. Synthetic analgesics. II. dithienylbutenyl- and dithienylbutylamines. J Pharmacol Exp Ther. 1953;107:385-393.

23. Koster R, Anderson M, De-Beer E. Acetic acid for analgesic screening. Fed Proc. 1959;18:412-418.

24. Winter CA, Risley EA, Nuss GW. Carrageenin-induced edema in hind paw of the rat as an assay for antiinflammatory drugs. Exp Biol Med. 1962;111:544-547.

25. McMahon S, Koltzenburg M, Tracey I, Turk D. Wall and Melzack's Textbook of Pain. Anesthesia Progress. 2013;1-30.

26. Barrot M. Tests and models of nociception and pain in rodents. Neuroscience. 2012;211:39-50.

27. Schmauss C, Yaksh TL. *In vivo* studies on spinal opiate receptor systems mediating antinociception. II. Pharmacological profiles suggesting a differential association of mu, delta and kappa receptors with visceral chemical and cutaneous thermal stimuli in the rat. J Pharmacol Exp Ther. 1984;228:1-12.

28. Deraedt R, Jouquey S, Delevallée F, Flahaut M. Release of prostaglandins E and F in an algogenic reaction and its inhibition. Eur J Pharmacol. 1980;61:17-24.

29. Lee CR, McTavish D, Sorkin EM. Tramadol. A preliminary review of its pharmacodynamic and pharmacokinetic properties, and therapeutic potential in acute and chronic pain states. Drugs. 1993;46:313-340.

30. Dühmke R, Cornblath D, Hollingshead J. Tramadol for neuropathic pain. In: Dühmke RM (ed). Cochrane Database of Systematic Reviews. Chichester; John Wiley & Sons, Ltd; 2004;CD003726.

31. Soares AC, Leite R, Tatsuo MAKF, Duarte IDG. Activation of ATP-sensitive K^+ channels: mechanism of peripheral antinociceptive action of the nitric oxide donor, sodium nitroprusside. Eur J Pharmacol. 2000;400:67-71.

32. Meller ST, Gebhart GF. Nitric oxide (NO) and nociceptive processing in the spinal cord. Pain. 1993;52:127-136.

33. Talarek S, Fidecka S. Role of nitric oxide in benzodiazepines-induced antinociception in mice. Pol J Pharmacol. 2002;54:27-34.

34. Tokunaga A, Saika M, Senba E. $5\text{-}HT_{(2A)}$ receptor subtype is involved in the thermal hyperalgesic mechanism of serotonin in the periphery. Pain. 1998;76:349-355.

35. Bruehl S, Burns JW, Chung OY, Chont M. Pain-related effects of trait anger expression: neural substrates and the role of endogenous opioid mechanisms. Neurosci Biobehav Rev. 2009;33:475-491.

36. Romberg R, Sarton E, Teppema L, Matthes HWD, Kieffer BL, Dahan A. Comparison of morphine-6-glucuronide and morphine on respiratory depressant and antinociceptive responses in wild type and μ-opioid receptor deficient mice. Br J Anaesth. 2003;91:862-870.

37. Schramm CL, Honda CN. Co-administration of δ- and μ-opioid receptor agonists promotes peripheral opioid receptor function. Pain. 2010;151:763-770.

38. Stein C, Lang LJ. Peripheral mechanisms of opioid analgesia. Curr Opin Pharmacol. 2009;9:3-8.

39. Vadivelu N, Mitra S, Hines RL. Peripheral opioid receptor agonists for analgesia: a comprehensive review. J Opioid Manag. 2011;7:55-68.

40. Posadas I, Bucci M, Roviezzo F, Rossi A, Parente L, Sautebin L, Cirino G. Carrageenan-induced mouse paw oedema is biphasic, age-weight dependent and displays differential nitric oxide cyclooxygenase-2 expression. Br J Pharmacol. 2004;331:318-331.

41. Verri WA, Cunha TM, Parada CA, Poole S, Cunha FQ, Ferreira SH. Hypernociceptive role of cytokines and chemokines: targets for analgesic drug development? Pharmacol Ther. 2006;112:116-138.

42. Ong CKS, Lirk P, Tan CH, Seymour RA. An evidence-based update on nonsteroidal anti-inflammatory drugs. Clin Med Res. 2007;5:19-34.

Turk J Pharm Sci 2020;17(6):593-598
DOI: 10.4274/tjps.galenos.2019.71542

ORIGINAL ARTICLE

Development of a New Approach for Standardization of the Herb *Centaurium erythraea* Rafn. by High Performance Liquid Chromatography

Centaurium erythraea Rafn. Bitkisinin Yüksek Basınçlı Sıvı Kromatografisi Yöntemi ile Standardizasyonu İçin Yeni Bir Yaklaşımın Geliştirilmesi

Svitlana M. GUBAR[1], Anna S. MATERIIENKO[2]*, Nataliia M. SMIELOVA[1], Liana G. BUDANOVA[3], Victoriya A. GEORGIYANTS[1]

[1]National University of Pharmacy, Department of Pharmaceutical Chemistry, Kharkiv, Ukraine
[2]National University of Pharmacy, Department of Quality, Standardization and Certification of Medicines, Kharkiv, Ukraine
[3]National University of Pharmacy, Department of Foreign Languages, Kharkiv, Ukraine

ABSTRACT

Objectives: The aim of this study was the development a new, fully validated high performance liquid chromatography (HPLC) method for the quantitative analysis of secoiridoid glycosides by an active marker swertiamarin in the herb *Centaurium erythraea* Rafn. The article describes a new approach to the standardization of *C. erythraea* and more specifically the development of a new validated HPLC method for the quantitative determination of secoiridoid glycosides by swertiamarin.

Materials and Methods: The quantitative determination of swertiamarin was performed in isocratic mode on a Symmetry C18 column using water and acetonitrile as solvents for the mobile phase.

Results: Validation characteristics of the developed method showed that it was linear in the whole range of concentrations from 0.01 mg/mL to 0.05 mg/mL swertiamarin. All validation characteristics met the established acceptance criteria.

Conclusion: This method can be used in the standardization of raw materials, as well as in the analysis of medicinal products and dietary supplements that include *C. erythraea*. The established chromatographic method was successfully applied for the analysis of raw materials of *C. erythraea* with the quantitative content determination of swertiamarin in the analyzed samples.

Key words: Common centaury herb, method development, HPLC, swertiamarin, validation

ÖZ

Amaç: Bu çalışmanın amacı, *Centaurium erythraea* Rafn. bitkisinde bulunan sekoiridoidleri glikozitlerinin aktif göstergesi olan swertiamarinin yeni, tam valide bir yüksek basınçlı sıvı kromatografisi (HPLC) yöntemiyle kantitatif analizidir. Bu makale *C. erythraea*'nın standardizasyonunu ve daha spesifik olarak da swertiamarin ile sekoiridoid glikozitlerini yeni valide HPLC yöntemi geliştirerek kantitatif olarak belirlenmesinden söz etmektedir.

Gereç ve Yöntemler: Swertiamarinin kantitatif belirlenmesi mobil faz için su ve asetonitril kullanılarak bir Symmetry C18 kolonu üzerinde izokratik modda yapılmıştır.

Bulgular: Geliştirilen yöntemin validasyon karakteristikleri 0,01 mg/mL swertiamarinden 0,05 mg/mL swertiamarine dek olan geniş bir konsantrasyon aralığında yöntemin doğrusal olduğunu göstermiştir. Tüm validasyon karakteristikleri kabul edilebilir kriterlere uymuştur.

Sonuç: Bu yöntem, *C. erythraea* içeren hammadde ve medisinal ürünler ve diyetsel suplemanların analizinde standardizasyon için kullanılabilir. Bu kromatografik yöntem analiz edilen *C. erythraea*'nın hammaddelerine swertiamarinin kalitatif içeriğini başarılı bir şekilde belirlenmesi için uygulanmıştır.

Anahtar kelimeler: Kantaron bitkisi, yöntem geliştirme, HPLC, swertiamarin, validasyon

*Correspondence: **E-mail:** anna.materienko@gmail.com, **Phone:** +380971142384 **ORCID-ID:** orcid.org/0000-0003-4184-2944
Received: 24.05.2019, **Accepted:** 17.10.2019

INTRODUCTION

Centaurium erythraea Rafn. is a valuable source of various biologically active compounds (BACs), including bitters.[1] Due to the presence of this particular group of BACs, the plant is widely used to treat diseases of the gastrointestinal tract and is included in the composition of drugs and dietary supplements.[2] The main representatives of secoiridoid glycosides, which determine the pharmacological action of this raw material, are swertiamarin, sweroside, and gentiopicroside (Figure 1).

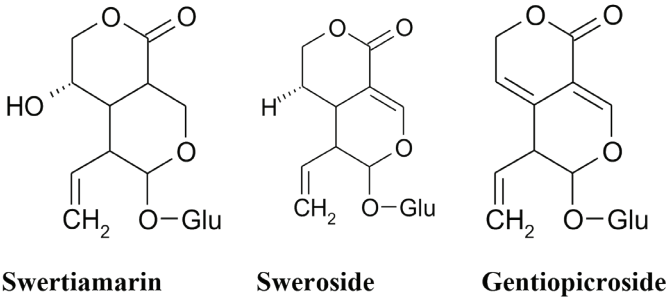

Figure 1. Structural formulas of secoiridoid glycosides of centaury

Bitters improve intestinal motility, increase the reduced secretory function of the stomach, and are used in the treatment of hypoacidic and chronic atrophic gastritis as well. In addition, secoiridoid glycosides show anti-inflammatory and antibacterial activity.[3]

The results of studies on the biological action of a secoiridoid glycoside of centaury, namely swertiamarin, are widely described in the literature. It has antihyperlipidemic,[4] hypoglycemic,[5] insulinotropic,[6,7] and antinociceptive[8] actions. In addition, swertiamarin exhibits an anticholinergic effect[9] and depressant effect, inhibits human DNA lipase, and has a central nervous system depressant effect[10] as well as inhibiting the growth of *Bacillus cereus*, *Bacillus subtilis*, *Citrobacter freundii*, *Escherichia coli*, *Proteus mirabilis*, and *Serratia marcescens*.[2]

It is important to mention that there are only a few publications regarding the description of the methods of *C. erythraea* analysis. Kaluzova et al.[11] described the analysis of gentiopicroside by high performance liquid chromatography (HPLC) in *C. erythraea*. Valentao et al.[12] analyzed xanthones (validation is not described). Glatz et al.[13] described the method for determining gentiopicroside in extracts of *C. erythraea* using micellar electrokinetic capillary chromatography, and Nikolova-Damyanova and Handjieva[14] carried out a quantitative determination of swertiamarin and gentiopicroside using the densitometric method.

In the European Pharmacopoeia, there are no methods for the quantitative analysis of secoiridoid glycosides in this raw material.[15] In the article on centaury for the quantitative evaluation of raw materials it is suggested to use the pharmacognosy method "Bitterness value", an organoleptic method of determination, which is based on the individual sensitivity of taste receptors and the subjective assessment of each expert.

The rate of bitterness represents the reciprocal dilution of the mixture, liquid, or extract, which still has a bitter taste. This indicator is determined by comparison with quinine hydrochloride, whose rate of bitterness is 200,000 (Eur.Ph. 2.8.15). This method is characterized by great subjectivity and high inaccuracy of determination, which means it is not recommended for the analysis of raw materials in modern conditions.

In the literature it is also stated that secoiridoid glycosides have different values of bitterness.[15] It is proved that swertiamarin is not the most bitter of them, and such a method, as a bitterness value, does not allow the objective evaluation of the content of swertiamarin in raw materials.

The European Pharmacopoeia[16] suggests the use of swertiamarin as a marker compound during the test "Identification" by the thin-layer chromatography method. Based on this, as well as on the results of the study of its biological activity, we suggested choosing swertiamarin as an active marker in the development of methods for standardization of *C. erythraea*.

The literature describes approaches for the quantitative determination of swertiamarin in other types of raw materials, such as its estimation in *Enicostemma littorale*[17] and its analysis in different *Swertia* species.[18] When developing the methodology, all the described approaches to the analysis of swertiamarin were studied and a new selective, sensitive, and accurate HPLC method for its quantitative determination in *C. erythraea* was developed. The most optimal conditions for the quantitative analysis of swertiamarin in the common centaury herb by the HPLC method are proposed: isocratic elution mode and more acceptable chromatographic time, based on the characteristics of this raw material in order to ensure maximum specificity (exclusion of influence on the analysis of ballast substances and other BAS groups of this raw material).

During the course of the experiment, a new, fully validated method was developed for the quantitative analysis of secoiridoid glycosides by the active marker swertiamarin in *C. erythraea* by HPLC method. This method can be used in the standardization of raw materials, as well as in the analysis of medicinal products and dietary supplements that include *C. erythraea*.

MATERIALS AND METHODS

HPLC

Quantitative analysis of swertiamarin in *C. erythraea* was carried out on a ProStar liquid chromatograph equipped with an autosampler 410 and two detectors, spectrophotometric PDA 325 and photodiode array detector PDA 330, made by Varian (USA). A Symmetry C18 column (150x4.6 mm, particle size 3.5 µm) with a precolumn was also used. A mixture of water and acetonitrile at the ratio of 91:9 was used as the mobile phase. The separation was carried out in isocratic mode. The flow rate of the mobile phase was 1 mL/min, the injection volume was 20 µL, the detection was carried out at a wavelength of 238 nm, and the column temperature was 40°C.

The sampling was carried out on an analytical balance, Ohaus Adventurer brand AR2140 (USA), by standard procedure for raw materials, according to the European Pharmacopoeia (Eur. Ph. 2.9.12). During the sample preparation, the following items were also used: a 355 sieve (SL-200) and a medical laboratory centrifuge with a rotor RU-180 OPN-12 "OAO TNK DASTAN".

Raw materials and reagents

To conduct the research, 20 series of *C. erythraea* plants were collected in various regions of Ukraine during the flowering period. Macroscopic and microscopic identification of raw materials was carried out at the Department of Botany of the National University of Pharmacy, Ukraine. The plant species were deposited in the herbarium section of the same department (code - BDC 12703).

The following reagents were used: acetonitrile (Sigma Aldrich, gradient grade, for HPLC), methanol (Sigma Aldrich, gradient grade, for HPLC), and water for chromatography (Millipore). A standard sample of swertiamarin (purity 99.5%), series OS10475 (Carbosynth, UK), was also used.

Solutions for the analysis were prepared according to the following methods:

Test solution: 0.500 g (accurately weighed) of the powdered raw material (355 μm, Eur.Ph. 2.9.12) was supplemented with 20 mL of methanol, shaken for 15 min, and centrifuged and the supernatant was removed into a 50-mL volumetric flask. The extraction was repeated with a further 20 mL of methanol, with collection of the supernatant as before. The volume of the solution was made up to the mark with methanol and mixed. Then 10 mL of the obtained solution was diluted to 50 mL with water. The solution was filtered through a 0.45 μm membrane filter.

Reference solution: 0.010 g of swertiamarin (accurately weighed) was placed into a 100 mL volumetric flask, dissolved in 50 mL of methanol, and then the volume was made up to the mark with the same solvent and mixed. Then 10 mL of the obtained solution was diluted to 50 mL with water, mixed, and filtered through a 0.45 μm membrane filter.

Validation

Validation of the developed method was carried out in accordance with the recommendations of the ICH,[19] the requirements of article 2.2.N.2 of SPhU,[20] and the standard procedure of quantitative methods validation using an external standard by studying its linearity, as well as its accuracy, robustness, and precision.

To study the specificity, the following solutions were prepared: a blank solution, a reference solution (a solution of a standard sample of swertiamarin), and a test solution.

To confirm the linearity of the method, five model solutions were prepared, the concentration of which varied uniformly within the application range to the extent of 50-250% (step 50%).

To determine the accuracy and precision within the range of use of the analytical method, five test solutions were prepared, in compliance with all the stages of the analytical procedure. The concentration of swertiamarin in the prepared solutions ranged from 0.01 mg/mL to 0.05 mg/mL.

In order to determine the intra-laboratorial precision, one sample was examined six times by two analysts on different days during one working week using various measuring glassware.

Statistical analysis

The analytical performance of the HPLC method was verified for compliance with the requirements. All tests were performed on three replicate injections and standard deviations for each analysis were calculated.

RESULTS AND DISCUSSION

Analysis of medicinal plant raw materials

An HPLC method was developed for analyzing the quality control of the medicinal plant raw material, *C. erythraea*. Swertiamarin was chosen as the active marker. It is suggested for the standardization of the raw material, as it was previously established that centaury contained the highest amount of swertiamarin and other secoiridoid glycosides, such as sweroside and gentiopicroside, in smaller amounts.[21]

The HPLC method for analyzing secoiridoid glycosides in centaury was developed on the basis of the State Research Laboratory for Quality Control of Medicines of the NUPh.

The results of quantitative determination of the swertiamarin content in the analyzed samples of the medicinal plant raw materials are shown in Table 1.

Statistical analysis

Method validation

When choosing the criterion for rationing the quantitative content of swertiamarin in the centaury, we used the results of the analysis of the raw materials for all indicators applicable to medicinal plant raw materials. It was found that the raw materials, in which the content of swertiamarin was less than 3%, did not meet the requirements of the Pharmacopoeia for such parameters as "foreign matter" and "total ash". On this basis, the quantitative content of swertiamarin in the centaury was not less than 3% in terms of dried raw materials. The results obtained during the analysis showed that 15 series of raw materials met these requirements.

The total uncertainty of the developed method was calculated, which in this case is related to the limits of the analyte content in the medicinal plant raw materials. For the centaury, the established content of swertiamarin is normalized at a level of at least 3%. In accordance with the requirements of SPhU 2.0 for quantitative determination (one-sided rationing "no more"), the maximum permissible total uncertainty of the analysis method is $max\ \Delta_{AS}$ ‹6.4%.[17]

The criterion of insignificance compared with the maximum permissible uncertainty of the results is ($\Delta_{AS,\ insig}$): $\Delta_{AS,\ insig} \leq max\Delta_{AS}$, %*0.32=6.4% *0.32=2.048%.

Table 1. The results of experimental studies of the swertiamarin content in centaury by HPLC method

No series	The region of collection of raw materials	Quantitative content of swertiamarin, %
1	2	3
1	Dnipropetrovsk region	3.6
2	Dnipropetrovsk region	3.9
3	Dnipropetrovsk region	1.7
4	Ivano-Frankivsk region	7.7
5	Kharkov region	4.5
6	Kharkov region	6.4
7	Kharkov region	2.8
8	Kiev region	8.3
9	Lviv region	7.3
10	Lviv region	4.8
11	Lviv region	2.4
12	Poltava region	6.6
13	Poltava region	7.1
14	Poltava region	1.5
15	Rovenskaya region	9.1
16	Sumy region	7.8
17	Sumy region	8.4
18	Sumy region	2.2
19	Volyn region	7.8
20	Volyn region	6.0

HPLC: High performance liquid chromatography

The calculation of the uncertainty of the final analytical operation Δ_{FAO} was carried out for the test solution and the reference solution. When calculating the intervals, Student's one-sided coefficient was used for a probability of 95% and the corresponding number of freedom degrees. Confidence intervals for the reference solution and the testing solution were calculated for an average of five results.

According to the requirements of suitability of the chromatographic system in the determination procedure, the relative standard deviation for five parallel determinations should be no more than 2.0%.

When n=5, t (95%, n-1)=2.1318:

$$\Delta^{cm}_{FAO} = \frac{1}{\sqrt{5}} * 2.1318 * 2.0\% = 1{,}907\% \quad \Delta^{smp}_{FAO} = \frac{1}{\sqrt{5}} * 2.1318 * 2.0\% = 1.907\%$$

The total uncertainty of the final analytical operation:

$$\Delta^{cm}_{FAO} = \sqrt{(\Delta^{smp}_{FAO})^2 + (\Delta^{cm}_{FAO})^2} = 2.70\%$$

Complete uncertainty of the analysis techniques Δ_{AS}%:

$$\Delta_{AS} = \sqrt{(\Delta_{sp})^2 + (\Delta_{FAO})^2} = 3.39\%$$

Thus, the calculated total uncertainty of the analysis Δ_{AS}% is less than max Δ_{AS} (3.39% < max Δ_{AS}=6.4%), which meets the requirements for this parameter.

Specificity

Under the conditions of the developed method, the determination of the active substance of swertiamarin was not interfered with by the solvent or the mobile phase, or other co-eluting impurities from the raw material at a detection wavelength of 238 nm, which indicates the specificity of the developed method.

Chromatograms of the blank solution, the test solution, and the reference solution are shown in Figure 2 in order to confirm the specificity of the method.

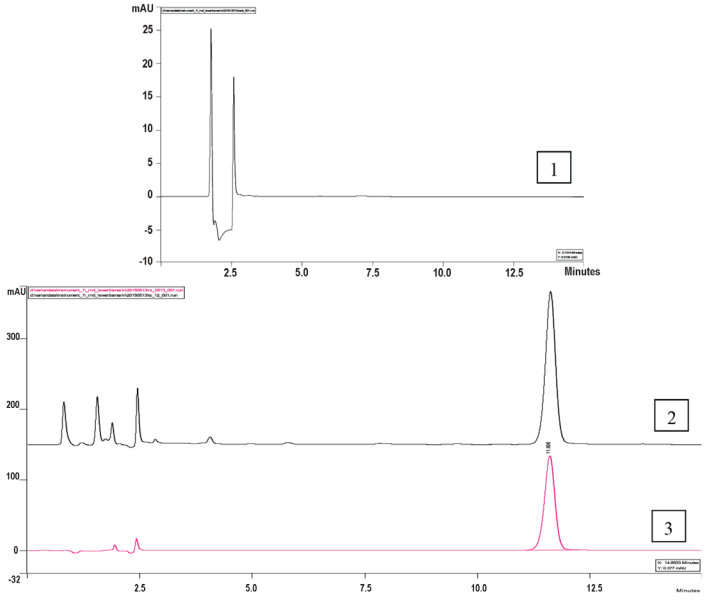

Figure 2. Chromatograms of the blank solution 1), the test solution 2), and reference solution 3)

Linearity

The method of quantification must be linear within the application range and must cover the possible values of the active substance concentrations. According to the requirements of the State Pharmacopoeia of Ukraine, the application range of the method of quantitative determination of swertiamarin in the medicinal plant raw materials must be from 50% to 250%.

Chromatograms of the solutions studied are shown in Figure 3.

The linearity curve is presented in Figure 4.

The linearity parameters, which are presented in Table 2, indicate the linearity of the method within the test range.

The results obtained confirm that the method developed for the quantitative determination of swertiamarin by HPLC in the concentration range from 0.01 mg/mL to 0.05 mg/mL is linear.

Accuracy, precision, and intermediate precision

Accuracy is characterized by two criteria:

- Criterion of statistical insignificance: $\delta\% = | Z - 100 \leq \frac{\Delta z}{\sqrt{5}} |$

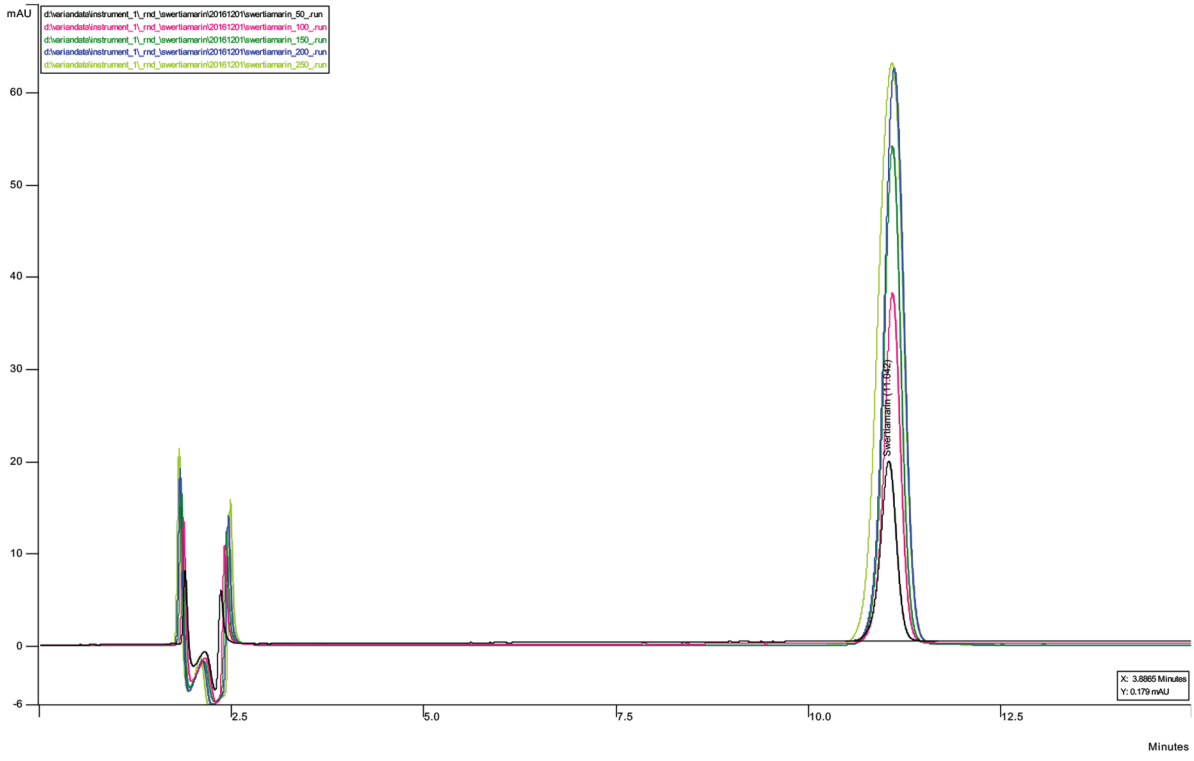

Figure 3. Chromatogram of swertiamarin solutions for linearity determination in the concentration range from 0.01 mg/mL to 0.05 mg/mL

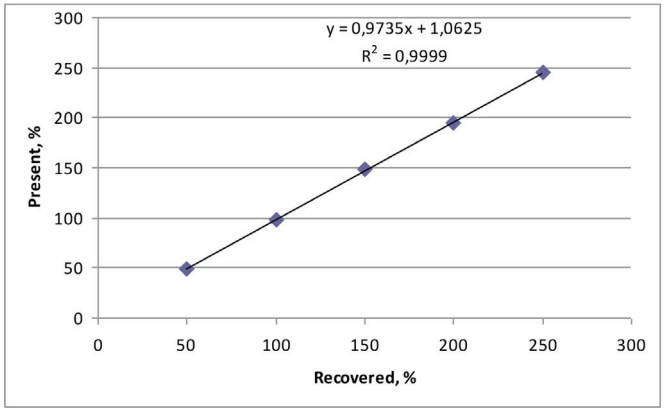

Figure 4. The linearity curve of swertiamarin concentration by HPLC method

HPLC: High performance liquid chromatography

δ% - criterion of practical insignificance - in the case the above ratio is not satisfied, we must use the criterion of insignificance of this systematic error compared with the maximum allowable uncertainty of the analysis:

$$\left|\bar{Z} - 100\right| \le \Delta_{AS,\ in\ sin\ g} = 2.048\%$$

The fulfillments of the criteria of accuracy, precision, and intermediate precision for determining swertiamarin in the common centaury herb by HPLC are given in Table 3.

The method of determining swertiamarin in centaury satisfies the criteria for acceptability of the validity indicators accuracy, precision, and intermediate precision.

Table 2. The linearity parameters of the quantitative determination method

No	Parameter	Requirements	Received value	Criterion fulfillment
1	|a|	≤5.1	1.0625	Performing
2	S_0	≤3.4	0.67	Performing
3	r	›0.9691	0.9999	Performing

Table 3. The results of the evaluation of the accuracy, precision, and intermediate precision of the HPLC method

Parameter	Index	Criterion		Criterion fulfillment
		Requirements for statistical insignificance	Requirements for practical insignificance	
|Z̄-100|	1.73	≤0.64%	≤2.048%	Performing by the second criteria
ΔZ	1.428	≤6.4%		Performing
Δintra	1.22	≤6.4%		Performing

Stability

The study of the stability of the reference solution was carried out immediately after the preparation and 12 h and 24 h later. The results are presented in Table 4.

Differences between the obtained values of the swertiamarin content must not exceed the criterion of insignificance in comparison with the maximum permissible uncertainty of the analysis results ($\Delta_{AS,\ insig}$), that is 2.048%. According to the results of the determination, for optimal chromatographic

conditions it is necessary to use a freshly prepared comparison solution within 12 h, which means in one working day.

Table 4. Determination of the stability of analytical solutions over time

No model solution	Parameter change, %	
	12 h later	24 h later
1	1.0214	6.1820
2	1.0296	5.8819
3	1.0762	6.4831
4	1.1395	6.1431
5	1.6306	6.3427
Δ_{ser}	1.18	6.21

CONCLUSION

This article presents a new method for the quantitative determination of swertiamarin as an active marker for the standardization of raw materials, i.e. *C. erythraea*. The method developed was fully validated and can be used to control the quality of both the raw material (*C. erythraea*) and in the analysis of medicinal products and dietary additives that include this plant.

Conflicts of interest: No conflict of interest was declared by the authors. The authors alone are responsible for the content and writing of the paper.

REFERENCES

1. European Medicines Agency (EMA), Assessment report on Centaurium erythraea Rafn. s.l. including C. majus (H. et L.) Zeltner and C. suffruticosum (Griseb.) Ronn., herba, for the development of a community herbal monograph, Doc. Ref.: EMA/HMPC/105535/2008, 2009. Available from: https://www.ema.europa.eu/en/documents/herbal-report/superseded-assessment-report-centaurium-erythraea-rafn-s-l-including-c-majus-h-et-l-zeltner-c_en.pdf
2. Kumarasamy Y, Nahar L, Cox PJ, Jaspars M, Sarker SD. Bioactivity of secoiridoid glycosides from Centaurium erythraea. Phytomedicine. 2003;10:344.
3. Tuluce Y, Ozkol H, Koyuncu I,Ine H. Gastroprotective effect of small centaury (Centaurium erythraea L) on aspirin-induced gastric damage in rats. Toxicol Ind Health. 2011;27:760-768.
4. Vaidya H, Rajani M, Sudarsanam V, Padh H, Goyal R. Swertiamarin: A lead from Enicostemma littorale Blume. for anti-hyperlipidaemic effect. Eur J Pharmacol. 2009;617:108-112.
5. Patel MB, Mishra SH. Hypoglycemic activity of C-glycosyl flavonoid from Enicostemma hyssopifolium. Pharml Biol. 2011;49:383-391.
6. Vaidya H, Prajapati A, Rajani M, Sudarsanam, V, Padh H, Goyal RK. Beneficial Effects of Swertiamarin on Dyslipidaemia in Streptozotocin-induced Type 2 Diabetic Rats. Phytotherapy Research. 2012;26:1259-1261.
7. Sonawane RD, Vishwakarma SL, Lakshmi S, Rajani M, Padh H, Goyal RK. Amelioration of STZ-induced type 1 diabetic nephropathy by aqueous extract of Enicostemma littorale Blume and swertiamarin in rats. Mol Cell Biochem. 2010;340:1-6.
8. Jaishree V, Badami S. Antioxidant and hepatoprotective effect of swertiamarin from Enicostemma axillare against D-galactosamine induced acute liver damage in rats. J Ethnopharmacol. 2010;130:103-106.
9. Yamahara J, Kobayashi M, Matsuda H, Akoi S. Anti-cholinergic action of Swertia japonica and an active constituent. J Ethnopharmcol. 1991;3:31-36.
10. Bhattacharya SK, Reddy PK, Ghosal S, Singh AK, Sharma PV. Chemical constituents of Gentinaceae XIX: CNS-depressant effects of swertiamarin. J Pharm Sci. 1976;65:1547-1549.
11. Kaluzova L, Glatz Z, Pospisilova J, Musil P, Unar J. Determination of gentiopicroside in Centaurium erythraea by high-performance liquid chromatography. Cesk Farm. 1995;44:203-205.
12. Valentao P, Andrade PB, Silva E, Vicente A, Santos H, Bastos ML, R.M. Seabra, Methoxylated xanthones in the quality control of small centaury (Centaurium erythraea) flowering tops. J. Agric. Food Chem. 2002;50:460-463.
13. Glatz Z, Pospísilová J, Musil P. Determination of gentiopicroside in extracts of Centaurium erythreae and Gentiana lutea by micellar electrokinetic capillary chromatography. J Liq Chromatogr Relat Technol. 2000;23:1831-1839.
14. Nikolova-Damyanova, B, Handjieva N. Quantitative determination of swertiamarin and gentiopicroside in Centaurium erythrea and C. turcicum by densitometry. Phytochemical Analysis. 1996;7:140-142.
15. Sharma Manish K, Mukesh B. Significance of Plant Bitters In The Field of Pharmacognosy. AJPTI. 2013; 01-14.
16. European Pharmacopoeia. 9th ed. Strasbourg: European Directorate for the Quality of Medicines Health Care, 2017. Available from: https://www.edqm.eu/
17. Alam P, Ali M, Singh R, Shakeel F. Estimation of swertiamarin in Enicostemma littorale and marketed formulations using HPLC-UV Method. Journal of Bioanalysis and Biomedicine. 2009;1:22-27.
18. Kshirsagar PR, Pai SR, Nimbalkar MS, Gaikwad NB. RP-HPLC analysis of seco-iridoid glycoside swertiamarin from different Swertia species. Natural product research. 2016;30:865-868.
19. ICH harmonised tripartite guideline Q2(R1). Validation of analytical procedures: text and methodology Q2(R1)," in Proceedings of the International Conference on Harmonization of Technical Requirements for Registration of Pharmaceuticals for Human Use, Geneva, Switzerland, 2005.
20. State Pharmacopoeia of Ukraine: in 3 volumes. Kharkiv: State enterprise "Ukrainian scientific pharmacopoeial center of medicines quality", 2nd ed. Vol. 3., 2014.
21. Gubar S, Materiienko A, Georgiyants V, Vasylieva O, Ivanauskas L. Comparative analysis of the qualitative composition of secoiridoid glycosides in Centaurium erythraea Rafn. and Centaurium pulchellum (Sw) Druce herbs. The 9th International Conference on Pharmaceutical Sciences and Pharmacy Practice, 2018;66. Available from: https://lsmuni.lt/media/dynamic/files/16960/9thconference_science_practice_1final.pdf

Turk J Pharm Sci 2020;17(6):599-609
DOI: 10.4274/tjps.galenos.2019.10846

ORIGINAL ARTICLE

Phytobiological-facilitated Production of Silver Nanoparticles From Selected Non-cultivated Vegetables in Nigeria and Their Biological Potential

Nijerya'da İşlenmemiş Sebzelerden Fitobiyolojikler ile Kolaylaştırılmış Gümüş Nanopartiküllerinin Üretimi ve Biyolojik Potansiyelleri

Oluwasesan M. BELLO[1]*, Olubunmi Stephen OGUNTOYE[1], Adewumi Oluwasogo DADA[2], Oluwatoyin E. BELLO[3], Tijjani ALI[4], Ahmad Abdullahi ALHAJI[4], Oluwatosin ADENIYI[4]

[1]University of Ilorin, Department of Chemistry, Ilorin, Kwara State, Nigeria
[2]University of Ilorin, Department of Crop Protection, Ilorin, Kwara State, Nigeria
[3]Landmark University Nanotechnology Laboratory, Department of Physical Sciences, Industrial Chemistry Programme, Omu Aran, Kwara State, Nigeria
[4]Federal University Dutsin-Ma, Department of Applied Chemistry, Dutsin-Ma, Katsina State, Nigeria

ABSTRACT

Objectives: Plant-mediated synthesis [silver (Ag) to form Ag nanoparticles (AgNPs)] is becoming progressively well accepted in many scientific and pharmaceutical fields. The aim of this study was to synthesize AgNPs using air-dried leaves of four neglected vegetables, i.e. *Ceratotheca sesamoides, Ceiba pentandra, Crassocephalum crepidioides,* and *Launaea taraxacifolia.*

Materials and Methods: Ultraviolet-visible (UV-Vis) spectroscopy, fourier transform infrared (FTIR) spectroscopy, and scanning electron microscopy (SEM) were used for characterization. Cell stabilization membrane and lipoxidase assays were used to determine used to assess the antiinflammatory activities while 2,2-diphenyl-1-picryl-hydrazyl-hydrate (DPPH) and 2,2'-azinobis(3-ethylbenzothiazoline-6-sulfonic acid (ABTS+) assays were used to assess the antioxidant activities of AgNPs [*L. taraxacifolia*-AgNPs, *C. sesamoides* Ag nanoparticles (CS-AgNPs), *C. pentandra* Ag nanoparticles (CP-AgNPs), and *C. crepidioides* AgNPs (CC-AgNPs)].

Results: The UV-Vis spectra of the synthesized NPs displayed absorption bands at around 360-440 nm, which is a characteristic band for AgNPs. The SEM image showed that the AgNPs formed were spherical in morphology. CC-AgNPs exhibited the most significant inhibitory activity against human red blood cell membrane stabilizasyonu [median inhibitory concentration (IC_{50}): 32.2 µg/mL] while CS-AgNPs displayed the most significant inhibitory activity against lipoxygenases (IC_{50}: 32.8 µg/mL). CP-AgNPs exhibited the most significant antioxidant effect against both ABTS and DPPH (IC_{50}: 5.5 and 6.4 µg/mL) when compared to ascorbic acid (IC_{50}: 4.7 µg/mL).

Conclusion: The synthesized AgNPs were found to be stable and the FTIR evidence suggested that the phytochemicals in the vegetables might have played an important role in the reduction and stabilization of AgNPs. This work showed that the synthesized AgNPs from non-cultivated vegetables can find relevance and application in health, drugs, food and environmental science. The evidences herein further confirmed their ethnopharmacological applications.

Key words: AgNPs, antiinflammatory, antioxidant, non-cultivated vegetables, nanoparticles

ÖZ

Amaç: Bitkiler aracılıklı sentez [gümüş nanopartikülleri (AgNP) oluşturmak için gümüş (Ag)] birçok bilimsel ve farmasötik alanda artan bir şekilde kabul görlmektedir. Bu çalışmanın amacı havada kurutulmuş işlem görmemiş sebze (*Ceratotheca sesamoides, Ceiba pentandra, Crassocephalum crepidioides* ve *Launaea taraxacifolia*) yapraklarını kullanarak AgNP'lerinin sentezidir.

Gereç ve Yöntemler: Karakterizasyon için ultraviyole-görünür bölge (UV-Vis) spektroskopisi, fourier transforme kızılötesi (FTIR) spektroskopisi ve taramali elketron mikroskopisi (SEM) kullanılmıştır. AgNP'lerin [*L. taraxacifolia*-AgNP'ler, *C. sesamoides* Ag nanopartikülleri (CS-AgNPs), *C. pentandra* Ag nanopartikülleri (CP-AgNP) ve *C. crepidioides* Ag nanopartikülleri (CC-AgNP)] antienflamatuvar aktivitesini belirlemek için hücre stabilizasyon membranı ve lipoksidaz yöntemleri kullanılırken antioksidan aktivitelerini değerlendirmek için 2,2-difenil-1-pikrilhidrazil hidrat (DPPH) ve 2,2'-azinobis(3-etilbenzotiyazolin-6-sulfonik asit (ABTS+) yöntemleri için kullanılmıştır.

*Correspondence: E-mail: obello@fudutsinma.edu.ng, Phone: +2348062320327 ORCID-ID: orcid.org/0000-0003-1431-7319
Received: 06.06.2019, Accepted: 19.09.2019

Bulgular: Sentez edilen NP'lerin UV-Vis spektrumları AgNP'leri için karakteristik bir bant olan 360-440 nm arasında absorpsiyon bantları göstermiştir. SEM görüntüleri AgNP'lerin küresel morfolojilerinin olduğunu göstermiştir. CC-AgNP'ler insan kırmızı kan hücresi membrane stabilizasyonu [medyan inhibitor konsantrasyon (IC_{50}): 32,2 µg/mL] için en yüksek inhibitor etkiyi gösterirken, CS-AgNP'leri lipoksijenazlara karşı en belirgin inhibitor etkiyi göstermiştir (IC_{50}: 32,8 µg/mL). CP-AgNP'leri hem ABTS+ hem de DPPH için (IC_{50}: 5,5 µg/mL ve 6,4 µg/mL) askorbik asitle karşılaştırıldığında (IC_{50}: 4,7 µg/mL) en belirgin antioksidan etki göstermişlerdir.

Sonuç: Sentez edilen AgNP'ler stabil bulunmuştur ve FTIR verileri sebzelerdeki fitokimyasalların AgNP'lerin redüksiyonunda ve stablizasyonunda önemli rol oynadıklarını göstermiiştir. Bu çalışma ilenmemiş bitkilerden sentez edilen AgNP'lerin sağlık, ilaç, gıda ve çevresel bilimlerde ilgi ve uygulama alanı bulabileceğini göstermiştir. Buradaki bilgiler etenoparmakolojik uygulamalarını onaylamıştır.

Anahtar kelimeler: AgNP'ler, antienflamatuvar, antioksidan, işlem görmemiş sebzeler, nanopartiküller

INTRODUCTION

For centuries, cultures around the world have continuously employed and taken advantage of edible but non-cultivated plants for sufficient nutrition, food security, and wealth creation.[1-3] These non-cultivated plants supply necessary and essential components of the human diet, supplying the body with various minerals, protein, and certain precursors of human hormones besides helping in the build-up of energy.[4-6]

Some of the plants studied here are non-cultivated due to their being tagged as "poor man's" vegetables but are eaten by the locals. *Ceratotheca sesamoides*[7] belongs to the family Pedaliaceae. It is mostly found in Africa and it grows as a wild and non-cultivated plant. However, in some parts of Africa, it is being cultivated, and because of its similarities with common sesame (*Sesamum indicum*), some call it false sesame.[8,9] Although widely regarded as a delicacy in most West African countries, literature on this plant and its consumption is scanty and not sufficient.[10] *C. sesamoides* is traditionally employed in the management of diarrhea in Nigeria. The plant is used as an aphrodisiac and in the treatment of jaundice, snake bites, and skin ailments. *C. sesamoides* leaf infusions are used to facilitate delivery in both humans and animals.[10-13] In northern Nigeria, *C. sesamoides* seeds are used to relieve circumcision pains.

Ceiba pentandra belongs to the family Malvaceae.[7] It is native to the Caribbean, Central America, northern South America, Mexico, and tropical West Africa. Besides its young leaves' nutritional benefits, in Nigeria many locals use its leaves for treating many ailments. This plant has many ethnobotanical uses (Table 1), i.e. to treat headache and diabetes and as a diuretic and aphrodisiac. Its use as one of the main ingredients in a hallucinogenic drink has also been reported.[14,15]

Crassocephalum crepidioides[7] is also called thickhead, fireweed, Okinawa spinach, and red flower ragleaf in English, Ebolo, or Ebire (Yoruba) in Nigeria. Its use is widespread in many tropical and subtropical regions, but is especially prominent in tropical Africa. It has also been widely cultivated in Asia due to its medicinal and nutritional properties.[16,17] In southern Nigeria, *C. crepidioides*' leaves have been reported to be valuable in the management of indigestion, stomach ache, and fresh wounds (in Uganda) and its leaves' decoction is employed in Nigeria against headache (Table 1). In Tanzania, a mixture of the leaf sap of *C. crepidioides* and *Cymbopogon giganteus* is taken by mouth against epilepsy. Its dried leaves are used to stop nose bleeds and aid in sleeping.[18]

Launaea taraxacifolia (synonymous to *Lactuca taraxacifolia*)[7] is a greenish leafy vegetable that is mainly eaten in the western part of Nigeria. This vegetable is eaten in most countries in Africa either cooked or as salad, i.e. Dahomey, Ghana, Senegal, and Sierra Leone.[19] Most people in West Africa call *L. taraxacifolia* by the name African lettuce or wild lettuce.[20] There are many ethno-medicinal applications of *L. taraxacifolia*. This leafy vegetable has been employed in managing many ailments for centuries, ailments such as diabetes, eye diseases (conjunctivitis), measles, skin diseases, and yaws (Table 1). Some cultures in Nigeria rubbed a concoction of its leaves on the limbs of toddlers to facilitate walking.[21,22]

Many studies have reported the green synthesis of leafy vegetable extracts employing various metals, i.e. the green synthesis of copper nanoparticles (NPs) using *Ocimum sanctum*[23] green synthesis of palladium NPs employing *Origanum vulgare* leaf extract[24] lemon fruits and turmeric powder to steady the green synthesis employing manganese NPs[25] and the synthesis of silver NPs (AgNPs) from *Curcuma longa*[26] and *Calotropis*. Beside their nutritional benefits, leafy and non-cultivated vegetables (Figure 1) are known to possess therapeutic uses.[13,27,28] However, many of these cheap but disease-preventing plant species are yet to be sufficiently studied and exploited. Hence, the aim of the present study was to investigate the phytochemical screening of these non-cultivated vegetables' leaves extract and experimentally carry out characterization and application of these medicinal plants species' AgNPs as antiinflammatory and antioxidant agents and acetylcholinesterase inhibitors.

MATERIALS AND METHODS

Fresh green plants of *Crassocephalum crepidioides* (I.U. 0345), *Ceratotheca sesamoides* (I.U. 011), *Ceiba pentandra* (UILH/001/957), and *Launaea taraxacifolia* (UILH/002/1020) were obtained in December 2016 from "Oja-Oba" market in Ilorin, in Kwara State of Nigeria located in the rain forest zone at latitude 10°00' North of the equator and longitude 8°00' East of the Greenwich meridian. The plants were identified and authenticated at the Plant Biology Department, University of Ilorin, and voucher numbers collected. The authenticated plant materials were air-dried at ambient temperature for 2 weeks to completely remove the moisture content and to effectively prepare the plants for the next stage of preparation. After drying, the dried leaves were crushed into fine powder using a ceramic pestle and mortar and the samples were kept in an air-tight plastic container.

Equipment and reagents

The equipment used comprised a pestle and mortal, extraction jar, rotary evaporator, centrifuging machine, ultraviolet-visible (UV-Vis) spectrophotometer, and fourier transform infrared spectrophotometer (FTIR). The reagents included n-hexane, methanol, silver nitrate, ferric chloride, potassium ferricyanide, chloroform, sulfuric acid, lead acetate, acetic anhydride, potassium hydroxide, and Fehling solution. They were purchased from Labtrade and Sunaf Nig. Ltd. All solvents used were of analytical grade.

Preparation of extracts

Powdered *C. sesamoides*, *C. pentandra*, *L. taraxacifolia*, and *C.*

Table 1. Ethnomedicinal importance of the non-cultivated[13-84]

S/N	Plant name	Other names	Country found	Ethnomedicine	Biological activities	Phytochemical present	References
1	*Crassocephalum crepidioides*	Thickhead, fireweed, red flower ragleaf (English); Okinawa spinach (Igbo); Efo Ebolo or Ebire (Yoruba), Sekkoteka Ekyakiragala (Southern Uganda)	Uganda, West African countries, Bangladesh, India, and Malaya	Epilepsy, indigestion, sickness, sleeping disorder, stomach-ache, swollen lips, tumor, diabetes, dizziness, fever, headache, hypertension, leprosy, mental diseases, peptic ulcer, crop yield improvement	β-cell protection, antidiabetic, antioxidant, anticholinesterases	Polyphenolic, pyrrolizidine alkaloid, tannin, dihydroisocoumarins, monoterpenes	52-58
2	*Ceratotheca sesamoides*	Eku (Yoruba-Western Nigeria); Bungu (Nigeria); Tchaba-laba (Guinea Bissau); Lalu-caminho (Senegal)	Senegal, Guinea Bissau, Angola, Namibia, Tanzania, Democratic Republic of Congo, Nigeria, Botswana, Mozambique, Zimbabwe, and Zambia	Diarrhea, conjunctivitis, emollient and lubricant, stomach ache, leprosy, tumor, relieve circumcision pains, malaria, aphrodisiac, jaundice, snake bites and skin ailments	Antiviral, antidiarrheal, antiplasmodial, antiplasmodial, antioxidant, hyaluronidase, phospholipase A2, proteolytic	Flavonoids, saponins, alkaloids, tannins, phenols, phenolics	59- 67
3	*Launaea taraxacifolia*	Yarin/Yamurin/ Odundun-Odo (*Yoruba*); Nononbarya, namijin dayii (Hausa); Ugu (Igbo); Yantotoé/ yantoto (*Fon*); Lantoto/ yantotoé (*Mahi*); Odôdô/ Odôdôlodôdô (*Idaach*)	Nigeria, Benin, Togo, Ghana, Cameroon	Malaria, ulcer, against high blood pressure, diabetes mellitus, pain in fresh wounds, dysentery, eye diseases (conjunctivitis), measles, skin diseases, and yaws	Antioxidant, hypolipidemic/ antidiabetics, antibacterial, antimalarial, antiviral, anticancer	Flavonoids,phenols, chlorogenic acid	13,22,59,68-78
4	*Ceiba pentandra*	Kapok, the Ceiba, Java cotton, Hara kapok, Silk cotton and Samauma is also known as Rimi (Hausa), Bamtami (Fulani), Araba ogungun (Yoruba) and Akpi (Igbo)	Indonesia, Nepal, Bahamas, the Caribbean, Mexico, South America, West African countries, Cape Verde, Chad and Angola	Diuretic, aphrodisiac, headache, diabetes, to banish evil spirits. hallucinogenic drink, bowel complaints, diarrhea, hypertension, headache, dizziness, constipation, mental diseases, fever, peptic ulcer, and leprosy	Antibacterial, antiinflammatory, antiallergic, antiviral, antioxidant, antimicrobial, antidiarrheal	Naphthaquinone, flavonoids, linoleic acids, fatty acids	15,79-84

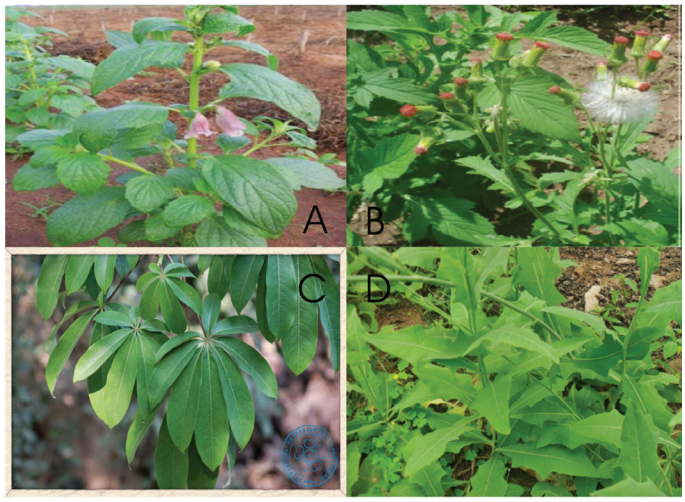

Figure 1. The leaves of A: *Ceratotheca sesamoides*, B: *Ceiba pentandra*, C: *Crassocephalum crepidioides*, D: *Launaea taraxacifolia*

crepidioides were macerated in 3 L of n-hexane in an extraction jar such that the level of the solvent was above that of the plant materials. The macerated mixtures were then left for 72 h at ambient temperature. The extracts were filtered out from the macerated mixture using Whatman 185 µm filter paper. The n-hexane extracts were concentrated in a vacuum rotary evaporator under reduced pressure and suitable temperature, transferred to appropriately labeled 250 mL beakers, and allowed to stand at ambient temperature to permit evaporation of residual solvents. The procedure was repeated using methanol after the residue of the n-hexane extract has been air-dried.

Phytochemical screening

Preparation for the test was done by pouring 3 mL of the leaf extracts into separate test tubes and diluting with 2-4 mL of deionized water. The various tests were carried out following the procedures described below. Standard techniques of screening and detecting secondary metabolites in plants were used.[29,30] The metabolites tested for were alkaloids, anthraquinones, cardiac glycosides, carbohydrates, flavonoids, saponins, steroids, phenolics, tannins, and triterpenes.

Synthesis of silver nanoparticles

The synthesis of AgNPs was carried out according to the method described in our previous study.[31] Ten milliliters of the leaf extract was measured and poured into a clean 250 mL beaker and reacted with 100 mL of 0.01 M $AgNO_3$ (prepared from stock $AgNO_3$-0.1 M of $AgNO_3$) from a burette (titration method) using $AgNO_3$ as the titrant and the extracts as the titrant at ambient temperature. A color change to yellow was observed. The synthesized mixture was left for 24 h and then separated by centrifugation using a centrifuging machine. Clear liquid was decanted and the settled layer (NPs) was stored in a 5 mL plastic sample vial and labeled accordingly. The following nomenclature was given to the synthesized NPs: *L. taraxacifolia* (LT)-AgNPs, *C. sesamoides* (CS)-AgNPs, *C. pentandra* (CP)-AgNPs, and *C. crepidioides* (CC)-AgNPs.

Characterization of silver nanoparticles

The characterization of LT-AgNPs, CS-AgNPs, CP-AgNPs, and CC-AgNPs was done using a combination of analytical and spectroscopic techniques, namely UV-Vis, FTIR, and scanning electron microscopy (SEM).

Ultraviolet-visible spectroscopy

The optical properties of the AgNPs of both plants were determined by UV-Vis spectroscopy on a Biochrom Libra PCB 1500 UV-VIS spectrophotometer. The wavelength with the highest absorbance was determined. The absorbance of AgNPs dispersed in a quartz cuvette with a 1 cm optical path was measured by withdrawing a small aliquot from the reaction mixture and a wavelength scan was taken every 60 min, then 90 min, and after 24 h. The wavelength was varied from 320 nm to 620 nm for *L. taraxacifolia*, from 320 nm to 670 nm for *C. crepidioides*, from 320 nm to 620 nm for *C. sesamoides*, and from 320 nm to 620 nm for *C. pentandra*.

Fourier transform infrared spectroscopy

The functional groups present in the methanolic extract of *L. taraxacifolia*, *C. crepidioides*, *C. sesamoides*, and *C. pentandra*, which were responsible for capping and efficient stabilization of the synthesized AgNPs, were determined using a Shimadzu FTIR model IR8400s spectrophotometer. The solutions were dried at 75°C and the dried powders were characterized in the range 4000-400 cm^{-1} by KBr pellet method.

Scanning electron microscopy

NPs of these plants' extracts were viewed using an Ultra Plus FEGSEM (Carl Zeiss, Germany) and the size and shape of the NPs were determined using the Smart SEM Ver. 5 software (Carl Zeiss, Germany).

Biological activities

Antiinflammatory activity

Cell stabilization membrane

The antiinflammatory activity of these extracts was tested by *in vitro* human red blood cell (HRBC) membrane stabilization method. The reaction mixtures (4.5 mL) consisted of 2 mL hypotonic saline solution, phosphate buffer (pH 7.4), and 1 mL of test solution in normal saline; 0.5 mL of 10% rabbit RBC in normal saline was added. For control tests, 1 mL of isotonic solution was used. The mixtures were incubated at 560°C for 30 min, cooled under running water, and centrifuged, while the absorbance of the supernatants was read at 560 nm. Percentage membrane stabilizing activity was calculated as follows:

% stabilization=(100-O.D. of drug sample/O.D. of control) x100

The control represents 100% lysis. The result was compared with STD (100 µg/mL) treated samples.[32,33]

Lipoxidase assay

The inhibitory activity against lipoxygenases (LOXs) was studied using linoleic acid as substrate and lipoxidase as enzyme. Test samples were dissolved in 0.25 mL of 2 M borate buffer pH 9.0 and 0.25 mL of lipoxidase enzyme solution (20,000 U/mL) was

added followed by incubation for 5 min at 250˚C. After that, 1.0 mL of lenoleic acid solution (0.6 mM) was added followed by thorough mixing and absorbance was measured at 234 nm. Indomethacin was used as reference standard. The percent inhibition was calculated from the following equation:

% inhibition=[(Abs control-Abs sample) /Abs control] x100

All tests and analyses were run in triplicate and averaged.[34,35]

Antioxidant activity

2,2-Diphenyl-1-picrylhydrazyl (DPPH) activity

The method employed was the one reported by Oguntoye et al.[28] but with slight modifications.[36] Mean ± standard error of the mean of two independent experiments run in duplicate was used to present the results.

2,2'-Azino-bis-(3-ethyl) benzothiazoline-6-sulfonic acid (ABTS) radical cation scavenging (ABTS) activity

The ABTS radical cation decolorization assay based on the scavenging of ABTS + radicals by antioxidant components of the extracts was used. The assay follows the procedure of Oguntoye et al.[28] with slight modifications.[36] All analyses were performed in duplicate.

Statistical analysis

Mean ± standard error of the mean of two independent experiments run in duplicate was used to present the results. The results are reported as mean ± standard deviation.

RESULTS AND DISCUSSION

Phytochemical screening

The phytochemical constituents of the extracts of *C. crepidioides*, *C. sesamoides*, *C. pentandra*, and *L. taraxacifolia* are shown in Table 2. On the whole, polyphenol, flavonoids, triterpenes, and steroids were identified in all the plants' extracts. Alkaloids and saponins are absent in most of these plants except for methanol extract of *C. crepidioides* and hexane extract of *C. pentandra*. The hexane extracts of *C. sesamoides* gave poor results for most groups of secondary metabolites investigated as shown in Table 2. The phytochemical screening reveals that flavonoids are present in the various extracts.

Characterization

UV-Vis spectroscopy study

Visual inspection showed color changes. The color changes that were witnessed indicate the formation of *C. crepidioides*, *C. sesamoides*, *C. pentandra*, and *L. taraxacifolia* AgNPs as shown in Table 3. Many studies have shown that AgNPs displayed these color changes in aqueous solution due to the excitation of surface plasmon resonance (SPR) of AgNPs, and this was the first confirmation test to show that AgNPs were formed.[37-41] The AgNPs formed were examined further by the use of UV-Vis spectroscopy, which is an important and popular tool used for characterization.

It was discovered that the aqueous extracts of *C. sesamoides* and *C. pentandra* were able to reduce silver nitrate to AgNPs at 450 nm, being the surface plasmon absorbance peak among others. Figure 2 shows the curve in each spectrum of synthesized AgNPs absorbed in the wavelength range 380-440 nm of AgNPs of *C. sesamoides* and *C. pentandra*. The absorption spectra showed SPR and peaks at 380 nm in the case of *L. taraxacifolia* (Figure 2), whereas the bands for *C. crepidioides* were observed at 410 nm as shown in Figure 2. This peak falls within the range of specification for NPs reported by previous authors.[42,43]

Fourier transform infrared spectroscopy study

FTIR spectroscopy measurements were employed to recognize and identify the biological reducing functional group, which will give a hint about the likely group of organic compounds present in these wild and non-cultivated vegetables responsible for the reduction of the Ag^{+} ions to elemental Ag^{0} and the ensuing capping resulting in efficient stabilization of the AgNPs formed.[44] The FTIR spectra of the synthesized AgNPs of the

Table 3. AgNPs' color changes observed

	Plant name	Color change	
		Initial	Final
1	*Crassocephalum crepidioides*	Black	Brown
2	*Ceratotheca sesamoides*	Black greenish	Yellow
3	*Ceiba pentandra*	Deep brown	Yellow
4	*Launaea taraxacifolia*	Light yellow	Reddish brown

AgNPs: Silver nanoparticles

Table 2. Phytochemical screening results

	Crassocephalum crepidioides		*Ceratotheca sesamoides*		*Launaea taraxacifolia*		*Ceiba pentandra*	
	MeOH	Hexane	MeOH	Hexane	MeOH	Hexane	MeOH	Hexane
Polyphenol	+++	+	+++	-	++	+	-	+
Flavonoids	+++	+	+++	-	+++	+	++	+
Triterpenes	++	++	++	++	-	+++	+++	+
Saponins	-	-	-	-	-	+	-	+++
Alkaloids	+++	-	++	-	++	-	-	-
Steroids	++	++	+++	-	+	-	++	++
Phenols	++	++	+++	++	+++	++	+++	++

+++: Very good, ++=Good, +: Fair, -: Not present, MeOH: Methanol

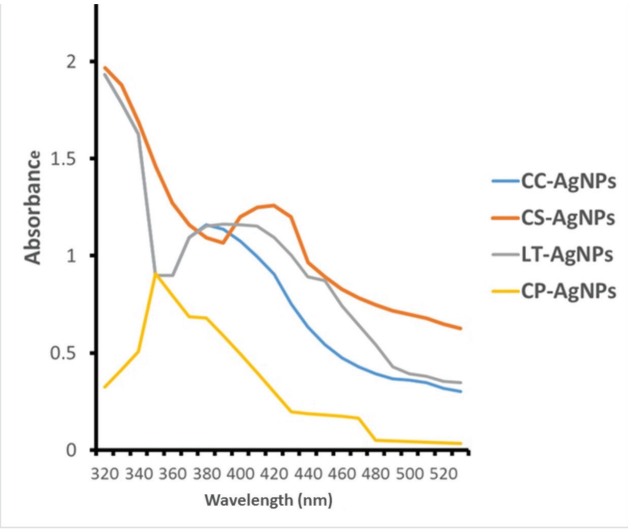

Figure 2. UV-visible spectra of the synthesized AgNPs

UV: Ultraviolet, AgNPs: Silver nanoparticles, CC: *Crassocephalum crepidioides*, CS: *Ceratotheca sesamoides*, LT: *Launaea taraxacifolia*, CP: *Ceiba pentandra*

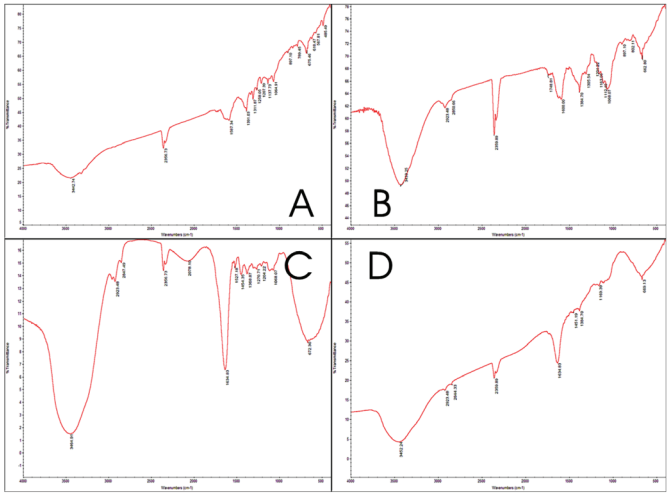

Figure 3. FTIR spectra of A=CC-AgNPs; B=CS-AgNPs; C=CP-AgNPs; D=LT-AgNPs

FTIR: Fourier transform infrared, CC: *Crassocephalum crepidioides*, CS: *Ceratotheca sesamoides*, LT: *Launaea taraxacifolia*, CP: *Ceiba pentandra*, AgNPs: Silver nanoparticles

four vegetables, i.e. A=CC-AgNPs, B=CS-AgNPs, C=CP-AgNPs, and D=LT-AgNPs, are shown in Figure 3. The infrared spectrum of CP-AgNPs showed the presence of an O-H functional group with a broad band at 3464.94 cm^{-1}, while the IR spectrum of CP-AgNPs further revealed a C=C structure with medium intensity at a wave number of 1634.33 cm^{-1}, which is sp^2 carbon. The IR spectrum of CS-AgNPs showed a very broad band at 3433.48 cm^{-1}, which was assigned to a -OH stretch. It showed a very sharp absorption band at 1748.81 cm^{-1}, which was assigned to a C=O stretch, while there was a C=C functional group at a wave number of 1600 cm^{-1}. Clear and broad absorbance bands were observed at 3452.24 (-OH), 2923.48-2844.33 (C-H, stretching), 1634.83 (C=C, stretching), 1451.19-1384.70 (C-H, bending), and 1169.39 (C-O) for the LT-AgNPs synthesized (Figure 3). The intense and broad bands observed at around 3452 cm^{-1} for all the AgNPs was due to the O-H stretching, which gives an indication for the presence of polyphenols. A medium band observed at around 1634 cm^{-1} in both the synthesized NPs was attributed to -C=C- stretching. The peaks at 1451 cm^{-1} correspond to C-H stretching of the aromatic compounds (Figure 3). The IR spectrum of CC-AgNPs showed an intense and broad band at 3442.74 (-OH, stretching), 1587.34 (C=C, stretching), 1391.03-1311.87 (N=O, stretching), and 1258.05-1064.91 (C-O, stretching). This indicated the presence of alkaloids, flavonoids, and others in this plant extract. The peaks at 1587 cm^{-1} correspond to C-H stretching of the aromatic compounds. As shown in Figure 3, most of these spectra proved distinctive functional groups of compounds, i.e. alkaloids, coumarins, flavonoids, and phenolic acids, which may all have had an active role in the reduction and capping of the synthesized AgNPs.

Scanning electron microscope

The scanning electron microscope identifies the surface characteristics, morphology, and the distribution of the CC-AgNPs, CS-AgNPs, CP-AgNPs, and LT-AgNPs depicted in the SEM micrograph (Figure 4), to determine the silver concentration of the NPs. AgNPs generally show a typical absorption characteristic peak at approximately 3 keV due to the surface plasma resonance phenomenon.[45] The cracked lines in the SEM micrographs (Figure 1A-1D) would enhance laminar flow, indicating the potential of the AgNPs for toxicant removal.[46,47] The NPs synthesized by these non-cultivated vegetables were

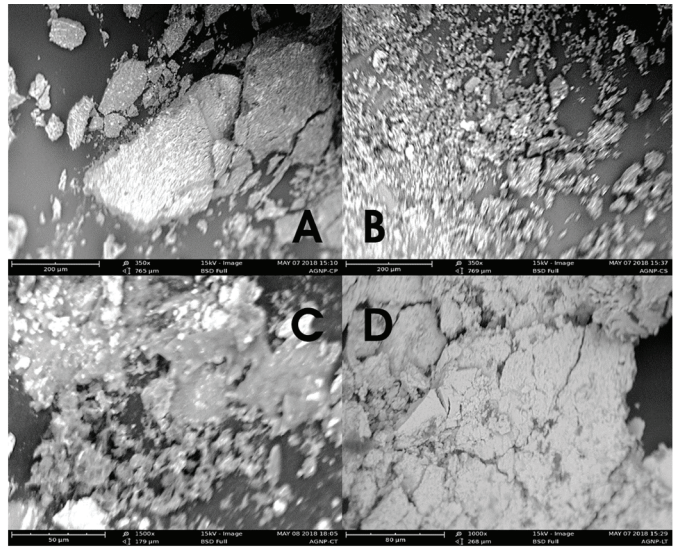

Figure 4. Scanning electron microscope picture: A=CC-AgNPs; B=CS-AgNPs; C=CP-AgNPs; D=LT-AgNPs

CC: *Crassocephalum crepidioides*, CS: *Ceratotheca sesamoides*, LT: *Launaea taraxacifolia*, CP: Ceiba pentandra, AgNPs: Silver nanoparticles

highly agglomerated except for CC-AgNPs, which displayed a scattered morphology (Figure 1). MubarakAli et al.[48] ascribes this cluster to a dehydration-induced combination of Ag NPs. However, CS-AgNPs, CP-AgNPs, and LT-AgNPs showed a trend in terms of differences in the dimensions and magnitude of the synthesized NPs. This can be accredited to the fact that the bigger and bulkier NPs can hold more Ag.

Table 4. Antioxidant activity of the synthesized AgNPs and extracts of the plant species

µg/mL	*Crassocephalum crepidioides*				*Ceratotheca sesamoides*				*Launaea taraxacifolia*				*Ceiba pentandra*				Ascorbic acid
	ABTS		DPPH		ABTS		DPPH		ABTS		DPPH		ABTS		DPPH		
	CC-AgNPs	Me-CC	CC-AgNPs	Me-CC	CS-AgNPs	Me-CS	CS-AgNPs	Me-CS	LT-AgNPs	Me- LT	LT-AgNPs	Me-LT	CP-AgNPs	Me-CP	CP-AgNPs	Me-CP	
100	11.4±2.1	13.4±1.5	15.4±3.1	13.4±1.5	12.4±0.1	14.7±1.6	9.4±0.1	13.3±1.6	11.3±0.9	18.5±4.3	13.3±1.9	16.4±2.3	5.5±18.2	27.9±6.5	6.4±1.2	14.9±0.5	4.7±0.6
200	13.9±0.2	24.2±1.8	18.9±0.2	24.2±0.2	13.4±0.1	17.2±2.	10.4±0.1	13.9±2.1	17.6±0.2	28.8±0.2	16.6±1.2	19.1±1.2	7.6±17.9	29.2±5.9	6.7±1.9	15.2±1.9	5.6±0.5
300	16.8±0.2	34.3±1.3	21.2±0.2	34.3±1.3	16.4±1.1	35.3±1.3	11.4±1.1	14.1±1.3	11.7±1.8	26.5±3.4	16.7±2.8	20.4±2.4	14.6±16.1	29.6±5.8	7.6±1.1	15.5±0.8	7.1±6.1
400	15.3±1.7	38.3±0.4	21.8±1.7	38.3±1.4	15.4±0.00	34.8±1.1	11.5±0.0	15.1±2.2	22.3±1.1	32.9±1.9	20.3±0.1	21.9±1.5	16.6±17.1	28.7±4.8	8.6±1.1	18.5±1.8	8.3±4.9
500	14.9±1.8	38.5±0.6	20.5±0.6	38.5±0.6	17.4±0.01	35.2±2.6	16.4±0.1	17.2±3.1	24.7±3.9	33.4±0.7	23.7±1.9	23.4±0.7	17.9±17.6	31.4±7.3	9.2±5.6	19.5±2.5	13.6±0.2

Me-CC: Methanol extract of *Crassocephalum crepidioides*, Me-CS: Methanol extract of *Ceratotheca sesamoides*, Me-LT: Methanol extract of *Launaea taraxacifolia*, Me-CP: Methanol extract of Ceiba pentandra, The IC_{50} values are means of three replicates (N=3 ± standard deviation), ABTS: 2,2′-azinobis(3-ethylbenzothiazoline-6-sulfonic acid, DPPH: 2,2-diphenyl-1-picryl-hydrazyl-hydrate, AgNPs: Silver nanoparticles

Table 5. Antiinflammatory activity of the synthesized AgNPs and extracts of the plant species

µg/mL	*Crassocephalum crepidioides*				*Ceratotheca sesamoides*				*Launaea taraxacifolia*				*Ceiba pentandra*				Indomethacin
	CSM		LIP		CSM		LIP		CSM		LIP		CSM		LIP		
	CC-AgNPs	Me- CC	CC-AgNPs	Me-CC	CS-AgNPs	Me-CS	CS-AgNPs	Me-CS	LT-AgNPs	Me- LT	LT-AgNPs	Me-LT	CP-AgNPs	Me-CP	CP-AgNPs	Me- CP	
100	32.2±0.1	39.1±0.1	57.6±0.1	63.1±0.1	38.5±0.1	62.9±1.1	32.8±0.1	51.9±1.1	56.4±2.1	59.2±0.1	55.4±1.1	59.2±0.1	34.7±1.0	53.1±0.1	48.5±1.0	53.0±0.1	28.1±0.0
200	32.5±0.1	39.9±1.1	55.5±0.1	59.9±1.1	43.2±1.1	58.3±2.1	33.8±2.1	58.3±2.1	58.2±1.1	59.2±0.1	52.6±2.1	59.2±0.1	34.9±2.1	55.5±2.6	51.1±2.1	58.3±1.6	34.4±0.0
300	33.1±0.1	38.4±2.1	49.1±0.1	58.4±2.1	44.2±1.2	61.1±1.2	34.5±1.2	61.1±1.2	57.1±1.9	61.3±1.1	47.1±1.1	61.3±1.1	41.2±1.1	56.2±1.1	47.8±1.2	61.1±0.1	34.8±0.0
400	34.4±0.1	43.3±1.0	49.4±0.1	63.3±1.0	46.6±0.2	64.5±0.1	34.7±0.1	64.5±0.1	58.9±2.2	59.3±2.1	52.3±1.0	59.3±2.1	42.3±1.2	57.5±0.2	37.7±1.1	64.5±0.1	37.3±0.0
500	35.9±0.1	45.4±1.3	45.9±0.1	61.4±1.3	51.2±1.3	63.6±0.1	35.1±1.1	63.6±0.1	61.2±0.0	57.2±0.1	54.2±0.0	57.2±0.1	43.2±0.1	57.8±1.1	31.2±0.1	63.7±1.1	36.3±0.0

Me-CC: Methanol extract of *Crassocephalum crepidioides*, Me-CS: Methanol extract of *Ceratotheca sesamoides*, Me-LT: Methanol extract of *Launaea taraxacifolia*, Me-CP: Methanol extract of *Ceiba pentandra*, The IC_{50} values are means of three replicates (N=3 ± standard deviation), CSM: Cell stabilization membrane, LIP: Lamprey immune protein, AgNPs: Silver nanoparticles

Biological activities

Antioxidant activity

The methanolic extracts of the four non-cultivated vegetables with their corresponding synthesized NPs were evaluated and compared employing two different assays for their antioxidant activity as shown in Table 4. The AgNPs and the methanol extract for each of these plants were evaluated for *in vitro* activity employing DPPH and ABTS assays. The results are expressed in terms of IC_{50} (the concentration that caused 50% inhibition) and are presented in Table 4. These were obtained by *in vitro* method at various concentrations (100, 200, 300...500 µg/mL) of the extracts and AgNPs formed. The synthesized AgNPs of the non-cultivated vegetables and the extracts tend to display significant antioxidant activity at the dose 100 µg/mL concentration; this was noted with the positive control as well. The higher the concentration the lower the antioxidant effect that was observed, although there was a climax at 400 µg/mL as shown in Table 4. Table 4 shows that there is an obvious trend: the synthesized AgNPs displayed better activity when compared to the extracts of these plants, i.e. AgNPs from *C. crepidioides*, *C. sesamoides*, *L. taraxacifolia*, and *C. pentandra* displayed better *in vitro* antioxidant activity (IC_{50}: 11.4, 12.4, 11.3, and 5.5 µg/mL) with the ABTS assay and (IC_{50}: 15.4, 9.4, 13.3, and 6.4 µg/mL) using the DPPH assay but the methanol extracts of these plants displayed values lower than those of the former. CP-AgNPs, CC-AgNPs, and LT-AgNPs exhibited the most significant antioxidant effect against ABTS (IC_{50}: 5.5, 11.3, and 11.4 µg/mL), while CP-AgNPs and CS-AgNPs displayed the most significant antioxidant activity against DPPH (IC_{50}: 6.4 and 9.4 µg/mL) when compared to the positive control used, ascorbic acid (IC_{50}: 4.7 µg/mL). Most of the AgNPs formed showed the most significant result at 100 µg/mL, although the positive control gave the best result at this dose as well (Table 4). Higher plants always contain constituents and substances with antioxidant effects. Flavonoids are among these naturally occurring substances that are widely renowned to exert scavenging ability against superoxide, free, and hydroxyl radicals.[49] In the present study, we assessed the antioxidant effects of the AgNPs of the non-cultivated vegetables and their methanolic extracts because of the multifaceted and complex nature of compounds in plants; the antioxidant nature of these AgNPs and their extracts cannot be studied by only a single method. As a result of this, the generally accepted assays, i.e. DPPH and ABTS methods, were used in the present study. CP-AgNPs displayed significant antioxidant activity in both assays employed, but CS-AgNPs only showed good antioxidant activity in the DPPH assay only. The DPPH and ABTS antioxidant assays proved that these neglected vegetables with their synthesized AgNPs show antioxidant activity. Bello et al.[15] examined the antioxidant effects of the leaves of *L. taraxacifolia* and *C. pentandra* (methanol extracts). These plant species displayed significant antioxidant activity when the ABTS assay was employed as compared with ascorbic acid.

Antiinflammatory activity

The methanolic extracts of the four non-cultivated vegetables with their corresponding synthesized NPs were evaluated and compared using cell-based assays for their antiinflammatory activity as shown in Table 5. The AgNPs and the methanol extract for each of these plants were evaluated for *in vitro* activity employing the HRBC membrane stabilization method and lipoxidase assay. The results are expressed in terms of IC_{50} (the concentration that caused 50% inhibition) and are presented in Table 5. These were carried out with an *in vitro* method at various concentrations (100, 200, 300....500 µg/mL) of the extract. The extract tends to display a significant antiinflammatory activity at 100 µg/mL concentration; this was noted with the positive control as well. The higher the concentration the lower the antiinflammatory effect that was seen, although there was a climax at 400 µg/mL as shown in Table 5. Table 5 shows that there is an obvious trend: the synthesized AgNPs displayed better activity when compared to the extracts of these plants, i.e. AgNPs from *C. crepidioides*, *C. sesamoides*, *C. pentandra*, and *L. taraxacifolia* displayed better *in vitro* antiinflammatory activity (IC_{50}: 32.2, 38.5, 56.4, and 34.7 µg/mL) against HRBC membrane and (IC_{50}: 57.6, 32.8, 55.4, 48.5 µg/mL) against LOXs but the methanol extracts of these plants displayed values lower than those of the former. AgNPs from *C. crepidioides*, *C. sesamoides*, *L. taraxacifolia*, and *C. pentandra* exhibited IC_{50} of 32.2, 38.5, 56.4, and 34.7 µg/mL against HRBC membrane and showed inhibitory activity (IC_{50}: 57.6, 32.8, 55.4, and 48.5 µg/mL) against LOXs. CC-AgNPs and CP-AgNPs exhibited the most significant inhibitory activity against HRBC (IC_{50}: 32.2 and 34.7 µg/mL), while CS-AgNPs and LT-AgNPs displayed the most significant inhibitory activity against LOXs (IC_{50}: 32.8 and 48.5 µg/mL) when compared to the positive control using indomethacin (IC_{50}: 28.1 µg/mL). Most of the AgNPs formed showed the most significant result at 100 µg/mL, although the positive control gave the best result at this dose as well. CS-AgNPs and LT-AgNPs displayed good activity against the LOX assay employed; they could serve as good LOX inhibitors. It was very surprising that they displayed moderate activity in the other assay used. Some authors have reported the antiinflammatory activity of *C. pentandra* through the LOX assay. It was reported that the methanol extract of its leaves displayed inhibitory activity against LOX with an IC_{50} of 102.4 µg/mL when compared with that of the positive control, 90.4 µg/mL (indomethacin).[22] This neglected vegetable's (*C. pentandra*) extracts exhibited inhibitory activity against LOX with an IC_{50} of 53.6 µg/mL. LOXs are present in the airway and stomach epithelium, leukocytes, and gut cells, and they aid in the introduction of an oxygen molecule to the 5-position of arachidonic acid to give the intermediate (5S)-hydroxy-(6E,8Z,11Z,14Z)-eicosatetraenoic acid or 5-HETE. This is an important aspect of antiinflammatory activity in the LOX assay, hence inhibiting the biological genesis of leukotriene and 5-HETE. Hence, the search for specific inhibitors of LOX activity from medicinal plants is ongoing and imperative. LOX inhibitors, i.e. CS-AgNPs and LT-AgNPs, could possess some great advantages for the treatment of allergic rhinitis, arthritis, asthma, atherosclerosis, cancer, osteoporosis, and psoriasis.[50,51]

CONCLUSION

Future studies will be carried out using various chromatographic techniques, spectroscopic techniques, and mass spectrometry to isolate and elucidate the bioactive compounds in the active fractions of wild and non-cultivated vegetables. The specific receptors these active plants' extracts and their corresponding synthesized AgNPs might be acting on to elicit antiinflammatory effects will be determined. There should be *in vivo* testing on small mammals to verify the antiinflammatory effects of these compounds in living organisms. Because AgNPs of both *C. crepidioides* and *C. sesamoides* significantly inhibited inflammatory response, it would be interesting to assay other plants from these families for antiinflammatory activity. The phytobiological facilitated production of AgNPs from selected non-cultivated vegetables proves to be ecofriendly and successful. In the current research, it has been shown that the synthesis of AgNPs by a simple, cost-effective, nontoxic, and reproducible green chemistry method allows for better antioxidant and antiinflammation worth. This study reports for the first time the synthesis, characterization, and antiinflammatory and antioxidant activities of CS-AgNPs, CP-AgNPs, and LT-AgNPs. The synthesized AgNPs were found to be stable and the FTIR evidence suggested that the phytochemicals might have played an important role in the reduction and stabilization of AgNPs. This work showed that the synthesized AgNPs from non-cultivated vegetables can find relevance and application in health, drugs, food, and environmental science. The evidence herein further confirmed their ethnopharmacological applications.

Conflicts of interest: No conflict of interest was declared by the authors. The authors alone are responsible for the content and writing of the paper.

REFERENCES

1. Antia BS, Akpan EJ, Okon PA ,Umoren IU. Nutritive and Anti. Nutritive Evaluation of sweet potatoes (Ipomoea batatas) Leaves. Pak J Nutr. 2006;5:166-168.
2. Dhellot JR, Matouba E, Maloumbi MG, Nzikou JM, Safoungoma DG, Linder M, Desobry S, Parmentier M. Extraction, chemical composition and nutritional characterization of vegetable oils: case of Amaranthus hybridus (var 1 and 2) Longo Brazzaville. Afr J Biotech. 2006;5:1095-1101.
3. Omoti O, Okyi PA. Characterization and composition of the pulp oil and cake of the African Dacryodes edulis. J Sci Food Agric. 1987;38:67-70.
4. Edmonds JM, Chweya JA. Promoting the conservation and use of under-utilized and neglected crops: Black nightshades (Solanum nigrum L.) and related species. International Plant Genetic Resources Institute;Rome, Italy;1997:1-90.
5. Fleuret A. The role of wild foidage plants in the Characterization and diet. A case study from Lushuto, Tanzania. Ecol Food Nutr. 1979;8:87-93.
6. Onyenuga VA, Fetuga BL. First National seminar on fruits and vegetables. In: proc and Recom. Nithort; Ibadan, Nigeria;1995.
7. Burkill HM. In: The useful plants of West tropical Africa, Vol 3, Royal Botanic Gardens; Kew, UK;1985:133-136.
8. Van Wyk BE, Gericke N. People's Plants: A Guide to Useful Plants of Southern Africa. Briza Publications; Pretoria, South Africa;2000:102.
9. Vanderjagt DJ, Freiberger C, Vu HTN, Mounkaila G, Glew RS, Glew RH. The trypsin inhibitor content of 61 wild edible plant foods of Niger. Plant Foods Hum Nutr. 2000;55:335-346.
10. Grubben GJH, Denton OA. Ceratotheca sesamoides Endl. In: Bedigian D, Adetula OA, eds. Plant Resources of Tropical Africa, vol. 2. Vegetables PROTA Foundation. Backhuys Publishers; Wageningen, Netherlands; 2004:56.
11. Bedigian D. Evolution of sesame revisited: domestication, diversity and prospects. Genet Resour Crop Evol. 2003;50:779-787.
12. Bedigian D, Adetula AO. Ceratotheca sesamoides Endl. Prota 2: Vegetables/ Legumes. PROTA, Wageningen; The Netherlands; 2004;34-36.
13. Bello OM, Zaki AA, Khan IS, Fasinu PS, Ali Z, Khan IA, Usman LA, Oguntoye OS. Assessment of selected medicinal plants indigenous to West Africa for antiprotozoal activity. S Afr J Bot. 2017;113:200-211.
14. Adebisi AA. Population of Neglected Indigenous Leafy Vegetables among the Yoruba tribe of South West Nigeria. CERNARD Development Series 06 CERNARD; Ibadan, Nigeria; 2000:86.
15. Bello OM, Ogbesejana AB, Tijjani A. Lipoxygenase (Lox) Inhibitory Activity of Leaves of Ceiba Pentandra (L.) Gaertn: A Neglected Vegetable from Nigeria. FUDMA Journal of Sciences. 2018;2:79-82.
16. Burkill HM. The useful plants of west tropical Africa 2ed. Royal Botanical Garden; Kew, London; 1995:160-164.
17. Robert OB. The Typification of Crassocephalum moench and Gynura cass. Kew Bulletin;London: 1955;10:455-465.
18. Arawande JO, Komolafe EA, Imokhuede B. Nutritional and phytochemical compositions of fireweed (Crassocephalum crepidioides). J Agr Tech. 2013;9:439-449.
19. Arawande JO, Amoo IA, Lajide L. Chemical and phytochemical composition of wild lettuce launaea taraxacifolia. JAPES. 2013;2:25-30.
20. Lydia EK. Safety Assessment of the Ethanolic Leaf Extract of Launaea Taraxacifolia (Willd) of the Family Asteraceae in Rodents. Master Thesis, Kwame Nkrumah University of Science and Technology, Kumasi, Ghana. 2012:110.
21. Adebisi AA. Launaea taraxacifolia (Willd.) Amin ex C. Jeffrey. In: PROTA 2: Vegetables/Legumes. Kew Bull. London. 1966;18:474.
22. Oluwasesan MB, Ogbesejana AB, Uduma A. Launaea taraxacifolia; a Neglected Vegetable from Nigeria, its Anti-inflammatory and Antioxidant Activities. Chem Search J. 2018;9:9-12.
23. Sathiraju A, Yathapu S, Bojja S, Ganghishetti B, Singh AK. Characterization of Green Synthesized Copper Nanoparticles Stabilized by Ocimum Leaf Extract. Mater Res Soc Symp Proc (India). 1704:6.
24. Mohammed RS, Zuhur J, Qandeel A, Mujeeb K, Mufsir K, Mohamed EA, Hamad ZA Abdulrahman, A-W, Rafiq HS, Merajuddin K, Syed FA. Green synthesis and characterization of palladium nanoparticles using origanum vulgare l. Extract and their catalytic activity. Molecules. 2017;22:165.
25. Jayandran M, Muhamed HM, Balasubramanian V. Green synthesis and characterization of Manganese nanoparticles using natural plant extracts and its evaluation of antimicrobial activity. J Appl Pharm Sci. 2015;5:105-110.

26. Ramar M. Synthesis of Silver Nanoparticles using Natural products from Acalypha indica and Curcuma longa. Int J Pharm Res Bio-Sci. 2015;4:151-164.
27. Bello OM, Ibitoye T, Adetunji C. Assessing antimicrobial agents of Nigeria flora Journal of King Saud University - Science; 2018.
28. Oguntoye S, Oluwasesan BM, Idowu OE, Dada AO, Hamid AA. Acetylcholinesterase inhibition and antioxidant evaluation of polyphenolic fractions and oil from four melon seeds used as condiments in Nigeria. Carpathian J Food Sci Technol. 2018;10:82-94.
29. Sofowora EA. Medicinal plants and traditional medicine in Africa. 2nd ed. Spectrum Books limited Ibadan; Nigeria;1993:289.
30. Trease GE, Evans WC. A Textbook of Pharmacognosy, 13th ed. Bailliere Tindall Ltd; London; 1989:134.
31. Dada AO, Inyinbor AA, Idu IE, Bello OM, Oluyori AP, Adelani-Akande TA, Okunola AA, Dada O. Effect of operational parameters, characterization and antibacterial studies of green synthesis of Silver Nanoparticles, using Tithonia diversifolia. Peer J. 2018;6:e5865.
32. Oyedapo OO, Akindele VR, Okunfolami KO. Effects of the extracts of Olax subcorpiodes and Aspilia Africana on bovine red blood cells. Phytotherapy Res. 1997;11:305-306.
33. Oyedapo OO, Akinpelu BA, Orefuwa SO. Anti-inflammatory effects of Theobroma cacao, L. root extract. J Tropical Med Plants (Malaysia). 2004;5:161-166.
34. Shinde UA, Kulkarni KR, Phadke AS, Nair AM, Dikshit VJ, Saraf MN. Mastcell stabilizing and lipoxygenase inhibitory activity of Cedrus deodara (Roxb.) Loud wood Oil. Indian J Exp Biol. 1999;37:258-261.
35. Steinhilber D. 5-Lipoxygenase: a target for anti-inflammatory drugs revisited. Curr Med Chem. 1999;6:69-83.
36. Atolani O, Omere J, Otuechere CA, Adewuyi A. Antioxidant and cytotoxicity effects of seed oils from edible fruits. J Acute Dis. 2012;1:130-134.
37. Kotakadi VS, Gaddam SA, Rao YS, Prasad TNV, Reddy VA, Gopal SDVR. Biofabrication of silver nanoparticles using Andrographis paniculata. Eur J Med Chem. 2014;73:135-140.
38. Kuppusamy P, Yusoff MM, Maniam GP, Govindan N. Biosynthesis of metallic nanoparticles using plant derivatives and their new avenues in pharmacological applications - an updated report. Saudi Pharmaceutical Journal; 2014.
39. Sharma S, Kumar S, Bulchandani BD, Taneja S, Banyal S. Green synthesis of silver nanoparticles and their antimicrobial activity against Gram-positive and Gram-negative bacteria. IJBB. 2013;4:711-714.
40. Stephen A, Seethalakshmi S. Phytochemical synthesis and preliminary characterization of silver nanoparticles using Hesperidin. Int J Nanosci. 2013;3-7.
41. Zhang, XF, Liu ZG, Shen W, Gurunathan S. Silver nanoparticles: Synthesis, characterization, properties, applications, and therapeutic approaches. Int J Mol Sci. 2016;17:1534.
42. Sigamoney M, Shaik S, Govender P, Krishna SBN, Sershen N. African leafy vegetables as bio-factories for silver nanoparticles: a case study on Amaranthus dubius C Mart. Ex Thell. S Afr J Bot. 2016;103:230-240.
43. Fafal T, Taştan P, Tüzüna BS, Ozyazici M, Kivcak B. Synthesis, characterization and studies on antioxidant activity of silver nanoparticles using Asphodelus aestivus Brot. aerial part extract. S Afr J Bot. 2017;112:346-353.
44. Kumar DA, Palanichamy V, Roopan SM. Green synthesis of silver nanoparticles using Alternanthera dentata leaf extract at room temperature and their antimicrobial activity. Spectrochim Acta A Mol Biomol Spectrosc. 2014;127:168-171.
45. Prasad TN, Kambala VSR, Naidu R. Phyconanotechnology: synthesis of silver nanoparticles using brown marine algae Cystophora moniliformis and their characterization. J Appl Phycol. 2012;25:177-182.
46. Dada AO, Adekola FA, Odebunmi EO. Kinetics and equilibrium models for sorption of Cu(II) onto a novel manganese nano-adsorbent. J Dispersion Sci Technol. 2016;37:119-133.
47. Dada AO, Adekola FA, Odebunmi EO. Liquid phase scavenging of Cd (II) and Cu (II) ions onto novel nanoscale zerovalent manganese (nZVMn): equilibrium, kinetic and thermodynamic studies. Environmental Nanotechnology, Monitoring Management. 2017;8:63-72.
48. MubarakAli D, Thajuddin N, Jeganathan K, Gunasekaran, M. Plant extract mediated synthesis of silver and gold nanoparticles and its antibacterial activity against clinically isolated pathogens. Colloids Surf B Biointerfaces. 2011;85:360-365.
49. Choi CW, Kim SC, Hwang SS, Choi BK, Ahn HJ, Lee MY, Park SH, Kim SK. Antioxidant activity and free radical scavenging capacity between Korean medicinal plants and flavonoids by assay-guided comparison. Plant Sci. 2002;163:1161-1168.
50. Fukuishi N, Takada T, Fukuyama Y, Akagi M. Antiallergic effect of ardisiaquinone A, a potent 5-lipoxygenase inhibitor. Phytomedicine. 2001;8:460-464.
51. Dana A, Ilse Z, Dingermann T, Müller WE, Steinhilber D, Werz O. Hyperforin is a dual inhibitor of cyclooxygenase-1 and 5-lipoxygenase. Biochem Pharmacol. 2002;64:1767-1775.
52. Asada Y, Shiraishi M, Takeuchi T, Osawa Y, Furuya T. Pyrrolizidine alkaloids from Crassocephalum crepidioides. Planta Medica. 1985;51:539-540.
53. Wilfried R, Kammermeier L, Schramm S, Towfique N, Adedeji NA, Ajayi SA, Poppenberger B. Quantification of the pyrrolizidine alkaloid jacobine in crassocephalum crepidioides by cation exchange high-performance liquid chromatography. Phytochem Anal. 2018;29:48-58.
54. Aniya Y, Koyama T, Miyagi C, Miyahira M, Inomata C, Kinoshita S, Ichiba T. Free radical scavenging and hepatoprotective actions of the medicinal herb, Crassocephalum crepidioides from the Okinawa Islands. Biol Pharm Bull. 2005;28:19-23.
55. Musa AA, Adekomi DA, Tijani AA, Muhammed OA. Some of the effect of Crassocephalum crepidioides on the frontal cortex, kidney, liver and testis of adult male Sprague Dawley rats: microanatomical study. Eur J Exp Biol. 2011;1:228-235.
56. Tomimori K, Nakama S, Kimura R, Tamaki K, Ishikawa C, Mori N. Antitumor activity and macrophage nitric oxide producing action of medicinal herb, Crassocephalum crepidioides. BMC Complement Altern Med. 2012;12:78.
57. Bukola AC, Oboh G, Oyeleye SI, Ejakpovi II, Boligon AA, Athayde ML. Blanching alters the phenolic constituents and *in vitro* antioxidant and anticholinesterases properties of fireweed (Crassocephalum crepidioides). J Taibah Univers Med Sci. 2015;10:419-426.
58. Ssegawa P, Kasenene JM. Medicinal plant diversity and uses in the Sango bay area, Southern Uganda. J Ethnopharmacol. 2007;113:521-540.
59. Obi RK, Iroagba II, Ojiako OA. Virucidal potential of some edible Nigerian vegetables. Afr J Biotechnol. 2006;5:1785-1788.

60. Toyin MY, Khadijat OF, Saoban SS, Olakunle AT, Abraham BF, Luqman QA. Antidiarrhoeal activity of aqueous leaf extract of Ceratotheca sesamoides in rats. Bangl J Pharmacol. 2012;7:14-20.

61. Benoit-Vical F, Soh PN, Saléry M, Harguem L, Poupat C, Nongonierma R. Evaluation of Senegalese plants used in malaria treatment: focus on Chrozophora senegalensis. J Ethnopharmacol. 2008;116:43-48.

62. Konan Y, Witabouna KM, Bassirou B, Kagoyire K. Antioxidant activity and total phenolic content of nine plants from Côte d'Ivoire (West Africa). J Appl Pharm Sci 2014;4:036-041.

63. Molander M, Nielsen L, Søgaard S, Staerk D, Rønsted N, Diallo D, Chifundera KZ, Van Staden J, Jäger AK. Hyaluronidase, phospholipase A2 and protease inhibitory activity of plants used in traditional treatment of snakebite induced tissue necrosis in Mali, DR Congo and South Africa J Ethnopharmacol. 2014;157:171-180.

64. Nadembega P, Boussim JI, Nikiema JB, Poli F, Antognoni F. Medicinal plants in Baskoure, Kourittenga Province, Burkina Faso: an ethnobotanical study. J Ethnopharmacol. 2011;133:378-395.

65. Diarra N, Klooster C, Togola A, Diallo D, Willcox M, Jong J. Ethnobotanical study of plants used against malaria in Sélingué subdistrict. Mali J Ethnopharmacol. 2015;166:352-360.

66. Abubakar MS, Musa AM, Ahmeda A, Hussaini IM. The perception and practice of traditional medicine in the treatment of cancers and inflammations by the Hausa and Fulani tribes of Northern Nigeria. J. Ethnopharmacol. 2007;111:625-629.

67. Fasola T, Ogunsola O. The proximate and phytochemical composition of Sesamum indicum Linn and Ceratotheca sesamoides Endl at different stages of growth. J Biol Agric Health. 2014;4:84-88.

68. Amujoyegbe OO, Idu M, Agbedahunsi JM, Erhabor JO. Ethnomedicinal Survey of medicinal plants used in the management of sickle cell disorder in Southern Nigeria. J Ethnopharmacol. 2015;85:347-360.

69. Olatunde O, Arinola GA. A vegetable, Launaea taraxacifolia, mitigated mercuric chloride alteration of the microanatomy of rat brain. J Dietary Supplements. 2017;4:613-625.

70. Obi RK, Umeh SC, Okurede OH, Iroagba II. Prevalence of Hepatitis B Virus among Pregnant Women attending an antenatal clinic in Port-Harcourt, Nigeria. Afr J Clin Exp Microbiol. 2006;7:2-6.

71. Thomford NE, Mkhize B, Dzobo K, Mpye K, Rowe A, Parker MI, Wonkam A, Skelton M, September AV. Dandara C. African lettuce (Launaea taraxacifolia) displays possible anticancer effects and herb-drug interaction potential by CYP1A2, CYP2C9, and CYP2C19 Inhibition. OMICS A J Integr Biol. 2016;20:528-534.

72. Adinortey MB, Sarfo JK, Quayson ET, Weremfo A, Adinortey CA, Ekloh W, Ocran J. Phytochemical screening, proximate and mineral composition of Launaea taraxacifolia leaves. Res J Med Plant 2012;6:171-179.

73. Olugbenga DJ, Ukpanukpong, Undigweundeye R, Ngozi UR. Phytochemical Screening, proximate analysis and acute toxicity study of launaea taraxacifolia ethanolic extract on albino rats. Int J Sci Techn. 2015;3;199-202.

74. Gbadamosi IT, Okolosi O. Botanical galactogogues: nutritional values and therapeutic potentials. J Appl Biosci. 2013;61:4460-4469.

75. Olugbenga DJ, Undigweundeye UR, Ngozi UR. Phytochemical screening, proximate analysis and acute toxicity study of Launea taraxacifolia ethanolic extract on albino rats. Int J Sci Tech. 2015;3:199-202.

76. Koukoui O, Agbangnan P, Boucherie S, Yovo M, Nusse O, Combettes L, Sohounhloué D. Phytochemical study and evaluation of cytotoxicity, antioxidant and hypolipidemic properties of launaea taraxacifolia leaves extracts on cell lines HepG2 and PLB98. Am J Plant Sci. 2015;6:1768-1779.

77. Ruffina AN, Maureen CO, Esther AE, Chisom IF. Phytochemical analysis and antibacterial activity of launaea taraxacifolia ethanolic leave extract. Sch Acad J Biosci. 2016;4:193-196.

78. Soelberg J, Asase A, Akwetey, G, Jäger AK. Historical versus contemporary medicinal plant uses in Ghana. J Ethnopharmacol. 2015;160:109-132.

79. Bamishaiye EI, Olayemi FF, Awagu EF, Bamishaiye MO. Proximate and phytochemical composition of Moringa oleifera leaves at three stages of maturation", Advance J Food Sci Technol. Vol. 3:233-237. Southern Nigeria. Int J Agri Food Sci. 2011;2:37-43.

80. Jimoh FO, Adedapo AA, Aliero AA, Koduru S, Afolayan AJ. Evaluation of the polyphenolic, nutritive and biological activities of the acetone, methanol and water extracts of Amaranthus asper. Open Complement Med J. 2010;2:7-14.

81. Adeniyi SA, Ehiagbonare JE, Nwangwu SCO. Nutritional evaluation of some staple leafy vegetables in Nigeria. Open Complement Med J. 2012;2:7-14.

82. Aloke C, Nachukwu N, Idenyi JN, Ugwuja EI, Nwachi EU, Edeogu CO. Hypoglycaemic and hypolipidaemic effects of feed formulated with ceiba pentandra leaves in alloxan induced diabetic rats. Aust J Basic Appl Sci. 2010;4:4473-4477.

83. Anigo KMB, Dauda MD, Sallau AB, Chindo IE. Chemical composition of Kapok (Ceiba pentandra) seed and physicochemical properties of its oil. Nig J Basic Appl Sci. 2012;21:105-108.

84. Enechi DC, Ugwu KK, Ugwu OPC, Omeh YS. Evaluation of the anti-nutrient levels of Ceiba pentandra leaves. IJRRPAS. 2013;3:394-400.

Turk J Pharm Sci 2020;17(6):610-619
DOI: 10.4274/tjps.galenos.2019.80037

ORIGINAL ARTICLE

An Investigation on the *In Vitro* Wound Healing Activity and Phytochemical Composition of *Hypericum pseudolaeve* N. Robson Growing in Turkey

Türkiye'de Yayılış Gösteren *Hypericum pseudolaeve* N. Robson Türünün *In Vitro* Yara İyileştirme Aktivitesi ve Fitokimyasal Kompozisyonu Üzerine Bir Araştırma

Bahar KAPTANER İĞCİ*, Zeki AYTAÇ

Gazi University Faculty of Science, Department of Biology, Ankara, Turkey

ABSTRACT

Objectives: The aim of this study was to investigate the in vitro wound healing effects of the methanolic and aqueous extracts of *Hypericum pseudolaeve* N. Robson obtained by two different methods as well as its cytotoxicity, antioxidant activity, and selected phytochemical constituents.

Materials and Methods: Total phenolic and flavonoid contents were measured using spectrophotometry-based methods. The cytotoxic effects of the extracts on L929 mouse fibroblast cells were evaluated by and 2h-tetrazolium,5-dimethylthiazol-2-yl)-2,5-diphenyltetrazolium bromide assay. Moreover, migration and spreading of the treated fibroblast cells were assessed by cell scratch assay as an *in vitro* wound healing model. In addition, the chemical content of the species was determined by high pressure liquid chromatography (HPLC).

Results: The results of the cytotoxicity assay indicated that the methanolic and aqueous extract did not have any cytotoxic effect on fibroblast cells at concentrations up to 500 µg/mL. Fibroblast migration was significantly increased by 62 µg/mL concentration of the aqueous extracts compared to the negative control. The extracts showed good antioxidant activity and 16 phytochemical compounds were detected by HPLC, with the highest amount for epicatechin.

Conclusion: The results showed that *Hypericum pseudolaeve* extracts have wound healing potential and contain several important antioxidant phenolic compounds. This species deserves further investigation aiming to isolate and identify the active compounds.

Key words: Wound healing, plant extract, antioxidant, phenolics, HPLC

ÖZ

Amaç: Bu çalışmanın amacı, *Hypericum pseudolaeve* N. Robson türünün iki farklı yöntemle elde edilmiş metanolik ve su ekstrelerinin *in vitro* yara iyileştirici etkisi ile sitotoksisitesini, antioksidan aktivitesini ve seçilmiş fitokimyasallarını araştırmaktır.

Gereç ve Yöntemler: Toplam fenolik ve flavonoit içerikleri spektrofotometri-temelli yöntemler kullanılarak ölçülmüştür. Ekstrelerin L929 fare fibroblast hücreleri üzerindeki sitotoksik etkileri 2h-tetrazolium,5-dimethylthiazol-2-yl)-2,5-diphenyltetrazolium bromide yöntemi ile değerlendirilmiştir. Ayrıca, uygulana yapılmış fibroblast hücrelerinin göçleri ve yayılmaları *in vitro* yara iyileşme modeli olarak kullanılan hücre çizik yöntemi ile değerlendirilmiştir. Ayrıca, türün kimyasal içeriği yüksek basınçlı sıvı kromatografisi (HPLC) ile belirlenmiştir.

Bulgular: Sitotoksisite deneyinin sonuçları, metanolik ve sulu ekstrelerinin, 500 µg/mL konsantrasyona kadar kullanıldığında fibroblast hücreleri üzerinde herhangi bir sitotoksik etkiye sahip olmadığını göstermiştir. Fibroblast göçü 62 µg/mL konsantrasyonunda sulu ekstreler uygulandığında negatif kontrole göre anlamlı derecede artış göstermiştir. Ekstreler iyi derecede antioksidan aktivite göstermiştir ve HPLC analizi ile içerinde en yüksek düzeyde epikateşin olmak üzere 16 fitokimyasal bileşik tespit edilmiştir.

*Correspondence: E-mail: +90 534 393 98 02, Phone: baharkaptaner123@gmail.com ORCID-ID: orcid.org/0000-0001-7102-6337
Received: 22.08.2019, Accepted: 31.10.2019

Sonuç: Sonuçlar *Hypericum pseudolaeve* ekstrelerinin, yara iyileşme potansiyeline sahip olduğunu ve çeşitli önemli antioksidan fenolik bileşikler içerdiğini göstermiştir. Bu türle ilgili aktif bileşiklerin izole edilmesi ve tanımlamasını amaçlayan daha fazla araştırma yapılmalıdır.

Anahtar kelimeler: Yara iyileşmesi, bitki ekstresi, antioksidan, fenolikler, HPLC

INTRODUCTION

Recent estimations show that approximately 6 million people suffer from chronic wounds worldwide. Wounds related to diabetes, gastric disorders, and duodenal ulcers and due to injuries such as cuts and burns continue to have serious impacts on the life quality of patients.[1] Wounds are generally caused by a cut or an opening in the skin as a result of physical damage, burns, infections, or chronic illnesses that disrupt normal skin anatomy and function. They cause loss of the connective tissue underlying the skin and integrity of the epithelial tissue. Chronic and delayed acute wounds are the most difficult to heal. Wound healing is a dynamic process involving the stages of inflammation (0-3 days), cellular proliferation (3-12 days), and remodeling (3-6 months), where cell-cell and cell-matrix interactions take place.[1] In the wound healing process, collagenase and elastase enzymes also play important roles by degrading extracellular matrix components such as collagen, elastin, and fibrin. However, their activity must be balanced by inhibition mechanisms and prolonged overexpression of these enzymes may cause impaired wound healing.[1] In recent years, the search for alternative and powerful remedies from nature (plants, animals, the marine environment, fungi, and other microorganisms) having potential to heal acute and chronic wounds especially in patients with metabolic disorders has increased considerably.[2] In folk medicine worldwide, many plants have traditional use for treating wounds. Wound healing activities of various plant extracts have also been demonstrated by scientific research using *in vitro* and *in vivo* methods.[2-8] Wound healing agents exert their effects by induction of keratinocyte differentiation and proliferation, stimulation of fibroblast proliferation and migration, increasing collagen formation, and exhibiting antioxidant, antimicrobial and antiinflammatory properties.[2]

The genus *Hypericum* is represented by 484 taxa from 36 taxonomic sections in the world according to the recent review of the genus[9] and by 119 taxa in Turkey, 49 of which are endemic.[10] *Hypericum pseudolaeve* N. Robson is grouped under the section *Hirtella* (*Drosanthe*) and distributed in central and eastern Anatolia in Turkey. The genus *Hypericum*, especially *Hypericum perforatum* (St. John's wort), is one of the most widely used medicinal plants for depression and its wound healing effects have been shown in both ethnobotanical and functional studies.[2,3,11-13] A common ethnobotanical preparation method for *Hypericum* spp. for wound healing is maceration of the aerial parts in olive oil under direct sunlight for at least 4 weeks.[11] However, there are no data in the literature regarding the ethnobotanical usage and wound healing potential of *H. pseudolaeve* to the best of the authors' knowledge and there is limited information on the chemical constituents of the species.

The aim of this study was to assess the wound healing potential of *H. pseudolaeve* extracts by *in vitro* methods, as well as to investigate their cytotoxicities, antioxidant activities, and phytochemical compositions with special emphasis on phenolic compounds. Moreover, we compared methanolic and aqueous extracts obtained by maceration and Soxhlet methods. Investigation on the chemical constituents and biological activities of this plant could be helpful in future studies searching for alternative drugs.

MATERIALS AND METHODS

Chemical compounds

The standards used for the high performance liquid chromatography (HPLC) analyses (except hypericin), thiobarbituric acid, and dimethylsulfoxide (DMSO) were purchased from Sigma; hypericin was from Santa Cruz Biotechnology; 2,2-diphenyl-1-picrylhydrazyl (DPPH) was from Aldrich; Folin-Ciocalteu reagent, ascorbic acid, sodium carbonate, potassium acetate, aluminum chloride hexahydrate, and sulfuric acid were from Merck; sodium phosphate was from Riedel-de Haën; ammonium molybdate was from Fluka; Dulbecco's modified Eagle's medium (DMEM) was from Gibco; fetal bovine serum (FBS), phosphate buffer saline (PBS), L-glutamine, and penicillin/streptomycin were from PAN Biotech; trypsin/ethylenediaminetetraacetic acid (EDTA) was from biological Industries; and (2h-tetrazolium,5-dimethylthiazol-2-yl)-2,5-diphenyltetrazolium bromide (MTT) was from Fisher Scientific.

Plant materials

Field studies were carried out by the authors in Nevşehir Province in Turkey for the collection of plant material. *H. pseudolaeve* was collected from dry igneous metamorphic slopes or steppes (1434 m, a.s.l.) between Ortahisar and Nevşehir on 06.06.2017 (Figure 1). Plant samples of a single population were used in the studies to minimize compositional variation. One of the collected plants was given a herbarium number (BK 1265) and deposited in the Herbarium of Gazi University. The aerial parts of the plants were dried in the shade and powdered with a commercial blender (waring). The powdered plant material was kept in the dark at room temperature until used.

Extraction procedure and determination of the yield

Extracts of *H. pseudolaeve* were obtained by maceration or Soxhlet extraction using methanol or water as solvents. After extraction, Whatman grade no.1 filter paper was used for the filtration procedure. Methanol was evaporated using a rotary vacuum evaporator (Heidolph-Rotar VV2000) at 40°C. Water extracts were frozen at -20°C and lyophilized by a freeze-dryer thereafter (Christ Gamma 2-16 LSC). The plant extracts were stored in the dark at 4°C until studied. Finally, four different

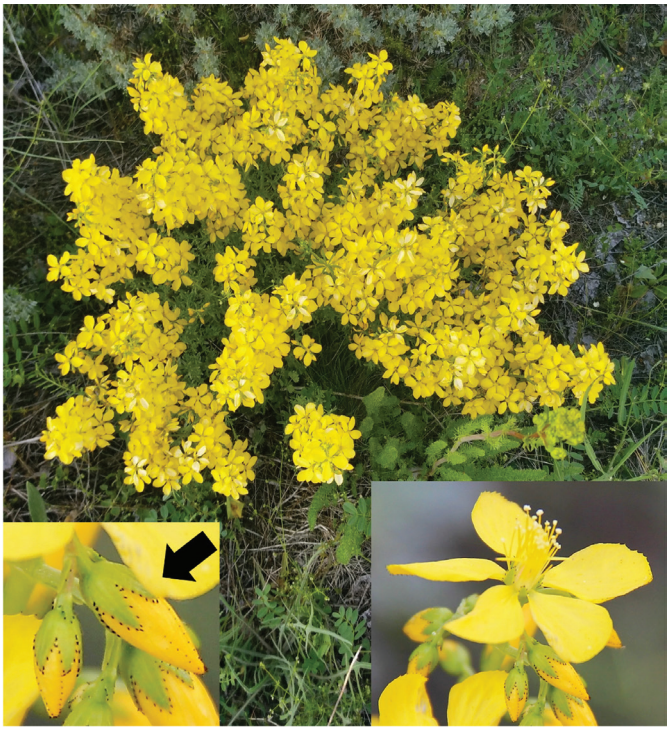

Figure 1. Photographs from the field of *Hypericum pseudolaeve*. Arrow indicates the dark secretion glands on the edges of the sepals and petals of *H. pseudolaeve*

Photographs: Bahar Kaptaner İğci

extracts were prepared and are abbreviated throughout the paper as follows: *H. pseudolaeve* maceration with methanol, maceration with water (HWM), soxhlet with methanol (HMS), and soxhlet with water (HWS). The extraction efficiencies of the plant materials were calculated using the following formula and expressed as percentages (%):

Percentage efficiency (w/w)=(weight of the dried extract, g)/(weight of dry plant material measured before the extraction process, g) ×100

Determination of total phenolic content

Total phenolic content was determined by the Folin-Ciocalteu method.[14] Gallic acid was used for the reference compound to obtain a standard curve (10 different concentrations were used between 10 and 100 µg/mL). Briefly, 0.5 mL of extracts (1 mg/mL) was mixed with 2.5 mL of 1:10 diluted Folin-Ciocalteu reagent and 2 mL of sodium carbonate solution (7.5% w/v) and allowed to stand for 15 min at 45°C. Blank, standards, and samples were transferred to cuvettes and read using a ultraviolet-visible spectroscopy (UV-VIS) spectrophotometer (PerkinElmer, Lambda 25) at 765 nm wavelength. Each sample was measured in triplicate and mean values were used. The results were presented as mg/g gallic acid equivalents (mg GAE/g).

Determination of the total flavonoid content

The total flavonoid content was determined by the aluminum chloride colorimetric method. Briefly, 0.5 mL of the extract solutions (0.5 mg/mL) was mixed with 0.1 mL of 10% aluminum chloride hexahydrate, 0.1 mL of 1 mol/L potassium acetate, and 2.8 mL of deionized water. After incubation at room temperature for 40 min, the blank, standards, and samples were transferred to cuvettes and the absorbance of the reaction mixture was measured at 415 nm against a blank by a UV-VIS spectrophotometer (PerkinElmer, Lambda 25). Rutin was used as a standard compound at 8 different concentrations between 10 and 80 µg/mL and the results were calculated as mg/g rutin equivalents (mg RUE/g). Each sample was measured in triplicate and mean values were used.

Determination of the total antioxidant capacity

First, 0.3 mL of extract (1 mg/mL) was mixed with 3 mL of the reagent solution (0.6 M sulfuric acid, 28 mmol/L sodium phosphate, and 4 mmol/L ammonium molybdate). Next, the tubes containing the reaction solution were incubated at 95°C for 90 min. Then the blank, standards, and samples were transferred into cuvettes and measured at 695 nm using a UV-VIS spectrophotometer (PerkinElmer, Lambda 25) after cooling to room temperature. Calibration graphics was plotted using ascorbic acid (AA) as a standard at concentrations between 3.9 and 500 µg/mL obtained by 2-fold serial dilution and the antioxidant activity was calculated as the equivalents of AA (EAA). The standards and samples were measured in triplicate and mean values were used.

2,2-Diphenyl-1-picrylhydrazyl free radical scavenging activity assay

The extracts were prepared in concentrations of 15.62, 31.25, 62.5, 125, and 250 µg/mL for this assay. First, 3 mL of extract of each concentration was mixed with 1 mL of the 0.1 mmol/L DPPH solution prepared in methanol. Next, the tubes were incubated in the dark at room temperature for 30 min and then read at 517 nm using a UV-VIS spectrophotometer (PerkinElmer, Lambda 25). Solvent without extract was used as a negative control and AA was used as a positive control. The effect of antioxidant capacity was observed as the color change of purple DPPH to yellow/light-yellow and % inhibition values of each extract were calculated using the following equation:

Inhibition (%)=[($A_{control}$ — A_{blank}) — (A_{sample} — A_{blank})]×100/($A_{control}$ — A_{blank}),

where $A_{control}$ is the absorbance of the negative control and A_{sample} is the absorbance of AA or extracts. Inhibitory concentration (IC_{50}) values were calculated with inhibition rates using a four-parameter logistic regression model after sigmoidal curves were plotted. Each of the standards and the samples were measured in triplicate and mean values were used for the calculations.

High performance liquid chromatography analysis and quantification

The chemical contents of the extracts were analyzed by reversed-phase HPLC-diode array detector (DAD) method. The reference compounds were selected mainly from phenolics that are common in plants as secondary metabolites. Chromatograms were recorded at 8 different wavelengths and 210, 260, 270, and 320 nm were chosen for the analyses

according to the maximum absorbances of reference peaks. All the standards and samples were filtered through 0.45-µm polytetrafluoroethylene membrane, measured in triplicate, and mean values were used.

Chromatographic separation was performed on a C18 column (Agilent Poroshell 120 SB-C18, 2.7 µm, 4.6x10 mm) using an Agilent 1220 Infinity HPLC system equipped with a DAD. The column temperature was set at 30°C, flow rate was 0.8 mL/min, and 20 µL of standard or sample was injected into the column. The reversed-phase separation was achieved using a gradient method with mobile phases A (deionized water acidified with 0.1% TFA) and B (acetonitrile acidified with 0.1% TFA). Gradient was applied as follows: 0-1 min 95% A, 2-30 min A 95% to 50%, 31-35 min A 50% to 5%, 36-37 min A 5%, 38-39 min A 5% to 95%, and A 95% for 1 min. As method validation parameters, limit of detection (LOD) and limit of quantitation (LOQ) values were calculated for each reference according to the Eurachem guide, 2nd edition.[15]

Cell culture and cell viability assay

The L929 (ATCC® CCL-1™) mouse fibroblast cell line (*Mycoplasma*-free) was obtained from the Republic of Turkey Ministry of Agriculture and Forestry Foot and Mouth Disease Institute (Ankara, Turkey) and used for *in vitro* experiments. The cells were grown in 25-cm^2 or 75-cm^2 cell culture flasks in DMEM supplemented with 10% FBS and 1% penicillin-streptomycin and 4 mM L-glutamine at 37°C in an incubator with 5% CO_2 and subcultured after reaching 80-90% confluence using trypsin-EDTA. Cells in all experiments were used between the 4th and 6th passages.

Cell viability was determined using a modified colorimetric MTT assay, which measures the mitochondrial reductase activity of viable cells.[16] Cells grown in 96-well plates were treated with plant extracts at concentrations of 31.25, 62.5 125, 250, and 500 µg/mL in the growth medium. Solvent alone (methanol or water) was added to the negative control wells. After 18, 24, and 48 h of incubation, MTT solution was added to the wells. Then all the solutions were removed and DMSO was added to dissolve the formazan crystals. The plates were incubated for 30 min and then read at 570 nm (Epoch™ Microplate Spectrophotometer, Biotek, Winooski, VT, USA). The experiment was carried out in quadruplicate and mean values were used.

Cell scratch wound healing assay

The migration capabilities of L929 mouse fibroblasts were assessed using a cell scratch *in vitro* wound healing assay, which measures the expansion of a cell population on surfaces. The cells were seeded into 48-well tissue culture dishes in the growth medium at a concentration of 2x10^4 cells/mL and cultured until nearly confluent cell monolayers formed. Then a linear wound was generated on the cell monolayer with a sterile 200-µL plastic pipette tip. Any cellular debris was removed by washing the wells with PBS. After that, growth medium containing plant extracts (62 µg/mL) was added followed by incubation for 24 h. Solvent (methanol or water) without the extract was added to the negative control wells. The cells were visualized under an inverted microscope. Three representative images from different parts (top, middle, and bottom parts of the well) of the scratched area for each replicate well were digitally photographed at 0 (the beginning) and 24 h to calculate the relative migration of cells.[17]

The area between the scratch edges was calculated by image processing using imageJ software. Firstly, the edges of the cells were contoured and then the cell-free area in between was calculated based on pixels. The mean values of the three photographs from the same well were used for each replicate well. The closure rate was calculated with these values using the following formula:

$$\text{Sclosure rate}=[(\text{Area}_{t0} - \text{Area}_{t24})/\text{Area}_{t0}] \times 100,$$

where Area_{t0} is the calculated area value at 0 h and Area_{t24} is the area value at 24 h. The experiment was performed in triplicate (three different replicate wells) and mean values were used.

Statistical analysis

All the results were obtained from at least three replicates and expressed as mean ± standard deviation. Statistical significance between groups was determined by One-Way ANOVA followed by Tukey's test for *post hoc* comparison. Mean values were considered statistically different if $p<0.05$.

RESULTS AND DISCUSSION

Plant extract yield and total phenolic and flavonoid contents

Extract yield was calculated and presented as percentage efficiency (Table 1). The yields of the extracts obtained with maceration were significantly higher than those of the extracts obtained with the soxhlet extraction method. When the solvents were compared, we found that methanolic extracts showed better yields than aqueous extracts (Table 1).

Since the correlation between the wound healing activity and antioxidant properties of plants was reported for some species in the literature,[2,7,18,19] special emphasis was placed on the phenolic compounds in the present study. Phenolics are among the most studied and important phytochemicals and there is a strong relationship between the phenolic content and antioxidant activity of plants.[2,14,19-21] The calculated total phenolic and flavonoid contents of the extracts of *H. pseudolaeve* are shown in Table 2. The results showed that the total phenolic content was highest in HMS with 177.21 mg GAE/g and lowest in HWM with 123.03 mg GAE/g values. Similarly, total flavonoid

Table 1. Amount of the total extracts and percentage efficiency of the extraction yield

Extracts	Dry plant material before extraction (g)	Extract after extraction (g)	Yield efficiency percentage (%)
HMS	20	5.89	29.45
HMM	60	24.05	40.08
HWS	20	2.22	11.10
HWM	60	10.25	17.08

HMS: Soxhlet with methanol, HMM: Maceration with methanol, HWS: Soxhlet with water, HWM: Maceration with water

Table 2. Total phenolic and flavonoid content, total antioxidant capacity and DPPH scavenging activity of the extracts

Extracts	Total phenolic content (mg/g GAE)	Total flavonoid content (mg/g RUE)	Total antioxidant capacity (mg/g AAE)	DPPH scavenging activity (IC50 values, µg/mL)
HMS	177.21±1.48[a]	123.40±2.61[a]	290.70±1.03[a]	14.32±0.13[a]
HMM	127.50±0.48[b]	114.2±0.45[b]	318.67±0.00[b]	14.68±0.07[b]
HWS	123.48±0.29[c]	44.32±1.10[c]	247.84±0.41[c]	13.04±0.03[c]
HWM	123.03±1.95[c]	21.79±0.17[d]	243.91±0.41[d]	13.29±0.10[c]
Ascorbic acid	-	-	-	1.49±0.01[d]

Values are the means of three replicates ± standard deviation. [a,b,c,d]The differences between the mean values with different letters in the same column are statistically significant ($p<0.05$), HMS: Soxhlet with methanol, HMM: Maceration with methanol, HWS: Soxhlet with water, HWM: Maceration with water, DPPH: 2,2-diphenyl-1-picrylhydrazyl

content was highest in HMS with 123.40 mg RUE/g and lowest in HWM with 21.79 mg RUE/g values. When the extraction solvents were compared, we observed that methanolic extracts had more phenolic substances than aqueous extracts. Our results are consistent with those of previous studies, which have shown that methanol extracts are richer in terms of phenolic content.[20,21] In the present study, it was found that a considerable amount of the phenolic compounds in *H. pseudolaeve* consisted of flavonoids, corroborating the previous reports on other *Hypericum* species.[22-26] Wound healing and antidepressant activities of the members of this genus have been associated with phenolic compounds such as hyperoside and epicatechin in some of the previous studies.[11,27] Therefore, phenolic content is important for the biological activities of *Hypericum* spp.

Methanolic extract of *H. pseudolaeve* was previously studied in terms of total phenolics and flavonoids and antioxidant activity[23], but we decided to present our results since we studied a different population. It is a well-known phenomenon that accumulation of phytochemicals in plants shows variation depending on the geographic region, season, phenological stage, and habitat properties.[28,29] Additionally, the previous study reported the results of methanol maceration extract only, while we present the results of both methanol and aqueous extracts obtained by two different methods in a comparative manner. According to the results of the present study, total phenolic and flavonoid contents were much higher than those reported previously. This shows that different geographical populations of *H. pseudolaeve* could vary in the accumulation of phenolic compounds. Moreover, in a study on the methanolic extract of *H. perforatum*, a widely used medicinal plant, its total phenolic content was found to be 191 mg GAE/g by the same method used in the present study.[30] When we compare our results with those in the literature, it can be seen that the total phenolic and flavonoid amounts of *H. pseudolaeve* are noteworthy and close to those of *H. perforatum*.

Antioxidant activity

According to the results of DPPH and total antioxidant capacity (phosphomolybdenum) assays, methanolic extracts expressed slightly better antioxidant activity than aqueous extracts, whereas the extraction method did not affect the activity significantly (Table 2). The antioxidant activities of several *Hypericum* species (including *H. perforatum*, *H. thymbrifolium*, *H. spectabile*, *H. scabrum*, *H. triquetrifolium*, *H. scabroides*, *H. lysimachioides*, *H. retusum*, and *H. pseudolaeve*) have been published using various methods including the DPPH scavenging assay.[22,23,26,31,32] Eroglu Ozkan et al.[23] reported the DPPH radical scavenging activity (expressed as EC_{50} values in mg/mL) of *H. pseudolaeve* methanolic extract as 0.916 mg/mL (916 µg/mL). We obtained approximately sixty times lower IC_{50} values for *H. pseudolaeve* extracts, ranging between 13.04 and 14.68 µg/mL. Such a difference may be observed due to technical variation or the calculation model of IC_{50}, since the authors did not state the model of the response curve (linear or sigmoidal). Geographical variation can be another issue, as discussed above. The antioxidant activity of a flavonoid-rich extract of *H. perforatum*, a well-known medicinal plant of the genus, was previously studied by DPPH assay and its IC_{50} value was reported as 10.63 µg/mL.[22] When we compared our results with those in the literature, we concluded that *H. pseudolaeve* has good antioxidant capacity among the other members of the genus close to that of *H. perforatum*. Antioxidant activity is important in the wound healing activity of plant extracts and generally listed as one of the properties that a good wound healing agent should possess.[2,4,7,19]

Chemical constituents revealed by HPLC analysis

In the present study, *H. pseudolaeve* plants growing in Turkey were analyzed for 17 different secondary metabolites (mainly phenolics) and the results were presented as mg/g DW (Table 3). Representative chromatograms in Figure 2 show the compounds identified. The coefficient of determination (R^2) values of linear regression of the calibration curves (calculated values were 0.9803 for quercetin and 0.9935-0.9999 for other compounds) and the LOD and LOQ values of the method were acceptable (Table 3). According to HPLC analysis of the present study, epicatechin was the main compound among the references we used, with 14.46-21.35 mg/g DW in all extracts. Apigenin was not detected in *H. pseudolaeve* extracts. The amounts of the compounds varied especially depending on the solvent, rather than the extraction method. As an exception, epicatechin concentration was significantly higher in HWM than in all the other extracts and quercitrin was also higher in maceration extracts. Moreover, kaempferol was detected only in HMS. The amount of chlorogenic acid was slightly higher in aqueous extracts, while p-coumaric acid and hyperoside (the second major compound) were higher in methanolic extracts. We used water as one of the extraction solvents since decoction is a widely used method and found that aqueous extracts of

Table 3. Comparison of the secondary metabolite content (mg/g DW mean values) of *H. perforatum* based on the reference compounds analyzed, with the LOD/LOQ values of the method for each reference measurement

	R_t (min)	Wavelength (nm)	HMS	HMM	HWS	HWM	LOD/LOQ
Gallic acid	2.57	270	7.79±0.01	7.73±0.02	7.87±0.00	8.00±0.04	0.008/0.02
4-hydroxybenzoic acid	7.37	260	+	0.10±0.04*	+	0.16±0.05*	0.08/0.29
(+)-Catechin	8.13	210	1.48±0.29	1.36±0.09	1.85±0.32	1.47±0.26	0.04/0.14
Chlorogenic acid	8.51	320	2.83±0.03	3.02±0.01	4.25±0.07	4.84±0.27	0.005/0.01
Vanillic acid	8.87	210	+	0.37±0.06*	+	+	0.28/0.93
Caffeic acid	9.21	320	0.77±0.02	0.71±0.00	0.82±0.05	1.33±0.11	0.08/0.28
Syringic acid	9.65	210	1.05±0.13	1.00±0.01	1.91±0.04	1.39±0.14	0.14/0.49
(-)-Epicatechin	10.04	210	14.79±0.16	14.49±0.08	14.46±0.07	21.35±0.07	0.11/0.39
p-Coumaric acid	11.77	320	3.37±0.02	2.60±0.01	0.95±0.04	0.08±0.07*	0.06/0.22
Rutin	13.07	210	1.72±0.11	2.04±0.15	1.75±0.02	1.53±0.05	0.35/1.17
Sinapic acid	13.24	320	0.53±0.03	0.44±0.00*	0.26±0.01*	-	0.15/0.51
Hyperoside	13.42	210	9.28±0.04	8.27±0.04	3.76±0.03	0.49±0.10*	0.23/0.77
Quercitrin	15.13	260	5.75±0.62	8.07±0.71	5.55±0.21	9.21±0.50	0.10/0.35
Quercetin	19.23	210	5.44±0.39	4.76±0.99	3.81±0.08	2.46±0.10	0.46/1.54
Apigenin	21.90	210	-	-	-	-	0.05/0.19
Kaempferol	22.40	210	0.28±0.01	-	-	-	0.08/0.27
Hypericin	33.59	590	+	-	-	-	2.49/8.30

*Values are the means of three replicates ± standard deviation. +: Peak detected but equal or <LOD and asterisk indicates that estimated concentration is >LOD, <LOQ
R_t: Retention time of the standard, LOD: Limit of detection, LOQ: Limit of quantitation, N/A: Not applicable for that sample, HMS: Soxhlet with methanol, HMM: Maceration with methanol, HWS: Soxhlet with water, HWM: Maceration with water

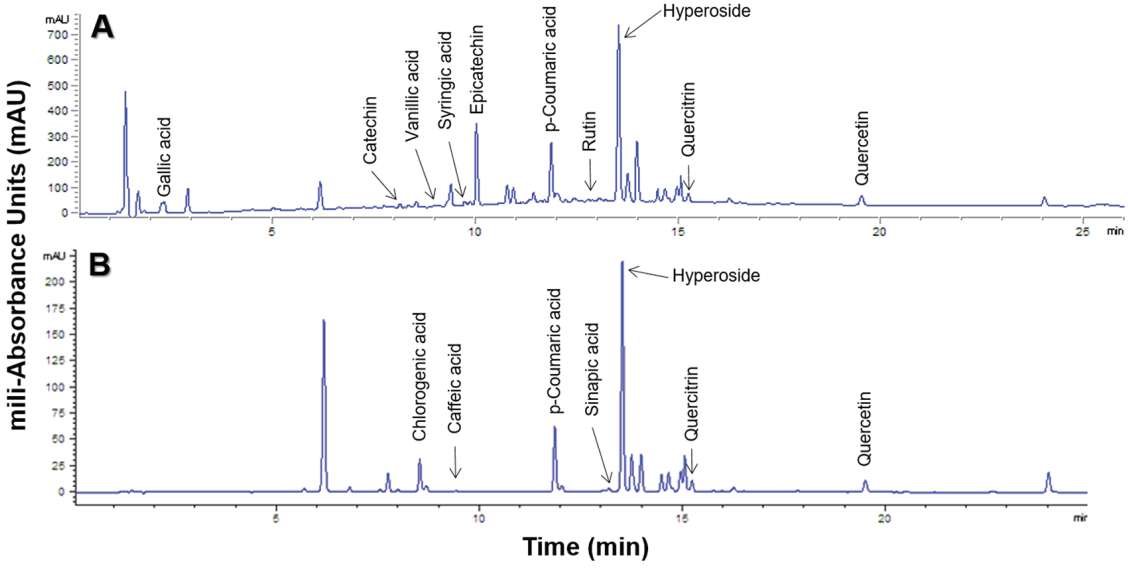

Figure 2. Representative HPLC chromatogram of *Hypericum pseudolaeve* methanolic extract obtained by maceration A. 210 nm wavelengths B. 320 nm wavelengths
HPLC: High performance liquid chromatography

H. pseudolaeve also contain considerable amounts of phenolics. However, hypericin, a naphthodianthrone molecule, was not detected in the aqueous extracts.

The chemical constituents of some *Hypericum* species were previously analyzed by chromatographic methods. In general, the secondary metabolites identified in *H. pseudolaeve* in the present study are in agreement with the previously published literature records.[11,23,25,33-38] The chemical composition of *H. pseudolaeve* from Turkey was studied by HPLC recently.[23] The authors gave yield (%) values for each compound and did not

specify the calculation, preventing comparison of their results with ours. However, even with this situation, it is observable that the amounts of some compounds show variation compared to our data. These results show that the amounts of the specific phenolic compounds may vary between different geographical populations of *H. pseudolaeve*. Moreover, catechin; epicatechin; vanillic, caffeic, syringic, p-coumaric, sinapic, gallic, and 4-hydroxybenzoic acids; and quercitrin were not included in the aforementioned study. Epicatechin was not included by Eroglu Ozkan et al.[23] while this compound was detected as one of the major constituents of *H. pseudolaeve* in the present study. Here we presented the results of all the reference compounds analyzed in the present study and provided more detailed and extended information on the chemical constituents of the species.

As a prominent result of this study, *H. pseudolaeve* was found to contain a high amount of epicatechin compared to published data of the other species of the genus. Epicatechin is an important antioxidant flavonoid that is beneficial for cardiovascular and neuropsychological health.[39] Moreover, the active fraction of *H. perforatum* with wound healing activity was also found to contain epicatechin in a previous study.[11] Our results show that *H. pseudolaeve* contains several phenolic compounds contributing to its biological activities.

The chemical constituents of *Hypericum* species are also analyzed for their chemotaxonomical importance. Secondary metabolites such as quercetin, quercitrin, hyperoside, and hypericin were considered useful biomarkers for chemotaxonomic analyses.[25] Chemical profiling can provide additional data for taxonomic classifications based on morphology and genetics. Our results are in concordance with previously published data reporting the chemical constituents of members belonging to the section *Drosanthe*.[25] As an exception, we detected caffeic acid in low amounts, whereas this compound was not found in the other members of the section.[25] Our results provide additional data for the chemotaxonomy of the genus *Hypericum*.

In vitro cytotoxicity and wound healing activity

We assessed wound healing activity using a well-established *in vitro* cell scratch assay, which is a widely used method to assess the wound healing activity of plant extracts.[40-44] To the best of our knowledge, this is the first report on the wound healing activity of the species studied. Before performing wound healing assay, we investigated the potential cytotoxic effect of the extracts on the L929 mouse fibroblast cell line since reduced levels of cell proliferation may affect the results. Moreover, toxicity assessment is also an important parameter for the quality control of pharmaceutical preparations.

None of the extracts showed significant cytotoxicity or reduced the cell viability by 50% on mouse fibroblast cells at 18 and 24 h at the highest concentrations of 250 and 500 µg/mL. However, a low level of inhibition (not more than 22%) was observed after 48 h of treatment (Table 4). We observed no significant difference in cytotoxic effects depending on the extraction solvent or extraction method. Similar studies on different species of *Hypericum* also showed that their extracts did not show a significant cytotoxic effect on fibroblasts, which makes them safer for topical applications.[45,46]

The cell scratch assay using skin cells such as fibroblasts and keratinocytes is a widely used method as an *in vitro* wound healing model that provides information about the activity of compounds and natural products.[40] In the present study, we used this assay and calculated the area closure percentages for comparison. Our results showed that HWM (76.7%) and HWS (68.4%) significantly increased ($p<0.05$) fibroblast migration compared to the negative control (Figure 3) at the tested concentration. Representative images in Figure 4 clearly show the induction of fibroblast migration.

Table 4. Cell viability percentages obtained by MTT assay after treatment with the highest extract concentrations (250 and 500 µg/mL)

	250 µg/mL			500 µg/mL		
Extracts	**18 h**	**24 h**	**48 h**	**18 h**	**24 h**	**48 h**
HMS	99.2%	91.9%	81.6%	94.9%	79.6%	78.0%
HMM	93.3%	92.5%	78.7%	91.2%	87.2%	78.6%
HWS	95.5%	90.5%	81.5%	97.2%	91.8%	79.7%
HWM	109.5%	93.1%	86.6%	112.1%	91.9%	83.9%

HMS: Soxhlet with methanol, HMM: Maceration with methanol, HWS: Soxhlet with water, HWM: Maceration with water, MTT: (2h-tetrazolium,5-dimethylthiazol-2-yl)-2,5-diphenyltetrazolium bromide

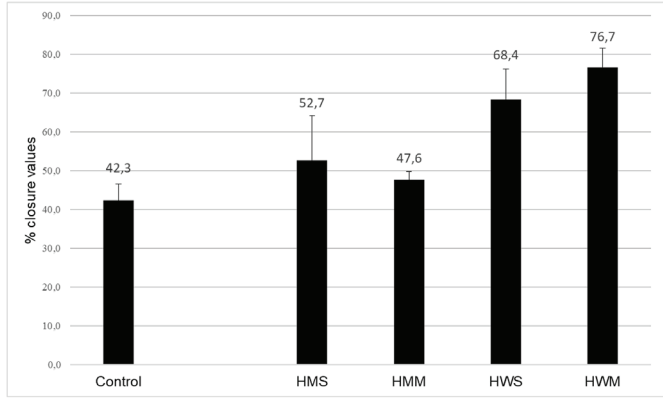

Figure 3. Graphic showing scratch assay closure percentages of *Hypericum pseudolaeve* (62 µg/mL, 24 h) on mouse dermal fibroblast (L929) migration in a wound scratch test assay. Mean values of three replicate wells were expressed with standard error bars. Results showed that HWM and HWS significantly increased ($p<0.05$) fibroblast migration compared to the negative control

HWM: Maceration with water, HWS: Soxhlet with water

In a study by Fronza et al.[40] the wound healing activity of *H. perforatum* oil was investigated by cell scratch assay using the 3T3 mouse fibroblast cell line. They found that the prepared oil was cytotoxic at concentrations higher than 0.5 µg/mL. However, wound healing activity of *H. perforatum* was shown by *in vivo* wound models and suggested it to be a potent natural wound healing product.[11] The results of the present study showed for the first time that *H. pseudolaeve*, a plant species distributed mainly in central and eastern Anatolia, has potential wound healing activity. The phytochemicals of *H. pseudolaeve*

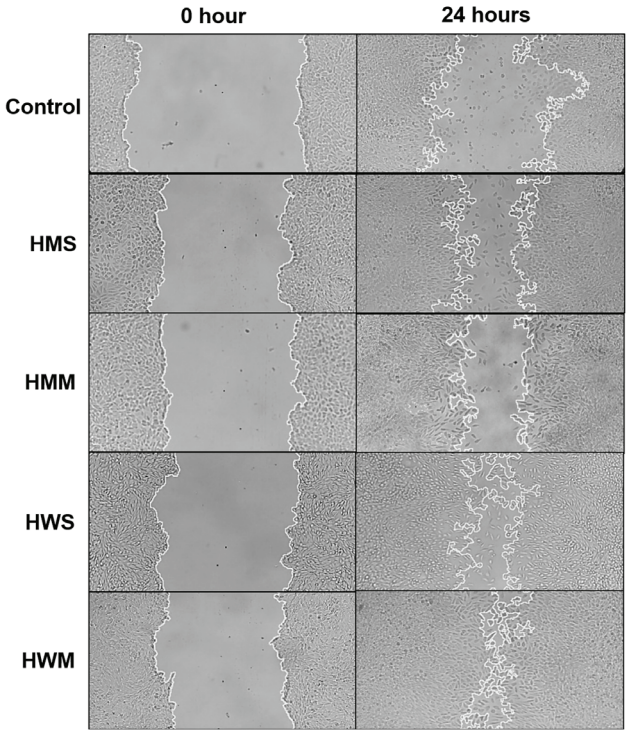

Figure 4. Representative image showing the effect of *Hypericum pseudolaeve* (62 µg/mL) on mouse dermal fibroblast (L929) migration in a wound scratch test assay. Magnification (4x)

HMS: Soxhlet with methanol, HMM: Maceration with methanol, HWS: Soxhlet with water, HWM: Maceration with water

and their synergistic actions are responsible for its biological activities.

Süntar et al.[11] investigated the wound healing potential of *H. perforatum* using *in vivo* wound models and detected hypericin, hyperoside, and rutin in the active fraction. These molecules were also detected in *H. pseudolaeve* in the present study. Previously published studies showed that hypericin has a broad range of molecular functions and biological activities, including the inhibition of protein kinase C and $CD8^+$ T-cell mediated cytotoxicity and antiviral activity.[12] Some limited studies also showed that purified hypericin may have wound healing potential.[47] According to our results, aqueous extracts were more potent regarding cell migration but we did not detect hypericin in these extracts and its concentration was low in methanolic extracts. Its contribution to the wound healing process should be investigated with more detailed studies using purified hypericin. Hyperforin (a phloroglucinol derivative) is another typical compound of the genus *Hypericum* and is considered one of the major antidepressant components of *H. perforatum*. Hyperforin also has other biological effects including antibacterial, antioxidant, anticancer, and anticyclooxygenase-1 activities.[12,48] However, hyperforin was not detected in the active fraction of *H. perforatum* by Süntar et al.[11] and the amount of hyperforin was very low in *H. pseudolaeve* (0.0023%) in a previous study.[23]

The most active extract in the cell scratch assay was HWM, which contains a significantly higher amount of (-)-epicatechin compared to the other extracts according to our HPLC analysis, indicating a correlation between the activity and the amount of this phenolic compound. In a study by Süntar et al.[11] epicatechin was identified in the active fraction of *H. perforatum* extract, showing remarkable wound healing activity. Wound healing activity of pure epicatechin gallate was reported previously.[49] These results suggest (-)-epicatechin as an important biologically active secondary metabolite of the genus *Hypericum*. The amounts of chlorogenic acid and quercitrin also show correlation with the *in vitro* wound healing activities of *H. pseudolaeve* extracts; HWM was found to contain the highest amounts of these compounds according to our HPLC analysis. Chlorogenic acid and quercitrin were also shown to have wound healing potential.[50,51] Our results and the data in the literature show that phenolic compounds may play important roles in the wound healing potential of the genus *Hypericum*.

Study limitations

Crude methanolic and aqueous extracts of *H. pseudolaeve* were investigated for their *in vitro* wound healing activity, antioxidant activity, and phytochemical content. Crude extracts showed promising results and this plant can be used for further investigations aiming to isolate active molecules.

CONCLUSION

Our results showed that *H. pseudolaeve* has potential wound healing activity and contains several important antioxidant phenolic compounds, as well as hypericin and hyperoside, which may be associated with its wound healing activity. We found that aqueous extracts, which are a common form of preparation of medicinal plants, also have good activity similar to methanolic extracts. Our results also showed that an *in vitro* scratch assay can be used for initial screening studies aiming to assess the wound healing potential of *Hypericum* spp. Using such *in vitro* tests will reduce animal use. The results of the present study, together with those in the literature, highlight that (-)-epicatechin is one of the possible contributors to the wound healing activity of the genus *Hypericum*. *H. pseudolaeve* accumulates this flavonoid in high amounts compared with the other members of the genus and deserves further investigation aiming to isolate and identify the active compounds.

ACKNOWLEDGMENTS

The authors are grateful to Gazi University Projects of Scientific Investigations for financial support of this study (project number: 05/2017-16). Bahar Kaptaner İğci acknowledges the Scientific and Technological Research Council of Turkey (TÜBİTAK) for the support under 2211/C National Scholarship Programme for PhD. students in priority areas. Special thanks are given to Nevşehir Hacı Bektaş Veli University Science and Technology Research and Application Center for HPLC facilities, and Prof. Dr. Aslıhan KARATEPE (Nevşehir Hacı Bektaş Veli University Department of Chemistry), Prof. Dr. Ceyda Sibel Kılıç (Ankara University Faculty of Pharmacy, Laboratory of Pharmaceutical Botany), and Prof. Dr. Belma Aslım (Gazi University Laboratory of Biotechnology) for providing access to laboratory infrastructure, and Prof. Dr. Hilal Özdağ (Ankara University Biotechnology Institute) and

Prof. Dr. Aykut Özkul (Ankara University Faculty of Veterinary Medicine and Biotechnology Institute) for their help obtaining the cell line. We also thank Ümmügülsüm Tükenmez Emre and Kübra Tan for their technical assistance during initial cell passaging, Derya Çiçek (Ankara University Faculty of Pharmacy) for her help during maceration extraction, and Dr. Naşit İğci (Nevşehir Hacı Bektaş Veli University Department of Molecular Biology and Genetics) for his assistance during HPLC analyses and critical review of the manuscript.

Conflicts of interest: No conflict of interest was declared by the authors. The authors alone are responsible for the content and writing of the paper.

REFERENCES

1. Menke NB, Ward KR, Witten TM, Bonchev DG, Diegelmann RF. Impaired wound healing. Clin Dermatol. 2007;25:19-25.
2. Agyare C, Bekoe EO, Boakye YD, Dapaah SO, Appiah T, Bekoe SO. Medicinal Plants and Natural Products with Demonstrated Wound Healing Properties. In: Alexandrescu VA, editors. Wound Healing - New Insights into Ancient Challenges 1st edition. London; Intech Open; 2016:487-535.
3. Süntar I, Akkol EK, Keleş H, Oktem A, Başer KHC, Yeşilada E. A novel wound healing ointment: A formulation of Hypericum perforatum oil and sage and oregano essential oils based on traditional Turkish knowledge. J Ethnopharmacol. 2011;134:89-96.
4. Süntar I, Tatlı II, Küpeli Akkol E, Keleş H, Kahraman Ç, Akdemir Z. An ethnopharmacological study on Verbascum species: from conventional wound healing use to scientific verification. J Ethnopharmacol. 2010;132:408-413.
5. Süntar I, Baldemir A, Coşkun M, Keleş H, Akkol EK. Wound healing acceleration effect of endemic Ononis species growing in Turkey. J Ethnopharmacol. 2011;135:63-70.
6. Koca U, Süntar IP, Keles H, Yesilada E, Akkol EK. *In vivo* anti-inflammatory and wound healing activities of *Centaurea iberica* Trev. ex Spreng. J Ethnopharmacol. 2009;126:551-556.
7. Balekar N, Katkam NG, Nakpheng T, Jehtae K, Srichana T. Evaluation of the wound healing potential of Wedelia trilobata (L.) leaves. J Ethnopharmacol. 2012;141:817-824.
8. Nicolaus C, Junghanns S, Hartmann A, Murillo R, Ganzera M, Merfort I. *In vitro* studies to evaluate the wound healing properties of Calendula officinalis extracts. J Ethnopharmacol. 2017;196:94-103.
9. Crockett SL, Robson NKB. Taxonomy and chemotaxonomy of the genus Hypericum. Med Aromat Plant Sci Biotechnol. 2011;5:1-13.
10. Güner A, Aslan S, Ekim T, Babaç T. List of Turkish Flora (Vascular Plants). 1st edition. Istanbul; Nezahat Gökyiğit Botanical Garden and Flora Research Society; 2012.
11. Süntar IP, Akkol EK, Yılmazer D, Baykal T, Kırmızıbekmez H, Alper M, Yeşilada H. Investigations on the *in vivo* wound healing potential of *Hypericum perforatum* L. J Ethnopharmacol. 2010;127:468-477.
12. Altan A, Damlar İ, Aras MH, Alparslan C. Effect of St. John's wort (*Hypericum perforatum*) on wound healing. Çukurova Ü Arşiv Kaynak Tarama Derg. 2015;24:578-591.
13. Mukherjee PK, Verpoorte R, Suresh B. Evaluation of *in-vivo* wound healing activity of Hypericum patulum (Family: *Hypericaceae*) leaf extract on different wound model in rats. J Ethnopharmacol. 2000;70:315-321.
14. Singleton VL, Orthofer R, Lamuela-Raventós RM. Analysis of total phenols and other oxidation substrates and antioxidants by means of folin-ciocalteu reagent. Methods Enzymol. 1999;299:152-178.
15. Magnusson B, Örnemark U. Eurachem Guide: The Fitness for Purpose of Analytical Methods - A Laboratory Guide to Method Validation and Related Topics. 2nd edition. Torino; Eurachem; 2014.
16. Mosmann T. Rapid colorimetric assay for cellular growth and survival: application to proliferation and cytotoxicity assays. J Immunol Methods. 1983;65:55-63.
17. Felice F, Zambito Y, Belardinelli E, Fabiano A, Santoni T, Di Stefano R. Effect of different chitosan derivatives on *in vitro* scratch wound assay: A comparative study. Int J Biol Macromol. 2015;76:236-241.
18. Öz BE, Ilhan M, Özbilgin S, Akkol EK, Acıkara ÖB, Saltan G, Keleş H, Süntar I. Effects of Alchemilla mollis and Alchemilla persica on the wound healing process. Bangladesh J Pharmacol. 2016;11:577-584.
19. Agar OT, Dikmen M, Ozturk N, Yilmaz MA, Temel H, Turkmenoglu FP. Comparative studies on phenolic composition, antioxidant, wound healing and cytotoxic activities of selected Achillea L. species growing in Turkey. Molecules. 2015;20:17976-18000.
20. Alali FQ, Tawaha K, El-Elimat T, Syouf M, El-Fayad M, Abulaila K, Nielsen SJ, Wheaton WD, Faklinham III JO, Oberlies NH. Antioxidant activity and total phenolic content of aqueous and methanolic extracts of Jordanian plants: an ICBG project. Nat Prod Res. 2007;21:1121-1131.
21. Mihailovic V, Kreft S, Benkovic ET, Ivanovic N. Chemical profile, antioxidant activity and stability in stimulated gastrointestinal tract model system of three Verbascum species. Ind Crops Prod. 2016;89:141-151.
22. Zou Y, Lu Y, Wei D. Antioxidant activity of a flavonoid-rich extract of *Hypericum perforatum L. in vitro*. J Agric Food Chem. 2004;52:5032-5039.
23. Eroglu Ozkan E, Ozsoy N, Yilmaz-Ozden T, Ozhan G, Mat A. Evaluation of Chemical Composition and *In vitro* Biological Activities of Three Endemic Hypericum Species from Anatolia (*H. thymbrifolium, H. spectabile* and *H. pseudolaeve*). Iran J Pharm Res. 2018;17:1036-1046.
24. Cirak C, Radusiene J, Jakstas V, Ivanauskas L, Seyis F, Yayla F. Secondary metabolites of seven *Hypericum* species growing in Turkey. Pharm Biol. 2016;54:2244-2253.
25. Cirak C, Radusiene J, Jakstas V, Ivanauskas L, Yayla F, Seyis F, Camas N. Secondary metabolites of *Hypericum* species from the *Drosanthe* and Olympia sections. South African J Bot. 2016;104:82-90.
26. Şeker Karatoprak G, Yücel Ç, Kaytan HÇ, İlgün S, Köngül Şafak E, Koşar M. Antioxidant and Cytotoxic Activities of Aerial and Underground Parts of *Hypericum* scabrum L. Iran J Sci Technol Trans A Sci. 2019: In press. Doi: 10.1007/s40995-019-00717-1
27. Ccana-Ccapatinta GV, Flores CS, Soria EJU, Crockett SL, Pari JC, Sanchez WG, Crockett SL, von Poser GL, Jimenez CC. Assessing the phytochemical profiles and antidepressant-like activity of four Peruvian Hypericum species using the murine forced swimming test. Phytochem Lett. 2014;10:107-112.
28. Çırak C, Radušiene J, Karpaviciene B, Çamaş N, Odabaş MS. Changes in phenolic content of wild and greenhouse-grown Hypericum triquetrifolium during plant development. Turkish J Agric For. 2013;37:307-314.
29. Kumar S, Yadav A, Yadav M, Yadav JP. Effect of climate change on phytochemical diversity, total phenolic content and *in vitro* antioxidant activity of Aloe vera (L.) Burm.f. BMC Res Notes. 2017;10:60.

30. Skerget M, Kotnik P, Hadolin M, Hras AR, Simonic M, Knez Z. Phenols, proanthocyanidins, flavones and flavonols in some plant materials and their antioxidant activities. Food Chem. 2005;89:191-198.

31. Kızıl G, Kızıl M, Yavuz M, Emen S, Hakimoğlu F. antioxidant activities of ethanol extracts of *Hypericum triquetrifolium* and *Hypericum scabroides*. Pharm Biol. 2008;46:231-242.

32. Barış D, Kızıl M, Aytekin Ç, Kızıl G, Yavuz M, Çeken B, Ertekin AS. *In Vitro* antimicrobial and antioxidant activity of ethanol extract of three Hypericum and Three Achillea species from Turkey. Int J Food Prop. 2011;14:339-355.

33. Mauri P, Pietta P. High performance liquid chromatography/electrospray mass spectrometry of *Hypericum* perforatum extracts. Rapid Commun Mass Spectrom. 2000;14:95-99.

34. Silva BA, Ferreres F, Malva JO, Dias ACP. Phytochemical and antioxidant characterization of Hypericum perforatum alcoholic extracts. Food Chem. 2005;90:157-167.

35. Ayan AK, Radušienė J, Çirak C, Ivanauskas L, Janulis V. Secondary metabolites of Hypericum scabrum and Hypericum bupleuroides. Pharm Biol. 2009;47:847-853.

36. Öztürk N, Tunçel M, Potoğlu-Erkara İ. Phenolic compounds and antioxidant activities of some Hypericum species: A comparative study with H. perforatum. Pharm Biol. 2009;47:120-127.

37. Çırak C, Radusiene J, Janulis V, Ivanauskas L, Arslan B. Chemical constituents of some *Hypericum* species Growing in Turkey. J Plant Biol. 2007;50:632-635.

38. Çırak C, Radusiene J, Jakstas V, Ivanauskas L, Seyis F, Yayla F. Secondary metabolites of seven *Hypericum* species growing in Turkey. Pharm Biol. 2016;59:2244-2253.

39. Bernatova I. Biological activities of (-)-epicatechin and (-)-epicatechin-containing foods: Focus on cardiovascular and neuropsychological health. Biotechnol Adv. 2018;36:666-681.

40. Fronza M, Heinzmann B, Hamburger M, Laufer S, Merfort I. Determination of the wound healing effect of Calendula extracts using the scratch assay with 3T3 fibroblasts. J Ethnopharmacol. 2009;126:463-467.

41. Balekar N, Nakpheng T, Katkam NG, Srichana T. Wound healing activity of ent-kaura-9(11),16-dien-19-oic acid isolated from Wedelia trilobata (L.) leaves. Phytomedicine. 2012;19:1178-1184.

42. Muhammad AA, Pauzi NAS, Arulselvan P, Abas F, Fakurazi S. *In Vitro* wound healing potential and identification of bioactive compounds from moringa oleifera lam. Biomed Res Int. 2013:974580:1-10.

43. Demirci S, Doğan A, Demirci Y, Şahin F. *In vitro* wound healing activity of methanol extract of *Verbascum* speciosum. Int J Appl Res Nat Prod. 2014;7:37-44.

44. Kim WS, Park BS, Sung JH, Yang JM, Park SB, Kwak SJ, Park, JS. Wound healing effect of adipose-derived stem cells: A critical role of secretory factors on human dermal fibroblasts. J Dermatol Sci. 2007;48:15-24.

45. Öztürk N, Korkmaz S, Öztürk Y. Wound-healing activity of St. John's Wort (Hypericum perforatum L.) on chicken embryonic fibroblasts. J Ethnopharmacol. 2007;111:33-39.

46. Dikmen M, Öztürk Y, Sagratini G, Ricciutelli M, Vittori S, Maggi F. Evaluation of the wound healing potentials of two subspecies of Hypericum perforatum on cultured NIH3T3 fibroblasts. Phytother Res. 2011;25:208-214.

47. Sayar H, Gergerlioglu N, Seringec N, Ozturk P, Bulbuloglu E, Karabay G. Comparison of efficacy of topical phenytoin with hypericin in second-degree burn wound healing: an experimental study in rats. Med Sci Monit Basic Res. 2014;20:36-46.

48. Zanoli F. Role of hyperforin in the pharmacological activities of St. John's Worth. CNS Drug Rev. 2004;10:203-218.

49. Kapoor M, Howard R, Hall I, Appleton I. Effects of epicatechin gallate on wound healing and scar formation in a full thickness incisional wound healing model in rats. Am J Pathol. 2004;165:299-307.

50. Bagdas D, Gul NY, Topal A, Tas S, Ozyigit MO, Cinkilic N, Gul Z, Etoz BC, Ziyanok S, Inan S, Turacozen O, Gurun MS. Pharmacologic overview of systemic chlorogenic acid therapy on experimental wound healing. Naunyn Schmiedeberg's Arch Pharmacol. 2014;387:1101-1116.

51. Seo SH, Lee SH, Cha PH, Kim MY, Min DS, Choi KY. Polygonum aviculare L. and its active compounds, quercitrin hydrate, caffeic acid, and rutin, activate the Wnt/β-catenin pathway and induce cutaneous wound healing. Phytother Res. 2016;30:848-854.

Turk J Pharm Sci 2020;17(6):620-625
DOI: 10.4274/tjps.galenos.2019.21548

ORIGINAL ARTICLE

Tualang Honey Improves Memory and Prevents Hippocampal Changes in Prenatally Stressed Rats

Prenatal Olarak Strese Maruz Kalan Erişkin Sıçanlarda Tualang Balının Hafızayı Güçlendirmesi ve Hippokampal Değişiklikleri Önlemesi

Che Badariah ABD AZIZ*, Hidani HASIM, Rahimah ZAKARIA, Asma Hayati AHMAD

Department of Physiology, Universiti Sains Malaysia, Kelantan, Malaysia

ABSTRACT

Objectives: This study investigated whether the alterations in memory and hippocampus morphology and levels of malondialdehyde (MDA) and N-methyl-D-aspartate (NMDA) receptor in the hippocampus of adult rats after prenatal stress could be prevented by administration of Tualang honey (TH).

Materials and Methods: Twenty-four pregnant rats were randomly grouped into a control group (C), a stress group (S), and a stress group treated with TH. Eight male pups from each group were randomly chosen and they were sacrificed at eight or ten weeks of age following the novel object recognition test. Their brains were removed and histological changes and levels of MDA and NMDA receptors in the hippocampus were determined.

Results: The offspring from TH group showed significantly increased preference index ($p<0.05$) with higher neuronal number compared to S group. A significantly lower level of MDA and NMDA receptors were shown in TH group ($P<0.01$; $P<0.05$ respectively) compared to S group. The parameters investigated were not significantly different between C and TH groups.

Conclusion: The study has shown that memory alteration, changes in hippocampus histology, MDA and NMDA receptor levels could be prevented by TH administration during prenatal stress. The results suggest the beneficial effects of Tualang honey in prenatally stressed rat offspring.

Key words: Prenatal stress, hippocampus, Tualang honey, malondialdehyde, NMDA receptor

ÖZ

Amaç: Bu çalışma prenatal olarak strese maruz kalan erişkin sıçanlarda Tualang balı (TH) uygulamasının hafıza ve hippokampal morfoloji değişikliklerini ve malondialdehit ve N-metil-D-aspartat (NMDA) reseptör düzeylerindeki farklılıkları önleyip önlemeyeceğini belirlemek için gerçekleştirilmiştir.

Gereç ve Yöntemler: Yirmi dört gebe sıçan kontrol grubu (C), stres grubu (S) ve TH uygulanan stres grubu olarak randomize olarak gruplanmıştır. Bu annelerden doğan 24 yavru erişkinliğe geldiklerinde yeni obje tanıma testi yapıldıktan sonra sakrifiye edilmiştir. Beyinleri çıkartılmış ve histopatolojik değişiklikler, MDA ve hipokampüsteki NMDA reseptör düzeyleri belirlenmiştir.

Bulgular: TH grubundan alınan yavrular, S grubuna kıyasla daha yüksek nöron sayısı ile belirgin bir şekilde artmış tercih indeksi ($p<0.05$) göstermiştir. TH grubundan alınan yavrularda, S grubuna göre MDA ve NDMA reseptör düzeylerinin belirgin bir şekilde düşük olduğu görülmüştür (sırasıyla $p<0,01$ ve $p<0,05$). İncelenen parametreler arasında C ve TH grupları arasında fark yoktur.

Sonuç: Bu çalışma, prenatal stres esnasında hafıza değişikliği, hipokampus histolojisi, MDA ve NMDA reseptör seviyelerindeki değişikliklerin TH uygulamasıyla önlenebileceğini göstermiştir. Bulgular, prenatal stresli sıçan yavrularında TH'nin faydalı etkilerini göstermektedir.

Anahtar kelimeler: Prenatal stres, hipokampüs, Tualang balı, malondialdehit, NDMA reseptörü

*Correspondence: E-mail: badariah@usm.my, Phone: 609-7676176 ORCID-ID: orcid.org/0000-0003-0102-1594
Received: 20.06.2019, Accepted: 31.10.2019

INTRODUCTION

Studies have reported that prenatal stress might lead to development of abnormal behaviors in adult offspring such as attention deficit hyperactivity disorder, schizophrenia, and depression as well as disruption of learning and memory processing of spatial information in the offspring.[1-3] The mechanisms that are responsible for the behavioral abnormalities following prenatal stress might be related to higher maternal corticosterone levels and lower placental 11-β-hydroxysteroid dehydrogenase type 2, an enzyme that deactivates the maternal corticosterone.[4] Changes in the hormone and enzyme will lead to higher levels of corticosterone in the fetus. Prolonged exposure to corticosterone will alter growth of the fetal brain and lead to oxidative stress as shown by increased lipid peroxidation and reduced in enzymatic antioxidant activities in the brain.[5,6]

The oxidative stress may contribute to damage of the neurons in the hippocampus of offspring and impairment of memory function.[7] Another report has shown that stress-induced elevation of N-methyl-D-aspartate (NMDA) receptors and corticosterone might mediate reduced learning ability, impaired memory, and other stress-induced neurologic disorders.[8] Studies have demonstrated that the hippocampus of prenatally stressed animals, e.g. rats and monkeys, was smaller compared to that of the nonstressed group and this suggests that prenatal stress is associated with reduced neurogenesis.[9,10] The reduced neurogenesis that occurs following prenatal stress might be associated with oxidative stress in the brain and with impairment of memory function.[5,6,8]

Tualang honey (TH) is a wild rainforest multifloral honey produced by bees of the species *Apis dorsata*. The honey can be collected from the hives, which are built on the branches of Tualang trees (*Koompassia excelsa*). It contains fructose, glucose, maltose, amino acids, vitamins, minerals, enzymes, flavonoids, and phenolic acids.[11,12] The composition will depend on the floral source and the environment surrounding the trees.[13,14] TH has been reported to have more antioxidant activity compared to Gelam and Manuka honey, which are monofloral honeys.[12,15]

Although direct administration of TH has been reported to reduce oxidant levels in stressed ovariectomized rats and improve memory function in ageing rats, its role in improving memory function in prenatally stressed rat offspring is not known.[16,17] Hence, this study investigated whether alteration of recognition memory and changes in morphology as well as malondialdehyde (MDA) and NMDA receptor levels in the hippocampus of adult rat offspring following prenatal stress could be prevented by TH administration to the pregnant dams.

MATERIALS AND METHODS

Twenty-four female and six male Sprague Dawley rats, 8 to 10 weeks of age, were obtained from the Animal Research and Service Centre (ARASC), Universiti Sains Malaysia. The rats were maintained on a 12-h light:12-h dark cycle (light phase 0700-1900) with adequate food and water available *ad libitum* with an adaptation phase for 3-5 days in the physiology laboratory before the experiment. The experiments were done in ARASC dring the day time. After mating, vaginal smears from the female rats were assessed in the morning between 0900 and 1000, and if sperms were detected, the day was labeled as day 0 of pregnancy.[18]

The rats were randomized into three groups (n=8 per group): control, stress, and stress treated with honey (TH). The stress was applied in the form of repeated restraint stress in a cylindrical restrainer measuring 23 cm x 6 cm. The stress was applied to the pregnant dams three times daily: 30 min each at 0800, 1200, and 1600.[18] The Federal Agricultural Marketing Authority supplied the TH. It was administered orally by gavaging to the pregnant rats (stress treated group) throughout pregnancy until delivery. The dosage used was 1.2 g/kg body weight/day and it was in the form of undiluted honey.[18] Each pregnant dam was kept in an individual cage until delivery. At least one male offspring from each pregnant dam was included in the study. A total of 24 male offspring (8 to 10 weeks old) weighing 200 g to 250 g were investigated.

Novel object recognition test (NORT)

Each rat was adapted to an empty open field (35 cm x 60 cm) for 10 min/day for 2 consecutive days. The open field was used for training and retention sessions. During the training session, two objects were placed in the field and each rat was permitted to explore freely for 10 min. The rats' behavior was recorded using a video camera and the time used to explore was assessed from the recorded video. Exploration was defined as the orientation of the animal's snout toward the object, sniffing, or touching with the snout.[19]

Retention was tested a day after the training session. One of the objects used in the training was substituted by a different object (novel object) and each rat was permitted to explore for 5 min.[20] The objects, which varied in shape and color and were made of plastic, were fixed to the floor. The objects were cleaned before each test to ensure lack of olfactory cues. The present study looked at exploratory preference, the ratio of time spent exploring any one of the two objects (training) or the novel one (retention) over the total time spent exploring both objects.[21] The preference index (PI) used was an indicator of recognition memory and Hammond et al.[22] suggested that a PI above 50% indicates novel object preference, below 50% familiar object preference, and 50% no preference.

Morphology of the hippocampus

The hippocampus was quickly identified and isolated. Ten percent formalin was used to fix the samples. The samples were then dehydrated in an automated tissue processor machine, blocked with paraffin wax, and kept at 0°C for 3 h. The tissues were cut using a microtome so that each section was about 5 µm thick. The tissues were then placed on glass slides, dried on a hot plate at 50-55°C for 30 min, and kept at 37°C. The slides were then stained using Nissl staining. After being completely dried of xylene, the slides were air-dried for 30 min, mounted in Cytoseal XYL mounting medium, and covered with cover slips. A light microscope was used to observe the histology of

the tissues and images were captured to assess the neuronal shape and arrangement.

Preparation of brain homogenate and malondialdehyde measurement

The hippocampus from each animal in each group was quickly removed from the brain. The isolated hippocampus was weighed and homogenate (10% w/v) was prepared in ice-cold 0.1 M phosphate-buffered saline (pH 7.4) by hand or grinder until no visible particles remained. The homogenates were centrifuged (10,000 x g) for 10 min and the samples were stored at -80˚C until assayed. The MDA level was analyzed in the hippocampus using commercially available kits (USCNK, Wuhan).

Assay procedures for N-methyl-D-aspartate receptors

The isolated hippocampus was homogenized and the sample was centrifuged at 2,000-3,000 rpm for 20 min. Supernatant was taken and kept at -80˚C until the assay. The assay was performed using a reagent kit bought from USCNK (Qayee-Bio, Shanghai, China). The NMDA receptor level in the sample was determined using a double antibody sandwich enzyme-linked immunosorbent one-step process.

Statistical analysis

The results were analyzed using SPSS version 22. One-Way ANOVA was used to analyze differences in the PI, number of Nissl-positive neurons, and MDA and NMDA receptor levels between the groups. The data were expressed as mean ± standard error of the mean. The differences were considered to be significant when p was less than 0.05.

RESULTS

Effect on the novel object recognition test in prenatally stressed male rat offspring

During the training session for the NORT, there were no significant differences in the PI (p=0.787) between the three groups. The PI for the novel object in the stress group was significantly lower [F(2.30)=0.007, p<0.01] compared to the other groups (Figure 1) during the retention session. The TH group spent significantly longer time exploring the novel object than the stress group did (p<0.05), while the difference between the TH and control groups was not statistically significant.

Effect on malondialdehyde level in prenatally stressed male rat offspring

There was a significant difference in MDA level when compared among the groups as determined by One-Way ANOVA [F(2.21)=18.53, p=0.001]. The level of MDA in the stress group (377.55±9.28 pmol/mL) was significantly higher (p<0.01) compared to the control (327.55±9.24 pmol/mL) and TH (297.75±9.61 pmol/mL) groups when analyzed using the Bonferroni post hoc test. There was no significant difference (p=0.116) between the control and TH groups (Figure 2).

Effect on N-methyl-D-aspartate receptor level in prenatally stressed male rat offspring

There was a significant difference in NMDA receptor level when compared among the groups as determined by One-Way ANOVA [F(2.21)=7.039, p=0.05]. The level of NMDA receptor was significantly higher in the stress group (20764.34±788.10 ng/mL) (p<0.05) compared to the control (18003.45±561.83 ng/mL) and TH (16999.95±826.28 ng/mL) groups (Figure 3) as analyzed using the Bonferroni post hoc test. There was no significant difference (p=1.000) between the control and TH groups.

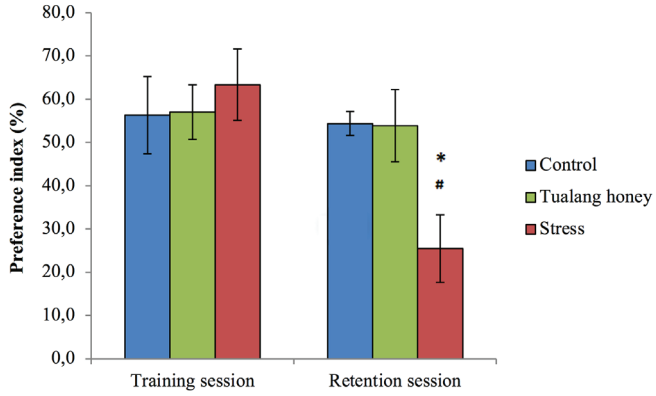

Figure 1. Preference index during training and retention sessions in the offspring from the control, stress and Tualang honey (TH) groups. Preference index (%)=any object/(familiar object 1+ familiar object 2) ×100 (%) in the training session or novel object/(familiar object + novel object) ×100 (%) in the retention session. *p<0.05 shows a significant difference between control and stress; #p<0.05 shows a significant difference between TH and stress. Data were analyzed using One-Way ANOVA followed by the Bonferroni test. Data are displayed as mean ± standard error of the mean for 8 rats in each group

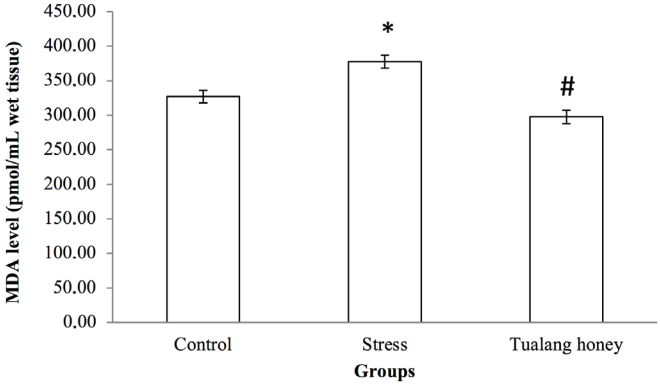

Figure 2. Level of malondialdehyde in the hippocampus of offspring from the control, stress, and Tualang honey (TH) groups. *p<0.01 comparison between control and stress groups and #p<0.01 comparison between stress treated with TH and stress group. Data were analyzed using One-Way ANOVA followed by the Bonferroni test. Data are represented as mean ± standard error of the mean for 8 rats in each group

MDA: Malondialdehyde

Effect on Nissl-positive neurons in the hippocampus of prenatally stressed male rat offspring

There was a significant difference in Nissl-positive neurons when compared among the groups as determined by One-Way ANOVA [F(2.21)=5.136, p<0.05]. The Bonferroni post hoc test revealed that the number of Nissl-positive neuron in the stress group (29.66±1.24 mm^2) was significantly lower

(p<0.05) compared to the TH (36.67±1.67 mm^2) group (Figure 4). However, there was no significant difference among the control, stress (p=1.000) and TH (p=0.127) groups. Meanwhile, normal hippocampus morphology was observed in the control group with abundant healthy neurons. The architecture was maintained and Nissl substances were clearly visualized in the cytoplasm. In contrast, the density and intensity of cytoplasmic staining of the hippocampus in the stress group were reduced

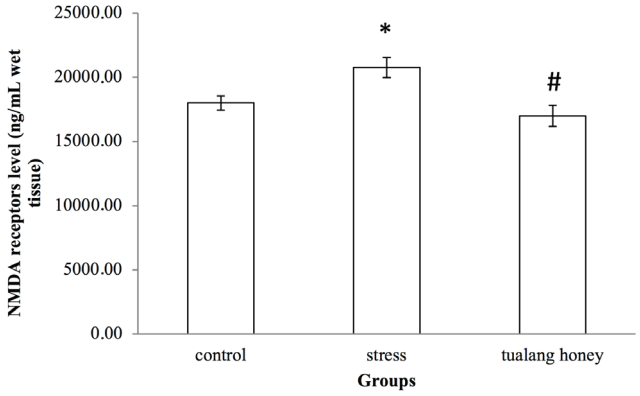

Figure 3. Level of N-methyl-D-aspartate receptors in the hippocampus of offspring from the control, stress, and Tualang honey (TH) groups. *p<0.01 comparison between the control and stress groups and #p<0.01 comparison between the stress treated with TH and stress groups. Data were analyzed using One-Way ANOVA followed by the Bonferroni test. Data are represented as mean ± standard error of the mean for 8 rats in each group

NMDA: N-methyl-D-aspartate

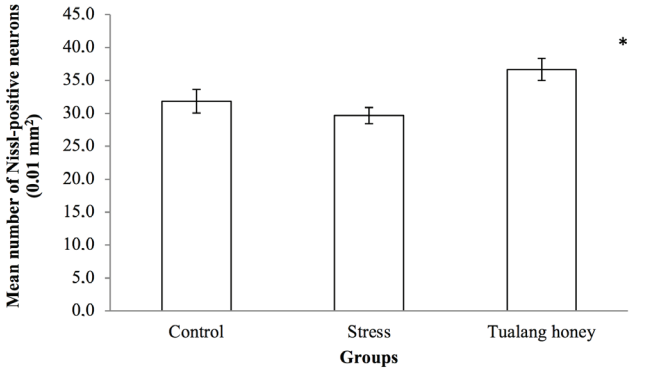

Figure 4. Mean number of Nissl-positive neurons in the hippocampus of offspring from the control, stress, and Tualang honey (TH) groups. *p<0.05 comparison between the stress and TH groups. Data were analyzed using One-Way ANOVA followed by the Bonferroni test. Data are represented as mean ± standard error of the mean for 8 rats in each group

with altered architecture compared to the control group. In the TH group the architecture was preserved with an increased number of neurons (Figure 5).

DISCUSSION

Recognition memory plays an important role in discriminating familiar from novel stimuli.[20] In the present study, there was no difference in the PI during the training session for the

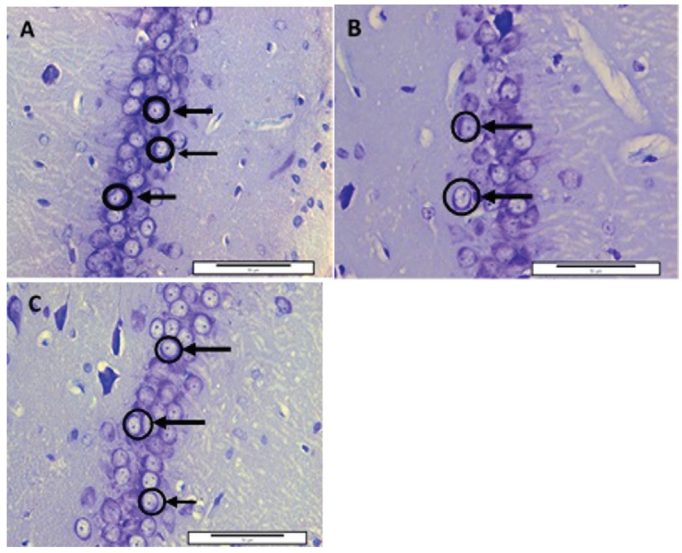

Figure 5. Neurons arrangement in the CA1 and CA2 (left side) of hippocampus section of the offspring from A) control, B) stress, and C) stress treated with Tualang honey (TH) groups. The arrows indicate the cells of interest (Nissl staining ×400, scale bar: 50 µm). Note the normal architecture with layers of pyramidal cells and vesicular nuclei in A). The architecture was altered and there was reduced intensity of cytoplasmic staining in B). The architecture was preserved with increased number of cells in C)

NORT; however, 24 h later the index was significantly lower in the stress group compared to the control and treated stress groups. The reduced PI indicating reduced recognition memory most probably is contributed to by structural changes in the hippocampus.[21] Although the number of Nissl-positive neurons was not significantly different between the stress and control groups, there were altered characteristics of the neuronal cells. Prenatal stress has been shown to induce histological changes in the brain of rat offspring, e.g., the amygdala, corpus callosum cerebral cortex, and hippocampus.[23]

In the present study, the number of Nissl-positive neurons in the stress group was not significantly different, but the morphology of CA2 of the hippocampus was altered. The altered morphology in the hippocampus could be attributed to oxidative stress as shown by the increased MDA level. Neuronal death due to oxidative stress has been shown to occur in the hippocampus in a rat model of status epilepticus and Alzheimer's disease.[24,25] Exposure to prenatal stress will activate the hypothalamic-pituitary-adrenal axis, leading to an increase in glucocorticoid level. There are abundant glucocorticoid receptors in the hippocampus and the hormone is able to modify neuronal structure and neuronal metabolism and may lead to oxidative stress in the brain of the offspring.[26] Furthermore, increased fetal glucocorticoid may increase activation of excitatory amino acid receptors such as NMDA receptors that upregulate increases in intracellular calcium concentration, contributing to accumulation of oxidants.[8]

The altered morphology of hippocampal cells may influence learning and memory in offspring as shown in the present study. Previous studies have shown that TH administration improved the number and histological features of neurons in the

hippocampus of rats exposed to various types of stress.[27,28] An increased number of neurons was also seen in the spinal cord of the offspring following TH administration during prenatal stress.[29] Luteolin, one of the flavonoids in TH, has been shown to stimulate neurogenesis in the hippocampus of a mouse model of Down's syndrome.[16,30] The increased neurogenesis was associated with improved learning and memory behavior.[30] The increased number of hippocampal neurons following TH administration in the pregnant dams suggests increased neurogenesis in the rats' offspring, which is associated with improved recognition memory.

Quercetin, another flavonoid in TH, has been reported to suppress mRNA expression of corticotropin-releasing hormone and reduce the level of adrenocorticotropic hormone and corticosterone.[31] A lower level of corticosterone plus the antioxidant activity of TH would reduce formation of reactive oxygen species and antioxidant utilization in the brain of the offspring, which may protect neuronal function.[29,32] Apart from quercetin and luteolin, TH contains other substances such as caffeic acid and vitamin C.[16,17] Koga et al.[33] reported that administration of caffeic acid in a group of mice led to reduced oxidative stress and less microglial activation in the hippocampus. Oxidative stress and microglial activation have been linked with various neurological and psychiatric disorders.[33] Vitamin C has also been shown to reduce oxidative stress and increase neurogenesis in the hippocampus in a rat model of aging.[16,34] All the reports suggest that the substances present in TH have beneficial effects on neurogenesis and have the potential to mitigate oxidative stress.

Study Limitations

The present study was conducted on a male offspring population and excluded a female population to avoid the influence of ovarian hormones on memory performance. In addition, no NMDA receptor subtype such as NR1 was assessed in this study because of financial limitations. Hence, it is recommended for future studies to investigate the effects of TH on different subtypes of NMDA receptor and different types of genes responsible for memory performance.

CONCLUSION

The present study has shown that prenatal stress was associated with memory impairment probably contributed to by altered hippocampal histology and increased levels of MDA and NMDA receptors in the hippocampus. Administration of TH was associated with improvements in the parameters investigated.

ACKNOWLEDGMENTS

This study was supported by a Bridging Grant (304/PPSP/6316130) awarded by Universiti Sains Malaysia.

Conflicts of interest: No conflict of interest was declared by the authors. The authors alone are responsible for the content and writing of the paper.

REFERENCES

1. Lodge DJ, Grace AA. Developmental pathology, dopamine, stress and schizophrenia. Int J Dev Neurosci. 2011;29:207-213.
2. Sternberg WF, Ridgway CG. Effects of gestational stress and neonatal handling on pain, analgesia, and stress behavior of adult mice. Physiol Behav. 2003;78:375-383.
3. de los Angeles GAM, del Carmen ROM, Sonia GA, RM S. Prenatal stress reduces learning and memory in pre-pubertal, young and adult rats of both sexes. Glob J Zool. 2017;2:13-20.
4. Mairesse J, Lesage J, Breton C, Bréant B, Hahn T, Darnaudéry M, Dickson SL, Seckl J, Blondeau B, Vieau D, Maccari S, Viltart O. Maternal stress alters endocrine function of the feto-placental unit in rats. Am J Physiol Endocrinol Metab. 2007;292:E1526-E1533.
5. Bingham BC, Sheela Rani CS, Frazer A, Strong R, Morilak DA. Exogenous prenatal corticosterone exposure mimics the effects of prenatal stress on adult brain stress response systems and fear extinction behavior. Psychoneuroendocrinology. 2013;38:2746-2757.
6. Sahu S, Madhyastha S, Rao G. Effect of prenatal stress on expression of glutathione system in neonatal rat brain. Turk Neurosurg. 2012;22:576-582.
7. Zhu Z, Li X, Chen W Zhao Y, Li H, Qing C, Jia N, Bai Z, Liu J. Prenatal stress causes gender-dependent neuronal loss and oxidative stress in rat hippocampus. J Neurosci Res. 2004;78:837-844.
8. Tavassoli E, Saboory E, Teshfam M, Rasmi Y, Roshan-Milani S, Ilkhanizadeh B. Effect of prenatal stress on density of NMDA receptors in rat brain. Int J Dev Neurosci. 2013;31:790-795.
9. Coe CL, Kramer M, Czeh B. Prenatal stress diminishes neurogenesis in the dentate gyrus of juvenile rhesus monkeys. Biol Psychiatry. 2003;54:1025-1034.
10. Lemaire V, Koehl M, Le Moal M, Abrous DN. Prenatal stress produces learning deficits associated with an inhibition of neurogenesis in the hippocampus. PNAS. 2000;97:11032-11037.
11. Ahmed S, Othman NH. Review of the medicinal effects of tualang honey and a comparison with manuka honey. Malays J Med Sc. 2013;20:6-13.
12. Khalil M, Alam N, Moniruzzaman M, Sulaiman S, Gan S. Phenolic acid composition and antioxidant properties of Malaysian honeys. J Food Sci. 2011;76:C921-C928.
13. Gheldof N, Wang XH, Engeseth NJ. Identification and quantification of antioxidant components of honeys from various floral sources. J Agric Food Chem. 2002;50:5870-5877.
14. Nurul SM, Gan S, Halim A, Shah NSM, Sukari H. Analysis of volatile compounds of Malaysian Tualang (*Koompassia excelsa*) honey using gas chromatography mass spectrometry. Afr J Tradit Complement Altern Med. 2013;10:180-188.
15. Kishore RK, Halim AS, Syazana MS, Sirajudeen KN. Tualang honey has higher phenolic content and greater radical scavenging activity compared with other honey sources. Nutr Res. 2011;31:322-325.
16. Azman KF, Zakaria R, Abdul Aziz CB, Othman Z. Tualang honey attenuates noise stress-induced memory deficits in aged rats. Oxid Med Cell Longev. 2016;11.
17. Al-Rahbi B, Zakaria R, Othman Z, Hassan A, Ahmad AH. Protective effects of Tualang honey against oxidative stress and anxiety-like behaviour in stressed ovariectomized rats. Int Sch Res Notices. 2014;Published online 2014 Sep 9. doi: 10.1155/2014/521065

18. Abd Aziz CB, Ahmad R, Mohamed M, Wan Yusof WN. The effects of Tualang honey intake during prenatal stress on pain responses in the rat offsprings. Eur J Integr Med. 2013;5:326-331.

19. Ennaceur A, Delacour J. A new one-trial test for neurobiological studies of memory in rats. 1. Behavioral data. Behav Brain Res. 1988;31:47-59.

20. Antunes M, Biala G. The novel object recognition memory: neurobiology, test procedure, and its modifications. Cogn Process. 2012;13:93-110.

21. Zhao D, Liu D, Chen X Wang K, Zhang A, Kang J, Zhou Q, Duan T. Prenatal stress disturbs hippocampal KIF17 and NR2B in spatial cognition in male offspring. J Neurosci Res. 2013;91:535-544.

22. Hammond RS, Tull LE, Stackman RW. On the delay-dependent involvement of the hippocampus in object recognition memory. Neurobiol Learn Mem. 2004;82:26-34.

23. Charil A, Laplante DP, Vaillancourt C, King S. Prenatal stress and brain development. Brain Res Rev. 2010;65:56-79.

24. Liu J, Wang A, Li L, Huang Y, Xue P, Hao A. Oxidative stress mediates hippocampal neuron death in rats after lithium-pilocarpine-induced status epilepticus. Seizure. 2010;19:165-172.

25. Yang R, Wang Q, Min L, Sui R, Li J, Liu X. Monosialoanglioside improves memory deficits and relieves oxidative stress in the hippocampus of rat model of Alzheimer's disease. Neurol Sci. 2013;34:1447-1451.

26. Joëls M. Functional actions of corticosteroids in the hippocampus. Eur J Pharmacol. 2008;583:312-321.

27. Al-Rahbi B, Zakaria R, Othman Z, Hassan A, Mohd Ismail ZI, Muthuraju S. Tualang honey supplement improves memory performance and hippocampal morphology in stressed ovariectomized rats. Acta Histochem. 2014;116:79-88.

28. Azman KF, Zakaria R, Othman Z, Abd Aziz CB. Neuroprotective effects of Tualang honey against oxidative stress and memory decline in young and aged rats exposed to noise stress. J Taibah Univ Sci. 2018. https://doi.org/10.1080/16583655.2018.1465275

29. Abd Aziz CB, Ahmad Suhaimi SQ, Hasim H, Ahmad Ah, Zakaria R. Effects of Tualang honey in modulating nociceptive responses at the spinal cord in offspring of prenatally stressed rats. J Integr Med. 2019;17:66-70.

30. Zhou WB, Miao ZN, Zhang B, Long W, Zheng FX, Kong J, Yu B. Luteolin induces hippocampal neurogenesis in the Ts65Dn mouse model of Down syndrome. Neural Regen Res. 2019;14:613-620.

31. Kawabata K, Kawai Y, Terao J. Suppressive effect of quercetin on acute stress induced hypothalamic-pituitary-adrenal axis response in Wistar rats. J Nutr Biochem. 2010;21:374-380.

32. Tronche C, Piérard C, Coutana M, Chauveau F, Liscia P, Béracochéa D. Increased stress-induced intra-hippocampus corticosterone rise associated with memory impairments in middle-aged mice. Neurobiol Learn Mem. 2010;93:343-351.

33. Koga M, Nakagawa S, Kato A, Kusumi I. Caffeic acid reduces oxidative stress and microglial activation in the mouse hippocampus. Tissue Cell. 2019;60:14-20.

34. Nam SM, Seo M, Seo JS, Rhim H, Nahm SS, Cho IH, Chang BJ, Kim HJ, Choi SH, Nah SY. Ascorbic acid mitigates D-galactose-induced brain aging by increasing hippocampal neurogenesis and improving memory function. Nutrients. 2019;11:E176.

Turk J Pharm Sci 2020;17(6):626-630
DOI: 10.4274/tjps.galenos.2019.05914

ORIGINAL ARTICLE

Evaluation of the Antioxidant Activity of Some Imines Containing 1*H*-Benzimidazoles

1*H*-Benzimidazol İçeren Bazı İminlerin Antioksidan Aktivitesinin Değerlendirilmesi

Rahman BAŞARAN[1]*, Gülgün KILCIGİL[2], Benay EKE[3]

[1]University of Leeds, School of Chemistry, Leeds, United Kingdom
[2]Ankara University Faculty of Pharmacy, Department of Pharmaceutical Chemistry, Ankara, Turkey
[3]Ankara University Faculty of Pharmacy, Department of Pharmaceutical Toxicology, Ankara, Turkey

ABSTRACT

Objectives: The *in vitro* antioxidant properties of some 2-(2-phenyl)-1*H*-benzo(d)imidazol-1-yl)-N'-(arylmethylene) acetohydrazide derivatives (**1-12**) were investigated in this study.

Materials and Methods: The *in vitro* antioxidant activity of compounds **1-12** was explored by determination of rat liver microsomal nicotinamide-adenine dinucleotide phosphate dependent inhibition on lipid peroxidation (LPO) levels and microsomal ethoxyresorufin O-deethylase (EROD) activity.

Results: All synthesised compounds had LPO inhibitory activity (15-57%) except compound **6**, which contains a thiophene ring. Almost all the compounds displayed slightly inhibitory activity (2-20%) on EROD.

Conclusion: The most active compound, **3** bearing a p-bromophenyl substituent at the second position of the benzimidazole ring, caused 57% inhibition of LPO level, while butylated hydroxytoluene showed 65% inhibition. None of the synthesised compounds had a marked inhibitory effect on EROD activity.

Key words: Antioxidant, benzimidazole, imine, lipid peroxidation, ethoxyresorufin O-deethylase activity

ÖZ

Amaç: Bu çalışmada, bazı 2-(2-fenil)-1*H*-benzo(d)imidazol-1-il)-N'-(arilmetilen) asetohidrazit türevlerinin *in vitro* antioksidan özellikleri araştırılmıştır.

Gereç ve Yöntemler: **1-12** numaralı bileşiklerin *in vitro* antioksidan aktiviteleri, lipit peroksidasyon (LPO) düzeylerine sıçan karaciğer mikrozomal nikotinamid adenin dinükleotid fosfat bağımlı inhibisyonunu ve mikrozomal etoksirezorufin O-deetilaz (EROD) aktivitesinin belirlenmesiyle incelenmiştir.

Bulgular: Tiyofen halkası içeren bileşik **6** dışında, sentezlenen tüm bileşikler LPO inhibitör aktivite (%15-57) göstermiştir. Hemen hemen tüm bileşikler az miktarda EROD inhibe edici aktivite (%2-20) göstermiştir.

Sonuç: Benzimidazol halkasının ikinci konumunda p-bromo fenil sübstitüenti taşıyan bileşik **3**, LPO seviyesinde %57 inhibisyona neden olan en aktif bileşik iken, butillenmiş hidroksitoluen %65 inhibisyon göstermiştir. Sentezlenen bileşiklerin hiçbiri EROD aktivitesi üzerinde belirgin bir inhibisyon etkisine sahip değildir.

Anahtar kelimeler: Antioksidan, benzimidazol, imin, lipit peroksidasyon, etoksirezorufin O-deetilaz

***Correspondence: E-mail:** cmrb@leeds.ac.uk, **Phone:** 00447902047533 **ORCID-ID:** orcid.org/0000-0001-9640-2730
Received: 30.09.2019, **Accepted:** 31.10.2019

INTRODUCTION

Antioxidant-defence mechanisms are present in living cells to maintain cellular homeostasis and survival by preventing cellular damage caused by oxidative stress in various diseases.[1,2] Impairment of antioxidant mechanisms causes the balance between antioxidant defences and oxygen-derived free radicals to shift in favour of free radicals, resulting in oxidative stress. Therefore, the synthesis of novel drugs with antioxidants and free radical scavenging properties can help to treat and/or prevent diseases induced by insufficient antioxidant capacity. It is well recognised that lipid peroxidation (LPO) is a free-radical-mediated chain process that results in oxidative damage to cell membranes and other lipid-containing structures.[3] It is an important tool to probe the antioxidant capacity of a novel compound. Almost all LPO products have long been reported to possess carcinogenic and/or mutagenic effects. Moreover, reactive oxygen species are generated by a variety of cellular mechanisms including cytochrome P450 (CYP450) enzymes, which catalyse a wide range of endogenous and exogenous substances, and particularly CYP1A1/2 have great importance in nicotinamide-adenine dinucleotide phosphate (NADPH)-dependent LPO. Probing the effects of synthesised compounds on LPO levels and the CYP450 system is, therefore, crucial.[4]

Benzimidazoles have become an attractive pharmacophore in drug design and discovery, and exhibit a wide range of biological activities, e.g., antimicrobial,[5-7] antiparasitic,[8] antihistaminic,[9] anticancer,[10-15] antiallergic,[16] and antioxidant.[17-26] The synthesis, characterisation, and antioxidant capacities of some benzimidazole derivates containing thiadiazole, triazole, oxadiazole, and thiazolidinone rings at the first position have been reported in previous studies,[6,18-21,23-25] and most of these compounds have been shown to possess substantial antioxidant properties. In the present study, the antioxidant properties of some benzimidazole derivatives having aryl-methylene amino acetamide (**1-12**) (Table 1), which have previously shown epidermal growth factor receptor kinase inhibitory activity, were investigated.[13]

MATERIALS AND METHODS

General synthetic method

All the desired benzimidazole-derived compounds were synthesised as described in Scheme 1 below. 2-phenyl-1*H*-benzo(d)imidazole (I) was produced via oxidative condensation of *o*-phenylenediamine, benzaldehyde, and sodium metabisulphite. Treatment of *I* with ethyl chloroacetate in KOH/dimethyl sulphoxide (DMSO) yielded the N-alkylated product ethyl 2-(2-phenyl)-1*H*-benzo[d]imidazol-1-yl) acetate (**II**). Hydrazine hydrate and the ester (**II**) in ethanol were refluxed for 4 h to obtain the desired hydrazide compound, 2-(2-phenyl)-1*H*-benzo(d) imidazol-1-yl) acetohydrazide (**III**). Compounds **1-12** were achieved by condensing acyl hydrazide **III** with the corresponding aromatic aldehyde derivatives in the presence of sulphuric acid.[13]

Treatment of animals

Male albino Wistar rats weighing 200-225 g were used throughout the experiments. All animals were housed in single cages under controlled laboratory conditions (22-25˚C room temperature; 12-h light/dark cycle; optimum humidity) and had access to standard rat chow and tap water *ad libitum*. They were deprived of feed for 24-h before sacrifice and then decapitated under anaesthesia. Their liver tissues were carefully dissected and immediately stored in a freezer at -80˚C. All procedures used in the present study were approved by the Ethics Committee for Animal Experiments of Ankara University (2015-8-117).

Isolation of rat liver microsomes

The rat liver tissues were weighed and homogenised with 1.15% KCl (w/v) at 3 000 rpm on ice and centrifuged at 11 000 x g for 25 min. Once the supernatant fractions had been centrifuged again at 108 000 x g for 60 min, the pellets were mixed with 20% glycerol and were then immediately stored at -80˚C until use. Total protein levels of the liver microsomes were measured as described by Lowry et al.[27] using bovine serum albumin as a standard.

In vitro antioxidant activity

Lipid peroxidation assay

The NADPH-dependent LPO level was determined based on the optimum conditions described previously.[28] In this protocol, the control activity was determined as the pure diluent in which the chemicals were dissolved. DMSO was used as a control for the synthesised compounds. The assay was, therefore, performed only in a solvent as a control or the determined concentrations of compounds. The protocol was carried out as described by Wills[29,30] with some modifications by Bishayee and Balasubramanian.[31] The measurement of thiobarbituric acid reactive substances (TBARS) is the well-established method for quantifying NADPH-dependent LPO levels. This method is based on the principle of spectrophotometrically measuring the coloured product formed by the reaction of TBA with malondialdehyde (MDA) at 532 nm. The amount of TBARS was then indicated as nanomoles of MDA/mg protein; 1 mL of reaction mixture contains 0.2 mg of microsomal protein, 62.5 mM potassium phosphate buffer (pH 7.4), 0.2 mM Fe^{2+}, 90 mM KCl, and cofactor (NADPH-generating system) consisting of 2.5 mM glucose-6-phosphate, 14.2 mM potassium phosphate buffer (pH 7.8), 2.5 mM $MgCl_2$, 0.25 mM $NADP^+$, and 1.0 U of glucose-6-phosphate dehydrogenase. The reaction was initiated by the addition of an NADPH-generating system and then allowed to incubate at 37˚C for 30 min in a shaking water bath. At the end of the incubation, the reaction was terminated by the addition of 500 µL of 25% trichloroacetic acid and then centrifuged at 5 000 rpm for 20 min to remove denatured proteins. Next, 1 mL supernatant was combined with 0.5 mL of TBA and the mixture was then boiled for 20 min in a hot water bath. Finally, the absorbance was read spectrophotometrically at a wavelength of 532 nm. Whilst butylated hydroxytoluene (BHT) was used as a standard, the control used in this assay was DMSO.

7-Ethoxyresorufin O-deethylase (EROD) assay

EROD activity in the rat liver microsomes was assayed as previously described by Burke et al.[32] 7-ethoxyresorufin is a substrate for CYP1A1, and this enzyme converts it to resorufin,

Table 1. ***In vitro*** **effects of compounds 1-12 on liver LPO levels and EROD enzyme activities. Concentration in incubation medium (10^{-3} M). All the values are means ± SD of three independent experiments**

Compounds	Ar	EROD (pmol/mg/min)	% of control	LPO (nmol/mg/min)	% of control
1	4-chlorophenyl 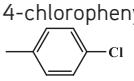	33.41±1.64	80	11.67±0.89	72
2	4-fluorophenyl 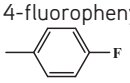	42.76±2.34	103	10.51±1.88	65
3	4-bromophenyl 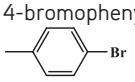	38.91±1.55	94	6.97±0.65	43
4	3-nitrophenyl 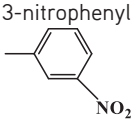	38.55±1.07	93	8.94±2.13	55
5	2-naphtyl 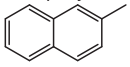	38.87±1.44	93	9.40±2.13	58
6	3-methylthiophene-2-yl 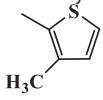	35.91±4.36	86	82.58±1.23	508
7	4-benzyloxyphenyl 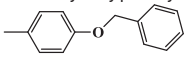	37.61±0.68	91	13.81±0.32	85
8	2-chloro-5-nitrophenyl 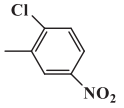	42.98±3.49	103	11.84±0.66	73
9	3,4-dibenzyloxyphenyl 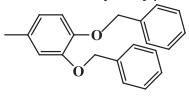	37.29±0.98	90	10.10±1.31	62
10	3-bromo-4-fluorophenyl 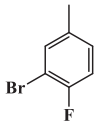	34.50±1.13	83	12.89±0.33	79
11	2,4-dichlorophenyl 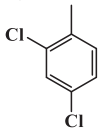	40.65±1.02	98	12.08±1.47	74
12	4-chloro-3-nitrophenyl 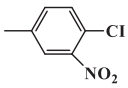	38.26±1.52	92	11.15±0.98	69
BHT		-	-	5.68±0.22	35
Caffeine		6.41±0.36	15	-	-
DMSO		41.53±0.99	100	16.25±1.45	100

LPO: Lipid peroxidation, EROD: 7-ethoxyresorufin O-deethylase, SD: Standard deviation, BHT: Butylated hydroxytoluene, DMSO: Dimethyl sulphoxide

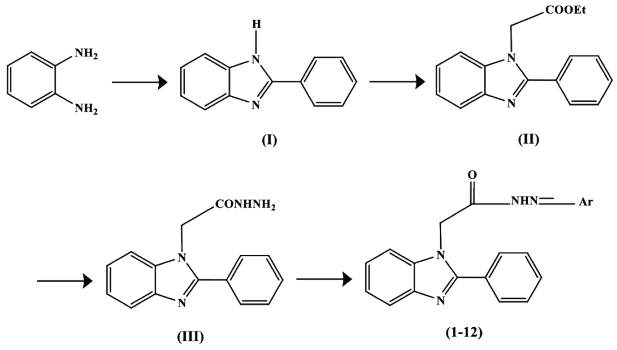

Scheme 1. Synthetic route to compounds **1-12**

which can be measured spectrofluorimetrically. 1 mL of typical optimized reaction mixture contains 0.2 mg of rat liver microsomal protein, 1.0 mM 7-ethoxyresorufin as a substrate, 100 mM Tris-HCl buffer (pH 7.8), 12 mM albumin, 10^{-3} M test compound, and an NADPH-generating system consisting of 2.5 mM glucose-6-phosphate, 14.2 mM potassium phosphate buffer (pH 7.8), 2.5 mM $MgCl_2$, 0.25 mM $NADP^+$, and 1.0 U of glucose-6-phosphate dehydrogenase. The reaction was initiated by the addition of the NADPH-generating system and then allowed to incubate at 37°C for 5 min. After incubation, the reaction was stopped by the addition of 3 mL of ice-cold methanol and then centrifuged at 5 000 rpm for 20 min to remove the denatured proteins. Finally, the absorbance was measured spectrofluorimetrically at the excitation wavelength of 538 nm and the emission wavelength of 587 nm. Whilst caffeine was used as a standard, the control used in this assay was DMSO.

RESULTS

The antioxidant effects of synthesised compounds on the rat liver microsomal NADPH-dependent LPO levels were ascertained by quantifying the amount of 2-TBARS formed in the reaction (Table 1). The results indicated that all synthesised compounds at a concentration of 10^{-3} M had LPO inhibitory activity except compound **6**, which contains thiophene, that well-known isoster of the phenyl ring as an aryl group, and the rates were in the range of 15-57%. Compounds **2**, **4**, **5**, **9**, and **12** have moderate inhibitory activity on LPO levels in the range of 31-45%. The most active compound, **3**, bearing a *p*-bromophenyl substituent at the second position of the benzimidazole ring, caused 57% inhibition of LPO level, while BHT displayed 65% inhibition at the same concentration.

The *in vitro* effects of compounds on rat liver microsomal EROD activity were also tested. The results showed that none of the synthesised compounds had a marked inhibitory effect on EROD activity. Almost all the compounds displayed slightly inhibitory activities (2-20%) on EROD when the value of caffeine was 85% (Table 1).

DISCUSSION AND CONCLUSION

In our previous studies, we described the synthesis and antioxidant effects of 2-[2-(4-chlorophenyl)benzimidazole-1-yl]-N-(2-arylmethylene amino)] acetamides on EROD activity and LPO levels.[21,33] When compared with the results obtained from these studies, benzimidazoles carrying a 4-chloro phenyl ring at the second position were found to be more effective than the benzimidazole counterpart carrying nonsubstituted phenyl rings for both assays.

Conflicts of interest: No conflict of interest was declared by the authors. The authors alone are responsible for the content and writing of the paper.

REFERENCES

1. Grune T. Oxidants and antioxidant defence systems. The Handbook of Environmental Chemistry Vol. 2: Reactions, Processes; Springer, Berlin, 2005.
2. Huang D, Ou B, Prior RL. The chemistry behind antioxidant capacity assays. J Agric Food Chem. 2005;53:1841-1856.
3. Halliwell B, Chirico S. Lipid peroxidation: its mechanism, measurement, and significance. Am J Clin Nutr. 1993;57:715S-25S.
4. Cadenas E, Packer L. Handbook of Antioxidants. 2nd ed. Revised and Expanded; Marcel Dekker: New York-Basel, 2002.
5. Ayhan-Kilcigil G, Tuncbilek M, Altanlar N, Goker H. Synthesis and antimicrobial activity of some new benzimidazole carboxylates and carboxamides, Il Farmaco. 1999;54:562-565.
6. Kus C, Sozudonmez F, Altanlar N. Synthesis and antimicrobial activity of some novel 2-[4-(substituted piperazin-/piperidin-1-ylcarbonyl) phenyl]-1H-benzimidazo-le derivatives. Arch Pharm Chem Life Sci. 2009;342:54-60.
7. Han-Bo L, Wei-Wei G, Vijai Kumar RT, Cheng-He Z, Rong-Xia G. Novel amino-pyrimidinyl benzimidazoles as potentially antimicrobial agents: Design, synthesis and biological evaluation. Eur J Med Chem. 2018;143:66-84.
8. Alp M, Goker H, Brun R, Yildiz S. Synthesis and antiparasitic and antifungal evaluation of 2'-Arylsubstituted-1H,1'H- [2,5']bisbenzimidazolyl-5-carboxamidi-nes. Eur J Med Chem. 2009;44:2002-2008.
9. Goker H, Ayhan-Kilcigil G, Tuncbilek M, Kus C, Ertan R, Kendi E, Ozbey S, Fort M, Garcia C, Farré A. Synthesis and antihistaminic H1-Activity of 1,2,5(6)-Tri-substituted benzimidazoles. Heterocycles. 1999;51:2561-2573.
10. Al-Douh Mh, Sahib H, Osman H, Hamid S, Salhimi S. Anti-proliferation effects of benzimidazole derivatives on Hct-116 colon cancer and mcf-7 breast cancer cell Lines. Asian Pac J Cancer P. 2012;13:4075-4079.
11. Yadav S, Sinha D, Sing KS, Singh K. Novel benzimidazole analogs as ınhibitors of EGFR tyrosine kinase. Chem Biol Drug Des. 2012;80:625-630.
12. Hu Z, Ou L, Li S, Yang L. Synthesis and biological evaluation of 1-cyano-2-amino-benzimidazole derivatives as a novel class of antitumor agents. Med Chem Res. 2014;23:3029-3038.
13. Demirel S, Ayhan Kilcigil G, Kara Z, Guven B, Onay Besikci A. Synthesis and pharmacologic evaluation of some benzimidazole acetohydrazide derivatives as EGFR inhibitors. Turk J Pharm Sci. 2017;14:285-289.
14. Jawaid AM, Anees AS, Ahsan AK, Zulphikar A. Design, synthesis, docking and QSAR study of substituted benzimidazole linked oxadiazole as cytotoxic agents. Eur J Med Chem. 2017;126:853-869.

15. Cheong JF, Zaffagni M, Chung I, Xu Y, Wang Y, Jernigan FE, Zetter BR, Sun L. Synthesis and anticancer activity of novel water soluble benzimidazole carbamates. Eur J Med Chem. 2018;144:372-385.

16. Nakano H, Inoue T, Kawasaki N, Miyataka H, Matsumoto H, Taguchi T, Inagaki N, Nagai H, Satoh T. Synthesis and biological activities of novel antiallergic agents 5-lipoxygenase ınhibiting action. Bioorg Med Chem. 2000;8:373-380.

17. Can Eke B, Puskullu MO, Buyukbingol E, Iscan M. Study on the antioxidant capacities of some benzimidazoles in rat tissues. Chem Biol Interact. 1998;113:65-77.

18. Ayhan-Kilcigil G, Kus C, Coban T, Can-Eke B, Iscan M. Synthesis and anti-oxidant properties of novel benzimidazole Derivatives. J Enzym Inhib Med Chem. 2004;19:129-135.

19. Ayhan-Kilcigil G, Kus C, Coban T, Can-Eke B, Ozbey SM. Iscan. Synthesis, Antioxidant and Radical Scavenging Activities of Novel Benzimidazoles. J Enzym Inhib Med Chem. 2005;20:503-514.

20. Ayhan-Kilcigil G, Kus C, Ozdamar ED, Can-Eke B, Iscan M. Synthesis and antioxidant capacities of some new benzimidazole derivatives. Arch Pharm. 2007;340:607-611.

21. Ayhan-Kilcigil G, Gurkan S, Coban T, Ozdamar ED, Can-Eke B. Synthesis and evaluation of antioxidant properties of novel 2-[2-(4-chlorophenyl) benzimi-dazole-1-yl]-n-(2-arylmethylene amino) acetamides and 2-[2-(4-chlorophenyl) benzimidazole-1-yl]-n-(4-oxo-2-aryl-thiazolidine-3-yl) acetamides-I. Chem Bio Drug Des. 2012;79:869-877.

22. Ayhan-Kilcigil G, Kus C, Coban T, Can-Eke B, Ozdamar ED, Can-Eke B. Identification of a novel series of n-phenyl-5-[(2-phenylbenzimidazol-1-yl)methyl]-1,3,4-oxadiazol-2-amines as potent antioxidants and radical scavengers. Arch Pharm. 2014;347:276-282.

23. Kus C, Ayhan-Kilcigil G, Can-Eke B, Iscan M. Synthesis and antioxidant properties of some novel benzimidazole derivatives on lipid peroxidation in the rat liver. Arch Pharm Res. 2004;27:156-163.

24. Kus C, Ayhan-Kilcigil G, Ozbey S, Kaynak FB, Kaya M, Coban T, Can-Eke B. Synthesis and antioxidant properties of novel n-methyl-1,3,4-thiadiazol-2-amine and 4-methyl-2h-1,2,4-triazole-3(4h)-thione derivatives of benzimidazole class. Bio Med Chem. 2008;16:4294-4303.

25. Kerimov I, Ayhan-Kilcigil G, Can-Eke B, Altanlar N, Iscan M. Synthesis, antifungal and antioxidant screening of some novel benzimidazole derivatives. J Enzym Inhib Med Chem. 2007;22:696-701.

26. Kerimov I, Ayhan-Kilcigil G, Ozdamar ED, Can-Eke B, Coban T, Ozbey S, Kazak C. Design and one-pot and microwave-assisted synthesis of 2-amino/5-aryl-1,3,4-oxadiazoles bearing a benzimidazole moiety as antioxidants. Arch Pharm. 2012;3457:549-556.

27. Lowry OH, Rosebrough NJ, Farr AL, Randall RJJ. Protein measurement with the Folin phenol reagent. Biol Chem. 1951;193:265-275.

28. Iscan M, Arinc E, Vural N, Iscan MY. In vivo effects of 3-methylcholantrene, phenobarbital, pyretrum and 2.4.5-T isooctylester on liver, lung and kidney microsomal mixed-function oxidase system of guinea-pig: a comparative study. Comp Biochem Physiol. 1984;77:77-190.

29. Wills ED. Mechanisms of lipid peroxide formation in animal tissues. Biochem J. 1966;99:667-676.

30. Wills ED. Lipid peroxide formation in microsomes. Relationship of hydroxylation to lipid peroxide formation. Biochem J. 1969;113:333-341.

31. Bishayee S, Balasubramanian AS. Lipid peroxide formation in rat brain. J Neurochem. 1971;18:909-920.

32. Burke MD, Thompson S, Elcombe CR, Halpert J, Haaparanta T, Mayer RT. Ethoxy-, pentoxy- and benzyloxyphenoxazones and homologues: a series of substrates to distinguish between different induced cytochromes P-450. Biochem Pharmacol. 1985;34:3337-3345.

33. Alp AS, Kilcigil GA, Ozdamar ED, Coban T, Eke B. Synthesis and evaluation of antioxidant activities of novel 1,3,4-oxadiazole and imine containing 1H-benzimidazoles. Turk J Chem. 2015;39:42-53.

Turk J Pharm Sci 2020;17(6):631-637
DOI: 10.4274/tjps.galenos.2019.68725

ORIGINAL ARTICLE

Evaluation of the Methylation and Acetylation Profiles of Dinitroaniline Herbicides and Resveratrol on the V79 Cell Line

Dinitroanilin Herbisitlerin ve Resveratrolün Metilasyon ve Asetilasyon Profillerinin V79 Hücre Hattında Değerlendirilmesi

Zehra SARIGÖL KILIÇ[1], Tuğbagül ÇAL[2], Ülkü ÜNDEĞER BUCURGAT[2]*

[1]Ammon Analytical Laboratory, Linden, USA
[2]Hacettepe University Faculty of Pharmacy, Department of Pharmaceutical Toxicology, Ankara, Turkey

ABSTRACT

Objectives: Herbicides are among the most widely used pesticide compounds for plant growth control worldwide. Risk assessment of the dinitroaniline-derived herbicides pendimethalin and trifluralin is important for foodborne or other means of exposure. In this study, we aimed to evaluate the methylation and acetylation profiles of pendimethalin and trifluralin, which we have high levels of exposure to in various ways. Furthermore, we also determined the protective effect of resveratrol, an antioxidant compound, against the possible toxic effects of these pesticides.

Materials and Methods: The effects of pendimethalin and trifluralin alone (25, 50, 100 µM) and in combination with resveratrol (100 µM) on DNA methyltransferase (DNMT1) 1, 3a, and 3b; and histone deacetylase (*HDAC*) *1* and *HDAC3* gene expression were evaluated by real-time polymerase chain reaction.

Results: According to the results, pendimethalin caused a significant decrease in DNMT1, 3a, 3b and HDAC expressions at all concentrations, whereas HDAC1 and 3 expression was increased at the concentration of 25 µM, when applied together with resveratrol. There were no changes in DNMT1 or 3b expression levels. Unlike pendimethalin, trifluralin increased DNMT1 expression in a concentration-dependent manner. While DNMT3a and DNMT3b expression levels increased significantly, HDAC1 and 3 expression levels did not change significantly. The expression levels of HDAC1 and HDAC3 increased at all concentrations of trifluralin combination with resveratrol. Moreover, DNMT levels increased at the concentrations of 50 and 100 µM.

Conclusion: Epigenetic gene expression results showed that pendimethalin and trifluralin might cause tissue function loss and chromosome damage as a result of direct effects on cell viability by causing expression level changes in all studied genes. It can also be concluded that the changes that occur in gene expression may induce tumor development. Further studies are needed to elucidate the possible toxicity mechanisms of these herbicides, considering the relationship between epigenetic changes and various diseases.

Key words: Pendimethalin, trifluralin, epigenetic, DNA methyltransferase, histone deacetylase

ÖZ

Amaç: Herbisitler, dünya genelinde bitki büyüme kontrolü için en yaygın kullanılan pestisit bileşiklerindendir. Dinitroanilin türevi herbisitlerden olan pendimetalin ve trifluralinin risk değerlendirmesinin yapılması, gıda kaynaklı veya diğer yollardan gerçekleşen maruziyetler açısından önemlidir. Bu çalışmada, çeşitli yollarla yüksek düzeylerde maruz kaldığımız pendimetalin ve trifluralinin metilasyon ve asetilasyon profillerini değerlendirmeyi amaçladık. Ayrıca, bir antioksidan bileşik olan resveratrolün, bu pestisitlerin olası toksik etkilerine karşı koruyucu etkisini belirledik.

Gereç ve Yöntemler: Pendimetalin ve trifluralinin tek başlarına (25, 50, 100 µM) ve resveratrol (100 µM) ile kombinasyon halinde DNA metiltransferaz (DNMT) 1, 3a, 3b; histon deasetilaz (*HDAC*) *1* ve *HDAC3* gen ekspresyonları gerçek zamanlı polimeraz zincir reaksiyonu yöntemiyle değerlendirilmiştir.

Bulgular: Sonuçlara göre pendimetalin tüm konsantrasyonlarda DNMT1, 3a, 3b ve HDAC ekspresyonlarında anlamlı ölçüde azalmaya neden olurken, resveratrol ile birlikte uygulandığında HDAC1 ve 3 ekspresyonları 25 µM konsantrasyonunda artmıştır. DNMT1 ve 3b ekspresyon düzeylerinde ise değişiklik olmamıştır. Pendimetalinin aksine, trifluarin DNMT1 ekspresyonunu konsantrasyonla bağımlı olarak artırmıştır. DNMT3a ve DNMT3b

This manuscript was presented at the 52nd Congress of the European Societies of Toxicology (EUROTOX) Fibes Congress Center Seville, Spain, 4th-7th September 2016.

*Correspondence: E-mail: uundeger@hacettepe.edu.tr, Phone: +90 535 368 53 91 ORCID-ID: orcid.org/0000-0002-6692-0366
Received: 11.09.2019, Accepted: 31.10.2019

ekspresyon düzeylerinde de anlamlı artış gözlenirken, HDAC1 ve 3 düzeylerinde anlamlı değişiklik gözlenmemiştir. Trifluarinin resveratrol ile kombinasyonunda ise, HDAC1 ve HDAC3 ekspresyon düzeyleri tüm konsantrasyonlarda artış göstermiştir. Ayrıca, DNMT düzeyleri 50 ve 100 µM konsantrasyonlarında artmıştır.

Sonuç: Epigenetik gen ekspresyonu sonuçları, pendimetalin ve trifluralinin çalışılan tüm genlerde ekspresyon düzeylerinde değişikliklere neden olarak hücre canlılığı üzerindeki doğrudan etkilerinin bir sonucu ile doku fonksiyon kaybına ve kromozom hasarına neden olabilir. Ayrıca, gen ifadelerinde meydana gelen değişikliklerin tümör gelişimini indükleyebileceği sonucuna varılabilir. Epigenetik değişikliklerin çeşitli hastalıklarla ilişkisi düşünülerek bu herbisitlerin olası toksisite mekanizmalarının aydınlatılması için ileri çalışmalara ihtiyaç bulunmaktadır.

Anahtar kelimeler: Pendimetalin, trifluralin, epigenetik, DNA metiltransferaz, histon deasetilaz

INTRODUCTION

The most important problem for humans since the establishment of residential life has been to produce sufficient nutrients. For this purpose, it is necessary to eliminate insects, fungi, weeds, and other harmful organisms that damage crops in order to increase the quantity and quality of the product. It is also important to combat these pests in terms of health, given the fact that they spread diseases.[1] Although the use of pesticides is necessary, toxic effects can be observed in organisms and in the environment as a result of widespread and uncontrolled use. Due to incorrect or careless use of pesticides, cases of mass poisoning can occur. In addition, long-term pesticide exposure is linked to cancer, immune system damage, and reproductive toxicity.[2]

Herbicides, which are among the most commonly used pesticide compounds in the world, are chemical compounds or cultured biological organisms controlling or suppressing plant growth.[3] Pendimethalin and trifluralin are dinitroaniline herbicides that provide the control of certain broad-leaf and grassy weeds inhibiting mitosis.[4-6] These herbicides have been used on vegetables, tobacco, oil seed, ornamentals, tomatoes, and cotton for a long time.[4,5] For this reason, they can affect health via environmental pollution or diet.[7]

Pendimethalin and trifluralin synthesis can cause the formation of reactive compounds known as nitrosamines. Nitrosamines are alkylating agents and can cause DNA damage by formation of adducts.[8] Additionally, epigenetic changes, which are basically related to DNA methylation and histone acetylation mechanisms, are as important as genetic changes because of the 1 genome/n epigenomes relation. The genome-epigenome relationship is thought to play an active role in basic biological functions such as cell viability, cell division, cell differentiation, and phenotypic changes.[9] Although epigenetic research has focused on embryonic development, aging, and cancer, recent research has been advancing in various areas such as the immune system, cardiovascular system, neurodegenerative diseases, obesity, and diabetes.[10,11]

In the present study, the epigenetic potential of pendimethalin and trifluralin on Chinese hamster lung fibroblast (V79) cells were investigated. We evaluated the DNA methyltransferase (DNMT) 1, 3a, and 3b; and histone deacetylase (HDAC) 1 and 3 levels on V79 cells after 24 h treatment of pendimethalin and trifluralin at the concentrations of 25, 50, and 100 µM, which were determined based on our previous study results from a neutral red uptake assay and comet assay.[12] The effects of resveratrol, a strong antioxidant compound, were also examined at the concentration of 100 µM.

MATERIALS AND METHODS

Pendimethalin, trifluralin, and resveratrol solution preparation

Pendimethalin (98.8% purity, CAS no: 40487-42-1), trifluralin (98.8% purity, CAS no: 1582-09-8), and resveratrol (99% purity, CAS no: R5010) were purchased from Sigma-Aldrich. Pendimethalin stock solution (500 mM) was prepared in dimethyl sulfoxide (DMSO): olive oil (1:3, v/v), and trifluralin (500 mM) and resveratrol stock solution (0.5 mM) were prepared in phosphate buffered saline containing DMSO [final DMSO concentration was 1% (v/v)].

Cell culture

V79 cells obtained from the American Type Culture Collection (ATCC; Rockville, MD, USA) were incubated in RPMI 1640 medium supplemented with 1% penicillin-streptomycin solution, 10% heat-inactivated fetal bovine serum (Lot: 094M3288), and 2 mM L-glutamine at 37°C and in 5% CO_2 for 24 h. After 24 h, the cells were harvested and were transferred to 6 well plates as 30,000 cells/2 mL medium of each. Pendimethalin and trifluralin solutions were added to the wells at the concentrations of 25, 50, and 100 µM after 24 h. Moreover, 100 µM resveratrol was used as a single concentration and additionally added to the concentrations of pendimethalin and trifluralin. For the negative control, 1% DMSO and 1% DMSO/3% olive oil were used. The cells were incubated for 24 h and harvested from the wells and centrifuged at 1000 rpm for 5 min.

Evaluation of gene expression profiles by reverse transcription-polymerase chain reaction (RT-PCR) assay

RNA isolation was performed according to the instructions of the RNeasy Mini Kit (QIAGEN). The cell suspensions were filtrated using a gDNA eliminator column after centrifugation. Then they were transferred to the RNeasy spin column and washed with the solutions as given in the kit procedure.

The measurement of the amount and quality of the eliminated RNA samples was performed by Maestrogen Nanodrop. Briefly, 1 µL of the sample was loaded to the base portion fiber terminal. All the samples' OD 260/280 ratios were found in the range of 1.6-1.8.

For the purpose of synthesizing cDNA from the RNA samples, an RT^2 First Strand Kit (QIAGEN) was used according to the instructions. The denaturation of the RNA samples was performed at 42°C for 5 min in the qRT-PCR device. To preserve linearity, the samples were placed on a cold surface. After that, reverse-transcription enzymes were added to the samples and the cDNA synthesis process was performed at 42°C for 15 min and 90°C for 5 min. The synthesized cDNA samples were stored at -20°C. The PCR primers used are listed in Table 1.

For measuring the expression levels of genes, cDNA samples were mixed with RT² SYBR Green qPCR MasterMix and RT² qPCR primers (DNMT1, DNMT3a, DNMT3b, HDAC1, HDAC3, and PPIA) and the expression performed with the qRT-PCR device under the conditions of hold at 95°C 15 min and cycle at 95°C 15 s and 60°C 30 s, for 40 cycles. The results were recorded at 60°C. The threshold limit was set to 0.05 and the cycle threshold (CT) values of the samples were calculated (Table 1).[13,14]

Statistical analysis

Statistics of the CT values were prepared using the online-based program RT² profiler PCR Data Analysis 3.5. The ΔΔCT method was used to interpret the gene expression data.[15] When evaluating the results, the upper limit CT value was taken as 35. Values higher than 35 were evaluated as 35. All experiments were performed twice.

RESULTS

Effects of trifluralin on gene expression

According to the ΔΔCT values, DNMT1 expression in V79 cells increased at a higher level and concentration relative to the control group with 24 h incubation of trifluralin. The levels of DNMT3a and 3b only increased significantly at high concentration. There were no significant changes in HDAC1 or 3 levels.

When resveratrol was administered alone, the levels of DNMT1, 3a, and 3b; and HDAC1 increased significantly compared to the control, but HDAC3 levels remained unchanged.

Furthermore, when trifluralin and resveratrol were co-administered, HDAC1 and 3 expression levels were significantly increased at all concentrations. DNMT levels were increased in 25 and 50 μM trifluralin and resveratrol, whereas 100 μM trifluralin and resveratrol were low in expression.

Generally, when the results of fold regulation and biological significance of trifluralin and resveratrol were examined, a significant increase in expression was observed in all genes except HDAC3 when resveratrol was administered alone. It was observed that trifluralin generally decreased HDAC1 and 3 expression. When trifluralin was combined with resveratrol, it caused an increase in HDAC1 and 3 expression, except 100 μM trifluralin and resveratrol administration. Additionally, DNMT1 showed a significant increase in all studied concentrations, whereas DNMT3a and 3b expression levels increased when 100 μM trifluralin was given. DNMT3b decreased at all concentrations when co-administered with resveratrol, while DNMT3a was significantly reduced only when 25 μM trifluralin and 100 μM resveratrol were co-administered.

The ΔCT, ΔΔCT, fold change, and fold regulation values of the genes are given in Tables 2-5.

Effects of pendimethalin on gene expression

When ΔΔCT values were compared, it was observed that DNMT and HDAC expression levels were significantly decreased in all concentrations of pendimethalin. Moreover, DNMT1 and HDAC1 and 3 expression levels were increased significantly at only 25 μM pendimethalin concentration when given together with resveratrol. However, all gene expression was significantly increased when resveratrol was administered alone.

When the pendimethalin and resveratrol fold-regulation and biological significance results were evaluated, it was seen that

Table 1. Gene sequences of primers[13,14]

Gene	Forward	Reverse
DNMT1	5'-AAC CTT CAC CTA GCC CCA G-3'	5'-CTC ATC CGA TTT GGC TCT TCA-3'
DNMT3a	5'-CGA CCC ATG CCA AGA CTC ACC TTC CAG-3'	5'- CCT GGT GGA ATG CAC TGC AGA AGG A-3'
DNMT3b	5'-TAC ACA GAC GTG TCC AAC ATG GGC-3'	5'-GGA TGC CTT CAG GAA TCA CAC CTC-3'
HDAC1	5'-CTG TCC GGT ATT TGA TGG CT-3'	5'-CAC GAA CTC CAC ACA CTT GG-3'
HDAC3	5'-TCT GAG GAC TAC ATC GAC TCC-3'	5'-GTC GCC ATC ATA GAA CTC AT TG-3'
PPIA	5'-ATG GTC AAC CCC ACC GTG T-3'	5'-TCT GCT GTC TTT GGG ACC TTG TC-3'

DNMT: DNA methyltransferase, HDAC: Histone deacetylase, PPIA: Peptidylprolyl isomerase A

Table 2. ΔCT values of trifluralin and resveratrol the values are expressed in mean ± standard deviation format

Gene	Control (1% DMSO)	r 100	t 25	t 50	t 100	t 25 + r 100	t 50 + r 100	t 100 + r 100
PPIA	0	0	0	0	0	0	0	0
DNMT1	11.29±2.55	3.465±19.70	6.755±0.346	5.085±2.84	4.67±0.226	3.855±16.94	2.07±14.07	4.785±14.61
DNMT3a	5.68±13.94	2.48±21.10	6.754±0.347	6.375±1.02	4.68±0.225	9.375±22.21	6.4±17.90	6.42±13.50
DNMT3b	7.3±14.96	3.18±20.11	6.756±0.344	6.374±1.02	4.65±0.224	9.135±22.54	9.66±18.76	24.305±3.81
HDAC1	5.275±13.88	2.83±20.60	6.753±0.347	6.373±1.01	4.68±0.227	(-) 3.93±5.99	(-) 6.905±5.16	(-) 7.11±21.41
HDAC3	2.54±8.71	2.565±19.93	6.755±0.345	6.376±1.04	4.69±0.223	(-) 6.36±1.61	(-) 7.875±0.86	(-) 6.115±3.58

The control gene PPIA value was taken as 0. The concentrations (25, 50, and 100 μM) of trifluralin are shown as t 25, t 50, and t 100. The concentration (100 μM) of resveratrol is shown as r 100), DNMT: DNA methyltransferase, *HDAC: Histone deacetylase, PPIA: Peptidylprolyl isomerase A,* DMSO: Dimethyl sulfoxide, CT: Cycle threshold

Table 3. ΔΔCT values of trifluralin and resveratrol the values are expressed as ΔΔCT values

Gene	Control (1% DMSO)	r 100	t 25	t 50	t 100	t 25 + r 100	t 50 + r 100	t 100 + r 100
PPIA	1	1	1	1	1	1	1	1
DNMT1	0.000399	0.090559	0.009259	0.029462	0.039282	0.069108	0.238159	0.036272
DNMT3a	0.019505	0.179244	0.009258	0.012049	0.039283	0.001506	0.011842	0.011679
DNMT3b	0.006346	0.110338	0.009260	0.012048	0.039280	0.001779	0.001236	0
HDAC1	0.025827	0.140632	0.009257	0.012047	0.039283	15.242208	119.842848	70.007239
HDAC3	0.171943	0.168989	0.009259	0.012050	0.039284	82.139257	234.753035	69.310403

The control gene PPIA value was taken as 1. The concentrations (25, 50, and 100 μM) of trifluralin are shown as t 25, t 50, and t 100. The concentration (100 μM) of resveratrol is shown as r 100), *DNMT: DNA methyltransferase, HDAC: Histone deacetylase, PPIA: Peptidylprolyl isomerase A,* DMSO: Dimethyl sulfoxide, CT: Cycle threshold

Table 4. The fold change values of trifluralin and resveratrol the control gene PPIA value was taken as 1

Gene	r 100	t 25	t 50	t 100	t 25 + r 100	t 50 + r 100	t 100 + r 100
PPIA	1	1	1	1	1	1	1
DNMT1	226.7565+	23.1831+	73.7719+	98.36+	173.0446+	596.343+	90.8239+
DNMT3a	9.1896+	0.4747*	0.6177	2.0139+	0.0772*	0.6071	0.5987
DNMT3b	17.3878+	1.459	1.8987	6.1903+	0.2803*	0.1948*	0*
HDAC1	5.4453+	0.3585*	0.4665*	1.521	590.1754+	4640.2924+	380.2803+
HDAC3	0.9828	0.0538*	0.0701*	0.2285*	477.7129+	1365.2978+	403.1017+

The concentrations (25, 50, and 100 μM) of trifluralin are shown as t 25, t 50, and t 100. The concentration (100 μM) of resveratrol is shown as r 100. A significant increase in gene expression is shown with +, a decrease in gene expression is shown with *. P<0.05 means significantly different from the negative control, *DNMT: DNA methyltransferase, HDAC: Histone deacetylase, PPIA: Peptidylprolyl isomerase A*

Table 5. The fold regulation values and biological significance of trifluralin and resveratrol the control gene PPIA value was taken as 1

Gene	r 100	t 25	t 50	t 100	t 25 + r 100	t 50 + r 100	t 100 + r 100
PPIA	1	1	1	1	1	1	1
DNMT1	226.757+	23.1831+	73.7719+	98.36+	173.0446+	596.3436+	90.8239+
DNMT3a	9.1896+	-2.1067*	-1.6189	2.0139+	-12.9511*	-1.6472	-1.6702
DNMT3b	17.3878+	1.459	1.8987	6.1903+	- 3.5677*	-5.1337*	-131527.049*
HDAC1	5.4453+	-2.7895*	-2.1435*	1.521	590.1754+	4640.2924+	-3.5677*
HDAC3	-1.0175	-18.57*	-14.271*	- 4.3772*	477.7129+	1365.2978+	403.1017+

The concentrations (25, 50, and 100 μM) of trifluralin are shown as t 25, t 50, and t 100. The concentration (100 μM) of resveratrol is shown as r 100. A significant increase in gene expression is shown with +, a decrease in gene expression is shown with *. P<0.05 means significantly different from the negative control, *DNMT: DNA methyltransferase, HDAC: Histone deacetylase, PPIA: Peptidylprolyl isomerase A*

Table 6. ΔCT values of pendimethalin and resveratrol the values are expressed in mean ± standard deviation format

Gene	Control (1% DMSO + %3 olive oil)	p 25	p 50	p 100	p 25 + r 100	p 50 + r 100	p 100 + r 100	r 100
PPIA	0	0	0	0	0	0	0	0
DNMT1	1.27±11.07	8.88±2.12	11.13±0.65	7.58±0.52	0.98±13.74	6.98±0.12	7.33±2.03	(-) 10.47±0
DNMT3a	5.545±16.22	10.28±0.14	11. 835±0.34	13.33±0.41	18.09±2.39	14.86±0.18	12.58±1.86	2.11±20.57
DNMT3b	5.36±18.69	10.215±0.049	11. 836±0.33	13.32±0.40	5.43±21.75	15.025±0.049	15.215±0.64	2.81±19.58
HDAC1	2.405±15.37	10.27±0.13	11. 834±0.34	13.34±0.41	(-) 8.165±2.05	13.83±1.06	14.26±0.70	(-) 11.74±0
HDAC3	8.485±0.34	9.53±0.91	11.02±0.80	10.765±1.05	(-) 0.545±11.32	9.175±0.17	8.395±1.09	2.21±20.43

The control gene PPIA value was taken as 0. The concentrations (25, 50, and 100 μM) of pendimethalin are shown as p 25, p 50, and p 100. The concentration (100 μM) of resveratrol is shown as r 100, DMSO: Dimethyl sulfoxide, *DNMT: DNA methyltransferase, HDAC: Histone deacetylase, PPIA: Peptidylprolyl isomerase A, CT: Cycle theshold*

pendimethalin caused a significant decrease in expression of all genes in all concentrations, whereas resveratrol increased expression in all genes when administered alone.

Additionally, when the biological significance of pendimethalin and resveratrol co-administered concentrations was evaluated, HDAC1 and 3 expression levels were increased with the effect

of resveratrol at a concentration of 25 μM of pendimethalin, but DNMT3a levels were significantly decreased. There were no changes in DNMT1 or 3b or HDAC3 levels, while expression of other genes was significantly reduced when 50 μM pendimethalin and 100 μM resveratrol were co-administered.

The ΔCT, ΔΔCT, fold change, and fold regulation values of the genes are given in Tables 6-9.

DISCUSSION

Although genetic material, which is the source of information and life of organisms, is very well protected against degradation by various mechanisms, it may be damaged by exposure to many factors, both internal and external. The DNA repair mechanisms are very active, but they are not sufficient or are repressed in some cases. These types of damage have temporary or permanent effects and may cause minor or major dysfunctions and diseases in the organism and affect future generations besides the organism first affected.

Within the scope of the present study, the possible epigenetic effects of pendimethalin and trifluralin, herbicide compounds that we are frequently exposed to in this country as well as the rest of the world, were investigated in the V79 cell line. It has been evaluated whether resveratrol, an antioxidant substance, has a protective effect on possible methylation and acetylation profile changes of these herbicides.

DNMT and HDAC expression levels were examined to investigate the effects of pendimethalin and trifluralin, dinitroaniline herbicide compounds whose genotoxicity potentials were determined,[12] on epigenetic changes. Based on the genotoxicity

Table 7. ΔΔCT values of pendimethalin and resveratrol the values are expressed as ΔΔCT values

Gene	Control (1% DMSO + 3% olive oil)	p 25	p 50	p 100	p 25 + r 100	p 50 + r 100	p 100 + r 100	r 100
PPIA	1	1	1	1	1	1	1	1
DNMT1	0.41466	0.002123	0.000446	0.005226	0.50698	0.007922	0.006215	1418.352095
DNMT3a	0.021418	0.000804	0.000274	0.000097	0.000004	0.000034	0.000163	0.231647
DNMT3b	0.024349	0.000841	0.000275	0.000096	0.023196	0.00003	0.000026	0.142595
HDAC1	0.188809	0.000803	0.000273	0.000098	287.018516	0.000069	0.000051	3420.520118
HDAC3	0.002791	0.001353	0.000482	0.000575	1.45902	0.00173	0.002971	0.216134

The control gene PPIA value was taken as 1. The concentrations (25, 50, and 100 μM) of pendimethalin are shown as p 25, p 50, and p 100. The concentration (100 μM) of resveratrol is shown as r 100), *DNMT: DNA methyltransferase, HDAC: Histone deacetylase, PPIA: Peptidylprolyl isomerase A, CT: Cycle threshold, DMSO: Dimethyl sulfoxid*

Table 8. The fold change values of pendimethalin and resveratrol the control gene PPIA value was taken as 1

Gene	p 25	p 50	p 100	p 25 + r 100	p 50 + r 100	p 100 + r 100	r 100
PPIA	1	1	1	1	1	1	1
DNMT1	0.0051*	0.0011*	0.0126*	1.2226	0.0191*	0.015*	3420.52+
DNMT3a	0.0376*	0.0128*	0.0045*	0.0002*	0.0016*	0.0076*	10.8153+
DNMT3b	0.0346*	0.0112*	0.004*	0.9526	0.0012*	0.0011*	5.8563+
HDAC1	0.0043*	0.0014*	0.000*	1520.1521+	0.0004*	0.0003*	18116.3+
HDAC3	0.4846*	0.1725*	0.2059*	522.7582+	0.6199*	1.0644	77.4396+

The concentrations (25, 50, and 100 μM) of pendimethalin are showed as p 25, p 50, and p 100. The concentration (100 μM) of resveratrol is shown as r 100. A significant increase in gene expression is shown with +, a decrease in gene expression is shown with *l. P<0.05 means significantly different from the negative control, *DNMT: DNA methyltransferase, HDAC: Histone deacetylase, PPIA: Peptidylprolyl isomerase A*

Table 9. The fold regulation values and biological significance of pendimethalin and resveratrol the control gene PPIA value was taken as 1

Gene	p 25	p 50	p 100	p 25 + r 100	p 50 + r 100	p 100 + r 100	r 100
PPIA	1	1	1	1	1	1	1
DNMT1	-195.361*	-929.3*	-79.3413*	1.2226	-52.3457*	-66.7178*	3420.52+
DNMT3a	-26.6304*	-78.249*	-220.5558*	-5976.1473*	-636.934*	-131.1433*	10.8153+
DNMT3b	-28.9401*	-88.955*	-250.7316*	-1.0497	-811.811*	-926.0845*	5.8563+
HDAC1	-234.753*	-689.78*	-1944.2527*	1520.1521+	-2749.5885*	-3704.3379*	18116.3+
HDAC3	-2.0634*	-5.7958*	-4.8568*	522.7582+	-1.6133	1.0644	77.4396+

The concentrations (25, 50, and 100 μM) of pendimethalin are shown as p 25, p 50, and p 100. The concentration (100 μM) of resveratrol is shown as r 100. A significant increase in gene expression is shown with +, a decrease in gene expression is showed with *. P<0.05 means significantly different from the negative control, *DNMT: DNA methyltransferase, HDAC: Histone deacetylase, PPIA: Peptidylprolyl isomerase A*

results, pendimethalin and trifluralin concentrations of 25, 50, and 100 μM were selected for study.

While pendimethalin caused a significant decrease in DNMT levels, trifluralin increased DNMT1 expression and increased all of the *DNMT* genes at a concentration of 100 μM, causing a decrease in all other genes. Embryo death was observed in mice with increased methylation in *DNMT1* gene disorder. Changes in DNMT1 expression lead to X chromosome inactivation and imprinting loss.[16] Disorders in *DNMT1* gene expression cause proliferation disorders and mitotic defects leading to cell death. These effects in human colorectal cancer cells have been clearly observed.[17] Similarly, it was reported that mouse fibroblast cells with DNMT1 defect were dragged into apoptosis via the p-53 pathway after several cell divisions,[18] and apoptosis was observed as a result of a decrease in DNMT1 expression in germ cells.[19] Studies have shown that the DNMT1 gene plays a critical role in cell proliferation and viability. In addition, DNMT1 function loss was directly associated with tumor formation, demonstrating tumor growth and chromosome instability in DNMT1-deficient mice.[20,21]

Similar to DNMT1, DNMT3a and 3b have also been reported to play a critical role in embryonic development in mice. It was observed that mouse embryos with DNMT3b deficiency died at 9.5 embryonic days and multiple developmental defects occurred; pups without DNMT3a deficiency did not develop and died shortly after birth.[22] Mutations in the *DNMT3b* gene in humans are the cause of a rare autosomal disease, immunodeficiency, centromere instability, and facial abnormalities syndrome.[23] Furthermore, mutations in the *DNMT3b* gene cause a decrease in DNA methylation specific to pericentromeric regions on chromosomes 1, 9, and 16, leading to chromosomal structure and function disorders.[24]

CpG methylation levels were found to be increased in lung cancer patients on two genes, SFTPA1 and SFTPA2, which encode surfactant protein A, associated with lung homeostasis and immunity.[25] In another study, when epigenetic changes were examined in 28 nonsmoking lung adenocarcinoma patients, it was found that methylation levels decreased in tumor tissues compared to neighboring nonmalignant tissues and methylation increased in tumor tissues in CpG islands.[26] Those findings were consistent with the results we obtained, and pendimethalin and trifluralin compounds significantly changed methylation levels.

Our evaluation of *HDAC* gene expression levels showed that both herbicidal compounds cause significant decrease in HDAC1 and 3 levels. HDAC1 and 3 consist of 93% structurally the same proteins and belong to the class I histone deacetylases group.[27,28] These genes are related to cell cycle control, cell survival, and differentiation. For this reason, the use of HDAC inhibitors for the treatment of cancer as an antineoplastic drug is contemplated.[29,30] In a study of non-small lung cancer cells, it was observed that HDAC levels were increased in cancer cells and it was possible to fight cancer cells using HDAC inhibitors.[31] However, these results are not consistent with our previous study, which was about the effects of pendimethalin and trifluralin on apoptosis and anti-apoptosis genes (p53, bax, bcl-2, casp3, casp9, and birc). According to our results, trifluralin downregulated the expression of all genes (1-500 μM), but pendimethalin upregulated bcl-2 (100 and 500 μg/mL) and birc5 (500 μg/mL) gene expression and had more effects on anti-apopitosis than trifluralin.[32] These differences in results confirm that in order to reduce the possible carcinogenic effects of pendimethalin and trifluralin in humans, the permissible values and residual limits on foods should not be exceeded.

When the change in the epigenetic expression levels due to resveratrol was examined, the capacity of resveratrol supplementation to reverse the expression changes caused by the herbicides studied was limited. Additionally, normal gene expression levels were not achieved despite resveratrol, especially in HDAC genes. Furthermore, administration of resveratrol alone led to undesirable increases in gene expression possibly as a result of the pro-oxidant effect of resveratrol.[33]

CONCLUSION

Methylation and deacetylation gene expression are among the main pathways of epigenetic changes and they are the main causes of embryonic development disorders and chronic diseases.

According to the epigenetic gene expression results, pendimethalin and trifluralin may cause tissue function loss and chromosome damage as a result of direct effects on cell viability by causing expression level changes in all studied genes. Since the groups of cells we studied were healthy lung fibroblast cells, it can be concluded that the changes that occur in gene expression may induce tumor development. Considering the concentrations used, the genotoxic effects appear to be high. However, both herbicidal compounds we investigated are considered group C, as a possible human carcinogen by the Environmental Protection Agency.

In addition to the beneficial effects of antioxidants such as resveratrol against oxidative DNA damage, there is also the risk of causing damage by pro-oxidant effects. Therefore, the use of dinitroaniline herbicides with high genotoxicity and epigenotoxicity potentials should be considered carefully and all the effects of antioxidant compounds should be examined in more detail.

ACKNOWLEDGEMENTS

This study was supported by Hacettepe University Scientific Research Projects Coordination Unit under Grant number THD-2015-5535 and by the Scientific and Technological Research Council of Turkey under Grant number 113S049.

Conflicts of interest: No conflict of interest was declared by the authors. The authors alone are responsible for the content and writing of the paper.

REFERENCES

1. Gupta P. Pesticide exposure-Indian scene. Toxicology. 2004;198:83-90.
2. Van Der Hoek W, Konradsen F, Athukorala K, Wanigadewa T. Pesticide poisoning: a major health problem in Sri Lanka. Soc Sci Med. 1998;46:495-504.
3. Grube A, Donaldson D, Kiely T, Wu L. Pesticides industry sales and usage - 2006 and 2007 Market Estimates. US EPA, Washington; 2011;15.
4. Grover R, Wolt JD, Cessna AJ, Schiefer HB. Environmental fate of trifluralin. Rev Environ Contam Toxicol. 1997;153:1-64.
5. Vighi M, Matthies M, Solomon KR. Critical assessment of pendimethalin in terms of persistence, bioaccumulation, toxicity, and potential for long-range transport. J Toxicol Environ Health B Crit Rev. 2017;20:1-21.
6. Hoffman J, Vaughn K. Mitotic disrupter herbicides act by a single mechanism but vary in efficacy. Protoplasma. 1994;179:16-25.
7. Wallace DR. Trifluralin. In: Wexler P, ed. Encyclopedia of Toxicology (3rd ed). London; Academic Press; 2014:846-848.
8. Montesano R, Hall J. Nitrosamine Metabolism and Carcinogenesis. In: Chu EHY, Generoso WM, eds. Mutation, Cancer, and Malformation. Environmental Science Research, vol 31. Boston; Springer; 1984:447-464.
9. Jiménez-Chillarón JC, Díaz R, Martínez D, Pentinat T, Ramón-Krauel M, Ribó S, Plösch T. The role of nutrition on epigenetic modifications and their implications on health. Biochimie. 2012;94:2242-2263.
10. Choi S-W, Friso S. Epigenetics: a new bridge between nutrition and health. Adv Nutr. 2010;1:8-16.
11. Niculescu MD. Nutritional epigenetics. ILAR Journal. 2012;53:270-278.
12. Sarıgöl Kılıç Z, Aydın S, Bucurgat Ündeğer Ü, Başaran N. In vitro genotoxicity assessment of dinitroaniline herbicides pendimethalin and trifluralin. Food Chem Toxicol. 2018;113:90-98.
13. Feng J, Zhou Y, Campbell SL, Le T, Li E, Sweatt JD, Silva AJ, Fan G. Dnmt1 and Dnmt3a maintain DNA methylation and regulate synaptic function in adult forebrain neurons. Nat Neurosci. 2010;13:423.
14. Chen S, Bellew C, Yao X, Stefkova J, Dipp S, Saifudeen Z, Bachvarov D, El-Dahr S. Histone deacetylase (HDAC) activity is critical for embryonic kidney gene expression, growth, and differentiation. J Biol Chem. 2011;286:32775-32789.
15. Livak KJ, Schmittgen TD. Analysis of relative gene expression data using real-time quantitative PCR and the 2-ΔΔCT method. Methods. 2001;25:402-408.
16. Sado T, Fenner MH, Tan SS, Tam P, Shioda T, Li E. X inactivation in the mouse embryo deficient for Dnmt1: distinct effect of hypomethylation on imprinted and random X inactivation. Dev Biol. 2000;225:294-303.
17. Chen T, Hevi S, Gay F, Tsujimoto N, He T, Zhang B, Ueda Y, Li E. Complete inactivation of DNMT1 leads to mitotic catastrophe in human cancer cells. Nat Genet. 2007;39:391.
18. Jackson-Grusby L, Beard C, Possemato R, Tudor M, Fambrough D, Csankovszki G, Dausman J, Lee P, Wilson C, Lander E, Jaenisch R. Loss of genomic methylation causes p53-dependent apoptosis and epigenetic deregulation. Nat Genet. 2001;27:31.
19. Takashima S, Takehashi M, Lee J, Chuma S, Okano M, Hata K, Suetake I, Nakatsuji N, Miyoshi H, Tajima S, Tanaka Y, Toyokuni S, Sasaki H, Kanatsu-Shinohara M, Shinohara T. Abnormal DNA methyltransferase expression in mouse germline stem cells results in spermatogenic defects. Biol Reprod. 2009;81:155-164.
20. Gaudet F, Hodgson JG, Eden A, Jackson-Grusby L, Dausman J, Gray JW, Leonhardt H, Jaenisch R. Induction of tumors in mice by genomic hypomethylation. Science. 2003;300:489-492.
21. Eden A, Gaudet F, Waghmare A, Jaenisch R. Chromosomal instability and tumors promoted by DNA hypomethylation. Science. 2003;300:455-455.
22. Okano M, Bell DW, Haber DA, Li E. DNA methyltransferases Dnmt3a and Dnmt3b are essential for de novo methylation and mammalian development. Cell. 1999;99:247-257.
23. Hansen RS, Wijmenga C, Luo P, Stanek AM, Canfield TK, Weemaes CM, Gartler SM. The DNMT3B DNA methyltransferase gene is mutated in the ICF immunodeficiency syndrome. Proc Natl Acad Sci USA. 1999;96:14412-14417.
24. Xu GL, Bestor TH, Bourc'his D, Hsieh CL, Tommerup N, Bugge M, Hulten M, Qu X, Russo JJ, Viegas-Péquignot E. Chromosome instability and immunodeficiency syndrome caused by mutations in a DNA methyltransferase gene. Nature. 1999;402:187.
25. Grageda M, Silveyra P, Thomas NJ, DiAngelo SL, Floros J. DNA methylation profile and expression of surfactant protein *A2* gene in lung cancer. Exp Lung Res. 2015;41:93-102.
26. Mansfield AS, Wang L, Cunningham JM, Jen J, Kolbert CP, Sun Z, Yang P. DNA methylation and RNA expression profiles in lung adenocarcinomas of never-smokers. Cancer Genet. 2015;208:253-260.
27. De Ruijter AJ, Van Gennip AH, Caron HN, Stephan K, Van Kuilenburg AB. Histone deacetylases (HDACs): characterization of the classical HDAC family. Biochem J. 2003;370:737-749.
28. Strahl BD, Allis CD. The language of covalent histone modifications. Nature. 2000;403:41.
29. Gallinari P, Di Marco S, Jones P, Pallaoro M, Steinkühler C. HDACs, histone deacetylation and gene transcription: from molecular biology to cancer therapeutics. Cell Res. 2007;17:195.
30. Dokmanovic M, Clarke C, Marks PA. Histone deacetylase inhibitors: overview and perspectives. Mol Cancer Res. 2007;5:981-989.
31. Chun SM, Lee JY, Choi J, Lee JH, Hwang JJ, Kim CS, Suh YA, Jang SJ. Epigenetic modulation with HDAC inhibitor CG200745 induces anti-proliferation in non-small cell lung cancer cells. PloS one. 2015;10:e0119379.
32. Sarıgöl Kılıç Z, Ündeğer Bucurgat Ü. The apoptotic and anti-apoptotic effects of pendimethalin and trifluralin on A549 cells *in vitro*. Turk J Pharm Sci. 2018;15:364-369.
33. De La Lastra CA, Villegas I. Resveratrol as an antioxidant and pro-oxidant agent: mechanisms and clinical implications. Biochem Soc Trans. 2007;35:1156-1160.

Turk J Pharm Sci 2020;17(6):638-644
DOI: 10.4274/tjps.galenos.2019.87094

ORIGINAL ARTICLE

Effects of Polyvinylpyrrolidone and Ethyl Cellulose in Polyurethane Electrospun Nanofibers on Morphology and Drug Release Characteristics

Elektro-Eğirme Yöntemi ile Üretilen Poliüretan Nanoliflerin Morfolojileri ve İlaç Salım Özellikleri Üzerinde Polivinilpirolidon ve Etil Selülozun Etkileri

Aslı GENÇTÜRK[1], Emine KAHRAMAN[2], Sevgi GÜNGÖR[2], Yıldız ÖZSOY[2]*, A. Sezai SARAÇ[1,3]

[1]İstanbul Technical University Faculty of Science and Letters, Department of Polymer Science and Technology, İstanbul, Turkey
[2]İstanbul University Faculty of Pharmacy, Department of Pharmaceutical Technology, İstanbul, Turkey
[3]İstanbul Technical University University Faculty of Science and Letters, Department of Nanoscience and Nanoengineering, İstanbul, Turkey

ABSTRACT

Objectives: Polyurethanes (PUs) are a popular choice for composing nanofibers due to their spinnability, biocompatibility, high chemical stability, and good mechanical and elasticity properties. The desired release behaviors are also achieved by using combinations of PUs and various polymers. In this study, we investigated effects of polyvinylpyrrolidone (PVP) and ethyl cellulose (EC) on PU electrospun nanofibers in terms of morphological structures and drug release characteristics.

Materials and Methods: Nanofibers were prepared using blends of PU with either EC or PVP in different ratios by electrospinning. The effects of PVP or EC on the morphology and diameter of the prepared nanofibers were examined with scanning electron microscope (SEM). The compatibility of the components used in the formulations of nanofibers was determined by attenuated total reflection (ATR)-fourier-transform infrared (FTIR). Donepezil hydrochloride (DNP), a water soluble compound, was selected as a model drug to examine its release characteristics from both PU/PVP and PU/EC electrospun nanofibers. *In vitro* drug release studies from electrospun nanofibers were performed according to the method defined in the monograph as the "paddle over disk method" of United States Pharmacopeia 38.

Results: The SEM images showed that addition of EC or PVP to PU solutions did not affect the generation of nanofibers, and those formed had a smooth surface without beads in nanoscale. The ATR-FTIR spectra disclosed that EC and PVP were separately incorporated into the PU matrix. The *in vitro* release data indicated that the presence of EC or PVP in PU nanofibers dramatically changed the release behavior of DNP. PU/EC nanofibers (F4) provided sustained drug release with the Korsmeyer-Peppas drug release kinetic mechanism, in which the release rate was controlled by diffusion of the drug, while all of the PU/PVP nanofibers exhibited fast drug release.

Conclusion: Overall, these characteristics of PU/EC (10/8) electrospun nanofibers has suggested their potential use as a drug carrier from which water-soluble drug release may occur in a sustained fashion.

Key words: Electrospun nanofibers, drug release, polyurethane, polyvinylpyrrolidone, ethyl cellulose

ÖZ

Amaç: Poliüretanlar (PU) eğirmelerinin kolaylığı, biyouyumlulukları, yüksek kimyasal stabiliteleri ve iyi mekanik ve elastik özelliklere sahip olmaları nedeniyle nanoliflerin kompoze edilmeleri için sıklıkla tercih edilirler. PU'lar ve çeşitli polimerlerle bileşimleri kullanılarak istenen salım davranışları da elde edilmektedir. Bu çalışmada, elektro-eğirme yöntemi ile üretilen PU nanoliflerin morfolojileri ve ilaç salım özellikleri üzerinde polivinilpirolidon (PVP) ve etil selülozun (EC) etkisini araştırdık.

Gereç ve Yöntemler: Nanolifler farklı karışımlardaki PU'nun farklı oranlarda EC veya PVP ile birlikte kullanılması ile elektro-eğirme yöntemiyle hazırlanmıştır. Hazırlanan nanoliflerin morfolojisi ve çapı üzerinde PVP veya EC'nin etkisi taramalı elektron mikroskobu (SEM) ile incelenmiştir. Nanolif formülasyonlarında kullanılan maddelerin geçimliliği zayıflatılmış toplam yansıma üniteli fourier dönüşümlü kızılötesi spektroskopisi (ATR-FTIR) ile belirlenmiştir. Hem PU/PVP hem de PU/EC nanoliflerin salım davranışlarını incelemek için suda çözünen bir madde olan donepezil hidroklorür (DNP) model ilaç olarak seçilmiştir. Elektro-eğirme yöntemi ile hazırlanan nanoliflerden ilaç salım çalışmaları Amerikan Farmakopesi 38'de tanımlanan "disk üzerinde palet yöntemine" göre yapılmıştır.

*Correspondence: E-mail: yozsoy@istanbul.edu.tr, Phone: +90 212 440 00 00-13498 ORCID-ID: orcid.org/0000-0002-9110-3704
Received: 03.09.2019, Accepted: 31.10.2019

Bulgular: SEM görüntüleri, EC'nin veya PVP'nin PU çözeltisine eklenmesinin nanolif oluşumunu etkilemediğini; oluşan nanoliflerin pürüzsüz yüzeye sahip olduğunu ve boncuk şeklinde yapılar içermediğini göstermiştir. ATR-FTIR spektrumları ise EC ve PVP'nin ayrı ayrı PU matrikse yüklendiğini ortaya koymaktadır. *İn vitro* salım verileri, PU nanoliflerde EC veya PVP varlığının DNP'nin salım davranışını önemli ölçüde değiştirdiğini göstermiştir. PU/PVP nanolifleri sürekli ilaç salımı sergilemiş ve PU/EC nanolifleri (F4) ise salım hızının ilacın difüzyonuyla kontrol edildiği Korsmeyer-Peppas kinetik mekanizması ile uyumlu uzatılmış ilaç salımı sağlamıştır.

Sonuç: Sonuçta, elektro-eğilme yöntemiyle üretilen PU/EC (10/8) nanoliflerin sürekli şekilde suda çözünür ilaç salımı sağlayan özellikleri, bu yapıların ilaç taşıyıcısı olarak potansiyel kullanımları olabileceğini göstermektedir.

Anahtar kelimeler: Elekro-eğirme yöntemi ile üretilen nanolifler, ilaç salımı, poliüretan, polivinilpirolidon, etil selüloz

INTRODUCTION

Electrospun nanofibers have attracted great attention because of their potential applications for biomedical devices, tissue engineering, biosensors, filtration, wound dressing, and enzyme immobilization in recent years.[1] They have also received considerable attention in drug delivery especially because of their high surface area to volume ratio, which might permit drug molecules to diffuse out of the matrix promptly due to the highly porous structure.[2,3] Additionally, electrospun nanofibers have other superiorities such as high drug loading capacity, cost effectiveness, and ease of fabrication.[4]

Polyurethanes (PUs) are widely used for composing nanofibers due to their spinnability, biocompatibility, chemical stability, and good mechanical and elasticity properties. They could generally be adapted for many applications such as filters, wound dressing, biosensors, biomedical devices, and tissue engineering, owing to their various structures.[5] The addition of a second component such as cellulose derivatives, polyethylene glycol, and polycaprolactone to PUs could give rise to the fabrication of a new type of nanofiber with different morphological and physical structures for special applications.[6,7] The desired release behaviors are also achieved using various polymer combinations.[8]

Ethyl cellulose (EC) is a non-ionic and physiologically inert cellulose derivative. This material, which is insoluble in aqueous media, has a moderately low swelling degree.[9] Thus, it is an appropriate compound for the production of a sustained drug release matrix[10] and does not require addition of release modifiers.[11]

Polyvinylpyrrolidone (PVP) is a nonionic, biodegradable, and biocompatible polymer produced from monomer N-vinylpyrrolidone.[12,13] It has outstanding spinnability in various solvents such as ethanol, methanol, and chloroform.[12,14] PVP has a hygroscopic property, so that it absorbs water up to 40% of its weight in atmospheric conditions and could result in unstable nanofibers. However, besides these properties, PVP is a hydrophilic polymer that leads to fast dissolution and immediate release of drugs.[15] PVP has already been used to modulate the release of drugs from nanofibers.[16] The drug release from PVP, EC, or PVP/EC nanofibers has been studied by various researchers.[17-20] However, the morphology and drug release characteristics of electrospun fibers composed of blends of PU with either EC or PVP are not yet available in the literature.

In the present study, we proposed to investigate effect of EC and PVP in PU electrospun nanofibers on morphology and drug release characteristics. At the second stage, fibers were prepared from PU and either hydrophobic polymer EC or hydrophilic polymer PVP blends in different combinations. PU/EC and PU/PVP fibers were assessed as a carrier system to determine the drug release profile. The developed PU/EC and PU/PVP nanofibers in different combinations were characterized morphologically and structurally. At the second stage, effects of EC or PVP on the release rates of donepezil hydrochloride (DNP), which is a water-soluble drug, were examined and their kinetic mechanisms were estimated based on *in vitro* release data.

MATERIALS AND METHODS

Materials

PU; Mw~93,000 g/mol was purchased from Flokser Corporation (Turkey). EC and PVP K30 were supplied by Dow (United States) and Hangzhou Sunflower Technology (China), respectively. N,N-dimethylformamide was obtained from Labkim (Turkey). DNP was given as a kind gift by Santa Farma Pharmaceutical Company (Turkey). All of the chemical materials were of analytical grade.

Production of electrospun nanofibers

Homogeneous PU solutions were prepared by dissolving PU (12.5%, w/v) in dimethylformamide. DNP was added to these clear polymer solutions and it was dissolved. Following the addition of either EC or PVP at different ratios to PU solutions (Table 1), the mixtures were stirred for 1 h to provide a homogeneous solution for electrospinning.

The conductivity of solutions was determined by a conductivity meter (Eutech Instruments, Netherlands) at 25°C. Each of the measurements was conducted at least three times.

In the electrospinning process (Figure 1), each of the mixed polymer solutions was loaded into a 10 mL syringe equipped

Table 1. Composition of nanofiber solutions

Formulation code	Ratio of PU/EC/DNP or PU/PVP/DNP	PU (g)	EC/PVP (g)	DNP (g)	Solvent (mL)
F1, F5*	10/1/1	12.5	1.25	1.25	100
F2, F6*	10/2/1	12.5	2.5	1.25	100
F3, F7*	10/4/1	12.5	5.0	1.25	100
F4, F8*	10/8/1	12.5	10.0	1.25	100

*Contains PVP instead of EC, PVP: Polyvinylpyrrolidone, PU: Polyurethane, EC: Ethyl cellulose, DNP: Donepezil hydrochloride

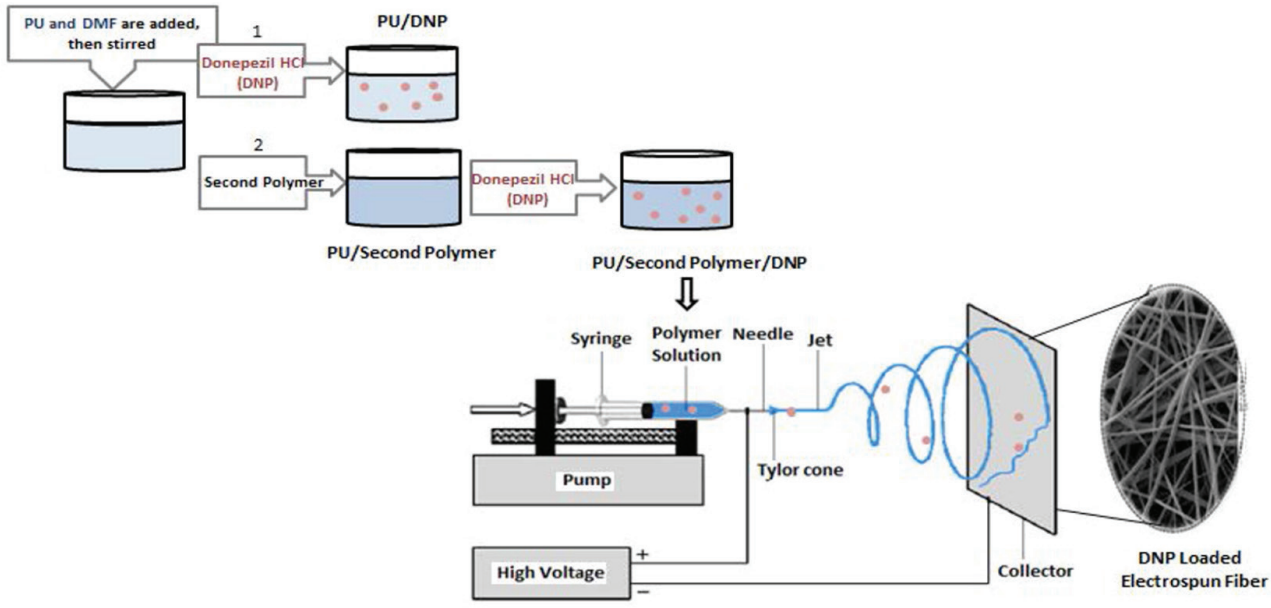

Figure 1. Schematic illustration of the setup of electrospinning and process of preparing polymer solution

PU: Polyurethane, DNP: Donepezil hydrochloride

with a metallic needle of outer diameter 0.8x38 mm. The syringe was mounted on a syringe pump (New Era Pump Systems, USA) and aluminum collector. A positive electrode of high voltage power supply (Gamma High Voltage Inc., USA) was attached to the syringe needle. The polymer solution was fixed at a rate of 1 mL/h. A high electric voltage was set to 15 kV and the distance between the needle tip and the aluminum collector was 15 cm. All solution preparations and electrospinning were performed at ambient temperature.

Morphology of electrospun nanofibers

The surface morphology of PU/EC and PU/PVP electrospun nanofibers was examined by a scanning electron microscope (SEM) (Philips-XL30 SFEG, Japan) after each of the samples was coated with a thin layer of gold/palladium alloy to render it electrically conductive. The SEM data were recorded at an accelerating voltage of 20 kV and average fiber diameter (AFD) was estimated via ImageJ by randomly measuring the diameters of 20 different nanofibers in the images for each sample.

Compatibility of components on electrospun nanofibers

The compatibility of components used in the formulations of nanofibers is crucial for the fabrication of stable nanofibers. For this reason, fourier transform infrared spectroscopy (FTIR) spectroscopic assessments of the nanofibers developed were carried out via attenuated total reflectance-FTIR (ATR) (PerkinElmer, USA).

In vitro drug release from electrospun nanofibers

In vitro drug release studies were carried out in accordance with method defined in the monograph as the "paddle over disk method" of United States Pharmacopeia 38.[21] 2.5 cm in diameter of fiber sections were immobilized between a glass holder and a stainless steel sieve. The samples were immersed into 500 mL of (phosphate buffer, pH 6.5) to maintain sink conditions for DNP. At specified time points (from 30 min up to 6 h), 2 mL aliquots of the samples were withdrawn periodically from the release medium and equal volumes of medium were immediately replaced to maintain a constant volume. Concentrations of DNP in the samples were analyzed via a ultraviolet (UV)-visible spectrophotometer (Shimadzu, Japan) at a wavelength of 229 nm. The cumulative amount of released DNP per cm^2 through the nanofibers was plotted versus time. Each experiment was conducted three times. UV-visible spectrophotometry was validated for selectivity, linearity, accuracy, and precision. It was determined to be linear over the concentration range 2.5-20 µg/mL with a high correlation coefficient (r^2>0.999) and accuracy (recovery >98%). There were no interfering absorbances with DNP, verifying selectivity of the method.

Determination of drug release kinetics and modeling

To understand the mechanism and kinetics of DNP release from electrospun nanofibers, the release results were fitted to kinetic models via the free open source software DDSolver®[22] as explained following equations 1-5:

Zero-order kinetic model:

$$C=k_0t+C_0 \quad (1)$$

First-order kinetic model:

$$\ln C=\ln C_0+k_1t \quad (2)$$

Higuchi square root kinetic model:

$$C=k_2t^{1/2}, \quad (3)$$

where C is the drug concentration released at time t, C_0 is the drug concentration at the beginning, and k_0, k_1, and k_2 are zero-order, first-order, and Higuchi release rate constants, respectively.

Hixson-Crowell kinetic model:

$$W_0^{1/3}-Wt^{1/3}=k_Ht, \quad (4)$$

where W_0 and W_t are the initial and remaining amounts of drug in the nanofiber at time t, respectively, and k_H is the Hixson-Crowell release rate constant.

Korsmeyer–Peppas kinetic model:

$$M_t/M_\infty = k_{KP} t^n, \quad (5)$$

where M_t is the drug concentration released at time t, M_∞ is the equilibrium concentration of drug that must be released at infinite time in the release medium, M_t/M_∞ is the fraction of drug in the release medium at time t, k_{KP} is the release rate constant, and n is the diffusional exponent showing the type of release mechanism. If n equals 1, the release mechanism is zero order; otherwise, if $0.5 < n < 1$, non-Fickian transport is the case. Moreover, the first 60% drug release data were fitted in this model.[23]

The coefficient of correlation (r^2) was calculated using linear curves generated by regression analysis of the drug release profile. The model with the highest r^2 value was selected as the most feasible.

RESULTS AND DISCUSSION

Production of electrospun nanofibers

The solution features (e.g., polymer type and concentration) as well as the electrospinning parameters including the flow rate, applied voltage, and tip-to-collector distance are very important to produce bead-free nanofibers.[24] Therefore, the preliminary nanofiber fabrication studies were performed using only PU solutions at diverse concentrations and the electrospinning process parameters (e.g., flow rates, applied voltages, and tip-to-collector distance) were tested to determine the optimal parameters and polymer concentration as described in our previous study.[25] The data had indicated that bead-free nanofibers might be produced with 12.5% (w/v) concentration of PU solution.[25] In the present study, DNP and either EC or PVP in different ratios (Table 1) were added to optimized PU solution and then conductivity of the solutions was determined to observe effect on the morphology of electrospun nanofibers. The conductivity of solutions and the AFD diameter of nanofibers are presented in Table 2. Interestingly, there was a correlated increase in conductivity with increasing AFD diameter of the PU/EC/DNP and PU/PVP/DNP nanofibers. However, this case did not show a linear increase between the conductivity of the polymer solutions and the AFD diameter of the nanofibers, as expected.

Morphology of electrospun nanofibers

To research effects of EC or PVP amounts on the morphology of PU/DNP electrospun nanofibers and to verify the production of bead-free nanofibers with smooth surfaces, the morphological features of PU/EC/DNP and PU/PVP/DNP nanofibers were examined using SEM analysis. Figures 2a, 2b, 3a and 3b present the morphological features and the diameter histograms of PU/EC/DNP and PU/PVP/DNP nanofibers with diverse ratios of EC and PVP. Most of the electrospun fibers (except for PU/PVP/DNP at a ratio of 10/8/1) had smooth surfaces and uniform structures without any "beads-on-a-string" morphology.

Table 2. The conductivity of the solutions and average fiber diameter of electrospun fibers (n=3)

Code	Conductivity (µS.cm-1)	Average fiber diameter (nm)
F1	109.33±4.15	410±47
F2	115.70±6.65	556±46
F3	116.66±1.65	518±39
F4	123.60±2.20	603±42
F5*	134.03±3.85	340±56
F6*	110.20±2.70	294±39
F7*	109.57±2.55	279±57
F8*	131.40±1.50	328±66

F1, F2, F3, and F4 are described for PU/EC/DNP, F5*, F6*, F7*, and F8* are described for PU/PVP/DNP nanofibers, PVP: Polyvinylpyrrolidone, PU: Polyurethane, EC: Ethyl cellulose, DNP: Donepezil hydrochloride

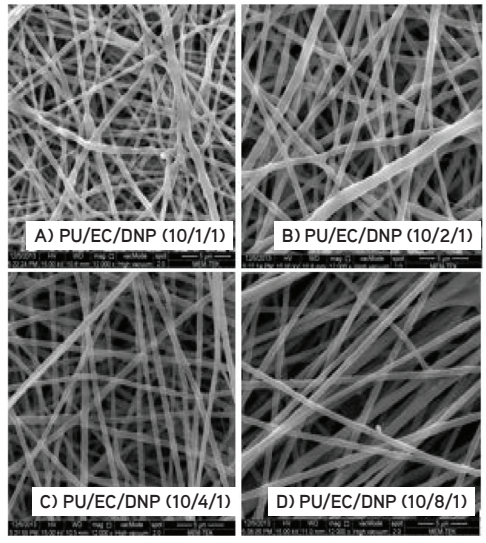

Figure 2a. SEM images of (PU/EC/DNP) (at different ratios) electrospun nanofibers (the scale bars represent 5 µm)

SEM: Scanning electron microscope, PU: Polyurethane, EC: Ethyl cellulose, DNP: Donepezil hydrochloride

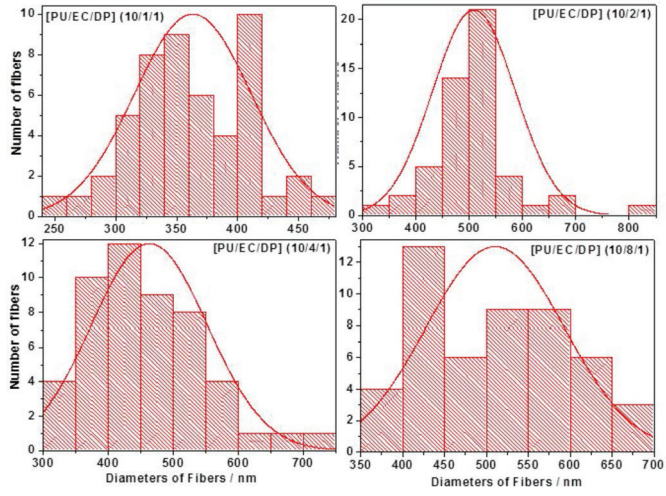

Figure 2b. Diameter histograms of (PU/EC/DNP) (at different ratios) electrospun nanofibers

PU: Polyurethane, EC: Ethyl cellulose, DNP: Donepezil hydrochloride

Furthermore, no drug particles were observed on the surface or outside of the nanofibers, revealing good compatibility between the polymers and drug and encapsulation of drug in the nanofibers. SEM images of the PU/EC/DNP nanofibers are given in Figure 2a. The diameter of PU/EC/DNP nanofibers relies upon the existence of EC in the formulation. PU/DNP (10:1) nanofibers without EC had a mean diameter of 775±16 nm[23] while the mean diameter of the nanofibers with addition of EC decreased to between 410±47 and 603±42 (Table 2). In addition, the shape and uniformity of PU/EC/DNP nanofibers were maintained even with increasing EC amount in the nanofibers.

SEM images of PU/PVP/DNP fibers are given in Figure 3a. PU/PVP/DNP nanofibers with diverse ratios of PVP had mean diameters from 279±57 nm to 340±56 nm. The mean diameter of nanofibers decreased with addition of PVP to the formulations, as also seen in PU/EC/DNP nanofibers. However, some clumps were observed in PU/PVP/DNP nanofibers at a ratio of 10/8/1, because of low PVP solubility in electrospinning solution (Figure 3a), as reported previously.[17] In conclusion, these data confirmed that PU/PVP/DNP and PU/EC/DNP nanofibers with smooth surfaces and bead-free were produced for nearly all of the ratios.

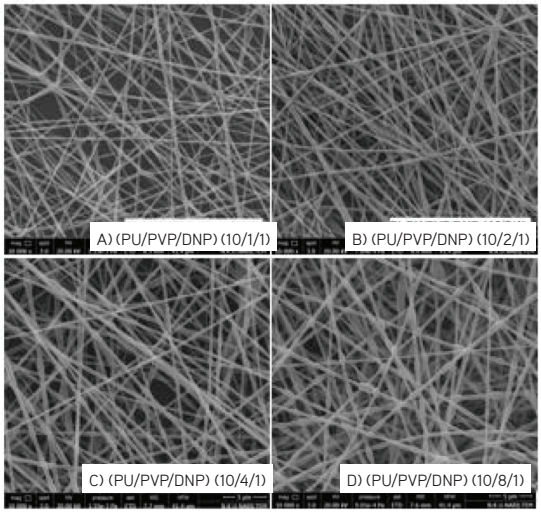

Figure 3a. SEM images of (PU/PVP/DNP) (at different ratios) electrospun nanofibers (the scale bars represent 5 µm)

PU: Polyurethane, DNP: Donepezil hydrochloride, PVP: Polyvingl pyrrolidone

Compatibility of components in electrospun nanofibers

The ATR-FTIR spectra of PU/EC/DNP and PU/PVP/DNP (10/2/1, 10/4/1, 10/8/1) are seen in Figures 4 and 5 in the wave number range of 4000-800 cm^{-1}; the spectra of 10/1/1 were not given because there were no differences between 10/1/1 and 10/2/1. The spectra of drug loaded PU/EC and PU/PVP nanofibers have similar characteristic FTIR bands, but the spectra of fibers also show some small difference. Characteristic absorption bands of PU were described in detail in our previous study,[25] such as: 1727 cm^{-1} band, because of carbonyl groups in urethane bonds (C=O); 1550 cm^{-1} band, assigned to secondary amide (RCONHR');

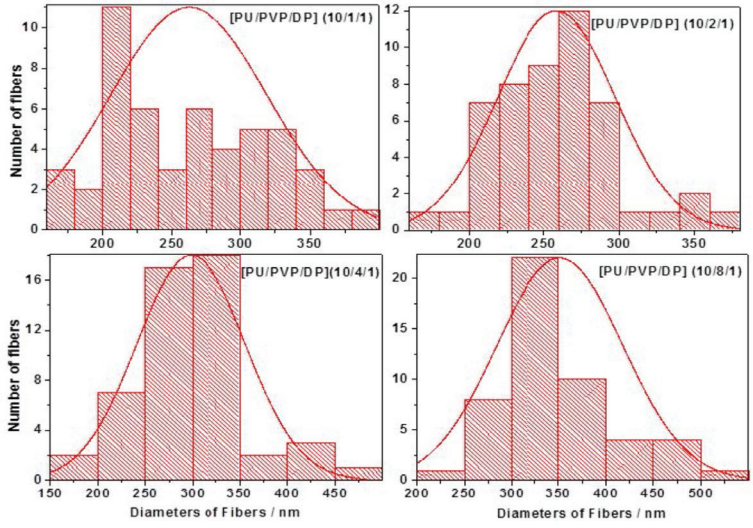

Figure 3b. Diameter histograms of (PU/PVP/DNP) (at different ratios) electrospun nanofibers

PU: Polyurethane, DNP: Donepezil hydrochloride, PVP: Polyvingl pyrrolidone

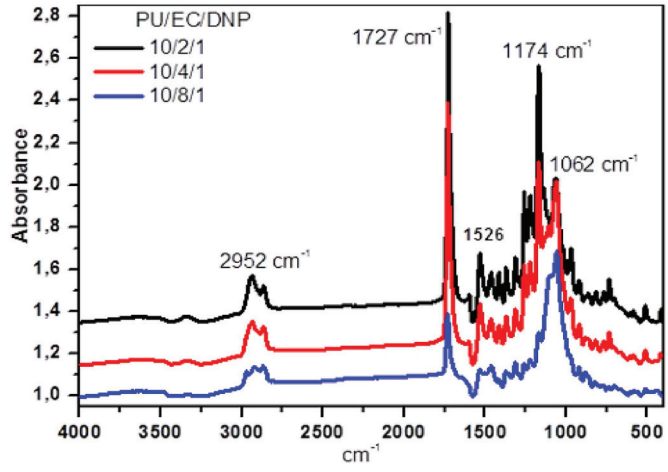

Figure 4. ATR-FTIR spectra of drug loaded electrospun nanofiber of PU/EC in various ratios

ATR: Attenuated total reflection, FTIR: Fourier-transform infrared, PU: Polyurethane, EC: Ethyl cellulose

1630 cm^{-1} band, assigned to carbonyl groups in urea bonds; 1170 cm^{-1} band because of C-O stretch and C-N stretch; 3350 cm^{-1} and 2944 cm^{-1} bands from N-H and C-H groups.

The decrease in characteristic absorption bands of PU at the 1727 cm^{-1} band from 10/2/1 to 10/8/1 (PU/EC/DNP) and also amendments at 1062 cm^{-1} and 2952 cm^{-1} clarify that EC is incorporated into the PU matrix in Figure 4. Because of the lower rate of the drug according to PU/EC and PU/PVP mixtures, characteristic absorption bands of the drug molecule may not be observed. Hence, the interactions could not be determined between the drug and polymers.

With addition of PVP to PU, new broad peaks located at 3434 cm^{-1} and 1658 cm^{-1} are observed in Figure 5. The new band at 3434 cm^{-1} is because of stretching vibration of the hydroxyl group and at 1658 cm^{-1} is because of stretching vibration of

the C=O. The increase at 2949 cm^{-1} is assigned to the C-H asymmetric stretching vibration from PVP.

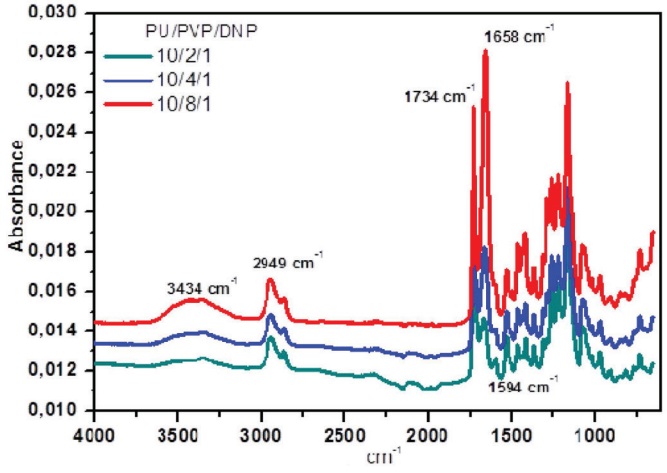

Figure 5. ATR-FTIR spectra of drug loaded electrospun fiber of PU/PVP in various ratios

ATR: Attenuated total reflection, FTIR: Fourier-transform infrared, PVP: Polyvinylpyrrolidone, PU: Polyurethane

In vitro drug release studies

PU/EC/DNP and PU/PVP/DNP nanofibers were used to research effect of EC and PVP amounts on drug release. The drug release profiles from PU/EC nanofibers are presented in Figure 6.

All of the nanofibers exhibited biphasic drug release with moderately fast release in 30 min. The highest amount of drug release was observed for PU/PVP/DNP (10/8/1) nanofibers with the highest ratio of PVP (data not given). Conversely, an increase in the EC amount in the formulation caused a reduction in drug release (Figure 6). While approximately 350 μg/cm^2 DNP from PU/PVP/DNP (10/8/1) nanofibers was released in 1 h (data not given), the concentration of released DNP from PU/EC/DNP (10/8/1) nanofibers was around 100 μg/cm^2 (approximately 20%) at the end of 1 h. This might be explained by the hydrophilic property of PVP, which could gradually accelerate the release of drug from PU nanofibers. In the case of EC, the slow drug release could be attributed to its hydrophobic character. Moreover, some clumps on the nanofibers with PVP (Figure 3a) could have resulted in high immediate drug release. Interestingly, for both nanofiber groups, no linear correlation between amount of drug released and ratios of PVP or EC was found. The data indicated that EC might induce retention of water-soluble drugs in the nanofibers, which resulted in inhibiting drug release and presenting sustained drug release, as reported previously.[26] Conversely, PVP might expedite the release of a water-soluble drug. Furthermore, it is well known that water-soluble drugs exhibit a fast release profile; this is a crucial point for controlled release of these drugs.[27] In the light of these data, sustained release of water-soluble drugs from PU/EC nanofibers might be possible, with increased ratio of EC (Figure 6).

Determination of drug release kinetics and modeling

The *in vitro* release results of nanofibers were analyzed using kinetic models aforementioned in the method section, in order to explain the release mechanism of DNP from PU/EC electrospun nanofibers. The drug release mechanism and kinetics were determined depending on r^2 values, which signify goodness of fit. Table 3 shows the r^2 values calculated via linear curves of PU/EC/DNP electrospun fibers. In addition, r^2 values were not estimated for kinetic models as drug release from PU/PVP/DNP electrospun fibers was immediate. The regressed results for PU/EC/DNP nanofiber (10/8/1) showed the highest r^2 value (0.999) (Table 3) for the Korsmeyer-Peppas model. This revealed that release of DNP from this nanofiber was controlled by a Fickian diffusion mechanism with a value of release exponent (n) of 0.31 (<0.5). DNP was released by molecular diffusion depending on drug gradient. A similar release kinetic has also been reported by Yu et al.[28] for ketoprofen-loaded PVP/EC nanofibers. However, the other nanofibers with EC did not fit the Korsmeyer-Peppas model (Table 3). In this case, an increase in EC ratio of the nanofibers could influence the release kinetics and mechanisms of a water-soluble drug, causing sustained-drug release. This improvement in PU/EC/DNP electrospun fiber (10/8/1) might be attributed to the hydrophobic nature of EC.

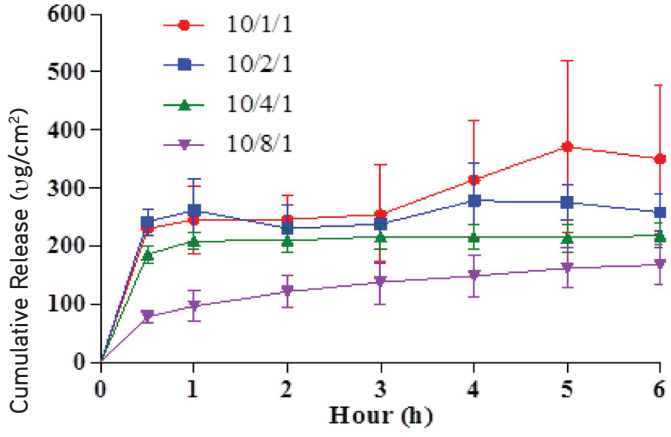

Figure 6. *In vitro* release profiles of DNP from PU/EC nanofibers

DNP: Donepezil hydrochloride, PU: Polyurethane, EC: Ethyl cellulose

Table 3. Coefficient of correlation (r^2) values for DNP loaded PU/EC nanofibers

	Ratio of PU/EC/DNP			
Kinetic models	10/1/1	10/2/1	10/4/1	10/8/1
Zero order	0.905	0.240	0.542	0.949
First order	0.922	0.241	0.530	0.896
Hixson-Crowell	0.917	0.241	0.534	0.915
Higuchi square root	0.863	0.358	0.658	0.994
Korsmeyer-Peppas	0.797	0.493	0.767	0.999
(n)	(0.14)	(0.04)	(0.05)	(0.31)

PU: Polyurethane, EC: Ethyl cellulose, DNP: Donepezil hydrochloride

CONCLUSION

Electrospun nanofibers composed of different blends of either PU/EC or PU/PVP have been utilized by electrospinning. DNP was loaded into these nanofibers as a water-soluble model drug. All electrospun nanofibers fabricated had smooth surfaces and uniform structures without any beads-on-a-string morphology. The PU/EC electrospun nanofibers showed a Korsmeyer-Peppas drug release kinetic mechanism in which the release rate was controlled by diffusion of drug when the EC ratios were increased in the nanofiber composition. The data also suggest that types and ratios of polymer blends need to be adjusted so as to optimize the drug release rate. Overall, this ability of PU/EC (10/8) electrospun nanofibers suggested their potential use as a drug carrier from which water-soluble drug release may be sustained.

ACKNOWLEDGEMENTS

This work was supported by the Scientific Research Projects Coordination Unit of İstanbul Technical University (project number: 37960).

Conflicts of interest: No conflict of interest was declared by the authors. The authors alone are responsible for the content and writing of the paper.

REFERENCES

1. Bhardwaj N, Kundu SC. Electrospinning: a fascinating fiber fabrication technique. Biotechnol Adv. 2010;28:325-347.
2. Luong-Van E, Grøndahl L, Chua KN, Leong KW, Nurcombe V, Cool SM. Controlled release of heparin from poly(epsilon-caprolactone) electrospun fibers. Biomaterials. 2006;27:2042-2050.
3. Vrbata P, Berka P, Stránská D, Doležal P, Lázníček M. Electrospinning of diosmin from aqueous solutions for improved dissolution and oral absorption. Int J Pharm. 2014;473:407-413.
4. Hu X, Liu S, Zhou G, Huang Y, Xie Z, Jing X. Electrospinning of polymeric nanofibers for drug delivery applications. J Control Release. 2014;185:12-21.
5. Akduman Ç, Akçakoca Kumbasar EP. Electrospun Polyurethane Nanofibers. In: Yılmaz F (ed). Aspects of Polyurethanes. London; IntechOpen; 2017: Chapter 2.
6. Raschip IE, Vasile C, Macocinschi D. Compatibility and biocompatibility study of new HPC/PU blends. Polym Int. 2009;58:4-16.
7. Uslu I, Aytimur A, Serincay H. Preparation of PVA/PAA/PEG/PVP nanofibers with HPMC and aloe vera. Curr Nanosci. 2013;9:489-493.
8. Wilmington DE. Polymer blend matrix for oral sustained drug delivery. Pharmaceutical Technology Report 016. Hercules Incorporated, Aqualon Division. 2002.
9. Callahan JC, Cleary GW, Elefant M, Kaplan G, Kensler T, Nash RA. Equilibrium moisture content of pharmaceutical excipients. Drug Dev Ind Pharm. 2008;8:355-369.
10. Huang LY, Branford-White C, Shen XX, Yu DG, Zhu LM. Time-engineeringed biphasic drug release by electrospun nanofiber meshes. Int J Pharm. 2012;436:88-96.
11. Emeje MO, Kunle OO, Ofoefule SI. Compaction characteristics of ethylcellulose in the presence of some channeling agents: Technical note. AAPS PharmSciTech. 2006;7:E18-E21.
12. Yang GZ, Li HP, Yang JH, Wan J, Yu DG. Influence of working temperature on the formation of electrospun polymer. Nanoscale Res Lett. 2017;12:55-65.
13. Illangakoon UE, Gill H, Shearman GC, Parhizkar M, Mahalingam S, Chatterton NP, Williams GR. Fast dissolving paracetamol/caffeine nanofibers prepared by electrospinning. Int J Pharm. 2014;477:369-379.
14. Li CC, Wang ZH, Yu DG, Williams GR. Tunable biphasic drug release from ethyl cellulose nanofibers fabricated using a modified coaxial electrospinning process. Nanoscale Res Lett. 2014;9:258-268.
15. Samprasit W, Akkaramongkolporn P, Ngawhirunpat T, Rojanarata T, Kaomongkolgit R, Opanasopit P. Fast releasing oral electrospun PVP/CD nanofiber mats of taste-masked meloxicam. Int J Pharm. 2015;487:213-222.
16. Xu J, Jiao Y, Shao X, Zhou C. Controlled dual release of hydrophobic and hydrophilic drugs from electrospun poly (l-lactic acid) fiber mats loaded with chitosan microspheres. Mater Lett. 2011;65:2800-2803.
17. Yu DG, Shen XX, Branford-White C, White K, Zhu LM, Bligh SW. Oral fast-dissolving drug delivery membranes prepared from electrospun polyvinylpyrrolidone ultrafine fibers. Nanotechnology. 2009;20:055104.
18. Yu DG, Branford-White C, Williams GR, Bligh SA, White K, Zhu LM, Chatterton NP. Self-assembled liposomes from amphiphilic electrospun nanofibers. Soft Matter. 2011;7:8239-8247.
19. Park JY, Kim JI, Lee IH. Fabrication and characterization of antimicrobial ethyl cellulose nanofibers using electrospinning techniques. J Nanosci Nanotechnol. 2015;15:5672-5675.
20. Yu DG, Wang X, Li XY, Chian W, Li Y, Liao YZ. Electrospun biphasic drug release polyvinylpyrrolidone/ethyl cellulose core/sheath nanofibers. Acta Biomater. 2013;9:5665-5672.
21. United State Pharmacopeia (USP) 38-NF33 Chapter Topical and transdermal drug products- Product Performance Tests for TDS. 750:764.
22. Zhang Y, Huo M, Zhou J, Zou A, Li W, Yao C, Xie S. DDSolver: An add-in program for modelling and comparison of drug dissolution profile. APPS J. 2010;12:263-272.
23. Dash S, Murthy PN, Nath L, Chowdhury P. Kinetic modeling on drug release from controlled drug delivery systems. Acta Pol Pharm-Drug Res. 2010;67:217-223.
24. Zamani M, Prabhakaran MP, Ramakrishna S. Advances in drug delivery via electrospun and electrosprayed nanomaterials. Int J Nanomed. 2013;8:2997-2917.
25. Gencturk A, Kahraman E, Güngör S, Özhan G, Özsoy Y, Sarac AS. Polyurethane/hydroxypropyl cellulose electrospun nanofiber mats as potential transdermal drug delivery system: characterization studies and *in vitro* assays. Artif Cells Nanomed Biotechnol. 2017;45:655-664.
26. Rowe RC, Sheskey PC, Quinn ME. Handbook of Pharmaceutical Excipients. London: Pharmaceutical Press; 2009.
27. Enayatifard R, Saeedi M, Akbari J, Tabatabaee YH. Effect of hydroxypropyl methylcellulose and ethyl cellulose content on release profile and kinetics of diltiazem HCl from matrices. Trop J Pharm Res. 2009;8:425-432.
28. Yu DG, Wang X, Li XY, Chian W, Li Y, Liao YZ. Electrospun biphasic drug release polyvinylpyrrolidone/ethyl cellulose core/sheath nanofibers. Acta Biomater. 2013;9:5665-5672.

Turk J Pharm Sci 2020;17(6):645-652
DOI: 10.4274/tjps.galenos.2019.53325

ORIGINAL ARTICLE

A Controlled Release Theophylline Delivery System Based on a Bilayer Floating System

İki Tabakalı Yüzen Sisteme Dayalı Kontrollü Salım Teofilin Taşıma Sistemi

John Afokoghene AVBUNUDIOGBA*, Christian Arerusuoghene ALALOR, Queen Dorcas OKOLOCHA

Delta State University, Pharmaceutics and Industrial Pharmacy Department, Abraka, Nigeria

ABSTRACT

Objectives: Bilayer floating drug delivery is an approach that helps to overcome the shortcomings of single-layered tablets. There is little or no fluctuation of the drug in the blood stream or tissue, while control is enabled over the time and site of drug release. In the current study, bilayer theophylline matrix tablets were formulated by double compression and evaluated using granules produced by polymeric granulation and simple coacervation techniques.

Materials and Methods: Bilayer floating theophylline tablets containing an immediate release layer (IRL) and a sustained release layer (SRL) were prepared. Granules for the IRL section were produced by wet granulation, while those for the SRL section were produced by polymeric granulation and simple coacervation techniques using Eudragit RL100 and carboxymethyl cellulose (CMC) as binder. The resulting granules were characterized for flowability and packing properties. Granules with adequate flow were compressed into flat-faced tablets 12 mm in diameter using a single punch tableting machine at an arbitrary load of 28 kgF on a load scale. The tablets were evaluated for hardness, weight variability, disintegration, friability, swelling index, floating time, and *in vitro* drug release.

Results: The angle of repose and Hausner ratio were 29.07±0.330 to 40.08±0.660 and 1.07±0.01 to 1.28±0.01, respectively. Tablets hardness values ranged from 4.74±0.36 to 9.84±0.49 kgF, while percentage friability ranged from 0.5% to 1.51%. Floating lag time was between 1±0.41 and 9±0.71 min, while the total floating time was between 1 min and 9 h. Over 50% of the drug was released within 7 h.

Conclusion: Drug release from the tablets showed a prompt release phase and an extended release phase. Therefore, appropriate combination of Eudragit and CMC and the right reagent can produce well retarded bilayer floating tablets.

Key words: Eudragit, carboxymethylcellulose, bilayer floating tablets, drug delivery

ÖZ

Amaç: İki tabakalı yüzen ilaç taşınması tek tabakalı tabletlerin eksikliklerinin üstesinden gelmeye yardımcı olan bir yaklaşımdır. Kan akımında veya dokuda ilaçla ilgili iniş çıkışlar olmazken, kontrol zamanla ve ilacın salıverildiği bölgeden sağlanır. Bu çalışmada, iki tabakalı teofilin matriks tabletleri çift kompresyon yöntemiyle formüle edilmiş ve polimerik granülasyon ve basit koaservasyonla üretilmiş granüller değerlendirilmiştir.

Gereç ve Yöntemler: Ani salım tabakası (ILR) ve sürekli salım tabakası (SRL) içeren iki tabakalı yüzen teofilin tabletleri hazırlanmıştır. IRL kısmı için olan granüller ıslak granülasyonla üretilirken, SRL kısmı için olanlar polimerik granülasyon ve basit koaservasyon teknikleriyle Eudragit RL100 ve bağlayıcı olarak karboksimetil selüloz (CMC) kullanılarak üretilmiştir. Elde edilen granüller alış ve paketlenme özellikleri için karakterize edilmiştir. Yeteri kadar akışkanlığa sahip granüller, tek vuruşlı tablet makinesinde yükleme skalasında 28 kgF rastlantısal yükte 12 mm çapında düz yüzeyli tabletler olarak komprese edilmiştir. Bu tabletler sertlik, ağırlık farklılığı, parçalanma, kırılabilirlik, şişme indeksi, yüzme zamanı ve *in vitro* ilaç salımı için değerlendirilmiştir.

Bulgular: Dinlenme açılarının ve Hausner oranlarının sırasıyla 29,07±0,330'den 40,08±0,660'e ve 1,07±0,01'den 1,28±0,01'e dek olduğu bulunmuştur. Tabletlerin sertlik değerleri 4,74±0,36'dan 9,84±0,49 kgF'ye dek bulunurken, yüzde kırılabilirlikleri %0,5 ile %1,5 arası değişmiştir. Yüzme gecikme zamanı 1±0,41 ve 9±0,71 arasındayken, toplam yüzme zamanları 1 dakika ve 9 saat arasındadır. Yedi saat içinde ilacın %50'si salınmıştır.

Sonuç: Tabletlerden ilaç salınımı ani salım fazı ve uzatmış salım fazı şeklinde görülmüştür. Eudragit ve CMC'nin uygun kombinasyonu ve doğru reaktifin uygun geciktirilmiş çift tabakalı yüzen tablet oluşturabilmektedir.

Anahtar kelimeler: Eudragit, karboksimetilsellüloz, çift tabakalı yüzen tabletler, ilaç taşınımı

*Correspondence: E-mail: avbunudiogba@yahoo.com, Phone: +2348033633331 ORCID-ID: orcid.org/0000-0002-1483-0860

Received: 20.04.2019, Accepted: 07.11.2019

INTRODUCTION

The oral route of drug administration is the most versatile, convenient, and often employed route. However, fluctuation in drug concentration in the blood stream and tissues with the resulting toxicity are some of the shortcomings associated with conventional oral tablets. Frequent drug administration *vis-à-vis* drug adherence are other problems associated with conventional dosage forms.[1-3] To obviate these shortcomings, controlled release formulations, especially those for oral administration, have been investigated and developed with the sole aim of maintaining a constant drug concentration in the blood stream for longer through slow release of drug into the gastrointestinal tract (GIT).[4] Although the oral route is the most preferred for drug administration, studies has demonstrated two physiological influences: short gastric residence time and variable gastric emptying time. Thus, bioavailability and time to achieve maximum plasma concentration cannot be predicted. It must be noted that most drugs are absorbed in the stomach and upper part of the intestine. However, residence time within these regions is short (2 to 3 h). Hence any methods to prolong the residence time of drugs within these regions will improve bioavailability and therapeutic outcome.[4,5]

The oral route has received greater attention and given more successful outcomes than any other route in controlled drug delivery systems.[6,7] This is not unconnected with the physiology of the GIT, which offers more flexibility in the design of oral dosage forms compared with other routes.[8-10] The most crucial challenge with an oral controlled drug delivery device is not just sustaining the drug release, but also ensuring that the dosage form is sufficiently prolonged within the GIT for complete release from the device. Scientists and the pharmaceutical industries, right from the first generation of controlled release (1952 to the 1970s) to the second generation (1980 to 2010), have made major breakthroughs in the development of oral controlled drug delivery systems by working against gastrointestinal emptying.[11]

One such device employs the concept of the gastroretentive drug delivery system (GRDDS).[12,13] Oral dosage forms for the GRDDS have received much attention over the years for enabling control over the time and site of drug release.[2,12] Prolongation of the gastric retention of drug delivery devices has numerous advantages. These include better absorption, enhanced bioavailability and therapeutic efficacy, and possible reduction of dose size.[14]

The major principle of the GRDDS is prolongation of stay of the dosage form and the release of drug at the absorption site. Many approaches have been adopted, but the most recent is "the floating device".[15] Floating dosage forms have low bulk density, hence their ability to float in the gastric fluid for a long time, thus contributing to improved bioavailability.[16] A floating device can also be improved upon by incorporating a combination of two or more active pharmaceutical ingredients (APIs) in a single dosage form (multilayer tablets). Multilayer tablets can be used to obviate chemical incompatibilities between APIs through physical separation and also to achieve different drug release profiles, e.g., immediate release and extended release segments.[17] Such an approach can be used for the formulation of sustained release tablets comprising an immediate release outer layer and a maintenance inner layer. This has been employed to overcome single-layered tablets' fluctuation in drug concentration both in the blood stream and at the site of action.[18,19] Drugs that are mainly absorbed from the upper part of the GIT, such as albuterol, furosemide, and theophylline, are worthy candidates. Development of these drugs in floating sustained release dosage form helps to prolong their limited bioavailability.[20]

Theophylline has an antiinflammatory property at the therapeutic regular dose and as such plays an important role in treating chronic obstructive pulmonary disease.[21] Theophylline has a narrow therapeutic index (10-20 µg/mL); thus the conventional preparations experience fluctuation between maximum and minimum blood concentration, resulting in poor therapeutic outcome. On the other hand, patients on regular sustained release preparations may experience delay in the onset of drug action since the initial release may not be therapeutic. Thus, in the current study, bilayer theophylline matrix tablets were formulated by double compression using granules produced by polymeric granulation and simple coacervation. One layer provides the immediate release component, while the second layer provides the sustained release segment.

MATERIALS AND METHODS

Materials

The test drug (theophylline powder) was obtained from Vital Biotic, Nigeria Ltd. as a free sample.

Excipients and reagents

Absolute ethanol, citric acid, and sodium bicarbonate (Guangdong Guanghua Sci-Tech Co. Ltd., Shantou, Guangdong, China); carboxymethyl cellulose (CMC) and lactose (Kermel); and normal saline (Unique Pharmaceutical Nigeria Ltd.) were obtained. Acrylic-methacrylic polymer (Eudragit RL100) was received as a gift sample from Evonik Industries AG-Werk Röhm, Darmstadt, Germany. Amaranth solution (Vinayak Ingredients Pvt Ltd, India) and magnesium stearate, talc, and maize starch (Kermel) were also used.

Ethical approval

No ethical approval is required by the Delta State University for research of this nature since the work does not involve animal studies or clinical trials; however, theophylline is a controlled drug in some countries, hence the need for ethical approval. The research work was approved by the Faculty of Basic Medical Sciences Research and Ethics Committee of the Delta State University, Abraka, Nigeria. The approval number is REC/FBMS/DELSU/19/45.

Methods

To formulate bilayer floating theophylline tablets, two sets of granules (conventional granules for the immediate release segment and a second set of granules for the prolonged release segment) were formulated.

Granules for the immediate release layer (IRL)

To form the immediate release section, conventional granules were formulated by wet granulation (F6, Table 1). A 1.5 g sample of maize starch powder was weighed and converted to mucilage with boiled water. Theophylline powder (25 g), lactose (18.5 g), and maize starch powder (2 g) were weighed and transferred into a clean porcelain mortar. A few drops of amaranth solution (colorant) were added and thoroughly blended. The blend was kneaded with maize starch mucilage to form a damp mass. This mass was forced through a 1 mm sieve and dried with a hot air oven (Lead Engineering, St Helens, UK. Model: GP/50/CLAD/100/HYD) at 60±0.5°C for 24 h. The dried mass was passed through a sieve (710 µm) and characterized by measuring the flow and packing property before storage.

Preparation of granules for the sustained release layer (SRL)

Granules for the SRL were prepared according to the formula in Table 1. A 5 g sample of Eudragit RL100 (10% w/w) was weighed and dissolved in 30 mL of absolute ethanol. A sample of theophylline powder (20 g) and a 10 g sample of CMC were weighed and transferred to a clean mortar and thoroughly blended. The powder blends were kneaded with the Eudragit-ethanol mixture to form a wet mass. The wet mass was forced through a 1 mm sieve and dried in a hot air oven at 50.0±1.0°C for 2 h. The dried granules were passed through a 710 µm sieve to form the required granules (batch F1, Table 1). In other experiments, the quantities of Eudragit and CMC were varied in order to form batches F2, F3, and F5.

Batch F4 was prepared by a simple coacervation technique. Here, a 10 g sample (20% w/w) of Eudragit RL100 was weighed and dissolved in 150 mL of absolute ethanol. A 20 g sample of theophylline powder was weighed and mixed with the Eudragit-ethanol mixture. Thereafter, 350 mL of normal saline solution (0.9% w/v of sodium chloride) was added followed by stirring to form coacervates. The coacervates so formed were allowed to settle, filtered, and dried in a hot air oven at 50.0±1.0 °C for 2 h. The dried mass was passed through a 710-µm sieve to form the required granules. The granules were characterized before storage for further study.

Preformulation studies

a- Angle of repose: A 20 g sample of granules was weighed and allowed to flow through a funnel orifice at a height of 7 cm. The height and diameter of the cone so formed were measured. The procedure was performed in triplicate and the mean value recorded. The angle of repose (θ) was computed from equation (1):

$$\text{Tan } \theta = \frac{2H}{D}, \quad (1)$$

where *H* and *D* are the height and diameter of the powder cone so formed.

b- Densities and compressibility index (CI): A sample of granules (20 g) was weighed and transferred into a 100-mL cylinder of an automated tapped density tester (Model C-TDA2, Campbell Electronics, Mumbai, India). The volumeter was allowed to tap 100 times and the tapped volume recorded. The bulk and tapped densities and the CI were computed from equations (2), (3), and (4). The procedure was performed in triplicate and the mean values recorded.

$$\text{Bulk density} = \frac{\text{Weight of granules}}{\text{Bulk volume of granules}} \quad (2)$$

$$\text{Tapped density} = \frac{\text{Weight of granules}}{\text{Tapped volume of granules}} \quad (3)$$

$$(\text{CI}) = \frac{(\text{Tapped} - \text{Bulk}) \text{ density}}{\text{Tapped densit}} \times 100 \quad (4)$$

c- Particle size analysis: A sample of granules (50 g) was weighed and transferred into the topmost sieve of a set of sieves arranged in descending order. The set of sieves was shaken with a sieve shaker (Endecott Ltd, UK) for 5 min. The quantity of granules in each sieve was weighed to determine the size distribution. The procedure was performed in triplicate and mean values recorded.

Compression of granules to tablets

A sample of granules (500 mg) for the SRL was weighed and poured into the die cavity of a single punch tableting machine (Kilian & Co GMBH Kolu-Niel, Type KS 043111-196, Buchschlag,

Table 1. Composition of sustained release layer of bilayer theophylline floating tablets

Ingredients	F1 (mg)	F2 (mg)	F3 (mg)	F4 (mg)	F5 (mg)	F6 (mg)
Theophylline	200.0	200.0	200.0	200.0	200.0	200.0
Eudragit RL 100	50.0	25.0	75.0	100.0	-	-
Carboxymethyl cellulose	100.0	125.0	75.0	50.0	150.0	-
Sodium bicarbonate	93.4	93.4	93.4	93.4	93.4	-
Citric acid	46.6	46.6	46.6	46.6	46.6	-
Amaranth solution	-	-	-	-	-	qs
Magnesium stearate	5.0	5.0	5.0	5.0	5.0	5.0
Talc	5.0	5.0	5.0	5.0	5.0	5.0
Maize starch (4%)	-	-	-	-	-	20.0
Maize starch (6%)	-	-	-	-	-	30.0
Lactose	-	-	-	-	-	240.0
Total	500.0	500.0	500.0	500.0	500.0	500.0

Germany). A 100 mg sample of granules for the IRL was weighed and transferred to the same die cavity. This was compressed into bilayer tablets at a force of 28 kgF without agitation. The compression force was kept constant and the procedure repeated for all the batches.

Evaluation of tablets

i- Percentage weight variability: Twenty tablets were selected at random and the mean weight of each was determined with the aid of an analytical balance (Shimadzu Philippines Manufacturing Inc.). The percentage weight variability was computed using equation (6):

$$Q = \frac{W_m - W_i}{W_m} \times \frac{100}{1}, \quad (5)$$

where w_m is the mean weight and w_i is the weight of each tablet.

ii- Tablets' tensile strength determination: The diameter (*d*), thickness (*t*), and crushing load (*P*) of each 10 tablets selected at random were determined using a Veego digital hardness test apparatus. The mean tensile strength of the tablets was determined using equation (6):

$$Ts = \frac{2p}{\pi dt} \quad (6)$$

iii- Disintegration test: The method described in the British Pharmacopoeia[22] was employed. Six tablets were selected at random from each batch and a tablet was placed in each of the six baskets of the disintegration apparatus (Manesty Machine, MK4, UK). The baskets were immersed in warm distilled water maintained at 37±1°C. The mean time taken for the tablets to break up and pass completely through the mesh was recorded as the disintegration time.

iv- Friability test: To evaluate the degree of friability of the tablets, ten tablets were picked at random and weighed. The tablets were placed in the drum of a friabilator (Erweka friabilator). The machine was operated at 25 rpm for 4 min. The tablets were removed from the friabilator, dedusted, and reweighed. The difference in the initial and final weights expressed as a percentage was recorded as the friability.

v- Dissolution test: This test was carried out using the rotating basket method (USP apparatus one). The dissolution medium was 0.1 N hydrochloric acid (pH 2.3). The apparatus consisted of a Pyrex glass vessel containing 900 mL of the dissolution medium maintained at 37±1°C and a cylindrical basket made of stainless-steel wire mesh (aperture size 425 µm). One tablet was placed in the basket, which was rotated at 100 rpm in the dissolution medium. Aliquots (5 mL) were withdrawn at specified time intervals and the amount of drug released was determined using a ultraviolet (UV) spectrophotometer (PG Instrument, USA) at a wavelength of 272 nm. Fresh dissolution medium (5 mL) was added each time a sample was withdrawn.

Theophylline analysis (calibration curve): To standardize theophylline release from the various formulations, a standard calibration curve of theophylline was prepared as follows. A sample of theophylline powder (100 mg) was weighed with an analytical balance and dissolved in 100 mL of medium (0.1 N hydrochloric acid) to obtain a solution of 1 mg/mL (i.e. dilution X_1). A 10 mL sample of X_1 was measured and diluted with 0.1 N HCl to 100 mL to obtain a solution of 0.1 mg/mL (X_2). This process of serial dilution continued until solutions of 3, 5, 7, 9, 11, 13, 15, and 17 µg/mL were obtained. The absorbances of these standard solutions were measured at a wavelength of 272 nm using a UV spectrophotometer. The tests were conducted in triplicate and mean values recorded. Plots of mean absorbance against concentrations were made and a linear regression coefficient (R^2 values) of 0.9947 obtained. The same procedure was used to compute the amount of theophylline released into the dissolution medium at various time intervals.

vi- Kinetic data analysis: Data obtained from the dissolution study were fitted into three well known release models [equations (7), (8), and (9)]:

a- Zero order: $C = k_0 t$ (7)

b- First order: $\ln C1 = \ln C_0 + k_1 t$ (8)

c- Higuchi Model: $C = k_H t^{1/2}$ (9)

Here C_0 is the initial amount of drug in the dosage form, *C* is the percentage amount of drug released, and C_1 is the percentage of residual drug at time *t*. K_0, K_1, and K_H, are the zero order, first order, and Higuchi constants, respectively.

vii- Buoyancy lag time and floating time: A tablet was selected from each batch at random and placed in a 1000 mL beaker containing 900 mL of 0.1 N HCl maintained at 37±1°C. The time required for the tablet to rise to the surface was recorded as the buoyancy lag time, while the duration of floating on the surface without rupturing was recorded as the total floating time determined by visual observation.

viii- Swelling time: The extent of swelling was measured in terms of percentage weight gained by the tablets. A tablet was selected from each batch, weighed, and kept in a beaker containing 900 mL of 0.1 N HCl solution at 37±1°C. The tablet was withdrawn from the beaker at a specified time interval (swelling time interval is 2 h); then excess HCl was blotted with tissue paper and the tablet weighed. Percentage weight gain by the tablet was computed with equation (10):

$$Q = \frac{W_s - W_d}{W_d} \times \frac{100}{1}, \quad (10)$$

where W_s and W_d represent the weight of the swollen tablet and initial weight before swelling, respectively.

ix- Assay procedure (content uniformity): The theophylline assay of the various batches was performed according to the pharmacopeia method.[23] In this method, 2 tablets from each batch were crushed and 375 mg (equivalent to 240 mg of theophylline) was weighed and dissolved in 100 mL of distilled water. A sample (20 mL) of 0.1 M silver nitrate was added and shaken properly for 10 min. The solution so formed was titrated with 0.1 M sodium hydroxide solution using bromothymol blue solution as indicator. Each milliliter of 0.1 M sodium hydroxide solution is equivalent to 18.02 mg of theophylline.

Statistical analysis

All data were expressed as mean ± standard deviation of three determinations. Differences between means were determined with One-Way ANOVA at $p<0.05$.

Table 2. Flow and packing properties of the various granules

	Flow rate (g/s)	Bulk density (g/mL)	Tapped density (g/mL)	Hausner ratio	Compressibility index (%)	Angle of repose (°)
IRL	2.21±0.01	0.57±0.01	0.62±0.01	1.07±0.02	7.59±0.85	32.77±0.13
F1	1.72±0.04	0.55±0.01	0.58±0.01	1.07±0.01	6.33±1.08	30.28±0.13
F2	1.91±0.02	0.46±0.01	0.50±0.01	1.08±0.00	7.26±0.32	29.07±0.33
F3	1.71±0.04	0.51±0.00	0.55±0.01	1.08±0.01	7.42±1.03	34.46±0.28
F4	-	0.41±0.00	0.53±0.00	1.28±0.01	22.15±0.87	40.58±0.66
F5	1.69±0.01	0.52±0.01	0.59±0.01	1.14±0.01	12.34±1.1	29.25±0.50
F6	2.07±0.03	0.51±0.00	0.57±0.00	1.12±0.01	10.5±0.69	33.12±0.37

IRL: Immediate release layer

RESULTS AND DISCUSSION

Packing and flow properties

The results for the packing and flow properties such as bulk and tapped densities, the Hausner ratio, Carr's CI, flow rate, and angle of repose are shown in Table 2. The angle of repose for all formulations was within the range of 29.07 ° to 34.46 ° except batch F4 (angle of repose was 40.58 °), which was prepared by simple coacervation technique. Angle of repose is an indication of powder flowability;[24] all formulations except batch F4 had good flow. Batch F4 exhibited passable (may hang up, flow aid needed) type of flow. The passable flow of batch F4 may be because most of the particles are below 250 µm in size (Figure 1).

"Particles larger than 250 µm are usually relatively free flowing but as the size falls below 100 µm, powders become cohesive and flow problems are likely to occur".[25]

The CI for all granule formulation varied between 6.33% and 10.45% except for batches F4 and F5. Batch F5's CI value was 12.34% (good flow), while that of batch F4 was 22.15%. These variations could be due to the type and concentrations of the binders used. Combination of Eudragit® RL100 and CMC produced granules with better flow.

Physicochemical properties of the bilayer floating tablets

The physicochemical properties of the various tablets such as hardness, weight variability, friability, and disintegration time are presented in Table 3. The hardness of the tablets in all batches ranged between 4.74 kgF and 9.84 kgF. The hardness value of the batch that contained only CMC (batch F5) was 6.08 kgF, while batches F1, F2, and F3 had hardness values of 9.84 kgF, 8.04 kgF, and 7.14 kgF, respectively. The higher the concentration of Eudragit polymer present in these formulations, the greater the hardness. These observations could be due to stronger bonds formed with the hydrophobic polymer (Eudragit). Other researchers reported similar findings when compacts formed with methacrylic polymers (Eudragit L100-55 and Eudragit L100) were compared with that formed with hydroxypropyl methylcellulose (HPMC). Tatavarti et al.[26] and Naveen et al.[27] observed weaker compact formation with HPMC than with methacrylic polymers.

The friability percentage ranged between 0.5% and 1.04%, except batch F5, with a friability percentage of 1.51%. Thus, most tablets met the pharmacopeia requirement for uncoated tablets. The results showed the ability of tablets to withstand some reasonable levels of abrasion during handling and transportation, except batch F5, which contained hydrophilic polymer (CMC) only.

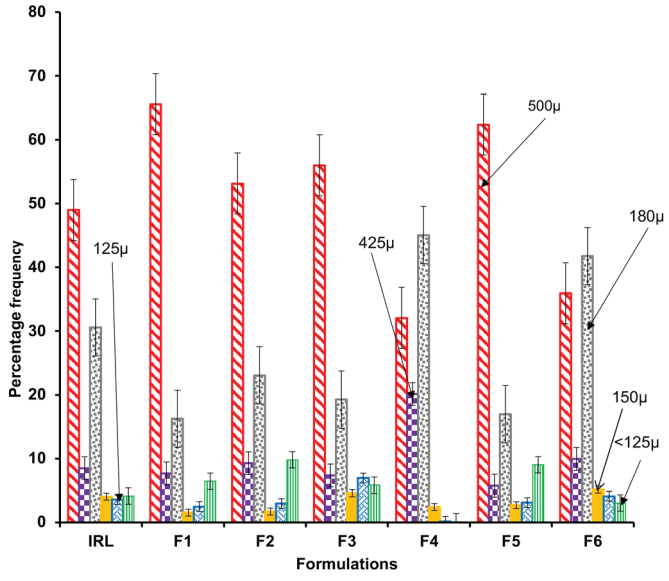

Figure 1. Particle size distribution of various formulations: 500 µm (●), 425 µm (●), 180 µm (●), 150 µm (●), 125 µm (●), <125 µm (●)

Floating and swelling properties of tablets

The floating lag time and floating time of the various tablets are shown in Table 4, while the swelling indices are shown in Figure 2. The floating lag time for batches F1 to F5 was within 49 min. Batch F4, prepared by coacervation, floated within 1 min but disintegrated immediately and lost its integrity. This may have been due to insufficient binder (batch F4 had the lowest concentration of CMC). Batch F5, which contained only CMC, had the lowest floating lag time. The results showed variation in floating lag time with different polymer ratios used. Of all the formulations that contained both Eudragit and CMC, batch F1, which contained Eudragit and CMC in 1:2 ratio, had the lowest floating time, while batch F3, with a Eudragit to CMC ratio of 1:1, had the highest floating lag time. The total floating time for batch F3 was 3 h, while batches F1, F2, and F5 floated for more

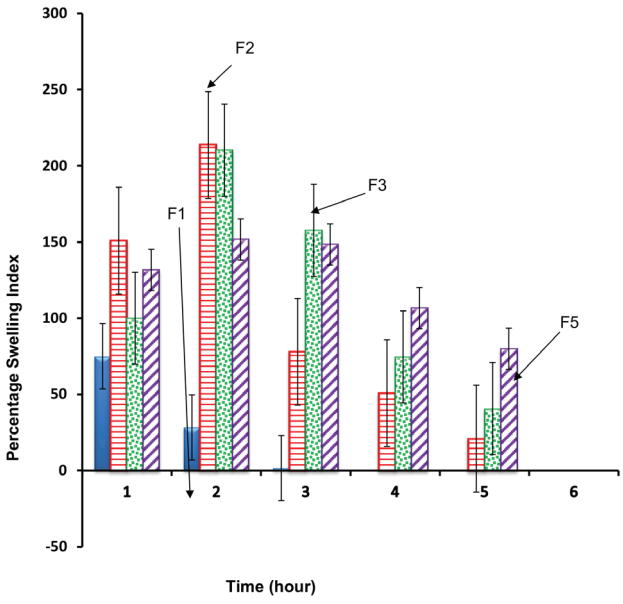

Figure 2. Swelling index of batches F1 (●), F2 (●), F3 (●), and F5 (●)

than 8 h.

It was observed from the present study that the floating lag time and total floating time were functions of both the hydrophilic (CMC) and hydrophobic (Eudragit) polymers present. The higher the concentration of hydrophilic polymer, the lower the floating lag time (see batch F5). Moreover, the higher the concentration of hydrophobic polymer, the higher the floating lag time (see batch F3).

Content uniformity

The assay results ranged from 96.82% to 102.12% as shown in Table 3. Controlled release theophylline bilayer floating tablets contained not less than 90.0% and not more than 110.0% of the labeled amount of theophylline.[28] From the result obtained (96.82-102.12%) as shown in Table 3, the bilayer floating tablets from all the formulations passed the drug content test. It is important for the tablets to have uniform content of the active ingredients, as this would guarantee the therapeutic effectiveness of all the tablets produced.

In vitro drug release profiles

Figure 3 shows the dissolution profiles of the various batches. Two distinct phases of release were observed in batches F1, F2, F3, and F4: one for the IRL and the other for the controlled release layer. All formulated bilayer tablets showed controlled release of drug over 8 h, while batch F6 (conventional tablets) released the entire drug content within 2 h. The maximum percentage drug release by batches F1, F2, F3, and F5 was 75%, 70%, 80%, and 73%, respectively. Batch F2, which contain Eudragit and CMC in 1:5 ratio, was better prolonged than any other batch (Figure 3). Table 5 illustrates the values of the release rate constants (K) and the regression coefficients (R^2) for each model for the six batches of tablets in 0.1 N HCl using a basket at 100 rpm. Research has shown that the model that best fits the release data should be the one with the highest R^2 values when analyzed for zero order, first order, and Higuchi models.[29] The Higuchi equation was found to have the highest R^2; thus release of theophylline from the various matrix tablets is by drug diffusion.

Table 4. Floating ability of various bilayer tablet formulations

Batches	Floating lag time mean ± SD (min)	Total floating time mean ± SD (h)
F1	20±1.08	>8±0.01
F2	33±1.47	>8±0.07
F3	49±0.71	3±0.01
F4	1±0.41	0.017±0.001
F5	18±1.25	>8±0.06

SD: Standard deviation

Table 5. Kinetic of theophylline release from the different formulations

Batches	Zero order		First order		Higuchi model	
	R^2	K_0	R^2	K_1	R^2	K_H
F1	0.9328	0.1353	0.9214	0.0010	0.9329	3.1328
F2	0.9139	0.1202	0.9180	0.0008	0.9534	2.8445
F3	0.8974	0.1295	0.8406	0.0010	0.9203	3.0366
F5	0.9112	0.1234	0.8977	0.0009	0.9448	2.9102
F6	0.9018	0.8372	0.5342	0.0173	0.8720	8.4363

CONCLUSION

Bilayer floating tablets of theophylline were the focus of this research. This is an approach to achieve *in vitro* immediate release, buoyancy, and prolonged release. The various sets of granules had a good flow property; combination of Eudragit

Table 3. Postcompression property of various theophylline tablets

Batch code	Thickness (mm)	Diameter (mm)	Hardness (kgF)	Weight variation (%)	Friability (%)	Drug content (%)
F1	3.79±0.09	12.36±0.10	9.84±0.49	0.40±0.95	0.67±0.04	101.00±0.82
F2	3.96±0.18	12.46±0.14	8.04±0.63	0.05±1.18	0.97±0.01	100.13±0.07
F3	4.00±0.05	12.51±0.06	7.14±0.31	0.23±0.93	0.60±0.00	099.44±0.04
F4	4.26±0.07	12.86±0.13	4.74±0.36	0.01±1.01	1.04±0.03	096.82±0.62
F5	4.07±0.11	12.51±0.07	6.08±0.54	0.32±1.11	1.51±0.01	099.03±0.02
F6	3.82±0.10	12.28±0.05	6.89±0.18	0.14±1.03	0.50±0.02	102.12±0.01

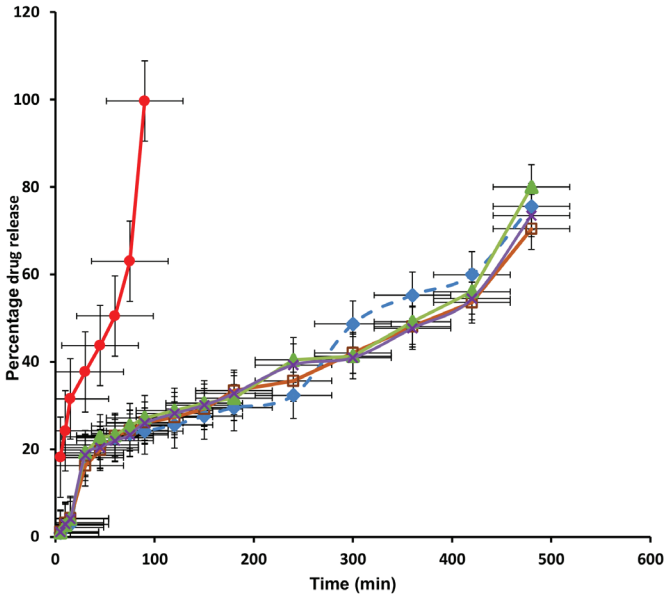

Figure 3. Dissolution profiles of the various formulations: F1 (- - - ■ - - -), F2 (—□—), F3 (—▲—), F5 (—x—), F6 (—●—)

RL100 and CMC produced granules with a better flow property. The presence of gel-forming polymers (CMC and Eudragit RL100) and a gas-producing agent (sodium bicarbonate) helps to achieve prolonged release. Citric acid helps to promote buoyancy under elevated pH of the stomach, thus enhancing drug release. A prolonged floating time and shorter floating lag time could be achieved by appropriate combination of CMC and Eudragit. The ratio of Eudragit and CMC affects the drug release rate and mechanism of release. The *in vitro* drug release profiles obtained with combination of Eudragit and CMC in 1:2 ratio (F1) produced a prolonged floating duration (>8 h) and a shorter floating lag time (20 min), attributes of a controlled released product. Thus, appropriate combination of hydrophobic and hydrophilic polymers can produce well retarded bilayer floating tablets.

ACKNOWLEDGEMENTS

The authors are grateful to the management of Evonik Industries AG, Werk Röhm, Darmstadt, for the gift of the Eudragit® RL100 sample. Also to be acknowledged is the management of Vital Biotic, Nigeria Limited, for providing the API (theophylline powder) at no cost. Special thanks to the laboratory staff of Pharmaceutics and Industrial Pharmacy Department, Delta State University, Abraka, Nigeria, for the use of the laboratory and for helping to operate some of the machines.

Conflicts of interest: No conflict of interest was declared by the authors. The authors alone are responsible for the content and writing of the paper.

REFERENCES

1. Khan GM. Controlled release oral dosage forms: some recent advances in matrix type drug delivery systems. J Med Sci. 2001;1:350-354.
2. Kumar AH, Kavitha K, Kumar SA, Kumar MR, Singh SDJ. Novel approach of bilayer tablet -a review. IJPCBS. 2013;3:887-893.
3. Park K. Controlled drug delivery systems: past forward and future back. J Control Release. 2014;190:3-8.
4. Ghosh DR, Rishikesh MD, Haque A, Banu MR, Rahman MM, Miah SH, Rahman M. Floating drug delivery system: a review. J Drug Discovery Therapeutics. 2013;1:52-59.
5. Majeed SM, Khalil YI. Formulation and evaluation of bilayer matrix tablets of amoxicillin and esomeprazole as an oral modified release dosage form for treatment of peptic ulcer. Int J Pharm Pharm Sc. 2014;6:134-142.
6. Gahlyan M, Jain S. Oral controlled drug delivery system -a review. Pharma Tutor. 2014;2:170-178.
7. Rishikesh G, Mohiuddin AB, Irin D, Drishti RG, Asraful I. Immediate release drug delivery system (tablets) an overview. Int Res J Pharm App Sci. 2012;2:88-94.
8. Nadigoti J, Shayeda. Floating drug delivery systems. Int J Pharm Sci Nanotech. 2009;2:595-604.
9. Panda S, Parida KR, Roy H, Talwar P, Ravanan P. A current technology for modified release drug delivery system: multiple unit pellet system (MUPS). Int J Pharma Sci Health Care. 2013;6:51-63.
10. Borse GC, Mahale NB, Chaudhari SR, Bhuktar DB, Datir MB. A review on emerging drug delivery system: "floating drug delivery system". JADD. 2016;3:12-19.
11. Lee PI, Li JX. Evolution of oral controlled release dosage forms. In: Wen H, Park K, editors. Oral Controlled Release Formulation Design and Drug Delivery. Hoboken; John Wiley & Sons, Inc. 2010;21-31.
12. Shaha SH, Patel JK, Pundarikakshudu K, Patel NV. An overview of a gastro-retentive floating drug delivery system. Asian J Pharma Sci. 2009;4:65-80.
13. Rishikesh G, Anwarul MD, Tripati RP, Al-Amin MA, Irin D. Bilayer tablet technology. World J Pharma Res. 2014;4:150-163.
14. Nayak AK, Maji R, Das B. Gastro-retentive drug delivery systems: a review. Asian J Pharma Sci Res. 2010;3:2-10.
15. Logidhasan L, Suresh S, Mathivanan M. Formulation and *in-vitro* evaluation of bilayer floating tablets of aceclofenac and ranitidine HCl. Int Res J Pharma App Sci. 2013;3:88-94.
16. Shruti S, Ashish P, Shikla A, Raju C. A review on: Recent advancement of stomach specific floating drug delivery system. Int J Pharma Bio Ach. 2011;2:1561-1568.
17. Gopinath C, Hima VB, Nischala M. An overview on bilayered tablet technology. J Global Trends Pharma Sci. 2013;4:1077-1085.
18. Reddy LH, Murthy RS. Floating dosage systems in drug delivery. Crit Rev Ther Drug Carrier Syst. 2002;19:553-585.
19. Vishwakarma AG, Mogal RT, Pawar AY. Bi-layer tablets - a new ways in oral drug delivery system. Int J Pharm Tech Res. 2014;6:1416-1428.
20. Bijumol C, William H, Kurien J, Kurian T. Formulation and evaluation of floating tablets of theophylline. Hygeia Drugs Med. 2013;5:23-31.
21. Barnes PJ. Theophylline. Am J Respir Crit Care Med. 2013;188:901-906.
22. British Pharmacopoeia. London; Her Majesty's Stationery Office; 2012;A320-A322.
23. British Pharmacopeoia. London; The Stationery Office; 2012;2135.

24. Staniforth JN, Aulton ME. Powder flow. In: Aulton ME, ed. Aulton's Pharmaceutics, The Design and Manufacture of Medicines (3rd ed). London; Churchill Livingstone, Elsevier. 2007;168-179.

25. Staniforth JN, Aulton ME. Powder flow. In: Aulton ME, ed. Aulton's pharmaceutics, the design and manufacture of medicines (3rd ed). London; Churchill Livingstone, Elsevier. 2007;170.

26. Tatavarti AS, Muller FX, Hoag SW. Evaluation of deformation behaviour of binary systems of methacrylic acid copolymers and hydroxyl propyl methyl cellulose using a compaction simulator. Int J Pharm. 2008;348:46-53.

27. Naveen KB, Helen JP, Gita NS. Influence of formulation factors on tablet formulation with liquid permeation enhancer using factorial design. J Am Ass Pharma Scientists. 2009;10:1437-1453.

28. British Pharmacopeoia. London; The Stationery Office; 2012;A342.

29. Avbunudiogba JA. Modification of the release profiles theophylline matrix tablets by inclusion of water leachable or water swellable excipients. NIJOPHASR. 2019;8:107-113.

Turk J Pharm Sci 2020;17(6):653-658
DOI: 10.4274/tjps.galenos.2019.46793

ORIGINAL ARTICLE

A Novel Genotyping Method for Detection of the Muscarinic Receptor *M1* Gene rs2067477 Polymorphism and Its Genotype/Allele Frequencies in a Turkish Population

Muskarinik Reseptör *M1* Geni rs2067477 Polimorfizmini Belirlemek için Yeni Bir Genotipleme Yöntemi ve Türk Popülasyonunda Genotip/Alel Sıklıkları

Fezile ÖZDEMİR[1], Yağmur KIR[2], Kenan Can TOK[1], Bora BASKAK[2], Halit Sinan SÜZEN[3]*

[1]Ankara University Institute of Forensic Sciences, Department of Forensic Toxicology, Ankara, Turkey
[2]Ankara University Faculty of Medicine, Department of Psychiatry, Ankara, Turkey
[3]Ankara University Faculty of Pharmacy, Department of Pharmacology and Toxicology, Ankara, Turkey

ABSTRACT

Objectives: Gene variation in the cholinergic muscarinic receptor 1 (CHRM1) has potential to become a candidate biomarker in the development of several disorders as well as drug response. In this study, a novel polymerase chain reaction-restriction fragment length polymorphism (PCR-RFLP) assay was developed to determine the C to A single nucleotide polymorphism at position 267 in the *CHRM1* gene.

Materials and Methods: A new reverse primer and a mismatched forward primer were designed to obtain 125 bp PCR products. The PCR products were then digested with the *Hae III* restriction enzyme to detect the rs2067477 polymorphism that comprises a C to A base change. The novel assay developed was tested in 51 Turkish schizophrenia patients.

Results: The genotyping assay was successfully performed in patients with schizophrenia in order to confirm the accuracy and validity of this method. The frequency of CC, CA, and AA genotypes was 72.5%, 25.5%, and 2%, respectively. On the basis of these findings, the allele frequency of C was 0.85 and the allele frequency of A was 0.15.

Conclusion: This genotyping assay is practical for screening the *CHRM1* C267A polymorphism in pharmacogenetic studies. The present polymorphism may be used as a candidate biomarker to determine genetic susceptibility to related diseases and may contribute to the implementation of individualized drug therapy for M1-related diseases.

Key words: CHRM1, C267A, Turkish, schizophrenia, PCR-RFLP

ÖZ

Amaç: Kolinerjik muskarinik reseptör 1'deki (CHRM1) gen varyasyonu, çeşitli bozuklukların gelişimi için ve ayrıca ilaç yanıtında aday biyogöstergelerden biri olma potansiyeline sahiptir. Bu çalışmada, *CHRM1* geninde 267. pozisyondaki C'den A'ya olan tek nükleotid polimorfizmini belirlemek için yeni bir polimeraz zincir reaksiyonu-kesim parçası uzunluk polimorfizmi (PCR-RFLP) analizi geliştirilmiştir.

Gereç ve Yöntemler: Yüz yirmi beş bç PCR ürünlerini elde etmek için yeni bir geri primer ve uyumsuz bir ileri primer tasarlanmıştır. PCR ürünleri daha sonra C'den A'ya olan baz değişikliğini içeren rs2067477 polimorfizmini tespit etmek için *Hae III* restriksiyon enzimi ile kesilmiştir. Geliştirilen yeni analiz, 51 Türk şizofreni hastasında test edilmiştir.

Bulgular: Genotipleme analizi, yöntemin doğruluğunu ve geçerliliğini onaylamak için şizofreni hastalarında başarıyla uygulanmıştır. CC, CA ve AA genotiplerinin sıklığı sırasıyla %72,5; %25,5 ve %2 olarak bulunmuştur. Bu verilere dayanarak, C alel frekansı 0,85 ve A alel için frekans 0,15 olarak bulunmuştur.

*Correspondence: E-mail: suzen@ankara.edu.tr, Phone: +90 533 345 37 99 ORCID-ID: orcid.org/0000-0003-1779-5850
Received: 20.08.2019, Accepted: 07.11.2019

Sonuç: Bu genotipleme yöntemi, farmakogenetik çalışmalarda *CHRM1* C267A polimorfizminin belirlenmesi için pratik bir yöntemdir. Bu polimorfizm, ilgili hastalıklara karşı genetik duyarlılığı göstermek için aday bir biyogösterge olarak kullanılabilir ve M1 ile ilgili hastalıklar için bireyselleştirilmiş ilaç tedavisinin uygulanmasına katkıda bulunabilir.

Anahtar kelimeler: CHRM1, C267A, Türk, şizofreni, PCR-RFLP

INTRODUCTION

Prenatal and perinatal risks, negative early life events, and genetic predisposition may cause neurodevelopmental alterations and sensitize the dopamine system in the brain, and the presence of these factors may contribute to the development of schizophrenia.[1,2] The prevalence of schizophrenia varies from 3 to 7 per 1000 worldwide and the average lifetime prevalence is 4/1000 while the lifetime risk is 7.2 per 1000.[3,4] However, studies about the prevalence of schizophrenia have shown that the disorder differs in all societies and can vary according to the characteristics of the society.[5,6] A systematic review based on a limited number of general population surveys conducted in Turkey showed that the prevalence of schizophrenia was 8.9 in 1000.[7]

The risk of schizophrenia is 10% for first-degree relatives and 40% for children if both parents have schizophrenia.[8] In addition to heredity in the development of this disease, the gene differences involved in the pharmacokinetics and pharmacodynamics of the drugs used in the treatment of schizophrenia also play a major role in treatment, response, and adverse drug reactions.

Antipsychotic drugs used in the treatment of schizophrenia such as clozapine (CLZ) and olanzapine have been found to be antagonistic to muscarinic receptors.[9] CLZ is prescribed especially in treatment-resistant schizophrenia patients and it is a weak muscarinic receptor 1 (M1) agonist, while its active metabolite, N-desmethylclozapine (NCLZ), is a potent M1 agonist receptor.[9] In addition, M1 receptor agonist DCLZ plays an important role in determining the clinical effects and pharmacotherapy in the treatment of psychotic disorders. Studies have also pointed out that a decreased density of M1 receptors particularly in the neocortical regions was associated with schizophrenia.[10] Similarly, some studies showed reduced M1 receptor mRNA levels in brain samples from schizophrenia patients.[11] Considering all of these, M1 receptor is an important target in the development and also treatment of schizophrenia.

There are five types of cholinergic muscarinic receptors, designated as M1 to M5. Among these, M1 is mostly located in the nervous system. M1 is typically found in the parasympathetic ganglia, cortical and hippocampal regions of the brain, and less in airway epithelial cells and is involved in cognitive functions such as learning and memory, as well as regulation of cardiac contractions.[12,13] M1 is encoded by the *CHRM1* gene located on chromosome 11q12.3. There are 15 single nucleotide polymorphisms (SNPs) in the *CHRM1* gene region; one of them is the C267A (rs2067477) base change. This polymorphism is a silent mutation that is a transversion of cytosine (C) to adenine (A) at position 267 in the *CHRM1* gene region. It is in the wobble site of the codon (GG**C**→GG**A**), so the protein sequence is preserved.[13,14]

In short, the determination of the SNPs in the gene regions that are potentially involved in schizophrenia are important because they could affect disease susceptibility, cognitive performance, drug response, or adverse drug reactions. The polymerase chain reaction-restriction fragment length polymorphism (PCR-RFLP) assay is one of the most common, simple, effective, fast, and inexpensive methods used to determine SNPs. Thus, our aim was to develop a novel PCR-RFLP method for genotyping the *CHRM1* C267A polymorphism. Subsequently, the PCR-RFLP assay developed was performed for validation of the method and determination of genotype and allele frequencies in Turkish patients with schizophrenia.

MATERIALS AND METHODS

Study subjects and DNA isolation

Whole blood samples were obtained from 51 consecutive Turkish schizophrenia outpatients admitted to Ankara University Medical Faculty Psychiatry Department and diagnosed using the Diagnostic and Statistical Manual of Mental Disorders fourth edition[15] between October 2016 and April 2018. The inclusion criteria were being between 18 and 65 years of age and having signed the written informed consent. Patients with any additional psychiatric diagnosis or general medical comorbidity were excluded. Informed consent was obtained from all subjects and the protocol was approved by the Research Ethics Committee of the Medical Faculty, Ankara University. Genomic DNA was extracted with the high salt method from the peripheral blood of the 51 subjects.[16] The absorbance level of DNA samples for 260 and 280 nm was detected with spectrophotometric analysis and the purity of the samples was between 1.7 and 2.0.

PCR primers and conditions

The sequence data of the C267A (rs2067477) polymorphism in the human *CHRM1* gene region were obtained from the NCBI website (http://www.ncbi.nlm.nih.gov) and the new primers were designed as follows based on the published sequence: forward primer: 5'-TACTTCCTGCTGAGCCTAGCC-3'; reverse primer: 5'-GCCAGCCAGAGGTCACAAGCC-3'. The PCR reaction was carried out in a volume of 25 µL, which contained 10X PCR buffer (Amplicon, Denmark; containing 10X ammonium and 15 mM Mg), 1.1 mM $MgCl_2$, 0.1 mM dNTP, 10 pmol from each primer, 1.5 µL of DMSO, 0.45 U of *Taq* DNA polymerase (Amplicon, Denmark), approximately 100 ng of genomic DNA, and distilled water to complete the final volume to 25 µL. Moreover, 125 bp PCR product was obtained using the following PCR cycling conditions: initial denaturation at 94°C for 3 min, followed by 30 3-graded cycles, which were denaturation at 94°C for 30 s, annealing for 30 s at 59°C, and elongation at 72°C for 45 s. At the end, a final extension for 5 min at 72°C was carried out.

The PCR products (125 bp) were visualized under an ultraviolet illuminator on 1% agarose gel stained with ethidium bromide.

Restriction fragment length polymorphism conditions

The RFLP was carried out in a 20-µL volume mixture consisting of 2 µL of 10X buffer, 10 U of *Hae III* enzyme (New England Biolabs, USA), 10 µL of PCR product, and 7 µL of distilled H_2O. The reactions were incubated at 37°C overnight and the digested products were visualized under an ultraviolet transilluminator after they had been electrophoresed on 3% agarose gel containing ethidium bromide for 1 h. The digested RFLP products were obtained for a wild-type genotype, while there were undigested RFLP products for a mutant genotype on the agarose gel.

To further assess the reliability of the presented assay, the PCR product of each different genotype was verified by direct sequencing using the same set of primers.

Statistical analysis

Allele and genotype frequencies were calculated by genotype counting method. The observed genotype frequencies of *CHRM1* C267A were compared with the expected frequencies according to the Hardy-Weinberg equilibrium. The data obtained were compared with previously reported representative data in other ethnic groups. Differences in allele frequencies between schizophrenic groups were tested by Pearson's chi-square test and a p value <0.05 was considered statistically significant.

RESULTS

A novel PCR-RFLP assay was designed to detect C267A SNP in the *CHRM1* gene region in schizophrenic patients. We also evaluated the accuracy and validity of this novel method. New primers were designed and the PCR products were digested with *Hae III* restriction enzyme for determination of the variant genotypes. A schematic illustration of the assay is given in Figure 1.

The previous genotyping method for rs2067477 by Liao et al.[17] could not be perfectly applied to analyze this SNP due to the difficulties in finding primer sites. This method also did not include any information about PCR product fragments, PCR conditions, or base pairs of the restriction fragments for genotyping. In the present study, a novel genotyping assay was developed and successfully performed by utilizing a reverse primer and mismatch forward primer, which are explained above. As shown in Figure 2, the underlined A (adenine base) is the mismatched base in the forward primer, which was replaced with the ancestral base G (guanine base) to eliminate the recognition site of the *Hae III* restriction enzyme (GG▼CC) in the primer binding site. This was also confirmed by sequencing (data not shown).

The individuals with the CC genotype (wild type) yielded two bands of 83 bp and 42 bp, while those with the AA genotype (mutant type) gave an undigested band (125 bp) on 3% agarose gel. The agarose gel electrophoresis results of the RFLP products on 3% agarose gel are given in Figure 3.

One sample of each different genotype PCR product was sequenced to confirm the expected sequence of each genotype and the data obtained were consistent with our findings. The sequencing results of the three genotypes are given below in Figure 4. The PCR products of each different genotype sequencing result precisely demonstrated the reliability of our novel assay.

The allele and genotype frequencies in the 51 Caucasian Turkish schizophrenic patients are shown in Table 1 for the C267A polymorphism in the *CHRM1* gene. This is the first study to document the frequencies and genotypes of *CHRM1* C267A alleles in Turkish patients with schizophrenia. The molecular analyses revealed that, among the 51 patients tested for the C267A genotype, 37 (72.5%) were CC, 13 (25.5%) were CA, and 1 (2%) was AA. On the basis of these data, the allele frequency of C was 0.85 and the frequency of A was 0.15. The distribution of *CHRM1* genotypes in our samples is presented in Table 1. The

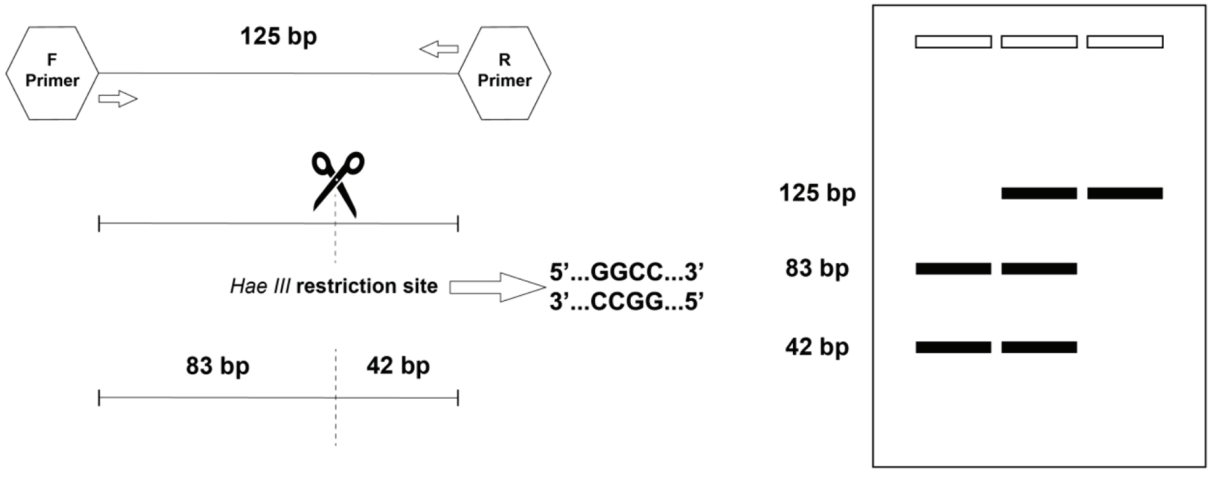

Figure 1. Diagrammatic representations of recognition sites of the *Hae III* enzyme and a schematic illustration of the restriction fragments for each genotype of *CHRM1* C267A SNP

CHRM1: Cholinergic muscarinic receptor 1, SNP: Single nucleotide polymorphism

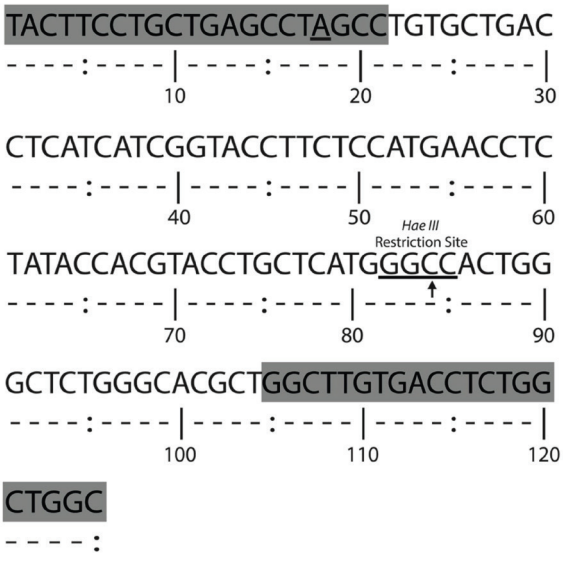

Figure 2. Restriction analysis of *CHRM1* with *Hae III* endonuclease. Forward and reverse primers are highlighted in gray. The mismatch base (A), which is used to eliminate the recognition site of *Hae III* in the forward primer, is underlined. The Hae III recognition site is depicted by underlining in the middle of the *CHRM1* sequence. This recognition site also includes rs2067477 SNP, which is depicted with capital and bold letters in the recognition site (C). In the case of the ancestral C allele at position 267 of the *CHRM1* gene 83 bp and 42 bp DNA fragments are obtained, after *Hae III* digestion. Conversely, no digestion site for *Hae III* endonuclease is found, when the C allele is replaced by an A allele at position 267, giving one fragment of 125 bp

CHRM1: Cholinergic muscarinic receptor 1, SNP: Single nucleotide polymorphism

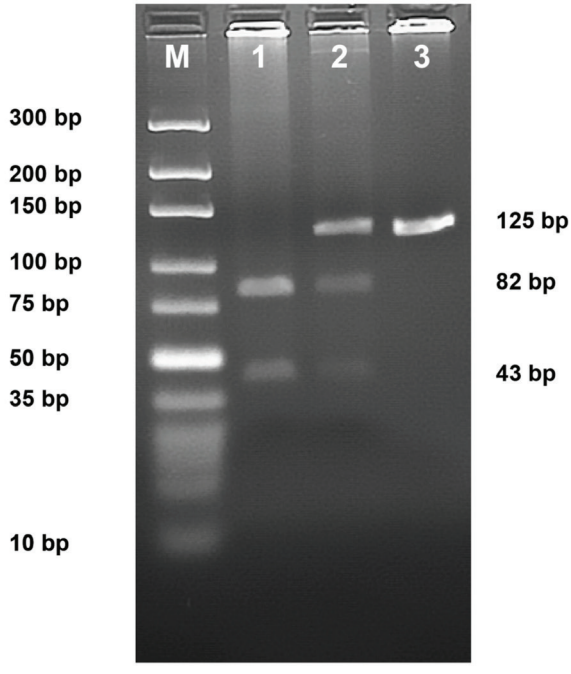

Figure 3. Agarose gel electrophoresis demonstrated the expected RFLP product sizes. The results shown in 1, 2, and 3 were in the same order as in Figure 1 (M: Thermo Fisher Scientific GeneRuler Ultra Low Range DNA Ladder Marker (10-300 bp, SM1211). 1: CC genotype, 2: CA genotype, and 3: AA genotype)

RFLP: Restriction fragment length polymorphism, PCR: Polymerase chain reaction

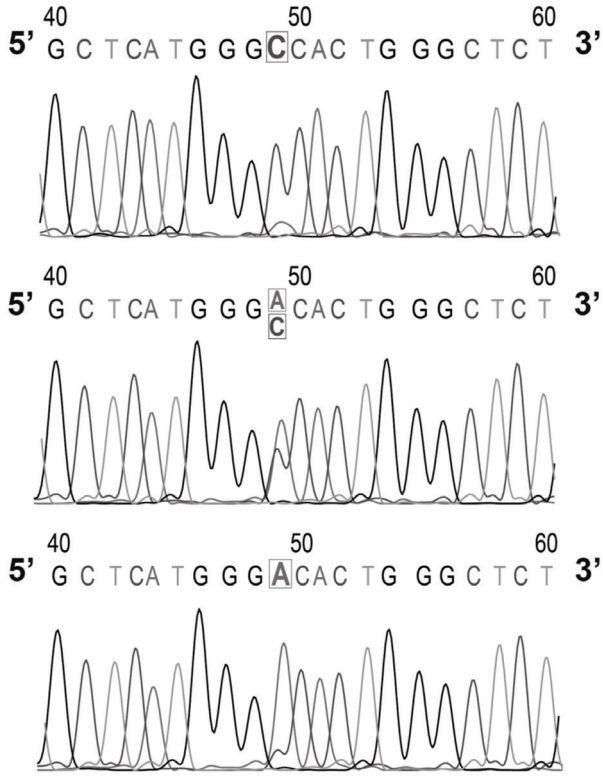

Figure 4. Examples of DNA sequencing of the polymerase chain reaction product of the *CHRM1* gene. From top the bottom the three figures represent the genotype of CC, CA, and AA, respectively, and the sequenced result of the heterozygote genotype with C and A alleles in the same position

CHRM1: Cholinergic muscarinic receptor 1

p value of the present results was p>0.05 and it was in good accordance with expected genotype distributions, calculated using the Hardy-Weinberg equilibrium (χ^2: 0.013; p=0.9).

DISCUSSION

Due to several gene variations that are potentially involved in the physiopathology of mental disorders, the *CHRM1* C267A polymorphism has the probability to become a genetic biomarker. In addition, this variation might play a role in psychopharmacotherapy since the muscarinic M1 receptor is a prominent target for a considerable number of medications. There were three primary objectives in the present study. The

Table 1. The distribution of the *CHRM1* gene polymorphism in Turkish patients with schizophrenia

Gene	Genotype	Observed frequency	Expected frequency	Allele frequencies
CHRM1	CC	37	37.1	C: 0.85 A: 0.15
	CA	13	12.8	
	AA	1	1.1	
Total		51	51	1.00

CHRM1: Gene variation in the cholinergic muscarinic receptor 1

main purpose was to develop a novel genotyping assay for the *CHRM1* C267 polymorphism and to test the accuracy and validity of the developed method. The other two aims were to draw attention to the importance of the *CHRM1* gene in the pathology of schizophrenia and to determine the genotype and allele frequencies of the *CHRM1* C267 polymorphism in Turkish patients with schizophrenia.

M1 receptors could be important for neuronal disorders and cognitive function in the pathophysiology of schizophrenia due to the location in the medial prefrontal cortex and hippocampus.[18,19] Lower levels of muscarinic receptors in the central nervous system of people with schizophrenia have been found in some studies.[18,20] Scarr et al.[21] showed that decreased M1 levels in the cortical region of the brain could contribute to the pathophysiology of schizophrenia. Thus, a brain imaging test before treatment could be useful in identifying patients with low M1 levels who could be treatment resistant. Another neuroimaging study also showed that muscarinic receptors were extensively decreased in schizophrenia patients under treatment during neuroimaging.[20]

At the molecular level, Mancama et al.[22] demonstrated that the levels of *CHRM1* cDNA in schizophrenia patients were 28% lower than those in their control group. Moreover, research suggested that there could be a relationship between rs2067477 SNP and a reduction in gray matter volume in patients with schizophrenia.[23] Other studies have shown that rs2067477 might be associated with cognitive performance. In these studies the Wisconsin Card Sorting Test performance, which is a measure of prefrontal and executive functions, was better in heterozygous individuals than in homozygous wild-type carriers.[17,24] In one of these studies, 243 schizophrenic patients were assessed according to the rs2067477 genotype and the genotypes differed in responses in the Wisconsin Card Sorting Test but not in other parameters including age of onset, chlorpromazine equivalents, and Brief Psychiatric Rating Scale.[17] Contrary to these, Cropley et al.[23] indicated that the homozygous CC genotype did not have an impact on attention, visuospatial construction, verbal fluency, or working memory but they did not assess the patients using the Wisconsin Card Sorting Test. All of these studies showed the importance of the determination of *CHRM1* C267A alleles in schizophrenic patients. To the best of our knowledge, ours is the first study to document the frequencies of *CHRM1* C267A alleles and its genotype distribution in Turkish schizophrenia patients.

In the present study, the genotype distribution and allele frequencies of the *CHRM1* C267A polymorphism were obtained from 51 Turkish schizophrenia patients. The data obtained were compared with previously reported representative data in other schizophrenia patients as shown in Table 2. The present results showed that the C and A allele frequencies in Turkish patients with schizophrenia were 0.85 and 0.15, respectively. The C267A variant frequency ranged between 0.07 and 0.11 in Australian patients with schizophrenia or schizoaffective disorder, while it was 0.09 in Chinese schizophrenia patients.[17,23-26] The difference in frequency of C267A SNP between Turkish schizophrenia patients and other populations patients was not statistically significant ($p>0.05$).

CONCLUSION

In summary, a novel, practical, low-cost, and reproducible PCR-RFLP method was developed for genotyping the *CHRM1* C267A polymorphism. The method is based on elimination of the recognition site of *Hae III* in the forward primer binding site by utilizing a mismatch base in the forward primer. As a result of this study, the validity and accuracy of the present novel method have been proven. Thus, the genotype and allele frequencies of the *CHRM1* C267 polymorphism in Turkish patients with schizophrenia have been determined for the first time. The number of samples should be increased in further studies for more certain and reliable results. Additionally, the effect of the *CHRM1* gene in the pathology and treatment of schizophrenia is explained with the data in the literature. The developed genotyping assay and results could be useful and provide a perspective for future studies.

Financial and Conflict of interest: This work was supported in part by grant from the Research Fund of Ankara University under Project 18L0217001. The author declares no conflict of interest, financial or otherwise.

Table 2. Genotypes and allele frequencies of C267A SNP in *CHRM1* in this study and other populations

Study population	n	Genotype frequency n (%)			Allele frequency		Reference
		CC	CA	AA	C	A	
Turkish patients with schizophrenia	51	37 (72.5)	13 (25.5)	1 (2)	0.85	0.15	Present study
Chinese patients with schizophrenia	243	202 (83.1)	40 (16.5)	1 (0.4)	0.91	0.09	7
Australian patients with schizophrenia and schizoaffective disorder	97	83 (86)	14 (14)	-	0.93	0.07	24
Australian patients with schizophrenia or schizoaffective disorder	267	191 (84.1)	35 (15.4)	1 (0.4)	0.92	0.08	23
Australian patients with schizophrenia and schizoaffective disorder	176	147 (83.5)	29 (16.5)	-	0.92	0.08	25
Australian patients with schizophrenia and schizoaffective disorder	147	114 (77.6)	33 (22.4)	-	0.89	0.11	26

CHRM1: Cholinergic muscarinic receptor 1, SNP: Single nucleotide polymorphism

Ethical conduct of research: All authors state that the appropriate institutional review board approval had obtained and the informed consent has been obtained from the participants involved study. The authors state that all experiments had followed the principles outlined in the Declaration of Helsinki.

Conflicts of interest: No conflict of interest was declared by the authors. The authors alone are responsible for the content and writing of the paper.

REFERENCES

1. Howes OD, Murray RM. Schizophrenia: an integrated sociodevelopmental cognitive model. Lancet. 2014;383:1677-1687.
2. Owen MJ, Sawa A, Mortensen PB. Schizophrenia. Lancet. 2016; 388:86-97.
3. Mc Garth J, Saha S, Chant D, Welham J. Schizophrenia: a concise overview of incidence, prevalence, and mortality. Epidemiol Rev. 2008;30:67-76.
4. DSM, American Psychiatric Association. Section 2: Diagnotic Criteria and Codes, Schizophrenia Spectrum and Other Psychotic Disorders. In: Diagnostic and Statistical Manual of Mental Disorders, 5th edition. Ed: First MB, Ward MN. American Psychiatric Publishing, Washington, DC. 2013;99-105.
5. Saha S, Chant D, Welham J, McGrath J. A systematic review of the prevalence of schizophrenia. PLoS Med. 2005;2:413-433.
6. Esan OB, Ojagbemi A, Gureje O. Epidemiology of schizophrenia-An update with a focus on developing countries. Int Rev Psychiatry. 2012;24:387-392.
7. Binbay T, Ulaş H, Elbi H, Alptekin K. The psychosis epidemiology in Turkey: a systematic review on prevalence estimates and admission rates. Turk Psikiyatri Derg. 2011;22:40-52.
8. Ayano G. Schizophrenia: a concise overview of etiology, epidemiology diagnosis and management: review of literatures. J Schizophr Res. 2016;3:1-7.
9. Weiner DM, Meltzer HY, Veinbergs I, Donohue EM, Spalding TA, Smith TT, Mohell N, Harvey SC, Lameh J, Nash N, Vanover KE, Olsson R, Jayathilake K, Lee M, Levey AL, Hacksell U, Burstein ES, Davis RE, Brann MR. The role of M1 muscarinic receptor agonism of N-desmethylclozapine in the unique clinical effects of clozapine. Psychopharmacology (Berl). 2004;177:207-216.
10. Scarr E, Cowie TF, Kanellakis S, Sundram S, Pantelis C, Dean B. Decreased cortical muscarinic receptors define a subgroup of subjects with schizophrenia. Mol Psychiatry. 2009;14:1017-1023.
11. Michel MC, Teitsma CA. Polymorphisms in human muscarinic receptor subtype genes. Handb Exp Pharmacol. 2012;208:49-59.
12. Hamilton SE, Schlador ML, McKinnon LA, Chmelar RS, Nathanson NM. Molecular mechanisms for the regulation of the expression and function of muscarinic acetylcholine receptors. J Physiol Paris. 1998;92:275-278.
13. Lucas JL, Sadee W, DeYoung JA. Single nucleotide polymorphisms of the human M1 muscarinic acetylcholine receptor gene. AAPS Pharmsci. 2001;3:57-61.
14. Brann MR, Ellis J, Jorgensen H, Hill- Eubanks D, Jones SV. Muscarinic acetylcholine-receptor subtypes - localization and structure-function. Prog Brain Res. 1993;98:121-127.
15. The American Psychiatric Association. DSM-IV-TR: Diagnostic and Statistical Manual of Mental Disorders 4th Revised Edition, American Psychiatric Press Inc. 2000. Avaialable from: https://dsm.psychiatryonline.org/doi/abs/10.1176/appi.books.9780890420249.dsm-iv-tr
16. Miller SA, Dykes DD, Polesky HF. A simple salting out procedure for extracting DNA from human nucleated cells. Nucleic Acid Res. 1988;16:1215.
17. Liao DL, Hong CJ, Chen HM, Chen YE, Le SM, Chang CY, Chen H, Tsai SJ. Association of muscarinic M1 receptor genetic polymorphisms with psychiatric symptoms and cognitive function in schizophrenic patients. Neuropsychobiol. 2003;48:72-76.
18. Dean B, McLeod M, Keriakous D, McKenzie J, Scarr E. Decreased muscarinic1 receptors in the dorsolateral prefrontal cortex of subjects with schizophrenia. Mol Psychiatry. 2002;7:1083-1091.
19. Yohn SE, Conn PJ. Positive allosteric modulation of M1 and M4 muscarinic receptors as potential therapeutic treatments for schizophrenia Neuropharmacol. 2018;136:438-448.
20. Raedler TJ, Knable MB, Jones DW, Urbina RA, Gorey JG, Lee KS, Egan MF, Coppola R, Weinberger DR. *In vivo* determination of muscarinic acetylcholine receptor availability in schizophrenia. Am J Psychiatry. 2003;160:118-127.
21. Scarr E, Hopper S, Vos V, Seo MS, Everall IP, Aumann TD, Chana G, Dean B. Low levels of muscarinic M1 receptor-positive neurons in cortical layers III and V in Brodmann areas 9 and 17 from individuals with schizophrenia. J Psychiatry Neurosci. 2018;43:338-346.
22. Mancama D, Arranz MJ, Landau S, Kerwin R. Reduced expression of the muscarinic 1 receptor cortical subtype in schizophrenia. Am J Med Genet. 2003;119B:2-6.
23. Cropley VL, Scarr E, Fornito A, Klauser P, Bousman CA, Scott R, Cairns MJ, Tooney PA, Pantelis C, Dean B. The effect of a muscarinic receptor 1 gene variant on grey matter volume in schizophrenia. Psychiatry Res. 2015;234:182-187.
24. Scarr E, Sundram S, Deljo A, Cowie TF, Gibbons AS, Juzva S, Mackinnon A, Wood SJ, Testa R, Pantelis C, Dean B. Muscarinic M1 receptor sequence: Preliminary studies on its effects on cognitionand expression. Schizophr Res. 2012;138:94-98.
25. Carruthers SP, Gurvich CT, Cropley VL, Pantelis C, Bousman C, Lenroot RK, Bruggemann JM, Weickert T; Australian Schizophrenia Research Bank, Rossell SL. The effects of a muscarinic receptor 1 gene variant on cortical thickness and surface area in schizophrenia. Psychiatry Res Neuroimaging. 2018;280:62-64.
26. Carruthers SP, Cropley V, Bousman C, Everall IP, Neill E, Pantelis C, Sumner PJ, Tan EJ; Australian Schizophrenia Research Bank, Bozaoglu K, Thomas EHX, Van Rheenen TE, Gurvich CT, Rossell SL. The effects of a muscarinic receptor *1* gene variant on executive and non-executive cognition in schizophrenia spectrum disorders. Psychiatry Res. 2019;273:178-180.

Turk J Pharm Sci 2020;17(6):659-666
DOI: 10.4274/tjps.galenos.2019.33602

ORIGINAL ARTICLE

Evaluation of the Neurobehavioural Toxic Effects of Taurine, Glucuronolactone, and Gluconolactone Used in Energy Drinks in Young Rats

Genç Sıçanlarda Enerji İçeceklerinde Kullanılan Taurin, Glukuronolakton ve Glukonolaktonun Nörodavranışsal Etkilerinin Değerlendirilmesi

Revathi BOYINA[1]*, Sujatha DODOALA[2]

[1]MLR Institute of Pharmacy, Department of Pharmacology, Hyderabad, India
[2]Sri Padmavati Mahila Visvavidyalayam, Institute of Pharmaceutical Technology, Department of Pharmacology, Tirupati, India

ABSTRACT

Objectives: The neurotoxic effects of food additives used in energy drinks have been investigated since the 1900s but safety concerns are rising and reassurance via safety testing in animals is demanded by the public. Rigorous safety testing is performed for dose optimisation and duration of treatment and to detect the methods to assess changes in mood and behaviour. Hence, we studied the neurobehavioral effects of selected food additives used in energy drinks and their combination in rats when consumed in high doses.

Materials and Methods: Young Sprague Dawley rats were divided into six groups. Group 1 was treated with the vehicle, group 2 was treated with 25 mg/kg p.o. caffeine, group 3 was treated with 5 mg/kg p.o. glucuronolactone, group 4 was treated with 8 mg/kg p.o. taurine, group 5 was treated with 84 mg/kg p.o. gluconolactone, and group 6 was treated with a combination of the three food additives. Neurobehavioral changes were evaluated on days 7, 14, and 21 using behavioural parameters. Neurobehavioral scoring and neurotransmitter estimation in rat brain tissue was performed on day 21.

Results: Significant changes were observed in the neurobehavioral parameters and neurobehavioural scoring in group 4 and group 6, compared with the control group ($p<0.001$). Furthermore, the significant decreases in neurotransmitter levels in the brains of rats that were treated with food additives indicated the neurotoxic effects of these substances.

Conclusion: This study elaborated the neurobehavioral effects of selected food additives, namely glucuronolactone, taurine, and gluconolactone, when administered orally for 21 days in young rats. The highest toxic effects, including alterations in neurotransmitter levels, were observed in animals treated with a combination of food additives at high doses.

Key words: Energy drinks, food additives, taurine, glucuronolactone, gluconolactone

ÖZ

Amaç: Enerji içeceklerinde kullanılan gıda katkı maddelerinin nörotoksik etkileri 1900'lardan bu yana incelenmektedir; ancak, güvenlilik endişeleri artmaktadır ve hayvanlarda güvenliliklerinin test edilerek onaylanması halk tarafından talep edilmektedir. Sıkı güvenlilik testleri doz ve uygulama süresi optimizasyonu ve ruh hali ve davranıştaki değişiklikleri belirlemek için yapılmaktadır. Bu nedenle, biz enerji içeceklerinde kullanılan seçilmiş gıda katkı maddelerinin ve kombinasyonlarının sıçanlarda nörodavranışsal etkilerini yüksek dozlarda araştırdık.

Gereç ve Yöntemler: Genç Sprague Dawley sıçanlar altı gruba ayrıldı: Grup 1'e taşıyıcı, grup 2'ye 25 mg/kg p.o. kafein, grup 3'e 5 mg/kg p.o. glukuronolakton, grup 4'e 8 mg/kg p.o. taurin, grup 5'e 84 mg/kg p.o. glukonolakton ve grup 6'ya üç gıda katkı maddesinin karışımı uygulanmıştır. Davranışsal parametreler kullanılarak nörodavranışsal değişiklikler 7, 14 ve 21. günlerde değerlendirilmiştir. Nörodavranışsal skorlama ve sıçan beyin dokusundan nörotransmitter belirlemenmesi 21. günde yapılmıştır.

Bulgular: Kontrol grubuna kıyasla grup 4 ve grup 6'da nörodavranışsal parametreler ve nörodavranışsal skorlamada belirgin değişiklikler gözlenmiştir ($p<0,001$). Dahası, gıda katlı maddeleri uygulanan hayvanların beyinlerindeki nörotransmiter düzeylerindeki belirgin düşüşler bu maddelerin nörotoksik etkilerini göstermektedir.

*Correspondence: E-mail: revspharma@gmail.com, Phone: +918985223029 ORCID-ID: orcid.org/0000-0002-8561-724X
Received: 03.06.2019, Accepted: 07.11.2019

Sonuç: Bu çalışma 21 gün boyunca oral olarak genç sıçanlara uygulanan seçilmiş gıda katkı maddelerinden glukuronolakton, taurine ve glukunolaktonun nörodavranışsal etkilerini ayrıntılı bir şekilde göstermiştir. Nörotransmitter düzeyleri dahil en fazla toksik etkiler yüksek dozlarda gıda katkı maddelerinin kombinasyonu uygulanan grupta görülmüştür.
Anahtar kelimeler: Enerji içecekleri, gıda katkı maddeleri, taurine, glukuronolakton, glukonolakton

INTRODUCTION

We are exposed to neurotoxins naively through food products. Today the evaluation of the effects of food additives on behaviour and mood in adults is of great concern. Various regulatory bodies are encouraging scrutiny of the use of food additives rigorously for safety and reassurance. The Food and Drug Administration (FDA) and European Food Safety Authority have been evaluating and supporting risk assessment and safety in the use of appropriate doses of acceptable daily intake (ADI). The food additives used in many products like baby foods, cool drinks, energy drinks, and soft drinks are approved by the FDA after safety evaluation. However, various food additives like antioxidants, stabilisers, sweeteners, thickeners, preservatives, and flavouring agents have effects on behaviour when taken in high doses that are listed under the safety margin. As of 2006, FDA guidelines on food additives are classified based on level of concern and safety margin into Low concern level I (12-50 ppb), Intermediate concern level II (50-250 ppb), and High concern level III (250-1000 ppb) based on primary toxicological data.[1] The maximum level of additive that has no demonstrable toxic effect, called the "no-observed-adverse-effect level", and ADI are the check parameters for each food additive. Chronic consumption per day more than the ADI leads to toxicity. The risk to human health varies depending upon the type and time of exposure. Specific studies such as for neurotoxicity, immunotoxicity, and allergenicity are rigorously performed repeatedly to ensure the safety of food additives.[2]

Common food additives used in energy drinks like taurine, glucuronolactone, and gluconolactone are considered elevated risk. The daily exposure to taurine, glucuronolactone, and gluconolactone from energy drinks in young generations is higher than the mean daily exposure (1420 mL/day of energy drink or 2.6 cans/day). In adults, chronic habitual intake of energy drinks was reported to cause several neurological disorders including migraine, seizures, endocrine disorders, and neuropsychiatric disorders.[3] Hence, excessive consumption of energy drinks has toxic effects on the nervous system.

The safety of these food additives used in energy drinks was not documented by the Scientific Committee on Food. According to EFSA 2009 data, the stimulatory effect of taurine on the central nervous system was not clearly documented. The major constituents of energy drinks are taurine, glucuronolactone, and gluconolactone.[4] Based on this background, a research protocol was elaborated to assess systematically possible neurobehavioural toxic effects in animals of individual food additives and the combination of the food additives taurine, glucuronolactone, and gluconolactone used in energy drinks at high doses. The study included an evaluation of neurobehavioural effects, neurobehavioural scoring, and neurotransmitter estimation in the brain tissue of young rats to show possible neurobehavioural effects and ensure the safety level of food additives used in energy drinks, which are listed under the safety margin.

MATERIALS AND METHODS

Chemicals and reagents

Chemicals

Glucuronolactone, gluconolactone, and caffeine (food grade 99.5%) were procured from Srineelima Labs, Hyderabad, India. Taurine (food grade 99.6%) was obtained from Nutrija Lifesciences, Nagda, Madhya Pradesh, India. All other chemicals (analytical grade) were from Himedia Pvt Ltd., India.

Reagents

Hydrochloric acid [(HCl)-butanol solution (0.85 mL of 37% HCl in 1 L)], 0.4 M HCl (3.4 mL of concentrated HCl and made up to 100 mL with water), 0.1 M HCl (0.85 mL of concentrated HCl made up to 100 mL with water), 5 M NaOH (20 g of sodium hydroxide pellets dissolved in distilled water and volume made up to 100 mL with distilled water), and 10 M acetic acid (57 mL of glacial acetic acid and made up to 100 mL with distilled water) were used. Reagents and buffers like sodium acetate buffer (EDTA pH 6.9), heptane, sodium sulphite solution, and O-phthaldialdehyde (OPT) reagent were obtained from Sigma Aldrich, Hyderabad, India.

Equipment

A morris water maze (MWM), version 5.0, was obtained from Orchid Scientific. A wooden arena with 64 squares was prepared by Wood Works, Hyderabad. A tissue homogeniser 160 W, a refrigerated centrifuge from Gravity Labs, and a spectrofluorometer model, ALT 2380 (wavelength range 200 to 700), were also used.

Animals

Sprague Dawley albino rats of both male and female in equal ratio weighing 150-200 g were obtained from the animal house of MLR Institute of Pharmacy, Hyderabad. The animals were divided into four groups and housed under standard laboratory conditions (temperature 25±10˚C, relative humidity 55±5%, and 12.00:12.00 h dark:light cycle) with standard pellet diet and water *ad libitum*. The experimental procedure was approved by the Institutional Animals Ethics Committee (IAEC) as required by the Committee for the Purpose of Control and Supervision of Experiments on Animals (CPCSEA), MLR Institute of Pharmacy, Hyderabad (CPCSEA/IAEC/PR3/2019).

Experimental protocol

All the animals were divided into six separate groups and each group consisted of six animals with equal ratios of males and

females, 3:3 (n=6, 3 males + 3 females). All the doses were calculated based on the human dose available in the literature and were converted to animal dose.[3] High doses of food additives were administered and the animals were observed for neurotoxic effects. Group I animals served as controls, treated with water administered orally. Group II animals acted as the working standard treated with caffeine 25 mg/kg p.o. Group III animals were treated with glucuronolactone 5 mg/kg p.o., group IV animals were treated with taurine 8 mg/kg p.o., group V animals were treated with gluconolactone 84 mg/kg p.o., and group VI animals were treated with a combination of the three food additives (glucuronolactone 5 mg/kg p.o., taurine 8 mg/kg p.o., and gluconolactone 84 mg/kg p.o.). All the animals were treated with freshly prepared doses dissolved in water and administered through an oral gauge every day until day 21.

Assessment of neurobehavioural effects

Neurobehavioural changes were observed in animals treated with the respective doses for 21 days. On days 7, 14, and 21 the animals were screened for neurobehavioural effects by functional observational battery (FOB) and the Irwin protocol.[5] These include studies of behavioural alterations, the MWM test, a locomotor activity test, and the Katz protocol as described below.

Behavioural alterations

Behavioural changes were evaluated by measuring rearing and paw licking behaviour for 5 min.[6] The observations were noted by three blind observers.

Morris water maze test

Cognitive changes such as in learning, conditioning, memory, and attention were evaluated by MWM test in rats.[7] The maze was a round grey tank (0.45 m radius, 0.5 m tall) filled with water (22°C) to a depth of 0.15 m. An adjustable platform of size 0.06 m x 0.06 m made of steel was placed 0.01 m under the water level and 0.13 m from the edge. Milk (1 mL) was added to make the water cloudy and thus the platform was hidden. On the edge of the tank the four letters nominated as north (N), south (S), east (E), and west (W) divided the tank into four portions (N-W, N-E, S-E, and S-W). On day 1, the rats were allowed to swim in the tank for 1 min without the hidden platform. Thus, they were trained for swimming in the tank. On day 2 they were trained to identify and move onto the submerged platform for 6 trials per day until day 5. In each trial the rats were released into the tank with their faces pointing towards the water to confirm immersion. The latency from immersion in the tank to escape onto the hidden platform (maximum duration of trial 2 min) was noted. In 2 min, if the animal could not identify the platform it was physically directed to climb by using a glass rod. Then the score of 2 min was noted for these trials. The number of such unsuccessful trials was calculated. For learning and memorising the spatial cues each animal was given an interval of 0.5 min on climbing onto the platform.

Locomotor activity test

Locomotor changes such as coordination and equilibrium were assessed by locomotor activity test. This test consists of a square wooden field measuring 0.8x0.8x0.3 m and the flooring was divided into 64 squares of equal dimensions. Duration of immobility and locomotion in 5 min for each animal was recorded.[7]

Katz protocol (neurobehavioural scoring)[8]

Neurobehavioural scores were calculated for the animals after 21 days' treatment with high doses of food additives and they were evaluated for neurobehavioural toxic effects (Table 1). The observations were noted by three blind observers.

Estimation of neurotransmitters

Preparation of tissue extract[9]

On day 21 the rats were sacrificed, the whole brain was dissected out, and the subcortical region was separated and weighed. The weighed tissue was homogenised in a homogeniser with 5 mL of HCl butanol for about 1 min. The homogenised tissue was then centrifuged for 10 min at 2000 rpm. The supernatant layer

Table 1. Neurobehavioural scores by Katz protocol to evaluate neurotoxic effects

	Neurobehavioural effect	Scores
General behavioural deficit	Present	0
Consciousness	No attempt (coma)	20
Respiration	Normal	0
	Abnormal	20
Cranial nerve reflexes	Present	0
Olfactory (sniffing food)	Absent	4
Vision (follow hand)	Present	0
	Absent	4
Corneal reflex	Present	0
	Absent	4
Whisker (movement)	Present	0
	Absent	4
Hearing (turning to clapped hands)	Present	0
	Absent	4
Motor deficit:	Normal	0
(Leg/tail movement)	Stiff	5
	Paralysed	10
Sensory deficit	Present	0
Leg/tail (on pinching)	Absent	10
Coordination:	Present	0
Beam walking (1.5 cm)	Absent	5
Placing test	Present	0
	Absent	5
Righting reflex	Present	0
	Absent	5
Stopping at edge of table	Present	0
	Absent	5
Neurobehavioural toxicity	**Total**	**100**

(1 mL) was separated and added to a centrifuge tube containing 2.5 mL of heptane and 0.3 mL of 0.1 M HCl. After 10 min of shaking vigorously the tube was centrifuged under identical conditions. Two layers were separated, the supernatant layer (organic layer) was discarded, and the remaining aqueous extract was used to estimate noradrenaline, dopamine, and serotonin. All the steps were carried out at 0°C. The brain extracts were stored at -20°C until further experimentation.

Estimation of noradrenaline[10]

First 0.2 mL of the aqueous layer was taken from tissue extract stored at ice cool temperature after preparation of extract. Then 0.05 mL of 0.4 M HCl and 0.1 mL of EDTA (pH 6-9) were added to the aqueous extract accompanied by 0.1 mL of iodine solution for oxidation. The reaction was stopped after 2 min by adding 0.1 mL of Na_2SO_3 solution. Next, 0.1 mL of acetic acid was added after 1.5 min. The solution was heated to 100°C for 6 min. The sample was allowed to cool and excitation and emission spectra were noted from the spectrofluorometer. These interpretations were measured at 395-485 nm for noradrenaline.

Estimation of dopamine[10]

To 0.2 mL of aqueous phase extract were added 0.5 mL of HCl and 1 mL of EDTA (pH 6.9) accompanied by 0.1 mL of iodine solution for oxidation. The reaction was stopped after 2 min by adding 0.1 mL of Na_2SO_3 solution. Then 0.1 mL of acetic acid was added after 1.5 min. The solution was heated to 100°C for 6 min. The sample was allowed to cool and excitation and emission spectra were noted from the spectrofluorometer. These interpretations were measured at 330-375 nm for dopamine.

Estimation of serotonin[10]

First, 0.2 mL of aqueous tissue extract was added with 0.25 mL of OPT reagent. Then it was heated for 100°C for 10 min. After the sample reached ambient temperature, the readings were taken at 360-470 nm in the spectrofluorometer for the estimation of serotonin.

Tissue blanks for dopamine and noradrenaline were prepared by adding the reagents of the oxidation step in reverse order (sodium sulphite before iodine). For the serotonin tissue blank, 0.25 mL of concentrated HCl without OPT was added. Internal standard was prepared by taking 500 µg/mL each of noradrenaline, dopamine, and serotonin prepared in distilled water: HCl butanol in 1:2 ratio. The concentration of the neurotransmitters expressed in µg per gram wet weight of tissue was calculated by using the formula:[11]

$$\text{Concentration of unknown (Cu)} = \frac{\text{Sample O.D-Blank OD}}{\text{Standard O.D-Blank OD}} \times \text{Cs}$$

Cs: Concentration of standard (500 µg/mL)

OD: Optical density

Statistical analysis

Altogether the results were studied using ANOVA followed by Dunnett's multiple comparisons. GraphPad Prism version 7.0, 2019 was the software used for analysis.

RESULTS

Neurobehavioural changes

Behavioural alterations

Alterations in behavioural effects were observed in animals treated with high doses of individual food additives, with successive increases in the behavioural effects with increases in treatment duration on days 7, 14, and 21. Animals treated with taurine and the combination of food additives showed significant increases in rearing and hind paw licking ($p<0.001$) compared with the experimental group. Group VI, given the combination of food additives, showed a high significant difference ($p<0.05$) in behavioural activity compared with the group given caffeine as shown in Figure 1.

Morris water maze test

Taurine treated animals showed longer escape latency onto the submerged platform in the water maze compared with the controls. With an increase in the duration of treatment the increase in escape latency was significant ($p<0.001$). Animals treated with the combination of food additives showed significantly ($p<0.05$) longer escape latency on day 21, indicating altered cognitive effects compared with the caffeine treated animals (Figure 2).

Locomotor activity test

A significant increase in immobility duration was seen in animals treated with individual food additives and the combination of food additives ($p<0.001$) and with an increase

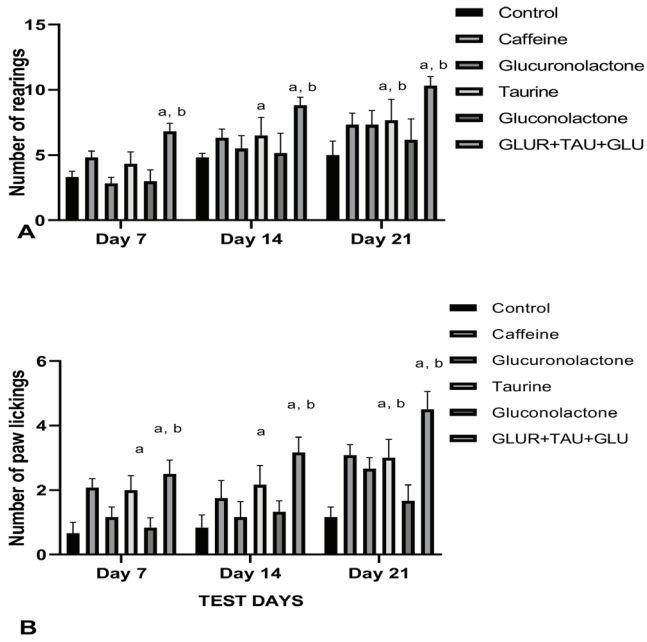

Figure 1. Assessment of neurobehavioural alterations of food additives on exposure to high doses for 7, 14, and 21 days in Sprague Dawley rats by (A) number of rearings and (B) number of paw lickings. Data were represented as mean ± SEM (n=6). [a]$p<0.001$ showed significant differences between the experimental group and the control group. [b]$p<0.05$ showed significant differences between the food additives treated group and the caffeine treated group

SEM: Standard error of the mean, GLUR: Glucuronolactane, TAU: Taurine, GLU: Glucanolactane

in duration of treatment compared to the control group when placed in the wooden arena. The combination of food additives caused a significant increase in immobility duration ($p<0.05$), indicating a decrease in locomotion compared to the caffeine treated animals (Figure 3).

Katz protocol of neurobehavioural scoring

In the Katz protocol animals treated with high doses of individual food additives showed high neurobehavioural scores on day 21. All the experimental groups showed significantly higher ($p<0.001$) scores than the control animals (Figure 4). The combination group exhibited the highest neurobehavioural scoring ($p<0.05$), indicating an increase in neurobehavioural toxic effects compared with the caffeine treated animals.

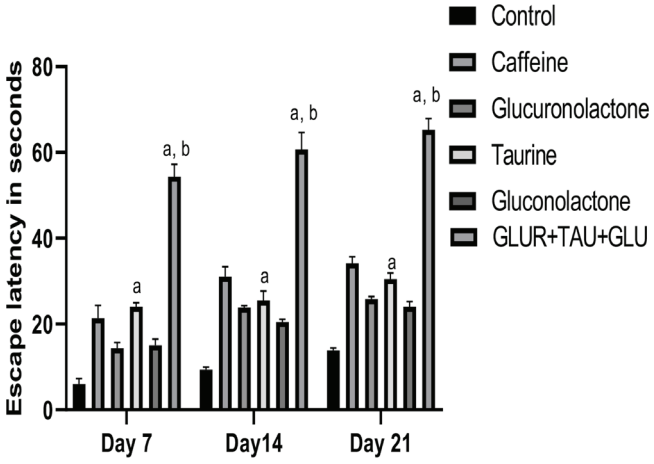

Figure 2. Assessment of neurobehavioural effects of food additives on exposure to high doses for 7, 14, and 21 days in Sprague Dawley rats by escape latency in seconds using the Morris water maze test. Data were represented as mean ± SEM (n=6). [a]$p<0.001$ showed significant differences between the experimental group and the control group. [b]$p<0.05$ showed significant differences between the experimental group and the caffeine treated group

SEM: Standard error of the mean, GLUR: Glucuronolactane, TAU: Taurine, GLU: Glucanolactane

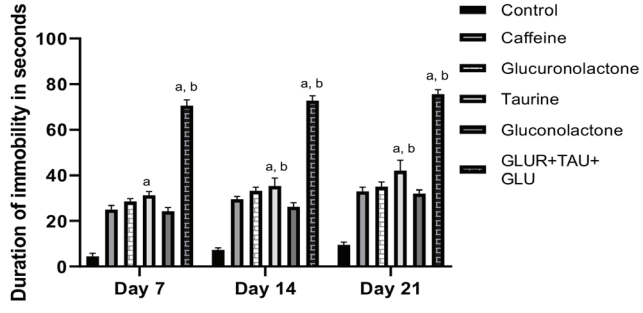

Figure 3. Assessment of neurobehavioural effects of food additives on exposure to high doses for 7, 14, and 21 days in Sprague Dawley rats by duration of immobility using a locomotor activity test. Data were represented as mean ± SEM (n=6). [a]$p<0.001$ showed significant differences between the experimental group and the control group. [b]$p<0.05$ showed significant differences between the food additives treated group and the caffeine treated group

SEM: Standard error of the mean, GLUR: Glucuronolactane, TAU: Taurine, GLU: Glucanolactane

Estimation of neurotransmitters

On day 21, tissue extract was prepared and neurotransmitters were estimated. The noradrenaline and serotonin levels were pointedly ($p<0.001$) lower in the taurine and combination of food additives treated animals than in the controls. The combination group animals showed high significance compared with the caffeine treated group ($p<0.05$) (Figures 5 and 6).

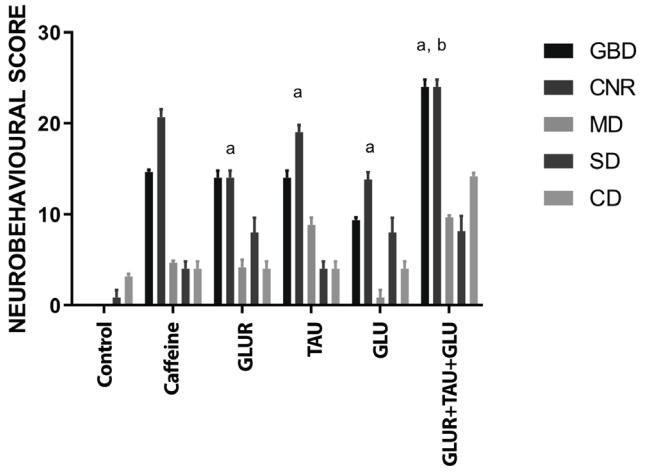

Figure 4. Assessment of food additives on exposure to high doses for 21 days in Sprague Dawley rats for neurobehavioural effects by neurobehavioural scoring using the Katz protocol. Data were represented as mean ± SEM (n=6). [a]$p<0.001$ showed significant differences between the experimental group and the control group. [b]$p<0.05$ showed significant differences between the experimental group and the caffeine treated group

GBD: General behavioural deficits (score 40), CNR: Cranial nerve reflexes (score 20), MD: Motor deficit (score 10), SD: Sensory deficit (score 10, CD: Coordination (score 20), SEM: Standard error of the mean, GLUR: Glucuronolactane, TAU: Taurine, GLU: Glucanolactane

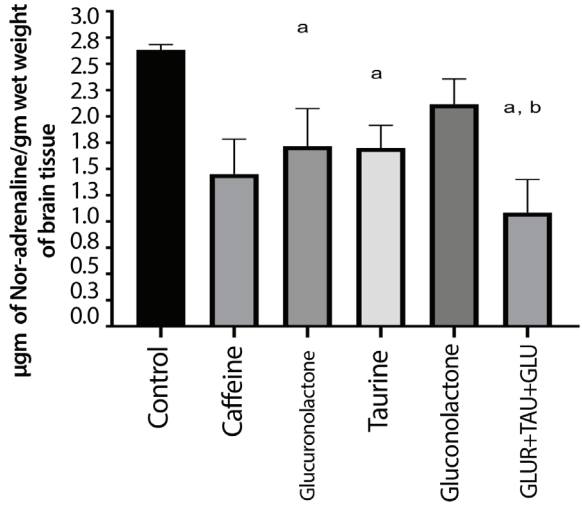

Figure 5. Effect of food additives on Nor-adrenaline levels in whole brain tissue of rats exposed to high doses for 21 days. Data were represented as mean ± SEM (n=6). a$p<0.001$ showed significant differences between the experimental group and the control group. b$p<0.05$ showed significant differences between the food additives treated group and the caffeine treated group

SEM: Standard error of the mean, GLUR: Glucuronolactane, TAU: Taurine, GLU: Glucanolactane

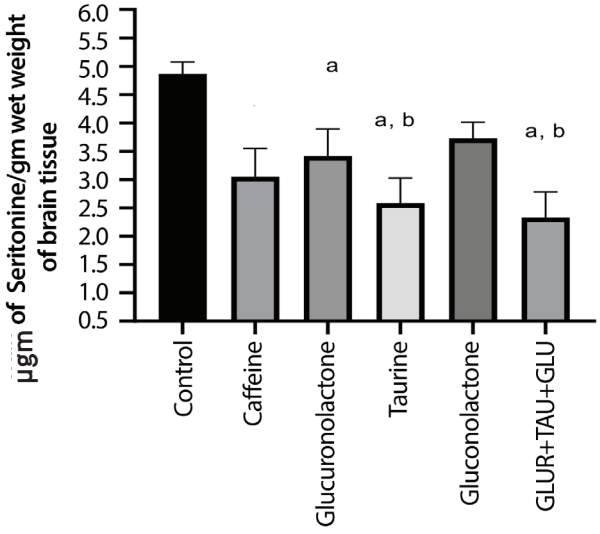

Figure 6. Effect of food additives on serotonin levels in whole brain tissue of rats exposed to high doses for 21 days. Data were represented as mean ± SEM (n=6). [a]p<0.001 showed significant differences between the experimental group and the control group. [b]p<0.05 showed significant differences between the food additives treated group and the caffeine treated group

SEM: Standard error of the mean, GLUR: Glucuronolactane, TAU: Taurine, GLU: Glucanolactane

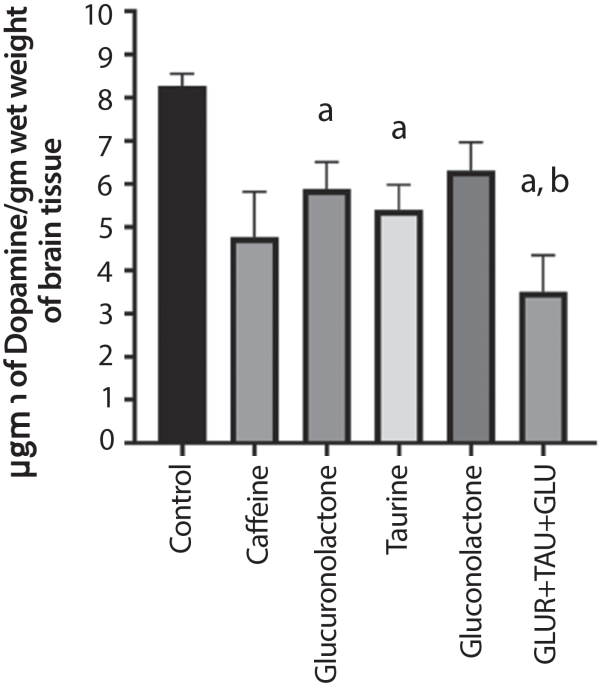

Figure 7. Effect of food additives on dopamine levels in whole brain tissue extract of rats exposed to high doses for 21 days. Data were represented as mean ± SEM (n=6). [a]p<0.001 showed significant differences between the experimental group and control the group. [b]p<0.05 showed significant differences between the food additives treated group and the caffeine treated group

SEM: Standard error of the mean, GLUR: Glucuronolactane, TAU: Taurine, GLU: Glucanolactane

Decreases in dopamine levels were observed in the taurine and combination group animals compared to the control (p<0.001). The combination animals showed highly significant results when compared with the caffeine treated animals, indicating altered neurotransmission in the brain (p<0.05) (Figure 7).

DISCUSSION

The food additives used in energy drinks, when consumed above the acceptable level, were reported to produce toxic effects, as stated by the EFSA. However, the exact ingredients and the dose responsible for toxic effects were not evaluated or documented clearly.[4] The present research provides evidence for neurobehavioural toxic effects for the selected FDA approved food additives used in energy drinks when consumed above the ADI. The neurobehavioural toxic effects of food additives when administered orally at doses of glucuronolactone 5 mg/kg p.o., taurine 8 mg/kg p.o., gluconolactone 84 mg/kg p.o., and a combination of the three food additives were evaluated and documented over 21 days of treatment in young rats.

Earlier studies suggested that the Irwin protocol (FOB test) explains many parameters and provides a multidimensional method for the explanation of neurobehavioural effects.[5] Based on the Irwin protocol, the Sprague Dawley rats were treated with food additives and neurobehavioural changes were evaluated using behavioural alterations test, the MWM test, and a locomotor test for clarification of neurobehavioural toxic effects.

Previous literature indicated that behaviour is a measure of the integration of neural function and alteration in behaviour was used to evaluate neurobehavioural toxic effect.[5] In the present study, alteration in behavioural activity was assessed by considering behavioural parameters like paw licking and rearing behaviours, which were considered indicators of grooming. An increased anxiety level due to any stimulus was reported to change paw licking and rearing behaviour.[12] Similar alterations in paw licking and rearing behaviour were caused by taurine and the combination, which clearly indicates the alteration in neuronal functioning with the selected food additives. Previous studies that evaluated cognitive effects in rats using a water maze test reported an increase in duration of escape latencies, indicating a decrease in cognition.[13] In the present study a significant increase in duration of escape latency to the submerged platform was observed in the taurine and combination groups. The decreased cognition may be due to the decrease in cyclic GMP levels as reported with cognitive impairment and neurobehavioural deficit reported in aluminium toxicity studies.[14] A similar decrease in cGMP levels was reported with taurine in cardiomyocytes.[15] Our study indicated that neurotoxicity caused by food additives progressively increased with days of exposure from day 7 to day 21. Earlier studies stated that locomotor activity indicates attentiveness.[16] In the present study, the decrease in locomotor activity indicated by an increase in duration of immobility in the taurine and combination groups affirms that a decrease in attentiveness leads to altered neurological functioning.[16]

Previous studies reported that taurine showed dose correlated behavioural changes in rats. Chewing of limbs after treatment with taurine indicated its central pharmacological and neuromodulator effects.[17] In the present study, the taurine treated group also showed altered behavioural activity, which confirmed its potent neuromodulator effect on neurotransmitters of the brain. In a subacute toxicity study for 14 days in rats, gluconolactone showed mortality, abnormal clinical signs, body-weight changes (on days 1, 2, 3, 7, 10, and 14), and gross pathological changes in the brain but was not focused on neurobehavioural symptoms.[18] Our study for the first time showed changes in behavioural activity in gluconolactone treated animals and may hint at neurotoxicity when consumed higher than the acceptable doses. These changes were high when given in combination with taurine.

Neurological scales/scores for motor, sensory and reflex functions in rats, mice, and dogs were used to detect effects on brain injury.[8] In the present research work, the Katz protocol of neurobehavioural scores was used considering various parameters like general behavioural deficits, cranial nerve reflexes, motor deficit, sensory deficit, and coordination to evaluate the neuronal damage in animals. High scores for neurobehavioural deficits were observed in animals receiving the food additives in combination, rather than individually. This indicates chances of increases in brain neuronal damage and can be correlated with the decrease in neurotransmitters.

Selected food additives were hypothesised to enhance neurotransmitter activity concentrated in the subcortical regions according to the literature.[19] Therefore, subcortical regions of whole brain extracts were used to estimate neurotransmitters. Decreases in noradrenaline, serotonin, and dopamine levels indicating neurochemical alterations and neurotoxic effects on subchronic drug administration were suggested previously.[20] In addition, earlier studies also focused on the participation of serotonin in cognition and memory, and altered serotonergic neurotransmission by toxic substances was reported.[21] The neurotransmitter modulatory effect of these selected food additives was mentioned.[22] Corroborating the earlier studies, noradrenaline, serotonin, and dopamine were decreased prominently in the current study. The combination of taurine, gluconolactone, and glucuronolactone caused more noticeable changes in neurotransmitter levels than when given alone, which indicates a risk of more neuronal damage, modulation, and toxicity. These changes support the observed neurobehavioural deficits caused by food additives.

The present study raises concern about the safety of the mentioned food additives at the doses studied considering the aspect of simultaneous consumption of these food additives via energy drinks, although the safety of these additives was established and approved but individually and at a different exposure level. Furthermore, histopathological studies are needed for correlation of neurobehavioural toxic effects.

CONCLUSION

This study elaborated the neurotoxic effects of glucuronolactone, taurine, and gluconolactone used in energy drinks when consumed above the ADI. It showed significant neurobehavioural toxic effects accompanied by altered neurotransmitter levels in rats treated with a combination of selected food additives. Furthermore, investigation is required to understand the mechanism and interaction between food additives. Appraisal of the developmental neurotoxic effects of these food additives in combination will also be valuable.

Conflicts of interest: No conflict of interest was declared by the authors. The authors alone are responsible for the content and writing of the paper.

REFERENCES

1. Carocho M, Barreiro MF, Morales P, Ferreira ICFR. Adding molecules to food, pros and cons: A review on synthetic and natural food additives. Compr Rev Food Saf. 2014:4:377-399.
2. Mepham B. Food additives: an ethical evaluation. Br Med Bull. 2011;99:7-23.
3. Aguilar F, Charrondiere UR, Dusemund B, Galtier P, Gilbert J, Gott DM, Grilli S, Guertler R, Kass GEN, Koenig J, Lambré C, Leblanc JC, Mortensen A, Parent-Massin D, Pratt I, Rietjens IMCM, Stankovic I, Tobback P, Verguieva T, Woutersen RA. The use of taurine and D-glucurono-γ-lactone as constituents of the so-called "energy" drinks, Scientific opinion of the panel on food additives and nutrient sources added to food, The EFSA J. 2009;935:1-31.
4. New information on ingredients in so-called "energydrinks" opinion of the panel on food additives, flavourings, processing aids, Materials in Contact with Food and Cosmetics of the Norwegian Scienific Committee for Food Safety,Vitenskapskomiteen for mattrygghet (VKM)11 May 2009. ISBN 978-82-8082-327-4. Available from: https://vkm.no/download/18.2994e95b15cc545071635320/1498417607794/a8859a2195.pdf
5. Virginia C. Moser, Functional assays for neurotoxicity testing. Toxicol Pathol. 2011;39:36-45.
6. Jintanaporn Wattanathorn, Nongnut Uabundit, Wanchailtarat, SupapornMucimapura, Pisamai Laopatarakasem, Bungorn Sripanidkulchai. Neurotoxicity of Coscinium fenestratum stem, a medicinal plant used in traditional medicine. Food Chem Toxicol. 2006;44:1327-1333.
7. Gasem M. Abu-Taweel, Jamaan S. Ajarem, Mohammad Ahmad, Neurobehavioural toxic effects of perinatal oral exposure to aluminium on the developmental motor reflexes, learning, memory and brain neurotransmitters of mice offspring. Pharmacol Biochem Behav. 2012;101:49-56.
8. Jeon H, Ai J, Sabri M, Tariq A, Shang X, Chen G, Macdonald RL. Neurological and neurobehavioral assessment of experimental subarachnoid hemorrhage. BMC Neuroscience. 2009;10:103.
9. Schlumfjf M, Liechtensteiner W, Langemann H, Waser PG, Hefti F. A Fluorometric micro method for the simultaneous determination of serotonin, noradrenaline and dopamine in milligram amounts of brain tissue, Pergamon Press, Printed M Great Britain. Biochem Pharmacol. 1974;23:2337-2446.
10. Habibur Rahman, Eswaraiah MC. Simple spectroscopic Methods for estimating. Brain Neurotransmitters, Antioxidant Enzymes of Laboratory animals like Mice: A review, 2017. Available from: http://www.pharmatutor.org/articles/simple-spectroscopicmethod-estimating-brain-neurotransmitter-antioxidnat-enzymes-lab-animals

11. Manikkoth S, Deepa B, Sequeira M, Joy AE, Rodrigues R. Assessment of brain dopamine levels to evaluate the role of Tylophora indica ethanolic extract on alcohol induced anxiety in Wistar albino rats. J Young Pharm. 2016;8:91-95.

12. Kalueff AV, Tuohimaa P. The grooming analysis algorithm discriminates between different levels of anxiety in rats: potential utility for neurobehavioural stress research. J Neurosci Methods. 2005;143:169-177.

13. Mesaram N, Nagapuri KK, Banala RR, Nalagoni CR, Karnati PR. Quercetin treatment against NaF induced oxidative stress related neuronal and learning changes in developing rats. Journal of King Saud University - Science. 2017;29:221-229.

14. Auti ST, Yogesh A. Kulkarni. Neuroprotective effect of Cardamom oil against Aluminium induced neurotoxicity in rats. Frontiers Neurol. 2019;10:399.

15. Yang Q1, Yang J, Wu G, Feng Y, Lv Q, Lin S, Hu J. Effects of taurine on myocardial cGMP/cAMP ratio, antioxidant ability, and ultrastructure in cardiac hypertrophy rats induced by isoproterenol. Adv Exp Med Biol. 2013;776:217-229.

16. P. Devi Raja Rajeswari, K. Aruna and S. Raja Sankar. The Effect of Biophytum sensitivum Extract Against the Behavioral Changes Induced by 1-Methyl - 4-Phenyl-1,2,3,6-Tetrahydropyridine (MPTP) in mice J Pharm Sci Res. 2016;8:1345-1348.

17. Red Bull Australia Pty Ltd, Submission on Review of Liquor Control Act 1988(WA), 25 February 2012.

18. Safety evaluation of certain food additives. IPCS, Inchem, WHO, Geneva 1999.

19. Miranda MI. Changes in Neurotransmitter Extracellular Levels during Memory Formation. In: Bermúdez-Rattoni F, editor. Neural Plasticity and Memory: From Genes to Brain Imaging. Boca Raton (FL): CRC Press/Taylor & Francis; 2007. Chapter 7. Available from: https://www.ncbi.nlm.nih.gov/books/NBK3921/)

20. Takata K, Sheng H, Borel CO, Laskowitz DT, Warner DS, Lombard FW Long-term cognitive dysfunction following experimental subarachnoid hemorrhage: new perspectives. Exp Neurol. 2008;213:334-336.

21. Ahuja M, Bishnoi M, Chopra K. Protective effect of minocycline, a semi-synthetic second generation teteracycline against 3-nitropropionic acid (3-NP) induced neurotoxicity. Toxicol. 2008;244:111-122.

22. Gamay, Aly (McLean, VA, US). Neurotransmitter and brain modulating oral delivery system for enhancement of cognitive functions and energy. United States Patent Application number 20180236016. Kind code A1. Publication date 08/23/2018. Filling date 02/14/2018.

Turk J Pharm Sci 2020;17(6):667-672
DOI: 10.4274/tjps.galenos.2019.65481

ORIGINAL ARTICLE

Antifungal and Antibiofilm Activities of Selective Serotonin Reuptake Inhibitors Alone and in Combination with Fluconazole

Selektif Serotonin Geri Alım İnhibitörlerinin Tek Başına ve Flukonazol ile Kombinasyonlarının Antifungal ve Antibiyofilm Aktiviteleri

Yamaç TEKİNTAŞ[1], Aybala TEMEL[1], Ayşegül ATEŞ[2], Bayrı ERAÇ[2], Dilek Yeşim METİN[3], Süleyha HİLMİOĞLU POLAT[3], Mine HOŞGÖR LİMONCU[2]*

[1]İzmir Katip Çelebi University Faculty of Pharmacy, Department of Pharmaceutical Microbiology, İzmir, Turkey
[2]Ege University Faculty of Pharmacy, Department of Pharmaceutical Microbiology, İzmir, Turkey
[3]Ege University Faculty of Medicine, Department of Medical Microbiology, İzmir, Turkey

ABSTRACT

Objectives: *Candida* spp. are clinically important pathogens that cause difficulties for treatment by biofilm formation. Considering antifungal resistance rates and the limitations in the discovery of new antifungals, the antifungal and antibiofilm effects of various drugs used for different therapeutic purposes are becoming more important. The goal of our study was to determine the antifungal and antibiofilm effects of the selective serotonin reuptake inhibitors (SSRIs), namely sertraline (SRT), paroxetine (PRX), and fluoxetine (FLX) alone and in combination with fluconazole (FLC) against *Candida* spp.

Materials and Methods: Twenty *Candida* spp. strains isolated from clinical samples from Ege University Hospital were identified by the Dalmau method and matrix-assisted laser desorption ionization time of flight mass spectrometry. The minimum inhibitory concentrations (MICs) of the SSRIs and FLC were detected by broth microdilution method. Synergistic interactions between the SSRIs and FLC were investigated by checkerboard assay. The antibiofilm effects of the SSRIs were determined by spectrophotometric microplate method.

Results: Among the isolates, five different *Candida* spp. (*C. albicans, C. glabrata, C. krusei, C. tropicalis,* and *C.parapsilosis*) were identified. The MICs of the SSRIs ranged between 16-512 µg/mL. While SRT showed the highest antifungal effect, the antibiofilm efficacy of FLX was higher than that of the other agents. Moreover, FLX and PRX showed a synergistic effect with FLC in 13 and 19 isolates, respectively. Four isolates were strong biofilm producers while nine isolates were moderate biofilm producers. *C. parapsilosis* strains showed higher biofilm production than the other species. At MIC/2 concentration, FLX and SRT alone inhibited mature biofilms in six and five isolates, respectively, while PRX caused increases biofilm formation in seven isolates.

Conclusion: This study revealed that MIC/2 concentrations of SSRIs could have antifungal and antibiofilm effects. SRT and FLX alone or in combination with antifungals may possibly have therapeutic potential for combating fungal infections.

Key words*: Candida* spp., fluconazole, EUCAST, synergistic effect, antibiofilm

ÖZ

Amaç: Klinik açıdan önemli fungal patojenlerden olan *Candida* türleri, biyofilm üretme kapasiteleriyle tedavide zorluklara yol açmaktadır. Antifungal direnç oranları ve yeni antifungallerin keşfinin sınırlılığı göz önüne alındığında, farklı terapötik amaç için kullanılan çeşitli ilaç moleküllerinin antifungal ve antibiyofilm etkileri daha fazla önem kazanmaktadır. Çalışmamızın amacı, selektif serotonin geri alım inhibitörleri (SSRI) olan sertralin (SRT), paroksetin (PRX), fluoksetinin (FLX), tek başına ve flukonazol (FLC) ile kombine halde *Candida* türlerine karşı antifungal ve antibiyofilm etkilerinin belirlenmesidir.

Part of this study was presented at the "12th International Symposium on Pharmaceutical Sciences, Ankara, Turkey" on June 26-29, 2018, and published as an abstract in the abstract book p 138.

*Correspondence: E-mail: minehosgorlimoncu@yahoo.com.tr, Phone: +90 232 3113983 ORCID-ID: orcid.org/0000-0002-4892-8639
Received: 27.09.2019, Accepted: 14.11.2019

Gereç ve Yöntemler: Ege Üniversitesi Hastanesi'nde klinik örneklerden izole edilen 20 *Candida* spp. kökeni Dalmau metodu ve Matriks aracılı lazer dezorpsiyon/iyonizasyon uçuş zamanı kütle spektrometresi kullanılarak tanımlanmıştır. SSRI moleküllerin ve FLC'nin minimum inhibitör konsantrasyon (MIC) değerleri sıvı mikrodilüsyon yöntemiyle belirlenmiştir. FLC ve SSRI moleküllerin sinerjistik etkileşimleri dama tahtası metoduyla araştırılmıştır. SSRI'ların antibiyofilm etkinlikleri spektrofotometrik mikroplaka yöntemiyle değerlendirilmiştir.

Bulgular: Yirmi izolat arasında beş farklı *Candida* türü (*C. albicans, C. glabrata, C. krusei, C. tropicalis* ve *C. parapsilosis*) belirlenmiştir. SSRI'ların MIC değerlerinin 16-512 µg/mL aralığında değiştiği saptanmıştır. SRT'nin yüksek antifungal etkisi gözlenirken, FLX'in antibiyofilm etkinliğinin diğer ajanlardan daha yüksek olduğu belirlenmiştir. Ayrıca, FLX ve PRX'in FLC ile kombinasyonlarında sırasıyla on üç ve on izolat üzerinde sinerjistik etkisi görülmüştür. Dört izolatın güçlü, dokuz izolatın ise orta düzey biyofilm üreticisi olduğu saptanmıştır. *C. parapsilosis* suşlarının biyofilm üretim kapasitelerinin diğer türlerden daha yüksek olduğu gözlenmiştir. MIC/2 konsantrasyonda, tek başlarına FLX ve SRT sırasıyla altı ve beş izolatta olgun biyofilm üzerinde inhibe edici etki gösterirken, PRX'in yedi izolatın biyofilm oluşumunda artışa yol açtığı saptanmıştır.

Sonuç: Bu çalışma, SSRI'ların MIC/2 konsantrasyonlarda antifungal ve antibiyofilm etkinliklerinin olabileceğini göstermiştir. SRT ve FLX'in tek başına veya antifungal ajanlarla kombine kullanımının fungal enfeksiyonlarla mücadelede terapötik potansiyeli olabilir.

Anahtar kelimeler: *Candida* spp., flukonazol, EUCAST, sinerjistik etki, antibiyofilm

INTRODUCTION

Fungal infections have received attention due to their higher prevalence and mortality rates in recent years.[1] Among the clinically important yeasts, *Candida* spp. are some of the most common opportunistic pathogens. Although species of this genus may live as members of the microbiota in healthy individuals, they may cause life-threatening infections in hospitalized and immunosuppressed patients.[2,3] One of the major reasons causing the increase in *Candida* infections is thought to be the greater use of medical devices such as catheters, cardiac pacemakers, or artificial hearts, which have suitable surfaces for biofilm formation.[4] A biofilm is a group of microbial cells embedded in extracellular polymeric substances, and recent studies have shown that these sessile cells in biofilms are much more resistant to both antimicrobials and host defense mechanisms compared to planktonic cells due to reduced penetration.[5]

The increased resistance rates to antifungals, the high biofilm production capacities, and the fact that certain *Candida* species are inherently resistant to some antifungals suggest that new antifungal molecules are needed for therapy. Because of the eukaryotic cell structures of fungal pathogens, antifungals should have selective mechanisms that target specific structures in microorganisms different from human cells. This situation makes it difficult to develop new antifungal agents. Consequently, it is becoming more and more beneficial to investigate the antifungal and antibiofilm activities of various molecules used for diverse therapeutic purposes.

Selective serotonin reuptake inhibitors (SSRIs) are used as antidepressants and as the first-line therapy for premenstrual syndrome. The antifungal activities of these agents were first discovered when three patients with chronic vulvovaginal candidiasis treated with sertraline (SRT) for premenstrual syndrome presented no symptoms of candidiasis during the treatment course.[6] Based on this knowledge, different studies have shown that these agents may have antifungal effects on yeast species. The main goal of the present study was to determine the antimicrobial activity and antibiofilm effects of SSRIs alone and in combination with fluconazole (FLC) against clinical *Candida* spp. isolates.

MATERIALS AND METHODS

Fungal isolates and identification

Twenty *Candida* spp. isolated from patients samples at Ege University Hospital, Mycology Laboratory of Medical Microbiology Department and *Candida parapsilosis* ATCC 22019 strain were examined. The yeast species were identified by the Dalmau method and matrix-assisted laser desorption ionization time of flight mass spectrometry (MALDI TOF-MS).

Agent solutions

FLC (Sigma, USA), fluoxetine (FLX) (Abdi Ibrahim, Turkey), paroxetine (PRX) (ARIS, Turkey), and SRT (Sanovel, Turkey) were provided in powder form. The agents were dissolved with using sterile water and dimethyl sulfoxide to a final concentration of 4096 µg/mL. The stock solutions were stored at -80°C until use.

Determination of minimum inhibitory concentrations (MICs)

MICs of the SSRIs and FLC were determined by broth microdilution method according to European Committee for Antimicrobial Susceptibility Testing (EUCAST) criteria.[7] Firstly, an appropriate volume of RPMI-1640 (Sigma, USA) supplemented with 2% glucose (Sigma, USA) was buffered with 0.165 M MOPS (Sigma, USA) at pH 7.0. Then the medium was added to 96-well U-bottom microplates. The agent solutions were added to the first well of the microplates and serially diluted. Fungal inoculums ($1x10^6$ cells) were added to the wells and the microplates were incubated at 37°C for 24 h. After incubation, the absorbance values were measured at 570 nm by spectrophotometric microplate reader (Varioskan Flash, Thermo Scientific, USA). The drug concentration that led to an approximately 50% reduction in growth relative to the drug-free well was accepted as the MIC. All experiments were performed in triplicate. The statistical analyses were performed using GraphPad Prism 5.03 (t-test).

Checkerboard assays

Interaction types between the SSRI agents and FLC were determined using the checkerboard method in 96-well plates. The types of interaction between the SSRI agents and FLC were evaluated based on the fractional inhibitory index (FIX) and the fractional inhibitory concentration (FIC) values for each combination. The following formulae were used to calculate the

FIC index:

FIC of drug A: (MIC of drug A in combination) / (MIC of drug A alone)

FIC index (FIX): (FIC of drug A) + (FIC of drug B)

Synergistic, indifferent, and antagonist interactions were defined by FIX values of ‹0.5, 0.5 to 4, and ›4, respectively.[8]

Biofilm formation and quantification

Biofilm formation was also quantified by a modification of the crystal violet (CV) staining assay.[9] Briefly, 100 µL of standardized *Candida* spp. cell suspensions prepared in tryptic soy broth (TSB) medium (Oxoid, UK) ($1x10^6$ cells) were transferred into wells of sterile, flat-bottomed, polystyrene 96-well microplates. The microplates were incubated at 37°C for 24 h for biofilm production. Following incubation, the cell suspensions were aspirated and the wells were washed three times with sterile phosphate buffered saline (PBS) (Oxoid, UK) 200 µL per well in order to remove nonadherent cells. After each washing step, the microplates were air dried to remove the PBS. Afterwards, the remaining attached microorganisms were fixed with 200 µL of methanol for 15 min. The contents of the wells were poured off, the methanol was discarded, and the wells were air-dried. Then 200 µL of 0.02% CV solution was added to the wells for 20 min at room temperature. After 20 min, the CV solution was removed by washing with PBS and the microplates were dried. Each well was destained with 200 µL of 95% ethanol for 15 min. Biofilm formation was quantified by measuring the optical density (OD) at 570 nm using a microplate reader (Varioskan Flash, Thermo Scientific, USA). OD values of wells without inoculum were used as negative controls. *Enterococcus faecalis* ATCC 29212 was used as a positive control strain. The cut-off OD (ODc) was defined as three standard deviations above the mean OD of the negative controls. The biofilm production capacities of the isolates were evaluated as shown in Table 1. All tests were carried out in triplicate. The statistical analyses were performed using GraphPad Prism 5.03 (t-test).

Antibiofilm effects of SSRIs

The antibiofilm effects of the SSRI agents at sub-MICs (MIC/2, MIC/4) were investigated by CV staining assay. Biofilm formation was performed by adding standardized cell suspensions to the wells of the microplates and incubating them for 24 h at 37°C as described above. After biofilm formation, the medium in the wells was aspirated, and nonadherent cells were removed by thoroughly washing all wells three times with sterile PBS. The SSRI agent solutions at sub-MICs (MIC/2 and MIC/4) were prepared in TSB and added to the wells that contained preformed biofilm. After these agents were added to the wells, the microplates were incubated for a further 24 h at 37°C. Then the CV staining assay was performed. The antibiofilm effects of the agents were evaluated by measuring the OD of the wells at 570 nm using a microplate reader.

Table 1. Categorizations of biofilm production capacities

OD ≤ ODc	**No biofilm production**
ODc ‹ OD ≤ (2×ODc)	**Weak biofilm producer**
(2×ODc) ‹ OD ≤ (4×ODc)	**Moderate biofilm producer**
(4×ODc) ‹OD	**Strong biofilm producer**

OD: Optical density of the isolate, ODc: The mean OD of negative controls

Statistical analysis

All tests were carried out in triplicate. The ODc was defined as three standard deviations above the mean OD of the negative controls. The statistical analyses were performed using GraphPad Prism 5.03 (t-test) and $p<0.05$ was considered statistically significant.

RESULTS

Fungal isolates and identification

The 20 clinical fungal isolates identified comprised six *C. albicans,* four *C. tropicalis,* four *C. krusei,* three *C. parapsilosis*, and three *C. glabrata* according to the Dalmau method and MALDITOF-MS.

Minimum inhibitory concentrations of fluconazole and SSRIs

Two isolates were resistant to FLC in addition to the inherently resistant *C. krusei* isolates. The MICs of SRT ranged from 16 µg/mL to 128 µg/mL by the broth microdilution method, while the MICs of PRX and FLX ranged from 64 µg/mL to 512 µg/mL. The MICs of all agents are shown in Table 2.

Table 2. Minimum inhibitory concentrations of fluconazole and SSRIs

Isolate	FLC (µg/mL)	SRT (µg/mL)	PRX (µg/mL)	FLU (µg/mL)
Candida glabrata	16	128	256	512
Candida glabrata	16	128	256	512
Candida glabrata	16	128	256	512
Candida albicans	0.25	128	256	512
Candida albicans	0.25	128	256	512
Candida albicans	0.25	128	256	256
Candida albicans	2	64	256	256
Candida albicans	1	64	256	256
Candida albicans	8	64	256	256
Candida tropicalis	1	32	128	128
Candida tropicalis	0.5	32	128	128
Candida tropicalis	4	32	128	256
Candida tropicalis	0.5	32	128	128
*Candida krusei**	-	64	64	128
*Candida krusei**	-	32	64	128
*Candida krusei**	-	32	64	64
*Candida krusei**	-	16	128	128
Candida parapsilosis	16	64	256	256
Candida parapsilosis	1	32	512	512
Candida parapsilosis	1	32	256	512
Candida parapsilosis ATCC 22019	2	128	256	512

*Intrinsically resistant to fluconazole, SSRIs: Selective serotonin reuptake inhibitors, SRT: Sertraline, PRX: Paroxetine, FLU: Fluoxetine, FLC: Fluconazole

Checkerboard assay

The interactions between the SSRI agents and FLC were examined by checkerboard assay. No antagonism was found between the agents tested. FLX showed a synergistic effect in the large number of isolates when it was compared to the other SSRIs. It was also determined that FLX is the only agent showing a synergistic interaction with FLC against five different *Candida* species. According to the checkerboard assay, SRT, FLX, and PRX were synergistic in six, thirteen, and ten isolates, respectively. The interaction types of the SSRI agents are shown in Table 3.

Biofilm formation and quantification

The biofilm quantification assays revealed that seven of the isolates have weak biofilm production capacity, nine isolates show moderate biofilm production, and four isolates have strong biofilm production capacity. The biofilm production capacities and the number of isolates are shown in Table 4.

Antibiofilm effects of SSRIs

In the presence of MIC/2 of FLX, biofilm formation decreased in six isolates, while it increased in two isolates. PRX and SRT, at MIC/2, inhibited biofilm in three and five isolates, respectively. The effects of sub-MIC of the SSRIs on mature biofilm formation in moderate and strong biofilm producer isolates are shown in Table 5.

Table 4. Biofilm production capacities of the isolates

	Biofilm production capacity		
Candida spp.	Weak	Moderate	Strong
Candida albicans (n=6)	3	3	-
Candida parapsilosis (n=3)	-	-	3
Candida krusei (n=4)	2	2	-
Candida tropicalis (n=4)	1	2	1
Candida glabrata (n=3)	1	2	-

Table 5. The effects of SSRIs on mature biofilm formation of the isolates

	Number of isolates					
Effects on mature biofilm	FLX (MIC/2)	FLX (MIC/4)	PRX (MIC/2)	PRX (MIC/4)	SRT (MIC/2)	SRT (MIC/4)
Decrease	6	4	3	-	5	3
Increase	2	4	7	7	3	3
No effect	5	5	3	6	5	7

SSRIs: Selective serotonin reuptake inhibitors, FLX: Fluoxetine, PRX: Paroxetine, SRT: Sertraline, MIC: Minimum inhibitory concentration

Table 3. Interaction types between SSRIs and fluconazole (FIX values)

	FLC + FLX		FLC + SRT		FLC + PRX	
Isolate	FIX	Profile	FIX	Profile	FIX	Profile
Candida glabrata	0.5078	I	0.5156	I	0.2656	S
Candida glabrata	0.375	S	0.5156	I	0.2656	S
Candida glabrata	0.5	S	0.5156	I	0.2656	S
Candida albicans	0.375	S	0.625	I	0.75	I
Candida albicans	0.5	S	1.0313	I	0.75	I
Candida albicans	0.5	S	1.25	I	0.75	I
Candida albicans	0.2813	S	0.3125	S	0.1563	S
Candida albicans	0.1406	S	1.5	I	0.75	I
Candida albicans	1.0625	I	1	I	1	I
Candida tropicalis	0.5	S	1.5	I	0.75	I
Candida tropicalis	1.0625	I	2	I	1.5	I
Candida tropicalis	0.2656	S	0.375	S	0.5	S
Candida tropicalis	1.0625	I	2	I	1	I
*Candida krusei**	0.625	I	0.25	S	0.5	S
*Candida krusei**	0.5	S	0.5	S	0.375	S
*Candida krusei**	0.5	S	0.5	S	0.375	S
*Candida krusei**	0.2813	S	0.75	I	0.25	S
Candida parapsilosis	0.3125	S	0.25	S	0.2813	S
Candida parapsilosis	1.0078	I	1.125	I	1.0078	I
Candida parapsilosis	1.0156	I	1.25	I	1.0156	I
Candida parapsilosis ATCC 22019	0.5	S	0.2656	S	0.625	I

*Intrinsically resistant to fluconazole, SSRIs: Selective serotonin reuptake inhibitors, FLC: Fluconazole, FLX: Fluoxetine, PRX: Paroxetine, SRT: Sertraline, FIX: Fractional inhibitory index, S: Synergistic, I: Indifferent

DISCUSSION

The significant increase in fungal infections over the past decade has increased the need for new antifungal agents and reliable and reproducible susceptibility testing methods.[10] There are two reference *in vitro* antifungal susceptibility testing methods for *Candida* spp. These reference methods have been developed by two scientific organizations, namely the Clinical and Laboratory Standards Institute and the EUCAST. Despite the differences such as in terms of media, plate types, and measurement methods between these methods, it was determined in several studies that these two methods give results consistent with each other.[10] Although the EUCAST method requires more material and equipment, it has the significant advantage of producing results after a 24-h incubation. Moreover, the measurement of absorbance by the automated device in the EUCAST method, instead of visual inspection, will be the major factor that reduces the error rate. Considering these reasons, we first investigated the *in vitro* activity of SSRIs and FLC by broth microdilution method according to EUCAST. The agent concentration that led to approximately 50% inhibition of growth relative to the controls, which was determined spectrophotometrically, was accepted as the MIC value (Table 2).

SRT was the prominent molecule with a lower MIC range (16-128 mg/mL) compared to FLX and PRX. According to the literature, SRT is generally more effective than the others, which is consistent with our study. In a study conducted on *Candida* spp., it was determined that SRT has antifungal effects on *Candida* species and it was also reported that SRT inhibits *Candida* virulence factors.[6] The inhibitory effects of SRT on different yeasts species, such as *Cryptococcus* isolates, are also shown by research.[11]

There are studies showing that FLX had antibiofilm activity at previously reported MIC values and even at sub-MIC values in the literature.[12] Oliveira et al.[12] reported that FLX was able to reduce biofilm metabolism at high concentrations by 96% (*C. krusei*) and biofilm biomass by 82% (*C. glabrata*), when compared to the control. They also detected that SRT achieved a reduction of 88% in biofilm biomass (*C. glabrata*) and 90% in biofilm metabolism (*C. parapsilosis*) under similar conditions. According to our results, FLX, at sub-MIC concentrations, showed an antibiofilm effect in six isolates, while SRT showed an antibiofilm effect in five isolates. It was also interesting that FLX's MIC ranges were lower on *C. krusei* isolates compared to other *Candida* species.

Unlike SRT and FLX, the number of studies about the antifungal effects of PRX is very limited in the literature. However, the results of a study conducted by Costa Silva et al.[13] and our data showed that PRX has antifungal activity at high concentrations. In parallel to this finding, the MICs of PRX were higher than those of FLX and PRX in our study. Considering our results on the antibiofilm effects of PRX, it was noteworthy that PRX, at MIC/2 levels, caused an increase in biofilm formation of seven isolates.

Even though it is not fully understood how SSRI agents provide their antifungal activities, the point of interest is that their antifungal activity is independent of the species and resistance properties of the *Candida* isolates. In a study investigating this situation, it was reported that the lethal effect of the agents is related to the induction of apoptosis due to damage to the plasma and mitochondrial membranes. It is thought that this condition may be related to genetic variation rather than factors such as species and resistance patterns.[13] Although antifungal activities of SSRIs have been shown in many studies in the literature, it is necessary to know more about the pharmacokinetics of these molecules, which are usually taken orally in clinical practice. The optimum concentrations that will be reached for these agents in several infection sites should be investigated in new studies. Considering the plasma drug concentration of SSRIs, it appears that the doses required for *Candida* inhibition are above the commonly used doses of these drugs.[14,15] On the other hand, it should be kept in mind that the commonly used dosage regimens and pharmacokinetic data of these drugs are regulated for oral therapeutic use. Undoubtedly, more research is needed to evaluate using different forms such as topical formulations of SSRIs as an antimicrobial agent.

A correlation between biofilm formation and antimicrobial resistance profiles was already shown in different studies and so the antibiofilm activities of drug molecules that have various known therapeutic effects are also gaining importance.[16,17] Therefore, we also analyzed the antibiofilm effects of SSRI molecules against mature biofilm of *Candida* isolates. Several different methods and devices could be used for the detection of biofilm formation such as the CV staining assay, light and fluorescence microscopy, bioluminescence, Congo red agar, and Christensen methods. The CV staining assay was used in our study, especially because more sensitive, specific, and quantitative results can be obtained by this method.[18,19] It has been demonstrated with the results of many studies that all *Candida* species could have biofilm forming ability.[20] In parallel with these data, the isolates in the present study identified as different *Candida* species showed moderate and strong biofilm production capacity (Table 4). It is thought that *C. parapsilosis* has the highest biofilm production capacity among non-*albicans* *Candida* species when considering the results of both previous reports and our study.[20,21]

CONCLUSION

It is understood that SSRI agents show *in vitro* antifungal and antibiofilm activity against *Candida albicans, C. tropicalis, C. parapsilosis*, and *C. glabrata* strains at different concentration levels, based on our findings and other studies in the literature. In addition to the antifungal activity of SSRIs, it was also detected that these agents in combination with FLC could have a synergistic effect against *Candida* spp. The effects of SSRIs on mature biofilms were investigated in the present study and it was found that SRT and FLX molecules could have antibiofilm effects against *Candida* species. Given all these results and studies, it is thought that these agents could have potential as adjuvant therapeutic agents. Research that will be conducted on the antibiofilm activities of SSRIs can be beneficial for the development of new antifungal and antibiofilm

drug combinations and understanding the mechanisms of their antifungal effects.

Conflicts of interest: No conflict of interest was declared by the authors. The authors alone are responsible for the content and writing of the paper.

REFERENCES

1. Guinea J, Sánchez-Somolinos M, Cuevas O, Peláez T, Bouza E. Fluconazole resistance mechanisms in Candida krusei: the contribution of efflux-pumps. Med Mycol. 2006;44:575-578.
2. Shin JH, Kee SJ, Shin MG, Kim SH, Shin DH, Lee SK, Suh SP, Ryang DW. Biofilm production by isolates of Candida species recovered from nonneutropenic patients: Comparison of bloodstream isolates with isolates from other sources. J Clin Microbiol. 2002;40:1244-1248.
3. Paulone S, Ardizzoni A, Tavanti A, Piccinelli S, Rizzato C, Lupetti A, Colombari B, Pericolini E, Polonelli L, Magliani W, Conti S, Posteraro B, Cermelli C, Blasi E, Peppoloni S. The synthetic killer peptide KP impairs *Candida albicans* biofilm *in vitro*. PLoS One. 2017;12:1-16.
4. Gao Y, Li H, Liu S, Zhang X, Sun S. Synergistic effect of fluconazole and doxycycline against *Candida albicans* biofilms resulting from calcium fluctuation and downregulation of fluconazole-inducible efflux pump gene overexpression. J Med Microbiol. 2014;63:956-961.
5. Pesee S, Angkananuwat C, Tancharoensukjit S, Muanmai S, Sirivan P, Bubphawas M, Tanarerkchai N. *In vitro* activity of Caspofungin combined with Fluconazole on mixed *Candida albicans* and *Candida glabrata* biofilm. Med Mycol. 2016;54:384-393.
6. Lass-Flörl C, Dierich MP, Fuchs D, Semenitz E, Ledochowski M. Antifungal activity against *Candida* species of the selective serotonin-reuptake inhibitor, sertraline. Clin Infect Dis. 2001;33:135-136.
7. Def EE. EUCAST E.DEF 7.3.1. EUCAST Method for the determination of broth dilution minimum inhibitory concentrations of antifungal agents for yeasts 2017; (January). Available from: https://www.eucast.org/astoffungi/publications_in_journals/
8. Lewis RE, Diekema DJ, Messer SA, Pfaller MA, Klepser ME. Comparison of E-test, chequerboard dilution and time-kill studies for the detection of synergy or antagonism between antifungal agents tested against Candida species. J Antimicrob Chemother. 2002;49:345-351.
9. Madariaga-Venegas F, Fernández-Soto R, Duarte LF, Suarez N, Delgadillo D, Jara JA, Fernández-Ramires R, Urzúa B, Molina-Berríos A. Characterization of a novel antibiofilm effect of nitric oxide-releasing aspirin (NCX-4040) on *Candida albicans* isolates from denture stomatitis patients. PLoS One. 2017;12:e0176755.
10. Pfaller MA, Castanheira M, Messer SA, Rhomberg PR, Jones RN. Comparison of EUCAST and CLSI broth microdilution methods for the susceptibility testing of 10 systemically active antifungal agents when tested against *Candida* spp. Diagn Microbiol Infect Dis. 2014;79:198-204.
11. Zhai B, Wu C, Wang L, Sachs MS, Lin X. The antidepressant sertraline provides a promising therapeutic option for neurotropic *Cryptococcal* infections. Antimicrob Agents Chemother. 2012;56:3758-3766.
12. Oliveira AS, Martinez-de-Oliveira J, Donders GGG, Palmeira-de-Oliveira R, Palmeira-de-Oliveira A. Anti-*Candida* activity of antidepressants sertraline and fluoxetine: effect upon pre-formed biofilms. Med Microbiol Immunol. 2018;207:195-200.
13. Costa Silva RA, da Silva CR, de Andrade Neto JB, da Silva AR, Campos RS, Sampaio LS, do Nascimento FBSA, da Silva Gaspar B, da Cruz Fonseca SG, Josino MAA, Grangeiro TB, Gaspar DM, de Lucena DF, de Moraes MO, Cavalcanti BC, Nobre Júnior HV. *In vitro* anti-*Candida* activity of selective serotonin reuptake inhibitors against fluconazole-resistant strains and their activity against biofilm-forming isolates. Microb Pathog. 2017;107:341-348.
14. DeVane CL. Pharmacokinetics of the selective serotonin reuptake inhibitors. J Clin Psychiatry. 1992;53:13-20.
15. Tremaine LM, Welch WM, Ronfeld RA. Metabolism and disposition of the 5-hydroxytryptamine uptake blocker sertraline in the rat and dog. Drug Metab Dispos. 1989;17:542-550.
16. Mukherjee PK, Chandra J. *Candida* biofilm resistance. Drug Resist Updat. 2004;7:301-309.
17. Azevedo MM, Cobrado L, Silva Dias A, Ramalho P, Pina-Vaz C and Rodrigues AG. Antibiofilm effect of cerium nitrate against bacteria and yeast. Microbiol Infect Dis. 2013;2011-2014.
18. Azeredo J, Azevedo NF, Briandet R, Cerca N, Coenye T, Costa AR, Desvaux M, Di Bonaventura G, Hébraud M, Jaglic Z, Kačániová M, Knøchel S, Lourenço A, Mergulhão F, Meyer RL, Nychas G, Simões M, Tresse O, Sternberg C. Critical review on biofilm methods. Crit Rev Microbiol. 2017;43:313-351.
19. Stepanović S, Vuković D, Hola V, Di Bonaventura G, Djukić S, Cirković I, Ruzicka F. Quantification of biofilm in microtiter plates: overview of testing conditions and practical recommendations for assessment of biofilm production by staphylococci. APMIS. 2007;115:891-899.
20. Udayalaxmi J, Shenoy N. Comparison between biofilm production, phospholipase and haemolytic activity of different species of *Candida* isolated from dental caries lesions in children. J Clin Diagn Res. 2016;10:DC21-DC23.
21. Dögen A, Sav H, Gonca S, Kaplan E, Ilkit M, Novak Babic M, Gunde-Cimerman N, de Hoog GS. *Candida parapsilosis* in domestic laundry machines. Med Mycol. 2017;55:813-819.

Turk J Pharm Sci 2020;17(6):673-678
DOI: 10.4274/tjps.galenos.2019.59862

ORIGINAL ARTICLE

In Situ Absorption Study of Acebutolol by Modulating P-glycoprotein with Verapamil in Rats

Sıçanlarda Asebutalolün P-glikoprotein ile Modüle Edildiği *İn Situ* Absorpsiyon Çalışması

Issam Mohammed ABUSHAMMALA[1]*, Elham Abed ABUWAKED[2], Hanan Mohammed FAYYAD[2], Ahmed Fadel ELQEDRA[2], Mai Abed Alrahman RAMADAN[1] , Ihab Mustafa ALMASRI[1]

[1]Al-Azhar University-Gaza Faculty of Pharmacy, Department of Pharmaceutics and Industrial Pharmacy, Gaza, Palestine
[2]Al-Azhar University-Gaza Faculty of Pharmacy, Department of Chemistry and Pharmaceutical Chemistry, Gaza, Palestine

ABSTRACT

Objectives: Acebutolol HCl (ABL) is a selective β-adrenergic receptor blocking agent that is preferably administered by the oral route despite its low bioavailability (30-50%). The purpose of this study was to evaluate the effect of verapamil HCl (VER) [as P-glycoprotein inhibitor (P-gp)] on the intestinal absorption of ABL by comparing the changes in the absorption rate constant (k_{ap}) of ABL.

Materials and Methods: *In situ* intestinal perfusion was conducted in healthy male Wistar albino rats to study the absorption phase of ABL. Eighteen rats were divided into three groups. The first group (the control group) was perfused with ABL alone (260 µg/mL). The second and third groups were perfused with ABL (260 µg/mL) in combination with VER at different concentrations (200 and 400 µg/mL, respectively). The analysis was performed using a simple, rapid, and validated spectroscopic method.

Results: The absorption study showed that k_{ap} of ABL in the first group was 0.47±0.045 h^{-1}. In the third group k_{ap} increased 3-fold (1.37±0.031 h^{-1}); however, the second group showed a statistically insignificant change in k_{ap} (0.39±0.076 h^{-1}).

Conclusion: The results revealed that VER at a concentration of 400 µg/mL has a pronounced effect on the absorption kinetics of ABL (increased k_{ap}). This could be linked to the inhibition of P-gp, which is considered a contributing factor in low bioavailability of ABL.

Key words: Acebutolol HCl, verapamil HCl, P-glycoprotein, intestinal perfusion technique, absorption

ÖZ

Amaç: Acebutolol HCl (ABL), düşük biyoyararlanımı (%30-50) olmasına rağmen oral yoldan uygulanan seçici β-adrenerjik reseptör bloke edici ajandır. Bu çalışmanın amacı verapamil HCl'nın (VER) [P-glikoprotein (P-gp) inhibitörü olarak] ABL'nin absorpsiyon hızı sabitindeki (k_{ap}) değişimleri karşılaştırarak ABL'nin intestinal emilimine etkisini değerlendirmektir.

Gereç ve Yöntemler: ABL'nin absorpsiyon fazını incelemek için sağlıklı Wistar albino erkek sıçanlarda *in situ* bağırsak perfüzyon tekniği uygulanmıştır. On sekiz sıçan üç gruba ayrılmıştır. Birinci grup (kontrol grubu) sadece ABL ile (260 µg/mL) perfüze edilmiştir. İkinci ve üçüncü gruplar, farklı konsantrasyonlarda (sırasıyla 200 ve 400 µg/mL) VER ile birlikte ABL (260 µg/mL) ile perfüze edilmiştir. Analiz basit, hızlı ve onaylanmış bir spektroskopik yöntem kullanılarak yapılmıştır.

Bulgular: Absorpsiyon çalışması birinci gruptaki ABL k_{ap}'nin 0,47±0,045 $saat^{-1}$ olduğunu gösterdi. Üçüncü grupta k_{ap}'nin 3 kat (1,37±0,031 $saat^{-1}$) arttığı belirlenmiş; ancak ikinci grupta istatistiksel olarak anlamlı olmayan bir değişiklik (0,39±0,076 $saat^{-1}$) görülmüştür.

Sonuç: Bulgular, 400 µg/mL konsantrasyondaki VER'nin, ABL'nin (artırılmış k_{ap}) absorpsiyon kinetiği üzerinde belirgin bir etkiye sahip olduğunu ortaya koymuştur. Bu etkinin, ABL'nin düşük biyoyararlanımına yol açan bir faktör olan P-gp'nin inhibisyonu ile bağlantılı olabileceği söylenebilir.

Anahtar kelimeler: Acebutolol HCl, verapamil HCl, P-glikoprotein, bağırsak perfüzyon tekniği, absorpsiyon

*Correspondence: E-mail: issam.abushammala@uv.es, Phone: +00970599019757 ORCID-ID: orcid.org/0000-0002-3371-4718
Received: 25.08.2019, Accepted: 21.11.2019

INTRODUCTION

Drug absorption is a key part of most pharmacokinetic processes and it represents the first step that can greatly influence drug bioavailability. Oral administration is the most common and preferable route of administration. The major site of absorption of orally administered drugs is the small intestine due to its large surface area. The rate and extent of drug absorption across the intestinal membrane are dependent on many drug and patient factors.[1] Drug-related factors involve physicochemical properties of the drug (molecular size, lipid solubility, degree of ionization, and chemical nature) and dosage characteristics (dosage form, formulation, and concentration of drug entering the intestine). Patient-related factors include the structure of the absorbing surface (efflux and influx protein transporters); vascularity; pH; gastrointestinal motility; presence of other substance such as foods, fluids, or drugs; and physiological characteristics of the patient such as malabsorption syndrome.[2,3] Drug transporters as one of the main factors affecting intestinal absorption have become increasingly evident in influencing orally administered drugs.[4,5]

P-glycoprotein (P-gp), a multidrug resistant protein 1, is one of the ATP binding cassette superfamily. This protein is found in many tissues including the intestine, liver, kidney, brain, testis, placenta, and lung and is also expressed in many cancer cells.[6] Its physiological role is to protect some tissues such as the brain from harmful substances. In the intestine P-gp plays an important role in drug absorption by returning the drug to the intestinal lumen. In addition, P-gp mediates drug-drug and food-drug interactions due to its broad specificity, which could affect the safety and efficacy of its substrate.[7,8] Induction or inhibition of P-gp leads to drug interactions in humans.[9] Previous kinetic studies emphasized the importance of using P-gp inhibitors to evaluate the effect of P-gp on the absorption and bioavailability of many drugs.[10,11]

Acebutolol HCl (ABL) is a cardioselective β1 adrenoceptor blocking agent.[12] The oral bioavailability of ABL is approximately 30-50% as it undergoes significant first-pass metabolism.[13] There is also evidence that ABL is a substrate for P-gp that plays a role as an absorption barrier.[14] Verapamil HCl (VER) is a calcium channel blocking agent and a competitive inhibitor of intestinal P-gp and is used as a tool for studying the effect of P-gp inhibition on the absorption and bioavailability of many drugs and significant changes in the absorption kinetics have been observed.[15-17] The aim of the present work was to study the effect of VER at different concentrations on the absorption of ABL using *in situ* intestinal perfusion on anesthetized rats as it is based on the disappearance of the drug in the luminal fluid.

MATERIALS AND METHODS

Materials and instruments

ABL and VER standards were purchased from Sigma-Aldrich Company. Normal saline (0.9% w/v) was obtained from B. Braun Melsungen AG (Germany). Thiopental sodium (500-mg vial) was obtained from Rotexmedica (Germany). A Shimadzu ultraviolet (UV)-spectrophotometer (UV-1601) was used. Centrifugation was performed with a Kokusan (H-103N) series centrifuge. A hotplate (J.P. Selecta) was also required.

Animals and study design

Eighteen healthy Wistar albino male rats (weight: 250-300 g) were purchased from the Center of Experimental Animals, Harlan Laboratories (Israel). The animals were housed 4 per cage in an air-conditioned room under constant temperature (22±2°C) with free access to food and drinking water.[10] The rats were subjected to a 12-h light-dark cycle.[18] The normal life conditions for the animals were based on guidelines of the International Animal Ethics Committee.

Approval for the study was obtained from the Helsinki Committee (Gaza, Palestine). All experiments with rats were conducted according to the Canadian Guide for the Use of Laboratory Animals.[19] *In situ* intestinal perfusion procedures were performed in rats according to the methods described previously.[20-22] The rats had been fasted for 12-18 h before the experiment with *ad libitum* access to water. Then they were anesthetized by intraperitoneal administration of thiopental (50 mg/kg). Anesthetized rats were placed on the fixing plate under a heating lamp maintaining their normal body temperature (37°C) during all experiments. The surgical procedure was initialized by a midline abdominal incision of approximately 10 cm to expose the small intestine and then two L-shaped cannulas were inserted carefully through the small narrow opening at the beginning of the duodenum and the end of the ileum. The cannulas were secured by ligation with silk sutures and the biliary duct also was ligated. Then the small intestine was returned to the abdominal cavity to maintain its integrity. The intestinal lumen was rinsed using a syringe containing normal saline (37°C) that was pumped slowly through the gut via the inlet duodenum cannula and out the ileal cannula until the effluent solution was free of feces and clear. After the intestine was cleaned the remaining perfusion solution was expelled from the intestine by air pumping via a syringe and 10 mL of drug solution was immediately introduced into the small intestine segment by the syringe.

In the first group 10 mL of solution containing ABL alone (concentration 260 µg/mL) in normal saline (0.9% w/v) was perfused into the small intestine segment of six rats. The second and third groups of rats were perfused with 10 mL of solution containing ABL (260 µg/mL) in combination with VER HCl (200 and 400 µg/mL, respectively). The surgical area was covered with a wet cotton pad and drops of normal saline (37°C) were added to the cotton to prevent disturbance of the circulatory system and dryness of the intestine. Next, 300 µL of perfused samples was collected from both sides alternatively every 5 min for a total of 30 min. The collected samples were transferred into 2 mL Eppendorf tubes, centrifuged at 5000 rpm for 10 min, and then 200 µL of the supernatant was transferred and diluted to 3 mL with normal saline to be analyzed by UV spectrophotometer on the same day. The absorbance was measured at 320 nm against a blank and then the concentration of each sample was determined using a calibration curve to determine the k_{ap} of ABL.

Analytical procedures

The determination of ABL in intestinal luminal fluid was performed using a spectrophotometric method that was validated for linearity, limit of detection (LOD), limit of quantification (LOQ), precision, and accuracy according to ICH guidelines.[23] For quantitative analysis of ABL, a calibration curve was constructed as follows: standard stock solution of ACH 200 µg/mL was prepared by dissolving 50 mg of standard sample (ABL powder) with normal saline solution in a 250 mL volumetric flask. Intestinal luminal fluid (blank) was collected from the rats by intestinal perfusion after administration of 10 mL of normal saline without drugs. From stock solution 0.1, 0.2, 0.4, 0.8, 1.6, and 3.2 mL were transferred into a 5 mL volumetric flask and diluted with intestinal luminal fluid (blank) collected previously to produce a series of ABL concentrations, 4, 8, 16, 32, 64, and 128 µg/mL, respectively. Next, 300 µL of diluted solutions was centrifuged at 5000 rpm for 10 min. Absorbance was measured against the blank at 320 nm. The calibration curve was constructed by plotting absorbance against ABL concentration.

Pharmacokinetic analysis

The intestinal absorption of ABL was evaluated using its apparent first-order rate constant, k_{ap}, calculated according to the following equation:

$$lnC_t = lnC_0 - k_{ap} \cdot t$$

(lnC_t: Intestinal luminal drug concentration collect postperfusion at time t, lnC_0: Initial perfused drug concentration preperfusion, and t: time of sampling)

Statistical analysis

The data obtained were treated and analyzed using Statistical Package for the Social Sciences (SPSS) version 16[24] (One-Way ANOVA and Bonferroni tests were applied in this study). The results were assumed to be statistically significant for a p value <0.05.

RESULTS

Analytical procedure

The analysis was performed by UV-spectrophotometric assay of ABL in intestinal luminal fluid collected during intestinal perfusion. No spectral interference was identified during the determination of ABL in the presence of VER and intestinal luminal fluid at the selected wavelength of 320 nm.

The calibration curve was repeated 5 times. The calculated regression lines showed a linear relationship between the absorbance and the concentrations of ABL in the range of 4-200 µg/mL. LOD and LOQ were determined by an empirical method consisted of analyzing series of solutions containing decreased amounts of ABL spiked with luminal intestinal fluid blank (Table 1).

The accuracy was checked at 3 different concentrations of ACH in intestinal fluid (8, 32, and 128 µg/mL) and the results of the recovery were in the range 99.8%-102.5%, which reveals good accuracy of the developed method with low standard deviation. Intraday and interday precision were evaluated by triplicate analysis of ACH solution at 3 different concentration levels for 3 consecutive days. Both interday and intraday precision results show low relative standard deviation (<2%), which indicates good precision (Table 2).

For the stability study, ABL in intestinal luminal fluid was established over 6 h at room temperature and no significant change in concentrations was noted. The validation parameters confirm that the method is appropriate and suitable for quantitative determination of ABL in intestinal luminal fluid.

Acebutolol HCl absorption

The allometric dose of ABL for the absorption study was calculated according to the following equation: human dose/human weight=animal dose/animal weight.[25] The absorption rate constants obtained for ABL in rat intestine were measured from intestinal sampling, which was based on disappearance of drug from the intestinal lumen. The means of ln remnant concentrations of ABL obtained experimentally from the three groups are collected in Table 3 and Figure 1 to show the differences in ABL absorption behavior among the three groups.The *in situ* intestinal perfusion model assumed that drug concentrations in the enterocytes and the intestinal lumen were

Table 1. Analytical parameters of the spectroscopic method

Regression equation	R^2	SD_a	SD_b	LOD (µg/mL)	LOQ (µg/mL)
Y=0.007X+0.003	0.999	$4.5x10^{-5}$	$1.4x10^{-3}$	0.670	1.938

R^2: Correlation coefficient, SD_a: Standard deviation of slope of regression line, SD_b: Standard deviation of intercept of regression line, LOD: Limit of detection, LOQ: Limit of quantification

Table 2. Intraday and interday precision of the spectroscopic method

ABL conc. (µg/mL)	Intraday precision (n=3)			Interday precision (n=3)		
	Mean	SD	% RSD	Mean	SD	% RSD
8	7.98	0.08	1.00	7.95	0.06	0.75
32	32.57	0.60	1.84	32.31	0.62	1.92
128	131.17	1.63	1.24	131.15	0.12	0.09

ABL: Acebutolol HCl, SD: Standard deviation, % RSD: Relative standard deviation

Table 3. The mean of ln remnant concentrations of all data obtained experimentally for the three groups

Time (min)	ABL (260 µg/mL) alonea	ABL/verapamil HCl (260/200 µg/mL)[a]	ABL/verapamil HCl (260/400 µg/mL)[a]
0	5.4864	5.5407	5.5452
5	5.3884	5.4692	5.3493
10	5.3290	5.4138	5.1967
15	5.3076	5.3585	5.1699
20	5.2934	5.3400	4.9122
25	5.2596	5.3150	4.8328
30	5.2053	5.2572	4.8185

ABL: Acebutolol HCl, [a]: Mean of ln remnant concentrations

in dynamic equilibrium after 5 min. Therefore, only samples obtained between 5 and 30 min, when ABL concentrations in the enterocytes were assumed to be proportional to the ABL concentrations in the intestinal lumen, were used for the calculation of k_{ap}.[22] This is due to the effect of membrane uptake, enterocyte loading, and other factors, resulting in lower predicted initial concentration (the intercept of the regression line at time zero) than actual initial concentration (concentration of nonperfused sample at time zero).[21,26] The gradual decrease in ABL concentration in the intestinal lumen indicates that ABL follows first-order kinetics and the dose used does not cause saturation of the transporter (Table 3, Figure 1). The mean absorption rate constants k_{ap} of the three groups are shown in Table 4.

The determination of k_{ap} using the control group was a necessary step to gain insight into the ABL absorption process because the k_{ap} value for the same drug is not constant as other pharmacokinetic parameters and many factors could affect it. Therefore, this group gives k_{ap} under the same conditions of all rats used in the present study and with the same dose of ABL, which can be compared with those values obtained in the presence of P-gp inhibitor.

Statistical analysis of data

The homogeneity between rats within a group was statistically evaluated and the results demonstrated low interindividual variation among rats (p value >0.05, Table 5).

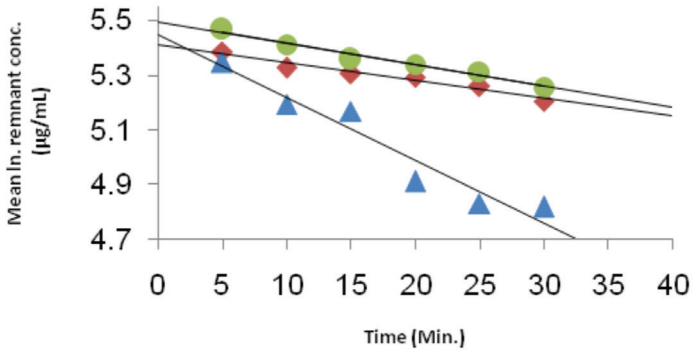

Figure 1. Graphical representation of the fit of the apparent first-order equation to the obtained mean data (remaining luminal concentrations of 260 µg/mL acebutolol HCl♦, acebutolol HCl with 200 µg/mL verapamil HCl●, and acebutolol HCl with 400 µg/mL verapamil HCl▲)

Table 4. Calculated parameters of ABL

	ABL (260 µg/mL) alone	ABL/verapamil HCl (260/200 µg/mL)	ABL/verapamil HCl (260/400 µg/mL)
k_a (h^{-1})	0.47±0.045	0.39±0.076	1.37±0.031
% A_0	99.06±0.22	97.66±0.32	98.23±0.06
R	0.98±0.0095	0.96±0.0514	0.97±0.0031

ABL: Acebutolol HCl, k_a: Absorption rate constant, % A_0: Estimated inclination of the absorption line, R: Correlation coefficient

Table 5. One-Way ANOVA for homogeneity study

Rat group	N	f value	p value
ABL (260 µg/mL) alone	6	1.012	0.428
ABL/Verapamil HCl (260/200 µg/mL)	6	0.198	0.961
ABL/Verapamil HCl (260/400 µg/mL)	6	0.122	0.986

ABL: Acebutolol HCl, N: Sample number

DISCUSSION

The data obtained in our study revealed a significant reduction in the remnant concentrations of ABL in intestinal luminal fluids of rats in the third group and the k_{ap} value increased 3-fold from 0.47±0.045 h^{-1} to 1.37±0.031 h^{-1} (Table 4). Statistical analysis using the Bonferroni test showed a p value <0.001 (Table 6). In contrast, no significant effect of VER, at a concentration of 200 µg/mL, on the k_{ap} value of ABL was found. As shown in Table 4, remnant concentrations of ABL in the rats' intestinal luminal fluid were not significantly decreased. The absorption rate constant of ACH obtained was 0.39±0.076 h^{-1} in the presence of VER (200 µg/mL), which is not significantly different from the k_{ap} value obtained for the control group, 0.47±0.045 h^{-1} (p=0.146, Table 6).

Table 6. A multiple comparisons Bonferroni test between the three groups

Group	Group	Standard error	p value
ABL 260 µg/mL alone	ABL + verapamil HCl 200 µg/mL	0.3100	0.146
	ABL + verapamil HCl 400 µg/mL	0.3100	<0.001*
ABL + verapamil HCl 200 µg/mL	ABL 260 µg/mL alone	0.3100	0.146
	ABL + verapamil HCl 400 µg/mL	0.3100	<0.001*
ABL + verapamil HCl 400 µg/mL	ABL 260 µg/mL alone	0.3100	<0.001*
	ABL + verapamil HCl 200 µg/mL	0.3100	<0.001*

*Statistically significant (p value ≤0.05), ABL: Acebutolol HCl

Despite the fact that anesthesia as used in this technique may decrease blood flow and intestinal motility, which may decrease both passive and active transport and affect the estimation of drug absorption, it has been reported that barbiturates have the least effect on intestinal permeability in rats.[27] Therefore, in the present study thiopental 50 µg/kg, which is a barbiturate, was used as the anesthetic drug in all experiments.

The oral drug bioavailability is directly related to the drug absorption and metabolism in the gut wall. In the case of ABL, intestinal metabolism was not observed.[28] The present study confirmed clearly the role of P-gp in intestinal absorption of ABL and thus may contribute to its low bioavailability. This also could explain the active secretion of ABL into the intestine after intravenous administration.[14] On the other hand, the obtained results revealed that VER at a concentration of 400 µg/mL is almost sufficient to saturate P-gp efflux transporter, which was

reflected in enhancement of ABL absorption. Other studies showed that an increase in the concentration of VER up to 5-fold did not significantly affect the absorption rate constant of P-gp substrate due to saturation of P-gp transporter.[11] Furthermore, a lower VER concentration (200 µg/mL) did not significantly affect the absorption rate constant of ABL, which indicates that VER 200 µg/mL was not sufficient to saturate P-gp efflux transporter or to affect the absorption of ABL. A similar effect of VER at the higher dose level was manifested with other β-blockers such as salbutamol,[29] labetalol,[30] and propranolol.[11] In addition, this effect was also seen with drugs other than β-blockers such as metformin and phenformin.[10,17]

CONCLUSION

ABL is actively secreted from the enterocytes by P-gp efflux pump as confirmed by the inhibition study performed with VER, which indicated that P-gp is a critical factor that participates in low oral bioavailability of ABL. The absorption rate constant (k_{ap}) of ACH was increased 3-fold in the presence of VER 400 µg/mL. In contrast, no effect of lower VER concentration (200 µg/mL) was seen on the k_{ap} of ABL.

ACKNOWLEDGMENTS

I wish to express my deepest gratitude thanks to all staff in the Faculty of Pharmacy at Al-Azhar University-Gaza for their kind support and help and many thanks to Mr. Mohamed Abu Affash, the director of Medical Relief Society-Gaza, for providing me the facilities to perform analysis in his laboratory.

Conflicts of interest: No conflict of interest was declared by the authors. The authors alone are responsible for the content and writing of the paper.

REFERENCES

1. Jamei M, Turner D, Yang J, Neuhoff S, Polak S, Rostami-Hodjegan A, Tucker G. Population-based mechanistic prediction of oral drug absorption. AAPS J. 2009;11:225-237.
2. Martinez M, Amidon G. A mechanistic approach to understanding the factors affecting drug absorption: a review of fundamentals. J Clin Pharmacol. 2002;42:620-643.
3. Chillistone S, Hardman J: Factors affecting drug absorption and distribution. Anaesth Intensive Care Med. 2008;9:167-171.
4. Shugarts S, Benet L. The role of transporters in the pharmacokinetic of orally administered drugs. Pharm Res. 2009;26:2039-2054.
5. Varma M, Ambler C, Ullah M, Rotter C, Sun H, Litchfield J, Fenner KS, El-Kattan AF. Targeting intestinal transporters for optimizing oral drug absorption. Curr Drug Metab. 2010;11:730-742.
6. Leslie E, Deeley R, Cole S. Multidrug resistance proteins: Role of P-glycoprotein, MRP1, MRP2, and BCRP (ABCG2) in tissue defense. Toxicol and Appl Pharmacol. 2005;204:216-237.
7. Friend D. Drug delivery to the small intestine. Curr Gastroenterol Rep. 2004;371-376.
8. Giacomini K, Huang S, Tweedie D, Benet L, Brouwer K, Chu X, Dahlin A, Evers R, Fischer V, Hillgren KM, Hoffmaster KA, Ishikawa T, Keppler D, Kim RB, Lee CA, Niemi M, Polli JW, Sugiyama Y, Swaan PW, Ware JA, Wright SH, Yee SW, Zamek-Gliszczynski MJ, Zhang L. Membrane transporters in drug development. Nat Rev Drug Discov. 2010;9:215-236.
9. Bauer M, Zeitlinger M, Karch R, Matzneller P, Stanek J, Jäger W, Böhmdorfer M, Wasdak W, Mitterhauser M, Bankstahl JP, Löscher W, Koepp M, Müller M, Langer O. P-glycoprotein mediated interaction between (R)-[^{11}C]verapamil and tariquidar at the human blood-brain barrier studied with positron emission tomography, a comparison with rat data. Clin PharmacolTher. 2012;91:227-233.
10. Song N, Li Q, Liu C. Intestinal permeability of metformin using single-pass intestinal perfusion in rats. World J Gastroenterol. 2006;12:4064-4070.
11. Abushammala I, Ramadan M, El-Quedra A. The effect of p-glycoprotein on propranolol absorption using in situ rats single pass intestinal perfusion. International Journal of Pharmaceutical Sci Rev Res. 2013;22:161-165.
12. Harvey RA. Drugs affecting the autonomic nervous system: Adrenergic antagonists, Pharmacology (5th ed). Lippincott; Wiliams and Wilkins;2012:87-97.
13. Roux A, Flouvat B, Fouache Y, Bourdarias J. Systematic bioavailability of acebutolol in man. Biopharm Drug Dispos. 1983;4:293-297.
14. Terao T, Hisanaga E, Sai Y, Tamai I, Tsuji A. Active secretion of drugs from the small intestinal epithelium in rats by P-glycoprotein functioning as an absorption barrier. J Pharm Pharmacol. 1996;48:1083-1089.
15. Saitoh H, Aungst B. Possible involvement of multiple P-glycoprotein-mediated efflux systems in the transport of verapamil and other organic cations across rat intestine. Pharm Res. 1995;12:1304-1310.
16. Dahmani FZ, Yang H, Zhou J, Yao J, Zhang T, Zhang Q. Enhanced oral bioavailability of paclitaxel in pluronic/LHR mixed polymeric micelles: Preparation, *in vitro* and in vivo evaluation. Eur J Pharm Sci. 2012;47:179-189.
17. Choi M, Song I. Blockade of P-glycoprotein decreased the disposition of phenformin and increased plasma lactate level. Bimol Ther (Soul). 2016;24:199-205.
18. Zakeri-Milania P, Valizadeha H, Tajerzadehc H, Azarmia Y, Islambolchilala Z, Barzegara S, Barzegar-Jalali M. Predicting human intestinal permeability using single-pass intestinal perfusion in rat. J Pharm Pharm Sci. 2007;10:368-379.
19. Ernest D, Alfert E.D, Brenda M, Cross B.M, McWilliam AA. Guide to the care and use of experimental animals Volume 1 (2nd ed). Ottava; Canadian Council on Animal Care;1993;15-52.
20. Doluisio J, Billups N, Dittert L, Sugita E, Swintosky J. Drug absorption I: An in situ rat gut technique yielding realistic absorption rates. J Pharm Sci. 1969; 58:1196-1200.
21. Sanchez-Pico A, Peris-Ribera JE, Toledano C, Torres-Molina F, Casabo VG, Martin-Villodre A, Pla-Delfina JM. Nonlinear intestinal absorption kinetics of cefadroxil in the rat. J Pharm Pharmacol. 1989;41:179-185.
22. Ruiz-Balaguer N, Nacher A, Casabo V, Matilde Merino. Nonlinear intestinal absorption kinetics of cefuroximeaxetil in rats. Antimicrob Agents Chemother. 1997;41:445-448.
23. ICH International Conference on Harmonization, Harmonized Tripartite Guideline.: Validation of analytical procedures: text and methodology. 2005;Q2 (R1). Available from: https://www.ema.europa.eu/en/documents/scientific-guideline/ich-q-2-r1-validation-analytical-procedures-text-methodology-step-5_en.pdf

24. SPSS for Windows, Version 16.0.: 2007; Chicago, SPSS Inc. Released. Available from: https://www.ibm.com/support/pages/how-cite-ibm-spss-statistics-or-earlier-versions-spss

25. Nair A, Jacob S. A simple practice guide for dose conversion between animals and human. J Basic Clin Pharm. 2016;7:27-31.

26. Martin-Villodre A, Pla-Delfina JM, Moreno- Dalmau J, Perez-Buendia MD, Miralles J, Collado EF, Sánchez-Moyano E, del Pozo A. Studies on the reliability of a bihyperbolic functional absorption model. I. Ring substituted anilines. J Pharm Biopharm. 1986;14:615-633.

27. Yuasa H., Matsuda K. and Watanabe J. Influence of anesthetic regimens on intestinal absorption in rats. Pharm Res. 1993;10:884-888.

28. Piquette-Miller M, Jamali F. Pharmacokinetics and multiple peaking of acebutolol enantiomers in rats. Biopharm Drug Dispos. 1997;18:543-556.

29. Valenzuela B, Nacher A, Ruiz-Carretero P, Martin-Villodre A, Lopez-Carballo G, Barettino D. Profile of P-glycoprotein distribution in the rat and its possible influence on the salbutamol intestinal absorption process. J Pharm Sci. 2004;93:1641-1648.

30. Abushammala I, Garrigues T, Casabó V, Nácher A, Martín-Villodre A. Labetalol absorption kinetics: rat small intestine and colon studies. J Pharm Sci. 2006;95:1733-1741.

Turk J Pharm Sci 2020;17(6):679-685
DOI: 10.4274/tjps.galenos.2019.25902

ORIGINAL ARTICLE

Spectrophotometric Determination of Dopamine in Bulk and Dosage Forms Using 2,4-Dinitrophenylhydrazine

2,4-Dintrofenilhidrazin Kullanılarak Dopaminin Yığın ve Dozaj Formlarının Spektrofotometrik Tayini

Mai Abed Alrahman RAMADAN*, Ihab ALMASRI, Ghada KHAYAL

Al-Azhar University-Gaza Faculty of Pharmacy, Department of Pharmaceutical Chemistry and Pharmacognosy, Gaza, Palestine

ABSTRACT

Objectives: Dopamine (DA) hydrochloride is a sympathomimetic agent used therapeutically for the correction of hemodynamic disorders associated with shock episodes. Although several analytical methods have been described, a spectroscopic assay of DA after chemical derivatization with 2,4-dinitrophenylhydrazine (DNP) is still unexamined. Therefore, the optimization of the reaction parameters and validation of developed method were required.

Materials and Methods: The method is based on coupling of DA as a phenolic compound with a diazonium salt to produce an intensely colored azo derivative. DNP was oxidized with potassium periodate to produce a diazonium salt that coupled with DA in basic media. The experimental parameters were then optimized. The developed method was validated according to International Conference on Harmonisation Guidelines and was applied to dosage forms. The results were compared with the data of a reference method.

Results: The method was linear in a concentration range between 5 and 50 µg/mL. The regression line equation was Y=0.042±0.0003X+0.0672±0.0015 with a regression coefficient of 0.9944 (n=5). The limit of detection and limit of quantification were 0.32 and 0.97 µg/mL, respectively. The precision was satisfactory; the percentage relative standard deviation did not exceed 2%. The average values of the recovery study were in the range 98.90-100.40±0.31-1.21%. The developed method was applied successfully for the determination of DA in injection and infusion fluid.

Conclusion: The method is accurate, sensitive, and practical for DA analysis in quality control laboratories.

Key words: Dopamine hydrochloride, 2,4-dinitrophenylhydrazine, spectrophotometric, validation

ÖZ

Amaç: Dopamin (DA) hidroklorür, şok epizodlarında hemodinamik bozuklukların düzeltilmesinde terapötik olarak kullanılan bir sempatomimetik ajandır. Çok sayıda analitik yöntem tanımlanmasına rağmen, 2,4-dinitrofenilhidrazin (DNP) ile kimyasal türevlendirme sonrası DA'nın spektroskopik analizi henüz incelenmemiştir. Bu nedenle, reaksiyon parametrelerinin optimizasyonu ve geliştirilen yöntemin geçerliliği gereklidir.

Gereç ve Yöntemler: Yöntem, DA'nın bir fenolik bileşik olarak diazonyum tuzu ile birleştirilmeyle yoğun renkli bir azo türevinin oluşturulmasına dayanır. DNP potasyum periyodat ile okside edilmiş, bazik ortamda DA ile birleştirilerek diazonyum tuzu oluşturulmuştur. Sonrasında reaksiyon parametreleri optimize edilmiştir. Geliştirilen yöntem Uluslararası Uyum Konferansı Kılavuzları'na göre valide edilmiş ve dozaj formlarına uygulanmıştır. Sonuçlar bir referans yönteminin verileriyle karşılaştırılmıştır.

Bulgular: Yöntemin doğrusallığı 5 ila 50 µg/mL arasındadır. Regresyon çizgisi denklemi Y=0,042±0,0003X+0,0672±0,0015, regresyon katsayısı ise 0,9944 (n=5) olarak saptanmıştır. Deteksiyon limiti ve kantifkasyon limiti sırasıyla 0,32 ve 0,97 µg/mL'dir. Hassasiyet düzeyi yeterli seviyede olup; yüzde bağıl standart sapma %2'yi geçmemiştir. Geri kazanım çalışmasının ortalama değerleri %98,90-100,40±0,31-1,21 arasında bulunmuştur. Geliştirilen yöntem enjeksiyon ve infüzyon sıvısında DA tayini için başarıyla uygulanmıştır.

Sonuç: Yöntem, DA analizi için doğru ve hassastır ve kalite kontrol laboratuvarlarında kullanımının pratik olduğu söylenebilir.

Anahtar kelimeler: Dopamin hidroklorür, 2,4-dinitrofenilhidrazin, spektrofotometrik, validasyon

*Correspondence: E-mail: m.ramadan@alazhar.edu.ps, Phone: +972-059-9906430 ORCID-ID: orcid.org/0000-0001-8032-5777

Received: 23.09.2019, Accepted: 21.11.2019

INTRODUCTION

The chemical name for dopamine (DA) hydrochloride is 1,2-benzenediol,4-(2-amonoethyl) hydrochloride. DA is an endogenous catecholamine that is a sympathomimetic agent with prominent dopaminergic and β_1-adrenergic effects at low to moderate doses and α-adrenergic effects at high doses. It is used for the correction of hemodynamic disorders associated with shock episodes.[1,2]

A literature survey of DA revealed several methods for its determination in injection. Spectrophotometric methods using bromanil, 2,6-dichloroquinone-4-chloroimide, 3-amiopyridine, chloramine T, and various oxidative coupling based methods were published.[3-10] In addition, different high performance liquid chromatography (HPLC),[11-15] flow injection,[16,17] fluorimetric,[18] capillary electrophoresis,[19] chemiluminescence,[20] and electrochemical[21-26] methods were reported.

Spectrophotometry is considered the most practical analytical procedure in quality control laboratories, since it does not need costly instrumentation or toxic solvents like chromatography does. 2,4-dinitrophenylhydrazine (DNP) is a derivatizing agent used in the analysis of many drugs.[27-31] Chemical derivatization prior to spectroscopic analysis enhances both sensitivity and selectivity.[32]

The current study was performed, in continuation of our interest in the development and validation of simple, sensitive, and rapid spectrophotometric methods for the analysis of drugs,[33,34] to determine DA depending on a derivatization reaction with DNP in pharmaceuticals.

MATERIALS AND METHODS

Instruments

The spectrophotometers used were a Shimadzu ultraviolet (UV)-1601 with UV-Pro software (Shimadzu, Japan) and a Lambda 25 with V5 ES software (PerkinElmer, USA) and 1-cm quartz cells (Innovative Lab Supply, USA).

Materials

All chemicals used were of analytical grade. DA hydrochloride standard was purchased from Merck (Germany). DA dosage forms were ampoules for infusion (200 mg/5 mL) and DA hydrochloride with 5% dextrose infusion fluid (800 µg/mL DA) obtained from a local hospital pharmacy (Gaza, Palestine).

Preparation of reagents

DNP, 0.005 M reagent: 0.10 g of DNP was accurately weighed and transferred into a 100 mL volumetric flask, dissolved in 2.5 mL of concentrated sulfuric acid, and completed up to the volume with distilled water. The solution was freshly prepared and protected from light during use because it is *light sensitive.*

Potassium periodate [(PPI), 0.0065 M] reagent: 0.15 g of PPI was accurately weighed and transferred into a 100 mL volumetric flask, dissolved, and completed up to the volume with distilled water.

Sodium hydroxide [(NaOH), 10 M]: 40.00 g of NaOH was accurately weighed and transferred into a volumetric flask, dissolved, and completed up to the volume of 100 mL with distilled water.

Standard stock solution

It was prepared by dissolving 0.02 g of DA hydrochloride standard in 100 mL of distilled water (200 µg/mL). Working solutions were prepared by diluting the stock solution. The stock solution was freshly prepared during use.

General procedure

An aliquot of standard stock solution was transferred into a 10 mL volumetric flask followed by 1.0 mL of DNP, 1.0 mL of PPI, and 0.5 mL of NaOH reagents. The mixture was mixed well and diluted to 10 mL with distilled water at room temperature. The absorbance was measured at absorption maximum (λ_{max}) 560 nm against a blank.

Determination of stoichiometric ratio (Job's method)

Job's method of continuous variation was employed.[35] Equimolar ($3x10^{-3}$ M) aqueous solutions of DA and DNP were prepared. Series of 1.0 mL portions of DA and DNP were made up comprising different complementary volumes (0.0:1.0, 0.1:0.9, 0.2:0.8, 0.3:0.7, 0.4:0.6, 0.5:0.5, 0.6:0.4, 0.7:0.3, 0.8:0.2, 0.9:0.1, 1.0:0.0) in 10 mL volumetric flasks. The process followed the general procedure. Absorbance was plotted against DNP molar fraction.

Optimization of reaction conditions

Different reaction parameters were studied. They included concentration and volume of DNP, PPI, and NaOH; temperature; reaction time; order of addition; and stability of the developed chromogen. The study was carried out by altering one factor and keeping the others constant.

Method validation

Validation parameters were determined according to International Conference on Harmonisation (ICH) guidelines.[36]

Assay of pharmaceutical formulations

The content of three ampoules for DA was mixed and an accurately measured volume equivalent to 0.020 g of DA was transferred to a 100 mL volumetric flask. Distilled water was added to bring the volume up to 100 mL.

For DA and 5% dextrose infusion fluid, the content of three bottles was mixed and an accurately volume equivalent to 0.02 g was transferred into a 100 mL volumetric flask and diluted with water. It was further diluted to get a concentration of working solutions. Analysis was performed as described in the general procedure.

Statistical analysis

Data analysis was performed using SPSS version 17 to calculate the regression equation, coefficient factor, standard deviation, relative standard deviation (RSD), t-test, and p value.

RESULTS

In order to enhance sensitivity a derivatization reaction of DA using DNP was performed. A red shifted DA derivative was

produced, which showed an λ_{max} at 560 nm (Figure 1). The reaction parameters were optimized (Table 1). The reaction was completed immediately at room temperature. Heating was not advantageous due to intermediate (diazonium) instability. To DA solution was added DNP followed by PPI and NaOH (Table 2). DNP was oxidized by PPI to form a diazonium ion and the pH was still acidic. Once diazonium formed it attacked the electron-rich phenolic DA. The last step required basic media. Addition of PPI to DA (Table 2) was unsuitable since it can lead to oxidation of the catechol moiety of DA. When NaOH was added to DA the absorption was decreased. This can be explained by phenoxide formation and inappropriate media for diazonium salt formation.[37-39] The best result was achieved when 1 mL of both DNP and PPI reagents and 0.5 mL of NaOH were added to DA in the mentioned order. After dilution the DA derivative was stable for at least 15 min (Figure 2), which allowed processing of samples and their comfortable measurement. The stoichiometric ratio of the DA-derivatization reaction was studied by Job's method. The molar ratio was 1:1

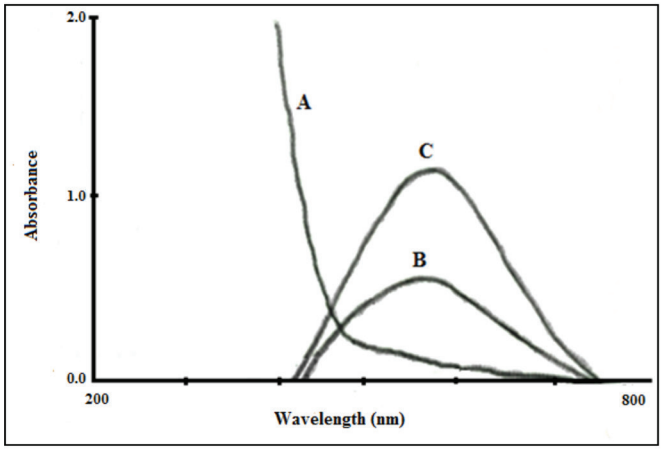

Figure 1. Absorption spectra. A) Blank spectrum against water; B, C) derivatization products against blank (DA: 10 and 30 µg/mL), respectively

DA: Dopamine

Table 1. Summary of optimum conditions for DA-derivatization reaction

Variable	Studied rangea	Optimum
DNP concentration	0.0015-0.010 M	0.005 M
Volume of DNP (0.005 M)	0.5-2.5 mL	1.0 mL
PPI concentration	0.0017-0.011 M	0.0065 M
Volume of PPI (0.0065 M)	0.5-2.5 mL	1.0 mL
NaOH concentration	5-10 M	10 M
Volume of NaOH (10 M)	0.2-2.0 mL	0.5 mL
Temperature	25-60°C	25°C
Time	0-60 min	0 min
Order of addition	Different	b

[a]: DA 10 µg/mL, DNP, PPI, and NaOH were mixed according to tested factor, H_2O diluting solvent, absorbance at 560 nm, [b]: For best order of addition see Table 2
DA: Dopamine, DNP: 2,4-dinitrophenylhydrazine, PPI: Potassium periodate, NaOH: Sodium hydroxide

for DA and DNP (Figure 3). Accordingly, a proposed mechanism of the reaction is illustrated in Figure 4 depending on the result for the molar ratio and the mechanism of azo formation.

Method validation

Linearity and sensitivity

For evaluation of linearity DA was determined at optimized conditions for five concentrations. The calibration curve was Y=0.042±0.0003X+0.0672±0.0015 (r=0.9944, n=5), where Y is

Table 2. Effect of order of addition on DA analysis

Sample	First	Second	Third	Fourth	Absorbance[a] (Mean ± SD)
1	DA	DNP	PPI	NaOH	0.473±0.005
2	DA	PPI	DNP	NaOH	0.451±0.013
3	DA	NaOH	PPI	DNP	0.442±0.001
4	DA	NaOH	DNP	PPI	0.447±0.001
5	DNP	PPI	DA	NaOH	0.450±0.010
6	DNP	PPI	NaOH	DA	0.438±0.009

[a]: Values are means of three determinations, DA 10 µg/mL, DNP (0.005 M, 1.0 mL), PPI (0.0065 M, 1.0 mL), NaOH (10 M, 0.5 mL), H_2O diluting solvent, at room temperature, absorbance at 560 nm
DA: Dopamine, DNP: 2,4-dinitrophenylhydrazine, PPI: Potassium periodate, NaOH: Sodium hydroxide, SD: Standard deviation

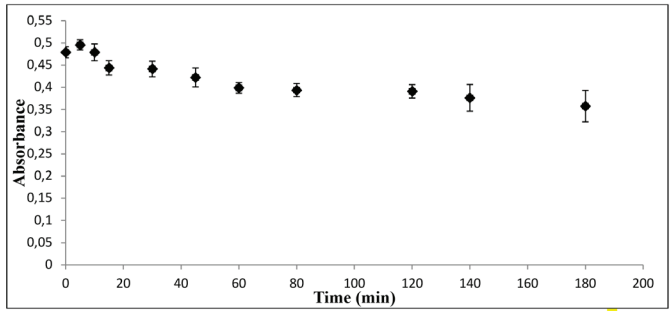

Figure 2. Stability of chromogen resulting from the reaction of DA with DNP. DA (10 µg/mL), absorbance is average of three determinations. Error bars represent standard deviation

DA: Dopamine, DNP: 2,4-dinitrophenylhydrazine

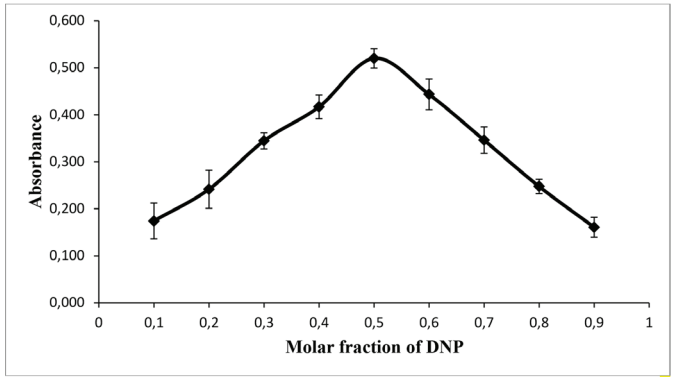

Figure 3. Determination of stoichiometric ratio by Job's method. DA and DNP are $3x10^{-3}$ M, absorbance is average of three determinations. Error bars represent standard deviation

DA: Dopamine, DNP: 2,4-dinitrophenylhydrazine

the absorbance at 560 nm and X is the concentration of DA (µg/mL). The linear range was 5-50 µg/mL. The molar absorptivity (ε) was 7.9x10^4 L/mol.cm. The limit of detection (LOD) and limit of quantitation (LOQ) were calculated as 3.3σ/S and 10σ/S, respectively,[36] where σ is the residual standard deviation of the regression line and S is the slope of the regression line. The LOD and LOQ were 0.32 and 0.97 (µg/mL), respectively.

Accuracy, precision, and specificity

The accuracy was evaluated by recovery studies for added standard concentrations to a pre-analyzed product at low, intermediate, and high concentrations. The recovery values were 99.5-101.9±0.21-1.12% (Table 3), indicating the accuracy of the method. Intraday precision was assessed at three different concentrations by analyzing five replicates per concentration on the same day. Interday precision was determined by analyzing samples for 6 consecutive days within a week (Table 4). The percentage of RSD did not exceed 2%, proving the high precision of the method. Before proceeding with the analysis of DA in its dosage forms, interference liabilities were determined to examine the effect of excipients that might be added during formulation. Samples were prepared by mixing 10 and 40 mg of DA with excipients like sodium bisulfate (0.05 g) and dextrose (5.0 g). These laboratory-prepared samples were analyzed by the developed method. The recovery values were 98.9-100.4±0.31-1.21% (Table 5). These data confirmed the absence of interference from excipients with DA determination by the developed method.

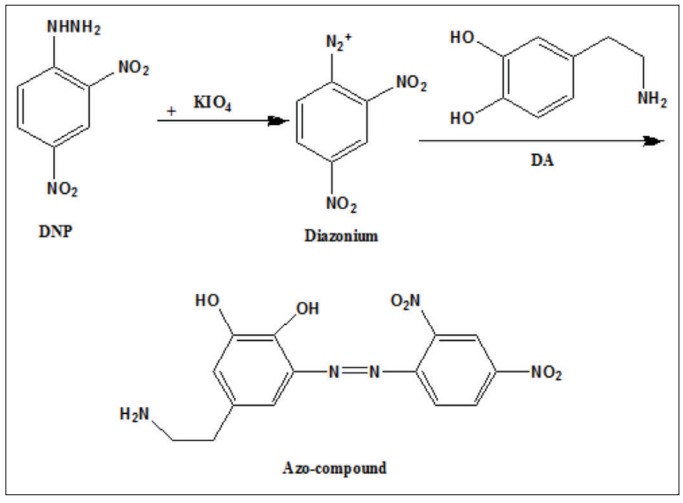

Figure 4. Suggested reaction of DA derivatization

DA: Dopamine, DNP: 2,4-dinitrophenylhydrazine

Table 3. Recovery studies for determination of DA by the developed method

Pre-analyzed product[a] (µg/mL)	Added DA (µg/mL)[b]	Recovery % (Mean ± SD)[c]
10	5	101.2±0.83
	10	99.5±1.01
	15	100.8±0.98
15	7.5	100.4±1.12
	15	101.8±0.21
	22.5	100.4±0.57
20	10	101.9±0.30
	20	100.5±0.73
	30	100.2±0.81

[a]: DA ampoule labeled to contain 200 mg/5 mL, found 198.6±0.1 mg/5 mL by the developed method, appropriate dilution was done, [b]: Standard DA was added to a pre-analyzed product at 50%, 100%, and 150%, [c]: Values are means of three determinations

DA: Dopamine, SD: Standard deviation

Table 4. Evaluation of intra- and interday precision

DA concentration (µg/mL)	Intraday (n=5)	Interday (n=6)
	RSD %	RSD %
5	0.99	1.5
20	1.14	0.65
40	0.64	0.42

DA: Dopamine, RSD: Relative standard deviation

Table 5. Interference liabilities from excipients

Excipients	DA concentration (µg/mL)	Recovery % (Mean ± SD)[a]
Sodium bisulfite	10	99.21±0.31
	40	100.4±0.73
Dextrose	10	98.9±1.21
	40	99.6±0.58

[a]: Values are means of three determinations, DA: Dopamine, SD: Standard deviation

Robustness and ruggedness

Robustness was evaluated by studying the influence of small variations in the method variables on its analytical performance. One parameter was changed while the others were kept unchanged and the recovery values were calculated each time. The recovery values were 98.6-101.1±0.31-1.12 (Table 6). This indicated the reliability of the method. Regarding ruggedness, lab-to-lab variations were examined by performing DA analysis using the same operational conditions but using two different instrumentations. The results obtained were reproducible, as RSD did not exceed 1.43% (Table 7).

Application of the method

DA pharmaceutical dosage forms (ampoule, infusion fluid) were analyzed successfully by the developed method. The results comply with the USP 29 specifications of DA content in injection (95-105%).[40] Comparison of the result with the reference data[5] by statistical analysis with respect to accuracy

Table 6. Robustness of the method

Parameter	Variation	Recovery% (Mean ± SD)[a]
DNP concentration		
	0.004 M	99.6±0.41
	0.006 M	98.9±0.64
Volume of 0.005 M DNP		
	0.8 mL	101.1±0.93
	1.2 mL	100.5±0.76
PPI concentration		
	0.0057 M	98.6±1.12
	0.0074 M	99.3±0.31
Volume of 0.0065 M PPI		
	0.8 mL	100.2±0.86
	1.2 mL	99.1±0.37
NaOH concentration		
	9.8 M	98.7±0.54
	10.2 M	99.2±0.62
Volume of 10 M NaOH		
	0.4 mL	101.5±1.5
	0.6 mL	99.3±1.5
Temperature		
	23°C	99.25±0.14
	27°C	100.55±0.39

[a]: Values are means of three determinations; the concentration of DA was 20 µg/mL DA: Dopamine, DNP: 2,4-dinitrophenylhydrazine, PPI: Potassium periodate, NaOH: Sodium hydroxide, SD: Standard deviation

Table 7. Ruggedness of the method

DA concentration (µg/mL)[a]	Shimadzu UV-1601		Perkin Elmer Lambda 25	
	Recovery % (Mean ± SD)	RSD %	Recovery % (Mean ± SD)	RSD %
5	98.3±1.41	1.43	98.6±1.22	1.24
20	100.7±0.47	0.47	98.8±0.58	0.59
40	98.6±0.43	0.44	99.7±0.29	0.29

[a]: Three determinations per concentration, RSD: Relative standard deviation, DA: Dopamine, UV: Ultraviolet, SD: Standard deviation

by t-test showed that there was no significant difference at the 95% confidence level. This confirms similar accuracy in the determination of DA by the two methods (Table 8).

DISCUSSION

DA contains a catechol group, which can be coupled with a diazonium cation in basic solution to produce a red shifted azo derivative. A simple one-step procedure was achieved for spectrophotometric analysis of DA after derivatization with DNP. The reaction was completed immediately at room temperature,

Table 8. Determination of DA in dosage forms by developed method and comparison with reference data

Dosage forma	Recovery % (Mean ± SD)[b]	
	DNP method	Reference data[5]
Ampoule	99.32±0.51 (t=1.6567, p value=0.1362)	98.56±0.89
DA and dextrose infusion solution	95.81±0.87	-

[a]: Labeled to contain 200 mg/5 mL DA per ampoule or 0.8 mg/mL DA and 5% dextrose infusion solution, [b]: Values are means of five determinations, p value >0.05 nonsignificant difference, DA: Dopamine, SD: Standard deviation, DNP: 2,4-dinitrophenylhydrazine

which is advantageous in comparison to other spectroscopic DA assays. Heating at 30, 40, and 75°C and adjustment of pH using a buffer were required for 4-aminoantipyrine-,[10] bromanil-,[6] and 2-hydroxynaphthaldehyde-based[11] spectroscopic analysis of DA, respectively. A derivatization reaction was described for spectroscopic analysis of DA based on the formation of intensely colored Prussian blue that required 35 min for completion.[9] In addition, the developed method exhibited enhanced sensitivity (ε $7.9x10^4$ L/mol.cm). The recorded molar absorptivities (ε) for spectrophotometric DA determination were $3.475x10^3$, $6.47x10^3$, and $7.4x10^3$.[4,6] A HPLC assay for DA analysis showed a range (12-40 µg/mL) comparable with that of the developed method.[12] Chromatographic methods require highly sophisticated instruments and expensive solvents.

The results of the validation studies were in good agreement with ICH guidelines. The method was accurate and precise. The results for interference liabilities proved the specificity of the developed method; thus it can be applied for DA analysis in its dosage forms. The statistical analysis showed that the developed method is comparable with a reference method[5] for analysis of DA.

CONCLUSION

The developed method has the advantages of being simple, rapid, sensitive, accurate, and low cost, and does not require any pretreatment of the drug. The method was applied successfully for analysis of DA in dosage forms without interference from excipients. Therefore, it can be suitable for routine analysis of DA in quality control laboratories.

ACKNOWLEDGMENTS

I would like to thank Al-Shifa hospital pharmacy (Gaza, Palestine) for supplying the DA dosage forms.

Conflicts of interest: No conflict of interest was declared by the authors. The authors alone are responsible for the content and writing of the paper.

REFERENCES

1. Ford SM, Roach SS. Roach's Introductory Clinical Pharmacology (10th ed). Philadelphia; Lippincott, Williams & Wilkins; 2013:350-362.

2. Boulain T, Runge I, Bercault N, Benzekri-Lefevre D, Wolf M, Fleury C. Dopamine therapy in septic shock: detrimental effect on survival? J Crit Care. 2009;24:575-582.
3. Al-Abachi MQ, Al-Da'amy MA. Spectrophotometric determination of catechol amine drugs in pharmaceutical preparations via oxidative coupling reaction with 3-amino pyridine and sodium periodate. Irq Nat J Chem. 2005;18:226-234.
4. Al-Sharook MM. Spectrophotometric determination of catecholamines in pharmaceutical preparations via charge transfer complex formation using bromanil reagent. J Edu Sci. 2007;19:1-11.
5. Idris RM, Gadkariem EA, Ibrahim KE, Mohamed MA. Development of spectrophotometric method for determination of dopamine hydrochloride in bulk and injectable forms. Res J Pharm Biol Chem Sci. 2012;3:1135-1145.
6. Nagaraja P, Murthy KC, Rangappa KS, Gowda NM. Spectrophotometric methods for the determination of certain catecholamine derivatives in pharmaceutical preparations. Talanta. 1998;46:39-44.
7. Nagaraja P, Murthy KC, Yathirajan HS, Mohan BM. Rapid spectrophotometric determination of dopamine hydrochloride with chloramine-T. Indian J Pharm Sci. 1998;60:99-101.
8. Nagaralli BS, Seetharamappa J, Melwanki MB, Ramesh KC, Keshavayya J. Spectrophotometric investigations of the assay of physiologically active catecholamines in pharmaceutical formulations. J AOAC Int. 2002;85:1288-1292.
9. Guo L, Zhang Y, Li Q. Spectrophotometric determination of dopamine hydrochloride in pharmaceutical, banana, urine and serum samples by potassium ferricyanide-Fe(III). Anal Sci. 2009;25:1451-1455.
10. Mohamed GG, Nour-El-Dien FA, El-Nahas RG. Spectrophotometric and standard addition methods for quantitative determination of dopamine hydrochloride and levodopa in tablets and ampoules. Afinidad. 2009;541:243-251.
11. Rajper AD, Arain GM, Rind FMA, Khuhawar MY. Spectrophotometric and liquid chromatographic determination of dopamine from pharmaceutical preparations using 2-hydroxynaphthaldehyde as derivatizing reagent. Asian J Chem. 2007;19:4817-4824.
12. Cosmin R, Marius B, Ancamaria N. Validation of a HPLC method of dopamine hydrochloride determination from injectable preparation. Clujul Med. 2009;82:520-523.
13. Sanchez A, Menezes M, Pereira O. Determination of catecholamines in plasma from rats by direct injection using HPLC. Salusvita. 2001;20:79-87.
14. Rao PS, Rujikarn N, Luber JM, Tyras DH. A specific sensitive HPLC method for determination of plasma dopamine. Chromatographia. 1989;28:307-310.
15. Zhao H, Mun H, Bai Y, Yu H, Hu Y. A rapid method for the determination of dopamine in porcine muscle by pre-column derivatization and HPLC with fluorescence detection. J Pharm Anal. 2011;1:208-212.
16. Nevado JJB, Gallego JML, Laguna PB. Flow-injection spectrophotometric determination of adrenaline and dopamine with sodium hydroxide. J Pharm Biomed Anal. 1996;14:571-577.
17. Al-Abachi MQ, Sinan R, Haddi H. Spectrophotometric determination of methyldopa and dopamine hydrochloride in pharmaceutical preparations using flow injection analysis. Nat J Chem. 2009;36:597-604.
18. Subrata K, Ghosh SK, Madhuri M, Anjali P, Tarasankar P. Fluorimetric determination of dopamine via its derivatization with 1,2-phenylenediamine. J Indian Chem Soc. 2004;81:868-873.
19. Kuo IT, Huang YF, Chang HT. Silica nanoparticles for separation of biologically active amines by capillary electrophoresis with laser-induced native fluorescence detection. Electrophoresis. 2005;26:2643-2651.
20. Nalewajko E, Wiszowata A, Kojto A. Determination of catecholamines by flow-injection analysis and high-performance liquid chromatography with chemiluminescence detection. J Pharm Biomed Anal. 2007;43:1673-1681.
21. Yu Z , Li X, Wang X, Ma X, Li X, Cao K. Voltammetric determination of dopamine and norepinphrine on a glassy carbon electrode modified with poly (L-aspartic acid). J Chem Sci. 2012;124:537-544.
22. Ören T, Birel Ö, Anık Ü. Electrochemical determination of dopamine using a novel perylenediimide-derivative modified carbon paste electrode. Anal Lett. 2018;51:1680-1693.
23. Lai GS, Zhang HL, Han DY. Electrocatalytic oxidation and voltammetric determination of dopamine at a nafion/carbon-coated iron nanoparticles-chitosan composite film modified electrode. Mikrochim Acta. 2008;160:223-233.
24. Stoytcheva M, Zlatev R, Velkova Z, Gochev V, Montero G, Toscano L, Olivas A. Advances in the electrochemical analysis of dopamine. Curr Anal Chem. 2017;13:89-103.
25. Redžić S, Kahrović E, Zahirović A, Turkušić E. Electrochemical determination of dopamine with ruthenium (III) modified glassy carbon and screen printed electrodes. Anal Lett. 2016;50:1602-1619.
26. Vinoth V, Wu JJ, Anandan S. Sensitive electrochemical determination of dopamine and uric acid using $AuNPs_{(EDAS)}$–rGO nanocomposites. Anal. Methods. 2016; 22:4379-4390.
27. Shravya A, Chandan RS, Gurupadayya BM, Sireesha M. Spectrophotometric determination of atorvastatin and ezetimibe using 2,4-DNP in bulk and pharmaceutical dosage forms. Int J Pharm Technol. 2010;2:1046-1056.
28. Nagaraja P, Shrestha AK. Spectrophotometric method for the determination of drugs containing phenol group by using 2,4-dinitrophenylhydrazine. J Chem. 2010;7:395-402.
29. Sowjanya K, Thejaswini JC, Gurupadayya BM, Priya MI. Spectrophotometric determination of pregabalin using 1,2-napthaquinone-4-sulfonic acid sodium and 2,4-dinitrophenylhydrazine in pharmaceutical dosage form. Pharm Lett. 2011;3:47-56.
30. Sai Praveen P, Anupama B, Jagathi V, Devala Rao G. Spectrophotometric determination of Tolperisone using 2,4-dinitrophenylhydrazine reagent. Int J Res Pharm Sci. 2010;1:317-320.
31. Abdelmageed OH. Development and validation of a spectrophotometric method for the determination of macrolide antibiotics by using 2,4-dinitrophenylhydrazine. J AOAC Int. 2007;90:364-371.
32. Watson GD. Pharmaceutical Analysis: A Textbook for Pharmacy Students and Pharmaceutical Chemists (2nd ed). London; Churchill Livingstone; 2005:97-116.
33. Ramadan M. O-Phthalaldehyde based spectrophotometric method for determination of sitagliptin in tablets. Int J Pharm Pharm Sci. 2014;6:125-129.
34. Ramadan M, Abuiriban A. NQS assisted spectrophotometric determination for aliskiren in pharmaceutical dosage form. Am J Anal Chem. 2013;3:105 113.
35. Job P. Advanced Physicochemical Experiments (2nd ed). Edinburgh; Oliver and Boyd; 1964:45.

36. ICH Harmonized tripartite guideline, Validation of analytical procedures: Text and Methodology Q2(R1). In Proceedings of the International Conference on Harmonization, Geneva; 2005.

37. Morrison RT, Boyd RN. Organic Chemistry (6th ed). New Jersey; Prentice Hall; 1992:864-866.

38. March J. Advanced Organic Chemistry: Reactions, Mechanisms and Structure. (4th ed). New York; John Wiley & Sons; 1992:635-637.

39. Herbst W, Hunger K. Industrial Organic Pigments: Production, Properties, Applications (3rd ed). Weinheim; Wiley-VCH; 2004:197-205.

40. United States Pharmacopeia 24 -National Formulary 19. Rockville; United States Pharmacopeial Convention Inc.; 2007:754-755.

Turk J Pharm Sci 2020;17(6):686-697
DOI: 10.4274/tjps.galenos.2020.76401

REVIEW

New Therapeutic Approaches in Cystic Fibrosis

Kistik Fibroziste Yeni Terapötik Yaklaşımlar

Dolunay Merve FAKIOĞLU[1], Beril ALTUN[2]*

[1]Gazi University Faculty of Pharmacy, Department of Clinical Pharmacy, Ankara, Turkey
[2]Gazi University Faculty of Pharmacy, Department of Pharmaceutical Toxicology, Ankara, Turkey

ABSTRACT

Cystic fibrosis (CF) is a hereditary, multisystemic disease caused by different mutations in the *CFTR* gene encoding CF transmembrane conductance regulator. CF is mainly characterized by pulmonary dysfunction as a result of deterioration in the mucociliary clearance and anion transport of airways. Mortality is mostly caused by bronchiectasis, bronchiole obstruction, and progressive respiratory dysfunction in the early years of life. Over the last decade, new therapeutic strategies rather than symptomatic treatment have been proposed, such as the small molecule approach, ion channel therapy, and pulmonary gene therapy. Due to considerable progress in the treatment options, CF has become an adult disease rather than a pediatric disease in recent years. Pulmonary gene therapy has gained special attention due to its mutation type independent aspect, therefore being applicable to all CF patients. On the other hand, the major obstacle for CF treatment is to predict the drug response of patients due to genetic complexity and heterogeneity. The advancement of 3D culture systems has made it possible to extrapolate the disease modeling and individual drug response *in vitro* by producing mini adult organs called "organoids" obtained from rectal cell biopsies. In this review, we summarize the advances in the novel therapeutic approaches, clinical interventions, and precision medicine concept for CF.

Key words: Cystic fibrosis, gene therapy, gene modulators, rectal organoids

ÖZ

Kistik fibrozis (CF), CF transmembran iletkenlik düzenleyicisini kodlayan *CFTR* genindeki farklı mutasyonların neden olduğu kalıtsal, multisistemik bir hastalıktır. CF, esas olarak hava yollarındaki mukosiliyer klerensin ve anyon transportunun bozulması sonucu gelişen pulmoner disfonksiyon ile karakterizedir. Mortalite, genellikle bronşektazi, bronşiyollerin tıkanması ve erken dönemde progresif solunum fonksiyon bozukluğundan kaynaklanır. Son on yılda, küçük molekül yaklaşımı, iyon kanal tedavisi ve pulmoner gen tedavisi gibi semptomatik tedaviden ziyade hastalığı tedavi etmeye yönelik yeni stratejiler geliştirilmiştir. Tedavi seçeneklerindeki önemli ilerlemeler sayesinde, CF son yıllarda pediatrik bir hastalıktan ziyade yetişkin hastalığı haline gelmiştir. Pulmoner gen tedavisi, mutasyon tipinden bağımsız olması ve tüm CF hastalarına uygulanabilirliği nedeniyle özellikle dikkat çekmiştir. Diğer taraftan CF tedavisindeki en büyük sorun, hastalardaki genetik karmaşıklık ve heterojenite nedeniyle ilaç yanıtını öngörememektir. 3D hücre kültürü sistemlerindeki ilerlemeler, rektal hücre biyopsilerinden "organoidler" adı verilen kişiye özel mini organlar üreterek hastalığın modellenmesini ve bireysel ilaç yanıtını *in vitro* olarak tahmin etmeyi mümkün kılmıştır. Bu derlemede, CF için yeni terapötik yaklaşımlar, klinik girişimler ve hassas tıp konseptindeki ilerlemeler özetlenmektedir.

Anahtar kelimeler: Kistik fibrozis, gen terapisi, gen modülatörleri, rektal organoidler

INTRODUCTION

Cystic fibrosis (CF) is a hereditary, multifactorial, multisystemic disease characterized by obstruction of airways, microbial infection, digestive disorders, and other complications. CF is known as the most common autosomal recessive disease in Caucasians.[1]

Although the incidence of disease varies greatly throughout the world, the highest incidence rate is seen in Northern Europe and the United States with 1/3,000 in white Americans, 1/4,000-10,000 in Hispanics, and 1/15,000-20,000 in African Americans. In Turkey, the incidence rate was reported as 1/3,400, close to that of the regions with the highest incidence rates. Globally, around 70,000 to 100,000 people suffer from CF.[2]

CF is caused by different mutations in the *CFTR* gene encoding CF transmembrane conductance regulator (CFTR), which regulates the mucociliary clearance and anion transport in airways.[3] The *CFTR* gene is located on the long arm of chromosome 7 and the CFTR protein product is 1,480 amino acids in length. CFTR acts as a cAMP regulated chlorine channel in apical membranes, providing Na^+ and water transport from epithelial cells in many organs and glands.[4] CFTR dysfunction primarily affects epithelial cells and causes chronic microbial infection and subsequently airway inflammation. Mortality from CF is commonly caused by bronchiectasis, bronchiole obstruction, and progressive respiratory dysfunction.[5] The severity of the disease is directly

*Correspondence: E-mail: berilaltun@gmail.com, Phone: +90 506 820 12 82 ORCID-ID: orcid.org/0000-0003-3083-9854
Received: 14.02.2020, Accepted: 04.05.2020

proportional to the extent the lungs are affected and varies by person.[6]

The pathophysiology of CF cannot be explained by a single hypothesis. The most common theory is the excessive reabsorption of Na^+ and water from the airway surface, resulting in a more viscous and elastic state of the airway secretions. These changes in the secretions cause dehydration of the airway surface and the formation of mucus plugs; mucociliary clearance becomes difficult. In addition to these changes, low HCO_3^- further affects the microenvironment by making the pH more acidic. Since bacterial eradication in the airways is pH dependent, changes in pH disrupt the natural immunity by attenuating the effectiveness of endogenous peptides.[7-9] In addition to these changes, decreased HCO_3^- levels contribute to the increase in mucus intensity.[10] This leads to accumulation of secretions and obstruction of the airways starting from the bronchioles. Mucociliary clearance of inhaled microorganisms that are trapped in mucus becomes gradually more difficult.[11] In a typical infant with CF, *Haemophilus influenzae*, *Staphylococcus aureus*, or both rapidly colonize and *Pseudomonas aeruginosa*, *Stenotrophomonas maltophilia*, and *Burkholderia cepacia* may all be present even in infants.[12] In a short time, *P. aeruginosa* becomes the most dominant microorganism in the airways. It is the main pathogen in CF patients and its prevalence is around 70% in adults with CF.[13] *P. aeruginosa* forms a polysaccharide film to protect itself from antimicrobial agents. Therefore, bacterial binding to the epithelial cells increases and bacterial clearance decreases with natural immune mechanisms.[14,15] The management of pulmonary infection is of great significance since it affects the time of survival.[16] The most important concern regarding CF treatment is the increasing bacterial resistance to standard antibiotics.

CF also affects various organs and systems such as the intestinal tract, biliary tract, pancreas, and genitourinary system. Co-morbidities are pancreatic malabsorption (malnutrition), biliary cirrhosis, and infertility. Pancreatic and bile duct epithelial cells are affected by CFTR dysfunction as well. Chronic obstructive pancreatitis is observed due to excessive mucus secretion. Severe pancreatic exocrine deficiency causes symptomatic fat malabsorption.[17] If the pancreatic insufficiency cannot be controlled, this may cause damage to islet cells and leads to insulin deficiency and CF related-diabetes mellitus (CF-DM). The vascular outcomes of diabetes are evidential in typical DM patients; however, in CF-DM patients, nutritional and pulmonary outcomes might be life-threatening. The first treatment option is insulin (i.m.) rather than oral antidiabetics in CF-DM patients after the endocrinologic consultation, unlike the typical type-2 DM patients.[18] The intravenous (iv) administration of aminoglycoside and CF-DM are the major causes of renal failure in CF patients.[19]

The main objective of treatment of CF is to remove excessive mucus from the lungs, to control pulmonary infection, and to reverse pancreatic insufficiency and malnutrition. This perspective has led to a significant increase in the life span and quality of CF patients in recent years. In this review, we aim to summarize the novel treatment options and innovative therapeutic approaches for CF.

Classification of CFTR mutations

To date, approximately 2,000 different types of mutations have been identified in the *CFTR* gene.[20] However 15% of those are not associated with CF.[21] The most common mutation, called ΔF508, is the 3 base deletion leading to loss of phenylalanine at position 508 in the CFTR protein.[22] The ΔF508 mutation accounts for two-thirds of all CF alleles.[23] Approximately 90% of CF patients carry at least one copy of the ΔF508 mutation.[24] Determination of the CFTR mutation type is of great importance, since the mutation type shows the disease phenotype and indicates the way for the treatment strategy. CF is classified according to the step in which the mutation takes place. The conventional classification system divides CFTR mutations into 6 categories according to CFTR synthesis, trafficking, or function. However, De Boeck and Amaral[20] grouped mutations into seven classes according to functional defects and separated the previous class I mutations into class I (stop-codon mutations) and a new class VII [no messenger RNA (mRNA) transcription] (Table 1).

Classification of mutations helps us to understand the CFTR defect; however, mutations might be more than just a feature, because they are the most important determinant of disease severity.[25] Class I, II, and III mutations are related to no CFTR function and severe phenotype. However, class IV, V, VI, and VII mutations involve residual functional CFTR protein and therefore moderate phenotype and pancreatic insufficiency.[5]

Mutations of class I include nonsense, frameshift, or mRNA splicing mutations leading to absence of CFTR expression, therefore resulting in a reduced number of CFTR channels. Class II mutations, including ΔF508, lead to faulty CFTR processing. Even if CFTR is properly synthesized, missense and in-frame deletion mutations interrupt CFTR folding and trafficking. Some class II mutations partially disrupt protein stability. In class III mutations, channel gating is defective due to diminished ATP binding to the channel and results in impaired chloride transport. In class IV mutations, chloride transport is disrupted due to the abnormal CFTR channel pore. Class IV mutations often result in a milder phenotype because of the partial CFTR function. A low amount of CFTR protein is available, but aberrant splicing defects lead to defective mRNA processing (no full length or stable mRNA). Class VI mutations are characterized by a functional but unstable CFTR protein, and premature degradation of CFTR results in high CFTR turnover at the cell surface. The last category, class VII mutations, consist of large deletions on the *CFTR* gene and therefore no mRNA transcription process.[20,21,26,27]

New treatment approaches

New options in the management of pulmonary infection

Ceftazidime/avibactam is a new cephalosporin-beta lactamase inhibitor combination that is effective for multiple drug resistant infections.[28] Although ceftazidime has been in clinical use for many years as an antipseudomonal, its efficacy is unclear due to decreased sensitivity in recent years. The ceftazidime/

Table 1. Classification of CFTR mutations[20,21]

Mutation class	Defect	Phenotype	Example	Treatment strategy
I	Reduced CFTR protein expression	No protein	Gly542X Trp1282X	Production correctors (ataluren)
II	Misfolded CFTR protein not transported to the cell surface	No traffic	Phe508del (ΔF508) Asn1303Lys Ala561Glu	Corrector + potentiator (lumacaftor + ivacaftor, VX-661+ ivacaftor)
III	Reduced/lack of CFTR channel opening	Impaired gating	Gly551Asp Ser549Arg Gly1349Asp	Potentiator (ivacaftor)
IV	Misshaped CFTR pore restricts Cl^- movement	Decreased conductance	Arg117His Arg334Trp Ala455Glu	Potentiator (ivacaftor)
V	Reduced CFTR protein production	Less protein	3849+10 kb C→T Ala455Glu 3272-26A → G	No data available
VI	High CFTR protein turnover at the cell surface	Less stable	120del23 rPhe508del	No data available
VII	No transcription due to large deletions on *CFTR* gene	No mRNA	dele2,3 (21kb) 1717-1G →A	Unrescuable (By pass therapies?)

Kb: Kilobases, CFTR: Cystic fibrosis transmembrane conductance regulator

avibactam combination offers a potential improvement for CF pulmonary infections involving *P. aeruginosa.*[29,30] Combination with avibactam increases the activity of ceftazidime against *Enterobacteriaceae* and *P. aeruginosa*, since avibactam inhibits serine β-lactamases including ESBL, AmpC, and KPC. On the other hand, avibactam does not increase ceftazidime activity against *Acinetobacter* spp., *Burkholderia* spp., or most anaerobic Gram (-) bacilli.[31] Co-administration of ceftazidime/avibactam and aztreonam gave successful results for extremely drug resistant *Burkholderia multivorans* infections.[32]

Ceftolozane/tazobactam is a novel β-lactam/β-lactamase inhibitor combination approved by the Food and Drug Administration (FDA) in 2014 for the treatment of complicated intraabdominal and urinary tract infections.[33] Ceftolozane/tazobactam is promising for the treatment of *P. aeruginosa* infection in CF patients, alone or in combination with tobramycin or amikacin. The efficacy of amikacin and the ceftolozane/tazobactam combination is higher than that of tobramycin-ceftolozane/tazobactam. This encouraging progress led to further clinical research on multidrug resistant *P. aeruginosa* infections in CF patients.[34] Neither the ceftazidime/avibactam nor the ceftolozane/tazobactam combination has been approved for patients under the age of 18 yet, but pediatric population studies are in progress and currently in phase 2.[35-37]

Inhaled antibiotics are another widely used treatment option alone or in conjunction with oral antibiotics to prevent pulmonary exacerbations. The use of inhaled antibiotics has advantages compared to iv administration or the oral route. Increased antibiotic concentration at the infection site through inhalation enhances bacterial eradication, and systemic side effects such as nephrotoxicity and ototoxicity can be avoided.[38]

The inhaled antibiotics used for CF are aztreonam lysine, tobramycin inhalation powder/solution, inhaled colistin, liposomal amikacin, liposomal ciprofloxacin, and inhaled levofloxacin.[39-42] Inhaled tobramycin and inhaled aztreonam are the two inhaled antibiotics with FDA approval. Liposomal amikacin was approved by the FDA in 2018.[43]

Inhaled colistin (colistimethate sodium) has been approved by the European Medicines Agency, but not the FDA yet. Other antibiotics, i.e. liposomal ciprofloxacin and inhaled levofloxacin, have not been approved for CF. These are under investigation in the earlier stages of development, in phase studies.[44]

Ion channel therapies: non-CFTR modulating therapies

Inhibition of Na^+absorption

Fluid hydration in the airway depends on Cl^--bicarbonate secretion by CFTR channels and sodium absorption mediated by epithelial sodium channels (ENaCs). Although the CFTR channel defect mainly affects the secretion of Cl^- and bicarbonate ions from epithelial cells, it also leads to deterioration in the secretions and absorption of electrolytes.[45] Increased Na^+ absorption (2-3 times higher than normal) is observed through the ENaCs, as well as impaired Cl^- secretion. Na^+ hyperabsorption leads to more dehydration of respiratory secretions and further deterioration of mucociliary clearance. Blockage of the epithelial Na^+ channel and prevention of Na^+ hyperabsorbion have been recommended as a treatment strategy.[46]

Amiloride is a first generation potassium-sparing ENaC antagonist, developed as a sodium channel inhibitor in the 1960s. Although intranasal administration of amiloride has reduced the pulmonary mortality rate, the risk of hyperkalemia

limited its use.[47] The study had to be terminated due to acute hyperkalemia caused by inhibition of ENaCs in the kidneys.[48]

AZD5634 is a new inhalable, second-generation amiloride derivate and it is well tolerated without considerable hyperkalemia risk.[49] ENaC antagonists QBW 276 and BI 443651 have undergone clinical investigation and demonstrated remarkable safety profiles in phase 1 trials. However, phase 2/ efficacy outcomes are still pending.[50,51]

SPX-101 is another inhalable ENaC inhibitor peptide that has undergone phase 2 trials.[52] SPX-101 showed positive and significant results without causing hyperkalemia. The aerosol administration of antisense oligonucleotides may provide an alternative approach.

Stimulation of Cl^- secretion

Luminal Cl^- secretion of epithelial cells is mediated by the CFTR and alternative chlorine channels. Increased activity of alternative chlorine channels like the calcium-activated chloride channel (CaCC) in the lower respiratory tract may compensate for decreased or absent CFTR function and improve the clinical status of CF patients.[53]

Activation of $P2Y_2$ nucleotide receptor activates the CaCCs by causing a rapid increase in cytosolic free calcium concentration. ATP and uridine 5'-triphosphate (UTP), endogenous $P2Y_2$ receptor ligands, increase ion and liquid secretion.[54] However, the short half-lives of extracellular ATP and UTP limit their clinical utility. To induce chlorine secretion by $P2Y_2$-mediated CaCC pathway, more stable inhaled $P2Y_2$ receptor agonists needed to be developed. Denufosol is an inhaled $P2Y_2$ receptor agonist that increases the Cl^- ion and fluid secretion in luminal clearance by $P2Y_2$-mediated CaCC stimulation. Although denufosol was found to be effective and well tolerated in mild CF patients,[55,56] it failed in the phase 3 step due to unsatisfactory results in terms of pulmonary function. Another reason for failure is its short half-life.[57]

Moli1901, also known as duramycin, a stable 19-residue-polycyclic peptide that is derived from *Streptomyces cinnamoneum*, interacts with phospholipids and thereby activates alternative chloride channels by elevated intracellular calcium levels.[58] Although Moli1901 showed promise as a chloride channel activator, it could not be further developed due to formulation problems.

Osmotic therapy

Airway surface fluid (ASL) is a thin layer of fluid that covers the lumen surface of the airway epithelium and maintains mucociliary clearance, ciliary function, and antimicrobial features of the airway, a key regulator of airway homeostasis.[59] ASL depletion is a significant factor in the pathogenesis of cystic fibrosis, so it has been shown that osmotic water withdrawal to the airway surface may improve the damaged mucociliary transport.[60,61] The main building block of CF treatment is actually correcting mucociliary clearance; a small molecule approach like CFTR modulators is able to do this by correcting dysfunctional CFTR as is an approach to targeting ion channels in airway epithelial cells pharmacologically. Hypertonic saline and dry mannitol powder, which directly correct mucociliary transport, produce an osmotic gradient by drawing water from the aquaporins of epithelial cells.[60,62] Hypertonic saline, usually used as a 7% solution, induces the release of inflammatory mediators such as prostaglandin E2, altering the rheology of the mucus and increasing mucociliary clearance.[63] Mannitol is a nonionic osmotic agent. The larger size of mannitol is a disadvantage over hypertonic saline, and it is difficult to accumulate in small airways; however, it is easier to administer via a metered dose inhaler (compared to nebulizer hypertonic saline).[64]

Small molecule approach: CFTR modulating therapies

CFTR modulators were described first by Verkmen in 2003. They are novel therapeutics that correct CFTR protein production, defective CFTR protein itself, and/or its intracellular function. CFTR modulators play a significant role in CF treatment since they provide a fundamentally therapeutic approach rather than symptomatic therapy by targeting the production or function of CFTR protein.[65-67]

The first group, called CFTR potentiators, increase the function of the expressed CFTR channels and ameliorate class III or IV defects even when CFTR reaches the cell surface but is nonfunctional. The second group, called CFTR correctors, are drugs that can act to improve the intracellular processing of proteins, thereby providing CFTR proteins to move to the appropriate site on the cell surface. Finally, the third group, CFTR production correctors, induce more CFTR protein production.[68]

The first small molecule defined as a CFTR potentiator (potential enhancer) is ivacaftor, which was developed as VX-770 at first.[69] Ivacaftor facilitates the transport of chloride by enhancing the channel opening of the CFTR protein on the cell surface. Ivacaftor is approved by the FDA for all class III mutations involving G1244E, G1349D, G178R, G551S, G1370D, S1251N, S1255P, S549N, S549R, and particularly G551D mutations for patients over 12 months of age.[70]

Ivacaftor has been shown to improve lung function and nutritional status and diminish the mortality rate associated with lung dysfunction.[71]

In *in vitro* studies, ivacaftor improves not only class III mutations, but also some mutant proteins of IV and V classes.[72] A class IV mutation, Arg117His, that leads to impairment of CFTR conductivity is seen in approximately 3% of patients with CF.[73]

Novel CFTR potentiator drugs are currently undergoing clinical trials. QBW251 is in the phase 2 stage of a randomized controlled trial involving 153 patients. Other candidates such as GLPG1837 and CTP-656 are also in phase 2.[74,75]

Despite the fact that ivacaftor improves channel opening time and chloride conductivity, it is not effective in patients who are homozygous for the ΔF508 mutation. The primary problem in the ΔF508 mutation is inaccurate folding of the protein and inability to reach the cell surface.[76] Therefore, co-administration of potentiators and correctors is recommended for patients homozygous for ΔF508. It has been shown that the combination

of corrective and potentiator therapies has been more effective than single regimens.[77] The FDA has approved the lumacaftor/ivacaftor combination for patients homozygous for the ΔF508 mutation who are 2 years old or older.[78] Lumacaftor, also known as VX-809, improves the conformational stability of the ΔF508-CFTR, thereby enhancing the processing of CFTR and its transfer to the cell surface.

Tezacaftor (VX-661) enhances the processing and transfer of CFTR proteins, including both normal and mutant ones (including ΔF508-CFTR), and thus increases the amount of protein reaching the cell surface. The tezacaftor/ivacaftor combination was approved by the FDA in 2018. It is indicated for the treatment of CF in patients at the age of 12 or older who are homozygous for the ΔF508 mutation.

The combination of tezacaftor/ivacaftor exhibits fewer side effects than the combination of lumacaftor/ivacaftor especially in terms of increased respiratory symptoms at the beginning of treatment. However, there is no therapeutic advantage of tezacaftor/ivacaftor when compared to lumacaftor/ivacaftor combination therapy.

To date, no combination therapy has been approved for patients who have heterozygous ΔF508 mutations (ΔF508 mutation in one allele + another mutation in another allele=ΔF508-MF) on the *CFTR* gene and minimal functional CFTR. Patients who carry two copies of the ΔF508 CFTR mutation (homozygous) are typically treated with a corrective and a potentiator, but this is not successful in heterozygotes.

The new generation CFTR correctors VX-659 and VX-440 are small molecule drugs that are expected to emerge as part of the triple combination regimen and phase 3 studies are in progress.[79]

VX-659 and VX-440 have different structures and different mechanisms of action.[80] Thus, the use of two distinct correctors in triple combination therapy acting via different mechanisms has come up. These drugs were developed for use in combination with tezacaftor and ivacaftor (VX-659/tezacaftor/ivacaftor or VX440/tezacaftor/ivacaftor) to restore the function of the ΔF508 CFTR protein of patients who have heterozygous ΔF508 CFTR (ΔF508-MF genotypes) and minimal CFTR function or homozygous ΔF508 mutations. Undoubtedly, the most important outcome of triple combination therapy is the success in treating the heterozygous ΔF508 mutation, for which CFTR modulator treatment is not available currently.[81]

Ataluren (PTC124): potential treatment for class I mutations

Stop codon mutations account for 10-12% of all CFTR mutations.[80] This mutation truncates CFTR protein production by introducing a premature stop in the mRNA and leads to unfinished protein formation. Ataluren is a novel oral drug that allows ribosomal reading of premature stop codons selectively. Ataluren activity for nonsense mutations has been shown *in vitro*, but its efficiency remains unclear due to inconsistent results in clinical trials.[82-86] The reason may be the suppression of ataluren activity by aminoglycosides.[85] Ivacaftor may increase the efficacy of ataluren by activating a specific protein. A recently completed study at the University of Alabama at Birmingham aimed to evaluate the effectiveness of ivacaftor with ataluren in a patient after one year of treatment.[87]

Personalized treatment and pulmonary gene therapy

The concept of precision medicine, which functions via the notion that "there is no disease, there is a patient", is defined as the planning of appropriate treatment by taking into account the patient's genetic background. Undoubtedly, gene therapy is one of the cornerstones of precision medicine and it gave direction to CF studies. Human gene therapy aims to alter, manipulate, or change the expression of a gene or the biological properties of living cells for therapeutic use.[88]

Gene therapy involves the correction of a defective *CFTR* gene by inserting an extra copy of a non-defective intact *CFTR* gene into the cell, which is called gene replacement, or using specially designed enzymes called nucleases, which also function as molecular scissors, which is called gene editing. The major obstacle for gene replacement/editing is gene delivery, which is hindered by the mucociliary barrier.

Gene editing uses the cell's own DNA repair machinery to correct the mutation in the DNA. Hence, a specific gene repair system should be designed for each type of mutation. Recently, the use of *CRISPR/Cas9* gene editing technology is on the rise due to its success. *CRISPR/Cas9* gene editing includes a "guide" that locates the mutated sequence in the *CFTR* gene and "scissors" that break the patient's DNA at the site of the mutation. This DNA damage gets the attention of the cell's DNA repair machinery, which will then fix the DNA breakage. This continuously corrects the mutation in the cell; therefore, its great advantage is that the effect is permanent. However, gene editing tools should be designed specifically for each type of CFTR mutation. This creates an obstacle since there are so many types of mutations in CF (approximately 2000 mutations). Moreover, gene editing tools can break the DNA in the wrong place (off-target) and cause an error resulting in new mutations in other genes. This might lead to unintended consequences, such as an increased risk of cancer.[89]

Although recent technological advances in gene editing (homologous recombination, zinc finger nucleases, transcriptional activator-like effector nuclease, CRISPR/Cas9) are promising, this option have been pushed into the background since there are many types of CF mutations and partially insufficient results.[90] However, the repair of a defective gene with the *CRISPR/Cas9* tool has huge advantages over gene replacement therapy. First of all, the corrected gene remains under the control of its endogenous promoter and therefore engages with life-long expression by the native regulation in the cell. Moreover, gene replacement has the potential to involve foreign DNA, thus increasing the risk of insertional mutations. *CRISPR/Cas9* gene editing technology is still being improved; promising results were obtained in CF tissue and animal models.[91] CF models, generated in 5 animal species (mice, rats, ferrets, pigs, and rabbits), clearly reflect the mechanisms of disease pathogenesis and CFTR function.[92] Recently, the sheep model has been proposed due to the similarity of lung anatomy between the two species.[93]

Some researchers have focused on gene replacement therapy for CF, which includes presentation of the nondefective *CFTR* gene (wild-type) into the lung cells. The entrance of functional CFTR DNA or RNA into the nucleus of lung epithelial cells through a vector and providing the expression of the functional *CFTR* gene instead of the mutant one are the main goals of the treatment.[94]

Mutation type is important for the small molecule approach, but not for gene replacement therapy. Since there is no need to identify the mutation type of the patient, gene replacement is suitable for all CF patients.[95] Pulmonary gene therapy is important since it is a non- symptomatic and mutation agnostic treatment, especially when compared with the other treatment strategies such as the potentiator and corrector regimens, which are limited by genotype. With the discovery of the *CFTR* gene in 1989, studies on gene therapy in CF have gained momentum.[24] Initially, viral and nonviral approaches were developed to deliver the *CFTR* gene (adeno-associated viruses, adenoviruses, plasmids formulated in cationic liposomes, and lentiviral and retroviral vectors). However, the lung, which has strong intracellular and extracellular barriers to protect itself from foreign particles, is a complex and difficult target organ.[95] Since gene transfer vectors can be deactivated by the immune system or inflammation products, this complicates pulmonary gene therapy. The vector carrying the gene reaches the cell surface but the receptors responsible for its uptake into the cell may be inadequate, which means inefficient gene transfer. CF is a lifelong disease and the life cycle of airway epithelial cells requires repetitive administration of the *CFTR* gene. All of these can account for the challenges of pulmonary gene therapy.[96,97] In general, viral vectors are more effective than nonviral alternatives. However, nonviral vectors are safer, cheaper, and easier to produce.[90]

In vitro studies have shown that the expression of the complementary DNA of the whole *CFTR* gene in the cell improves the anion channel activity. The most important question in this respect concerns at least how many cells must be corrected in order to benefit therapeutically. Studies showed that at least 6-10% of airway epithelial cells should be able to express functional CFTR for wild-type anion transport.[98] In 1992, with the production of animal models with CF, there was an increase in the number of gene therapy studies. In parallel with *in vitro* studies, transduction of up to 5% of the airway cells with the CFTR expressing vector has reached 50% of Cl^- transport levels in non-CF subjects in animal models.[99]

Clinical studies involving CF gene therapy were first performed in 1993 using viral and nonviral gene transfer agents from the nasal and bronchial epithelium. Adenoviruses were found to be safe in repetitive applications and did not trigger any immune response in animal experiments.[100] However, they caused immune response in clinical studies.[100,101] Despite vector modifications afterwards (such as the removal of all adenoviral genes in gutless vectors) to reduce immunodeficiency, there is little interest for the development of pulmonary gene therapy with adenoviruses.

The other promising application is recombinant adeno-associated viruses. Adeno-associated vectors are DNA based and lack some viral genes, such as gutless vectors (also called co-dependent vectors) that require assistance from a helper virus for replication. AAV2 is the first serotype to be clinically evaluated in CF patients but it has created frustration in repetitive applications due to changes in lung function.[96]

Lentiviruses are RNA-based vectors that belong to the family *Retroviridae*. Once lentiviruses enter the cell, they are reverse transcribed into DNA and the transcribed DNA is integrated into the genome of the host cell. The advantage of genomic integration is the transfer of undamaged *CFTR* gene into the daughter cells after the cell division. Therefore, it provides long-term expression. Recombinant lentiviral vectors can be modified to enhance their effectiveness by adding new surface proteins. Question marks remain as to whether the genomic integration of lentiviral vectors is safe.[90,96,102]

The failure of viral vectors has led to studies on the development of nonviral alternatives. The main objective in the development of nonviral (synthetic) vectors is to minimize the risk of immunogenicity. Nonviral vectors are circular, plasmid DNA (pDNA) molecules that are complexed with a series of cationic lipids and polymers called "lipoplexes" and "polyplexes".[96] However, nonviral vectors have no specific components required for cell entry. Nevertheless, delivery of the pDNA complicated by cationic liposomes to the lung epithelial by the aerosol system resulted in a 25% correction of the CFTR ion transport defect.[103]

In a randomized, double-blind, phase 2 trial, nonviral gene therapy pGM169/GL67A was administered for 1 year and pre- and posttreatment FEV1% values of 114 patients were calculated. The FEV1 results showed a modest but significant improvement in lung function compared with the placebo.[104]

To date, the presence of bacterial infection in the lungs has been ignored in terms of the efficacy of pulmonary gene therapy. In fact, the presence of infection can greatly affect the success of gene delivery. In recent years, several studies have focused on developing multifunctional models that will provide both antibacterial effects and gene distribution.[105] This method provides better protection of DNA during the delivery of the gene and better transfection into the bronchial epithelium, as well as contributing to bacterial eradication in the airways.

Organoids

As CF is a genetically heterogeneous disease, currently available treatment options do not cover all CFTR mutations. Many of the known CFTR mutations are associated with a variety of disease expression and this complicates the estimation of individual disease phenotypes. Moreover, phenotypic variations can be seen even in patients having identical CF mutations. CFTR genotype-based stratification for medication is challenging for many patients with rare CFTR mutations who are not included in clinical trials due to the low prevalence of the mutations ("orphan" mutations frequency <0.1%).[106,107] Due to genetic heterogeneity, there is great variability in drug responses such as to ivacaftor, lumacaftor, or their combination among

CF patients, from no clinical benefit to complete recovery. Therefore, there is an urgent need to elucidate the individualistic drug response from patients who have different types of CFTR mutations. *In vitro* organoid-based functional assays have been developed for this purpose. Organoids are a useful tool to predict the pharmacogenomics of diverse CFTR mutations and particularly CF drug response.

Organoids, also called mini-organs, are organ-specific 3D cell cultures derived from adult organs or pluripotent stem cells that reflect the features of the parental organ where they originated.[108] They are used to study heterogeneous medical conditions such as CF and cancer where genetics can influence disease severity, prognosis, and drug efficacy.[109,110] Organoids can be used to test drug efficacy and compare different combination treatments. Furthermore, patient-derived organoids represent an important tool of personalized medicine allowing the prediction of clinical disease phenotype and how a patient will respond to a drug (e.g., CFTR modulating drugs), since they have individuals' functional expressions of their own genomes.[111,112] Drug testing in patient-derived stem cells gathered by rectal biopsy offers an opportunity to select appropriate treatment on an individual basis. Scientists have demonstrated that CFTR function can be readily measured in colorectal organoids by a forskolin-induced swelling (FIS) assay.[107,113,114] The efficacy of Geneticin, ataluren, ivacaftor, and lumacaftor in combination therapy has been tested by FIS method in intestinal organoids with rare mutations.[86]

The first study to measure the correlation between *in vivo* and *in vitro* drug response in stem cell culture derived from CF patients was performed by Berkers et al.[111] in 2019. They showed a high correlation between the *in vitro* and *in vivo* effects of CFTR modulating drugs and demonstrated that organoids play an ideal role in CF modeling in a cost-effective and patient-friendly manner.

Immunotherapy for CF

Immunotherapy aims to improve how the immune system works. Chronic elevation in TNF-α, Interleukin-6 (IL-6), and IL-8, as well as IL-17, IL-13, and IL-5 levels in CF has shown to be important for disease exacerbation. IL-17 levels are found to be high in patients with *P. aeruginosa* infection.[115] IL-17, IL-5, and IL-13 levels increase with disease exacerbation and IL-17 was shown to be negatively correlated with FEV1 results. It is stated that the IL-17 increase was similar in CD4 + Th17 cells and lymph nodes.[116,117] Another study showed that tryptophan metabolism affects IL-17 levels and the RAR-related orphan receptor c (Rorc) expression. Reduction in tryptophan/kynurenine metabolism due to defective indoleamine 2,3-dioxygenase (IDO) causes susceptibility to *Aspergillus* infections and murine CF sensitivity due to type 17 helper T-cell/regulatory T-cell (Th17/Treg) imbalance. The importance of immunomodulation in CF through Th17-cell activation and IDO agonist is emphasized.[118]

The first clinical trial for immunomodulator therapy in CF is based on anti-pseudomonas aeruginosa IgY. Twenty patients with CF were involved in a phase 2 study. "Anti-pseudomonas IgY" was obtained from chicken eggs vaccinated with *Pseudomonas aeruginosa*. The preliminary results showed that it takes much longer to get a new infection and treated patients get fewer infections than controls. In addition, patients had no new opportunistic bacterial or fungal infections (*B. cepacia*, *S. maltophilia*, *A. xylosoxidans*, atypical *Mycobacteria*, *Aspergillus fumigatus*), antibiotic use was greatly diminished, and lung functions and nutritional status were stable.[119]

CONCLUSION

Over the last decade, CF has become one of the most studied hereditary diseases with novel treatment options. Since the availability to access new treatments, life quality of CF patients have increased and their survival has been prolonged. CF has become an adult disease rather than a pediatric disease in countries which devote more financial resources to health expenditures. However, the average life expectancy may still be in the 20s in low-income economies.

Recent advancements led to a paradigm shift from symptomatic treatment to therapeutic approach which targeted the mutant *CFTR* gene. The first one is to use small molecules, which covers a limited number of CF patients, and another one is pulmonary gene therapy, which represents an important tool for full recovery. Despite many efforts, there is no FDA-approved pulmonary gene therapy for CF. The major obstacle is the immune surveillance mechanisms of the lung, which hinder repeated administration of viral vectors.

CF treatment usually depends on the identification of the underlying genetic defect. Although the clinical outcome is mostly similar, CF patients differ from each other in terms of mutation type and disease progress. Thus, mutation-specific treatment and personalized therapy was an achievable goal for CF. CFTR modulators have become a remarkable step in terms of personalized treatment in CF. The CFTR potentiator ivacaftor and other correctors such as lumacaftor and tezacaftor, have been approved by the FDA for different types of mutations, such as the homozygous ΔF508 allele in CF. However, the treatment gap for the heterozygous ΔF508 allele still remains. New generation CFTR modulators have potential to fix the heterozygous ΔF508 allele, by improving CFTR folding and trafficking. The development of new generation modulator drugs (e.g., triple combinations) offers an alternative for a much larger CF population, including the patients having the heterozygous ΔF508 allele.

Significant efforts have been made to improve the treatment of patients with CF using various strategies targeting the underlying genetic defect and its subsequent results. However, the determination of CF drug efficacy is challenging because of the great heterogeneity of CFTR mutations, as well as other unknown factors that contribute to individual drug efficacy. The advancement in 3D culture systems made it possible to extrapolate the disease modeling and individual drug response *in vitro* by producing mini adult organs, which have been termed "organoids". Further studies are needed to confirm the

correlation between *in vitro* organoid-based functional assays and *in vivo* clinical phenotype and drug efficacy.

Over the 20 years following the cloning of the *CFTR* gene, the gene therapy for CF has evolved in two distinct areas: gene editing and gene replacement. Gene editing and gene replacement have advantages and disadvantages over each other. The repaired *CFTR* gene by gene editing technologies remains under the control of its endogenous promoter, and therefore a definitive and long-lasting treatment is guaranteed. However, the huge number of *CFTR* gene mutations is a major obstacle for gene editing tools. On the other hand, gene replacement requires repeated administration of the wild-type *CFTR* gene throughout the lifetime.

The full restoration of CFTR protein functionality was achieved by using *CRISPR/Cas9* gene editing technology in cultured intestinal stem cells (organoids) obtained from pediatric CF patients. An *ex vivo* repaired *CFTR* gene by *CRISPR/Cas9* in cultured organoids can be reinserted into the host successfully; this might be the beginning of a new era. In the near future, it may be possible to obtain lung stem cells from CF patients, engineering them with CRISPR/Cas9 to fix the CFTR mutation, and engraft them into lungs where stem cells find their suitable microenvironment to reconstruct the patients' airway.

In conclusion, gene therapies will continue to be an important strategy for CF as well as other genetic diseases, and organoid-based regenerative medicine designed with gene engineering technologies can provide an enormous innovation for CF therapy in the next years.

Conflicts of interest: No conflict of interest was declared by the authors. The authors alone are responsible for the content and writing of this article.

REFERENCES

1. Robert Kliegman RB, Hal Jenson, Bonita Stanton. Nelson Textbook of Pediatrics. Philadelphia, United States: Elsevier - Health Sciences Division; 2018.
2. Hangül M, Pekcan S, Köse M, Acıcan D, Şahlar TE, Erdoğan M, Kendirici M, Güney D, Demir O, Göçlü F, Öznavruz H, Ercan Ö. The Incidence of Cystic Fibrosis in the Central Region of Anatolia in Turkey Between 2015 and 2016. Balkan Med J. 2019;36:179-183.
3. Rudolp CD RA, Lıster GE, Fırst LR, Gershon AA. Rudolph's Pediatrics. New York: McGraw-Hill Education; 2011.
4. Anderson MP, Gregory RJ, Thompson S, Souza DW, Paul S, Mulligan RC, Smith AE, Welsh MJ. Demonstration that CFTR is a chloride channel by alteration of its anion selectivity. Science. 1991;253:202-205.
5. Elborn JS. Cystic fibrosis. Lancet. 2016;388:2519-2531.
6. WHO Human Genetics Programme. (2004). The molecular genetic epidemiology of cystic fibrosis: report of a joint meeting of WHO/IECFTN/ICF(M)A/ECFS, Genoa, Italy, 19 June 2002. World Health Organization. Available from: https://apps.who.int/iris/handle/10665/68702
7. Smith JJ, Travis SM, Greenberg EP, Welsh MJ. Cystic fibrosis airway epithelia fail to kill bacteria because of abnormal airway surface fluid. Cell. 1996;85:229-236.
8. Shah AV, McColley SA, Weil D, Zheng XT. Trichosporon mycotoxinivorans Infection in Patients with Cystic Fibrosis. J Clin Microbiol. 2014;52:2242-2244.
9. Berkebile AR, McCray PB. Effects of airway surface liquid pH on host defense in cystic fibrosis. Int J Biochem Cell B. 2014;52:124-129.
10. Elborn JS. CFTR Modulators: Deciding What Is Best for Individuals in an Era of Precision Medicine. Ann Am Thorac Soc. 2018;15:298-300.
11. Massip-Copiz MM, Santa-Coloma TA. Extracellular pH and lung infections in cystic fibrosis. Eur J Cell Biol. 2018;97:402-410.
12. Steinkamp G, Wiedemann B, Rietschel E, Krahl A, Gielen J, Barmeier H, Ratjen F, Emerging Bacteria Study Group. Prospective evaluation of emerging bacteria in cystic fibrosis. J Cyst Fibros. 2005;4:41-48.
13. Bensman TJ, Wang J, Jayne J, Fukushima L, Rao AP, D'Argenio DZ, Beringer PM. Pharmacokinetic-pharmacodynamic target attainment analyses to determine optimal dosing of ceftazidime-avibactam for the treatment of acute pulmonary exacerbations in patients with cystic fibrosis. Antimicrobial agents and chemotherapy. 2017;61:e00988-17.
14. Imudo L, Barasch J, Prince A, Alawqati Q. Cystic fibrosis epithelial-cells have a receptor for pathogenic bacteria on their apical surface. P Natl Acad Sci USA. 1995;92:3019-3023.
15. Matsui H, Wagner VE, Hill DB, Schwab UE, Rogers TD, Button B, Taylor 2nd RM, Superfine R, Rubinstein M, Iglewski BH, Boucher RC. A physical linkage between cystic fibrosis airway surface dehydration and Pseudomonas aeruginosa biofilms. P Natl Acad Sci USA. 2006;103:18131-18136.
16. Parkins MD, Somayaji R, Waters VJ. Epidemiology, Biology, and Impact of Clonal Pseudomonas aeruginosa Infections in Cystic Fibrosis. Clinical microbiology reviews. 2018;31:e00018-e00019.
17. Somayaji R, Ramos KJ, Kapnadak SG, Aitken ML, Goss CH. Common clinical features of CF (respiratory disease and exocrine pancreatic insufficiency). Presse Med. 2017;46:e109-e124.
18. Moran A, Brunzell C, Cohen RC, Katz M, Marshall BC, Onady G, Robinson KA, Sabadosa KA, Stecenko A, Slovis B, CFRD Guidelines Committee. Clinical care guidelines for cystic fibrosis-related diabetes: a position statement of the American Diabetes Association and a clinical practice guideline of the Cystic Fibrosis Foundation, endorsed by the Pediatric Endocrine Society. Diabetes Care. 2010;33:2697-2708.
19. Andersen HU, Lanng S, Pressler T, Laugesen CS, Mathiesen ER. Cystic fibrosis-related diabetes - The presence of microvascular diabetes complications. Diabetes Care. 2006;29:2660-2663.
20. De Boeck K, Amaral MD. Progress in therapies for cystic fibrosis. Lancet Resp Med. 2016;4:662-674.
21. Brodlie M, Haq IJ, Roberts K, Elborn JS. Targeted therapies to improve CFTR function in cystic fibrosis. Genome Med. 2015;7:101.
22. O'Riordan TG, Donn KH, Hodsman P, Ansede JH, Newcomb T, Lewis SA, Flitter WD, White VS, Johnson MR, Montgomery AB, Warnock DG, Boucher RC. Acute Hyperkalemia Associated with Inhalation of a Potent ENaC Antagonist: Phase 1 Trial of GS-9411. J Aerosol Med Pulm D. 2014;27:200-208.
23. Dell'Edera D, Benedetto M, Gadaleta G, Carone D, Salvatore D, Angione A, Gallo M, Milo M, Pisaturo ML, Pierro GD, Mazzone E, Epifina AA. Analysis of cystic fibrosis gene mutations in children with cystic fibrosis and in 964 infertile couples within the region of Basilicata, Italy: a research study. J Med Case Rep. 2014;8:339.

24. Cooney AL, McCray PB, Jr., Sinn PL. Cystic Fibrosis Gene Therapy: Looking Back, Looking Forward. Genes (Basel). 2018;9:538.
25. Welsh MJ, Smith AE. Molecular mechanisms of CFTR chloride channel dysfunction in cystic fibrosis. Cell. 1993;73:1251-1254.
26. Ratjen F, Bell SC, Rowe SM, Goss CH, Quittner AL, Bush A. Cystic fibrosis. Nat Rev Dis Primers. 2015;1:15010.
27. Kerem E. Cystic fibrosis: priorities and progress for future therapies. Paediatr Respir Rev. 2017;24:14-16.
28. Farfour E, Trochu E, Devin C, Cardot Martin E, Limousin L, Roux A, Picard C, Jolly E, Vasse M, Lesprit P. Trends in ceftazidime-avibactam activity against multidrug-resistant organisms recovered from respiratory samples of cystic fibrosis patients. Transpl Infect Dis. 2018;20:e12955.
29. Pitart C, Marco F, Keating TA, Nichols WW, Vila J. Activity of ceftazidime-avibactam against fluoroquinolone-resistant Enterobacteriaceae and Pseudomonas aeruginosa. Antimicrob Agents Chemother. 2015;59:3059-3065.
30. Rodriguez-Nunez O, Ripa M, Morata L, de la Calle C, Cardozo C, Feher C, Pellicé M, Valcarel A, Puerta-Alcalde P, Marco F, Garcia-Vidal C, Rio AD, Soriano A, Martinez-Martinez JA. Evaluation of ceftazidime/avibactam for serious infections due to multidrug-resistant and extensively drug-resistant Pseudomonas aeruginosa. J Glob Antimicrob Resist. 2018;15:136-139.
31. Lagace-Wiens P, Walkty A, Karlowsky JA. Ceftazidime-avibactam: an evidence-based review of its pharmacology and potential use in the treatment of Gram-negative bacterial infections. Core Evid. 2014;9:13-25.
32. Barlow G, Morice A. Successful treatment of resistant Burkholderia multivorans infection in a patient with cystic fibrosis using ceftazidime/avibactam plus aztreonam. J Antimicrob Chemoth. 2018;73:2270-2271.
33. Stokem K, Zuckerman JB, Nicolau DP, Wungwattana M, Sears EH. Use of ceftolozane-tazobactam in a cystic fibrosis patient with multidrug-resistant pseudomonas infection and renal insufficiency. Respir Med Case Rep. 2018;23:8-9.
34. Dassner AM, Sutherland C, Girotto J, Nicolau DP. In vitro activity of ceftolozane/tazobactam alone or with an aminoglycoside against multi-drug-resistant pseudomonas aeruginosa from pediatric cystic fibrosis patients. Infect Dis Ther. 2017;6:129-136.
35. Food and Drug Administration (FDA). These highlights do not include all the information needed to use ZERBAXA™ safely and effectively. See full prescribing information for ZERBAXA. 2014. Available from: https://www.accessdata.fda.gov/drugsatfda_docs/label/2014/206829lbl.pdf
36. ClinicalTrials.gov. MK-7625A Versus Meropenem in Pediatric Participants With Complicated Urinary Tract Infection (cUTI) (MK-7625A-034) Jully 26, 2017 [updated April 17, 2020. Available from: https://clinicaltrials.gov/ct2/show/NCT03230838?term=ceftolozane+tazobactam&age=0&draw=2&rank=4
37. ClinicalTrials.gov. Evaluation of Pharmacokinetics, Safety, and Tolerability of Ceftazidime-avibactam in Neonates and Infants. (NOOR) October 14, 2019 [updated April 3, 2020. Available from: https://clinicaltrials.gov/ct2/show/NCT04126031?term=ceftazidim+avibactam&age=0&draw=2&rank=2
38. Hewer SL. Inhaled antibiotics in cystic fibrosis: what's new? J R Soc Med. 2012;105(2):S19-24.
39. Zeitler K, Salvas B, Stevens V, Brown J. Aztreonam lysine for inhalation: new formulation of an old antibiotic. Am J Health Syst Pharm. 2012;69:107-115.
40. Vazquez-Espinosa E, Marcos C, Alonso T, Giron RM, Gomez-Punter RM, Garcia-Castillo E, Zamora E, Cisneros C, Garcia J, Valenzula C, Ancochea J. Tobramycin inhalation powder (TOBI Podhaler (R)) for the treatment of lung infection in patients with cystic fibrosis. Expert Rev Anti Infect Ther. 2016;14:9-17.
41. Antoniu SA, Cojocaru I. Inhaled colistin for lower respiratory tract infections. Expert Opin Drug Del. 2012;9:333-342.
42. Kirkby S, Novak K, McCoy K. Aztreonam (for inhalation solution) for the treatment of chronic lung infections in patients with cystic fibrosis: an evidence-based review. Core Evid. 2011;6:59-66.
43. Food and Drug Administration (FDA). These highlights do not include all the information needed to use ARIKAYCE safely and effectively 2018. Available from: https://www.accessdata.fda.gov/drugsatfda_docs/label/2018/207356s000lbl.pdf
44. ClinicalTrials.gov. MP-376 (Aeroquin™, Levofloxacin for Inhalation) in Patients With Cystic Fibrosis August 12, 2010. Last Accessed Date: 19.01.2018. Available from: https://clinicaltrials.gov/ct2/show/NCT01180634
45. Hobbs CA, Tan CD, Tarran R. Does epithelial sodium channel hyperactivity contribute to cystic fibrosis lung disease? J Physiol-London. 2013;591:4377-4387.
46. Shei RJ, Peabody JE, Kaza N, Rowe SM. The epithelial sodium channel (ENaC) as a therapeutic target for cystic fibrosis. Curr Opin Pharmacol. 2018;43:152-165.
47. Hirsh AJ, Zhang J, Zamurs A, Fleegle J, Thelin WR, Caldwell RA, Sabater JR, Abraham WM, Donowitz M, Cha B, Johnson KB, St. George JA, Johnson MR, Boucher RC. Pharmacological properties of N-(3,5-diamino-6-chloropyrazine-2-carbonyl)-N'-4-[4-(2,3-dihydroxypropoxy) phenyl] butyl-guanidine methanesulfonate (552-02), a novel epithelial sodium channel blocker with potential clinical efficacy for cystic fibrosis lung disease. J Pharmacol Exp Ther. 2008;325:77-88.
48. Moore PJ, Tarran R. The epithelial sodium channel (ENaC) as a therapeutic target for cystic fibrosis lung disease. Expert Opin Ther Tar. 2018;22:687-701.
49. ClinicalTrials.gov. To Assess the Safety, Tolerability and Pharmacokinetics of AZD5634 Following Inhaled and Intravenous (IV)Dose Administration February 10, 2016 . Last Accessed Date: 05.11.2018. Available from: https://clinicaltrials.gov/ct2/show/NCT02679729?term=NCT02679729&draw=2&rank=1
50. ClinicalTrials.gov. Safety, Pharmacokinetics and Pharmacodynamics Study of Inhaled QBW276 in Patients With Cystic Fibrosis October 1, 2015. Last Accessed Date: 17.07.2019. Available from: https://clinicaltrials.gov/ct2/show/NCT02566044?term=QBW+276&draw=2&rank=1
51. ClinicalTrials.gov. To Assess Safety, Tolerability and Pharmacokinetics of BI 443651 in Healthy Male Volunteers March 11, 2016. Last Accessed Date: 02.01.2020. Available from: https://clinicaltrials.gov/ct2/show/NCT02706925?term=BI+443651&draw=2&rank=3
52. Caldwell RA, Boucher RC, Stutts MJ. Neutrophil elastase activates near-silent epithelial Na+ channels and increases airway epithelial Na+ transport. Am J Physiol Lung Cell Mol Physiol. 2005;288:L813-L819.
53. Guilbault C, Saeed Z, Downey GP, Radzioch D. Cystic fibrosis mouse models. Am J Respir Cell Mol Biol. 2007;36:1-7.
54. Knowles MR, Clarke LL, Boucher RC. Activation by Extracellular Nucleotides of Chloride Secretion in the Airway Epithelia of Patients with Cystic-Fibrosis. New Engl J Med. 1991;325:533-538.

55. Deterding R, Retsch-Bogart G, Milgram L, Gibson R, Daines C, Zeitlin PL, Milla C, Marshall B, LaVange L, Engels J, Mathews D, Gorden JA, Schaberg A, Williams, Ramsey B. Safety and tolerability of denufosol tetrasodium inhalation solution, a novel P2Y2 receptor agonist: results of a phase 1/phase 2 multicenter study in mild to moderate cystic fibrosis. Pediatr Pulmonol. 2005;39:339-348.

56. Deterding RR, Lavange LM, Engels JM, Mathews DW, Coquillette SJ, Brody AS, Millard SP, Ramsey BW, Cystic Fibrosis Therapeutics Development Network and the Inspire 08-103 Working Group. Phase 2 randomized safety and efficacy trial of nebulized denufosol tetrasodium in cystic fibrosis. Am J Respir Crit Care Med. 2007;176:362-369.

57. Ratjen F, Durham T, Navratil T, Schaberg A, Accurso FJ, Wainwright C, Barnes M, Moss RB, The TIGER-2 Study Investigator Group. Long term effects of denufosol tetrasodium in patients with cystic fibrosis. J Cyst Fibros. 2012;11:539-549.

58. Grasemann H, Stehling F, Brunar H, Widmann R, Laliberte TW, Molina L, Döring G, Ratjen F. Inhalation of Moli1901 in patients with cystic fibrosis. Chest. 2007;131:1461-1466.

59. Haq IJ, Gray MA, Garnett JP, Ward C, Brodlie M. Airway surface liquid homeostasis in cystic fibrosis: pathophysiology and therapeutic targets. Thorax. 2016;71:284-287.

60. Robinson M, Hemming AL, Regnis JA, Wong AG, Bailey DL, Bautovich GJ, King M, Bye PT. Effect of increasing doses of hypertonic saline on mucociliary clearance in patients with cystic fibrosis. Thorax. 1997;52:900-903.

61. Williams HD, Behrends V, Bundy JG, Ryall B, Zlosnik JE. Hypertonic saline therapy in cystic fibrosis: do population shifts caused by the osmotic sensitivity of infecting bacteria explain the effectiveness of this treatment? Front Microbiol. 2010;1:120.

62. Boucher R. Human airway ion transport. Part two. Am J Respir Crit Care Med. 1994;150:581-593.

63. Assouline G, Leibson V, Danon A. Stimulation of prostaglandin output from rat stomach by hypertonic solutions. Eur J Pharmacol. 1977;44:271-273.

64. Tildy BE, Rogers DF. Therapeutic options for hydrating airway mucus in cystic fibrosis. Pharmacol. 2015;95:117-132.

65. Springsteel MF, Galietta LJ, Ma T, By K, Berger GO, Yang H, Dicus CW, Choung W, Quan C, Shelat AA, Guy RK, Verkman AS, Kurth MJ, Nantz MH. Benzoflavone activators of the cystic fibrosis transmembrane conductance regulator: towards a pharmacophore model for the nucleotide-binding domain. Bioorg Med Chem. 2003;11:4113-4120.

66. Suen YF, Robins L, Yang B, Verkman AS, Nantz MH, Kurth MJ. Sulfamoyl-4-oxoquinoline-3-carboxamides: novel potentiators of defective DeltaF508-cystic fibrosis transmembrane conductance regulator chloride channel gating. Bioorg Med Chem Lett. 2006;16:537-540.

67. Barry PJ, Ronan N, Plant BJ. Cystic Fibrosis Transmembrane Conductance Regulator Modulators: The End of the Beginning. Semin Resp Crit Care. 2015;36:287-298.

68. Rubin BK. Unmet needs in cystic fibrosis. Expert Opin Biol Th. 2018;18:49-52.

69. Van Goor F, Hadida S, Grootenhuis PDJ, Burton B, Cao D, Neuberger T, Turnbull A, Singh A, Joubran J, Hazlewood A, Zhou J, McCartney J, Arumugam V, Decker C, Yang J, Young C, Olson ER, Wine JJ, Frizzell RA, Ashlock M, Negulescu P. Rescue of CF airway epithelial cell function *in vitro* by a CFTR potentiator, VX-770. P Natl Acad Sci USA. 2009;106:18825-18830.

70. Food and Drug Administration (FDA). Orphan Drug Designations and Approvals. Last Accessed Date: 21.02.2014. Available from: https://www.accessdata.fda.gov/scripts/cdrh/cfdocs/cfcfr/CFRSearch.cfm?CFRPart=316&showFR=1

71. Bessonova L, Volkova N, Higgins M, Bengtsson L, Tian S, Simard C, Konstan MW, Sawicki GS, Sewall A, Nyangoma S, Elbert A, Marshall BC, Bilton D. Data from the US and UK cystic fibrosis registries support disease modification by CFTR modulation with ivacaftor. Thorax. 2018;73:731-740.

72. Van Goor F, Yu HH, Burton B, Hoffman BJ. Effect of ivacaftor on CFTR forms with missense mutations associated with defects in protein processing or function. Journal of Cystic Fibrosis. 2014;13:29-36.

73. Moss RB, Flume PA, Elborn JS, Cooke J, Rowe SM, McColley SA, Rubenstein RC, Higgins M, VX11-770-110 (KONDUCT) Study Group. Efficacy and safety of ivacaftor in patients with cystic fibrosis who have an Arg117His-CFTR mutation: a double-blind, randomised controlled trial. Lancet Resp Med. 2015;3:524-533.

74. ClinicalTrials.gov. Study of GLPG1837 in Subjects With Cystic Fibrosis (G551D Mutation) (SAPHIRA1) March 14, 2016. Last Accessed Date: 07.12.2016. Available from: https://clinicaltrials.gov/ct2/show/NCT02707562?term=NCT02707562&draw=2&rank=1

75. ClinicalTrials.gov. Study to Evaluate the Safety and Efficacy of CTP-656 in Patients With Cystic Fibrosis With CFTR Gating Mutations November 23, 2016. Last Accessed Date: 15.08.2018. Available from: https://clinicaltrials.gov/ct2/show/NCT02971839?term=NCT02971839&draw=2&rank=1

76. Boyle MP, De Boeck K. A new era in the treatment of cystic fibrosis: correction of the underlying CFTR defect. Lancet Resp Med. 2013;1:158-163.

77. Van Goor F, Hadida S, Grootenhuis PDJ, Burton B, Stack JH, Straley KS, Elborn JS, Melotti P, Bronsveld I, Fajac I, Malfroot A, Rosenbluth DB, Walker PA, McColley SA, Knoop C, Quattrucci S, Rietschel R, Zeitlin PL, Barth J, Elfring GL, Welch EM, Branstrom A, Spiegel RJ, Peltz SW, Ajayi T, Rowe SM, Cystic Fibrosis Ataluren Study Group. Correction of the F508del-CFTR protein processing defect in vitro by the investigational drug VX-809. P Natl Acad Sci USA. 2011;108:18843-18848.

78. Food and Drug Administration (FDA). ORKAMBI July 2, 2015. Available from: https://www.accessdata.fda.gov/drugsatfda_docs/label/2018/211358s000lbl.pdf

79. Relations I. Vertex Selects Two Next-Generation Correctors, VX-659 and VX-445, to Advance into Phase 3 Development as Part of Two Different Triple Combination Regimens for People with Cystic Fibrosis Feb 1, 2018. Available from: https://investors.vrtx.com/news-releases/news-release-details/vertex-selects-two-next-generation-correctors-vx-659-and-vx-445

80. Doull I. Cystic fibrosis papers of the year 2017. Paediatr Respir Rev. 2018;27:2-5.

81. Davies JC, Moskowitz SM, Brown C, Horsley A, Mall MA, McKone EF, Plant BJ, Prais D, Ramsey BW, Taylor-Cousar JL, Tullis E, Uluer A, McKee CM, Robertson S, Shilling RA, Simard C, van Goor F. Waltz D, Xuan F, Young T,Rowe SM, VX16-659-101 Study Group. VX-659-Tezacaftor-Ivacaftor in Patients with Cystic Fibrosis and One or Two Phe508del Alleles. N Engl J Med. 2018;379:1599-1611.

82. Du M, Liu XL, Welch EM, Hirawat S, Peltz SW, Bedwell DM. PTC124 is an orally bioavailable compound that promotes suppression of the human CFTR-G542X nonsense allele in a CF mouse model. P Natl Acad Sci USA. 2008;105:2064-2069.

83. Sermet-Gaudelus I, Boeck KD, Casimir GJ, Vermeulen F, Leal T, Mogenet A, Roussel D, Fritsch J, Hanssens L, Hirawat S, Miller NL, Constantine S, Reha A, Ajayi T, Elfring GL, Miller LL. Ataluren (PTC124) induces cystic fibrosis transmembrane conductance regulator protein expression and activity in children with nonsense mutation cystic fibrosis. Am J Respir Crit Care Med. 2010;182:1262-1272.

84. Kerem E, Hirawat S, Armoni S, Yaakov Y, Shoseyov D, Cohen M, Nissim-Rafinia M, Blau H, Rivlin J, Aviram M, Elfring GL, Northcutt VJ, Miller LL, Kerem B, Wilschanski M. Effectiveness of PTC124 treatment of cystic fibrosis caused by nonsense mutations: a prospective phase II trial. Lancet. 2008;372:719-727.

85. Kerem E, Konstan MW, De Boeck K, Accurso FJ, Sermet-Gaudelus I, Wilschanski M, Elborn JS, Melotti P, Bronsveld I, Fajac I, Malfroot A, Rosenbluth DB, Walker PA, McColley SA, Knoop C, Quattrucci S, Rietschel E, Zeitlin PL, Barth J, Elfring GL, Welch EM, Branstrom A, Spiegel RJ, Peltz SW, Ajayi T, Rowe SM, Cystic Fibrosis Ataluren Study Group. Ataluren for the treatment of nonsense-mutation cystic fibrosis: a randomised, double-blind, placebo-controlled phase 3 trial. Lancet Resp Med. 2014;2:539-547.

86. Zomer-van Ommen DD, Vijftigschild LA, Kruisselbrink E, Vonk AM, Dekkers JF, Janssens HM, de Winter_de Groott KM, van der Ent CK, Beekman JM. Limited premature termination codon suppression by read-through agents in cystic fibrosis intestinal organoids. J Cyst Fibros. 2016;15:158-162.

87. ClinicalTrials.gov. PTC Study to Evaluate Ataluren in Combination With Ivacaftor. 2018. Available from: https://clinicaltrials.gov/ct2/show/NCT03256968

88. Food and Drug Administration (FDA). Human Gene Therapy for Rare Diseases. 2018. Available from: https://www.fda.gov/regulatory-information/search-fda-guidance-documents/human-gene-therapy-rare-diseases

89. Hodges CA, Conlon RA. Delivering on the promise of gene editing for cystic fibrosis. Genes Dis. 2019;6:97-108.

90. Villate-Beitia I, Zarate J, Puras G, Pedraz JL. Gene delivery to the lungs: pulmonary gene therapy for cystic fibrosis. Drug Dev Ind Pharm. 2017;43:1071-1081.

91. Mention K, Santos L, Harrison PT. Gene and base editing as a therapeutic option for cystic fibrosis-learning from other diseases. Genes. 2019;10:387.

92. Marangi M, Pistritto G. Innovative therapeutic strategies for cystic fibrosis: moving forward to CRISPR technique. Frontiers Pharmacol. 2018;9:396.

93. Rosen BH, Chanson M, Gawenis LR, Liu J, Sofoluwe A, Zoso A, Engelhardt JF. Animal and model systems for studying cystic fibrosis. Journal of Cystic Fibrosis. 2018;17:S28-S34.

94. Martiniano SL, Sagel SD, Zemanick ET. Cystic fibrosis: a model system for precision medicine. Curr Opin Pediatr. 2016;28:312-317.

95. Griesenbach U, Pytel KM, Alton EW. Cystic Fibrosis Gene Therapy in the UK and Elsewhere. Hum Gene Ther. 2015;26:266-275.

96. Gill DR, Hyde SC. Delivery of genes into the CF airway. Thorax. 2014;69:962-964.

97. Burney TJ, Davies JC. Gene therapy for the treatment of cystic fibrosis. Appl Clin Genet. 2012;5:29-36.

98. Johnson LG, Olsen JC, Sarkadi B, Moore KL, Swanstrom R, Boucher RC. Efficiency of Gene-Transfer for Restoration of Normal Airway Epithelial Function in Cystic-Fibrosis. Nat Genet. 1992;2:21-25.

99. Dorin JR, Farley R, Webb S, Smith SN, Farini E, Delaney SJ, Wainwright BJ, Alton EW, Porteous DJ. A demonstration using mouse models that successful gene therapy for cystic fibrosis requires only partial gene correction. Gene Ther. 1996;3:797-801.

100. Zabner J, Petersen DM, Puga AP, Graham SM, Couture LA, Keyes LD, Lukason MJ, St George JA, Gregory RJ, Smith AE, et al. Safety and efficacy of repetitive adenovirus-mediated transfer of CFTR cDNA to airway epithelia of primates and cotton rats. Nat Genet. 1994;6:75-83.

101. Hay JG, McElvaney NG, Herena J, Crystal RG. Modification of nasal epithelial potential differences of individuals with cystic fibrosis consequent to local administration of a normal CFTR cDNA adenovirus gene transfer vector. Hum Gene Ther. 1995;6:1487-1496.

102. Valkama AJ, Leinonen HM, Lipponen EM, Turkki V, Malinen J, Heikura T, Ylä-Herttuala S, Lesch HP. Optimization of lentiviral vector production for scale-up in fixed-bed bioreactor. Gene Ther. 2018;25:39-46.

103. Prickett M, Jain M. Gene therapy in cystic fibrosis. Transl Res. 2013;161:255-264.

104. Alton EW, Boyd AC, Porteous DJ, Davies G, Davies JC, Griesenbach U, Higgins TE, Gill DR, Hyde SC, Innes JA, UK Cystic Fibrosis Gene Therapy Consortium. A Phase I/IIa Safety and Efficacy Study of Nebulized Liposome-mediated Gene Therapy for Cystic Fibrosis Supports a Multidose Trial. Am J Respir Crit Care Med. 2015;192:1389-1392.

105. Mottais A, Berchel M, Sibiril Y, Laurent V, Gill D, Hyde S, Jaffres PA, Montier T, Le Gall T. Antibacterial effect and DNA delivery using a combination of an arsonium-containing lipophosphoramide with an N-heterocyclic carbene-silver complex - Potential benefits for cystic fibrosis lung gene therapy. Int J Pharmaceut. 2018;536:29-41.

106. Rogan MP, Stoltz DA, Hornick DB. Cystic fibrosis transmembrane conductance regulator intracellular processing, trafficking, and opportunities for mutation-specific treatment. Chest. 2011;139:1480-1490.

107. Boj SF, Vonk AM, Statia M, Su J, Vries RR, Beekman JM, Clevers H. Forskolin-induced Swelling in Intestinal Organoids: An In Vitro Assay for Assessing Drug Response in Cystic Fibrosis Patients. J Vis Exp. 2017:55159.

108. van Mourik P, Beekman JM, van der Ent CK. Intestinal organoids to model cystic fibrosis. Eur Respir J. 2019;54:1802379.

109. Sachs N, de Ligt J, Kopper O, Gogola E, Bounova G, Weeber F, Balgobind AV, Wind K, Gracanin A, Begthel H, Korving J, van Boxtel R, Duarte AA, Lelieveld D, van Hoeck A, Ernst RF, Blokzijl F, Nijman IJ, Hoogstraat M, van de Ven M, Egan DA, Zinzalla V, Moll J, Boj SF, Voest EE, Wessels L, van Diest PJ, Rottenberg S, Vries RGJ, Cuppen E, Clevers H. A Living Biobank of Breast Cancer Organoids Captures Disease Heterogeneity. Cell. 2018;172:373-386 e10.

110. Broutier L, Mastrogiovanni G, Verstegen MM, Francies HE, Gavarro LM, Bradshaw CR, Allen GE, Arnes-Benito R, Sidorova O, Gaspersz MP, Georgakopoulos N, Koo BK, Dietmann S, Davies SE, Praseedom RK, Lieshout R, Ijzermans JNM, Wigmore SJ, Saeb-Pars K, Garnett MJ, van der Laan LJ, Huch M. Human primary liver cancer-derived organoid cultures for disease modeling and drug screening. Nat Med. 2017;23:1424-1435.

111. Berkers G, van Mourik P, Vonk AM, Kruisselbrink E, Dekkers JF, de Winter-de Groot KM, Arets HGM, Marck-van der Wilt REP, Dijkema JS, Vanderschuen MM, Houwen RHJ, Heijerman HGM, van de Graaf EA, Elias SG, Majoor CJ, Koppelman GH, Roukema J, Bakker M, Janssens HM, van der Meer R, Vries RGJ, Clevers HC, de Jonge HR, Beekman

JM, van der Ent C. Rectal Organoids Enable Personalized Treatment of Cystic Fibrosis. Cell Rep. 2019;26:1701-1708 e3.

112. Noordhoek J, Gulmans V, van der Ent K, Beekman JM. Intestinal organoids and personalized medicine in cystic fibrosis: a successful patient-oriented research collaboration. Curr Opin Pulm Med. 2016;22:610-616.

113. Dekkers JF, van der Ent CK, Beekman JM. Novel opportunities for CFTR-targeting drug development using organoids. Rare Dis. 2013;1:e27112.

114. Dekkers JF, Wiegerinck CL, de Jonge HR, Bronsveld I, Janssens HM, de Winter-de Groot KM, Brandsma AM, de Jong NWM, Bijvelds MJC, Scholte BJ, Nieuwenhuis EES, van den Brink S, Clevers H, van der Ent CK, Middendorp S, Beekman JM. A functional CFTR assay using primary cystic fibrosis intestinal organoids. Nat Med. 2013;19:939-945.

115. McAllister F, Henry A, Kreindler JL, Dubin PJ, Ulrich L, Steele C, Finder JD, Pilewski JM, Carreno BM, Goldman SJ, Pirhonen J, Kolls JK. Role of IL-17A, IL-17F, and the IL-17 receptor in regulating growth-related oncogene-α and granulocyte colony-stimulating factor in bronchial epithelium: implications for airway inflammation in cystic fibrosis. J Immunol 2005;175:404-412.

116. Tan HL, Regamey N, Brown S, Bush A, Lloyd CM, Davies JC. The Th17 pathway in cystic fibrosis lung disease. Am J Respir Crit Care Med. 2011;184:252-258.

117. Chan YR, Chen K, Duncan SR, Lathrop KL, Latoche JD, Logar AJ, Pociask DA, Wahlberg BJ, Ray P, Ray A, Pilewski JM, Kolls JK. Patients with cystic fibrosis have inducible IL-17+ IL-22+ memory cells in lung draining lymph nodes. Journal of allergy and clinical immunology. 2013;131:1117-1129. e5.

118. Iannitti RG, Carvalho A, Cunha C, De Luca A, Giovannini G, Casagrande A, Zelante T, Vacca C, Fallarino F, Pucceyyi P, Massi-Benedetti C, Defilippi G, Russo M, Porcaro L, Colombo C, Ratclif L, De Benedicts FM, Romani L. Th17/Treg imbalance in murine cystic fibrosis is linked to indoleamine 2, 3-dioxygenase deficiency but corrected by kynurenines. Am J Respir Crit Care Med. 2013;187:609-620.

119. ClinicalTrials.gov. Anti-pseudomonas IgY to Prevent Infections in Cystic Fibrosis (PseudIgY) March 11, 2008 [updated September 1, 2016]. Available from: https://clinicaltrials.gov/ct2/show/NCT00633191?term=immunotherapy&cond=Cystic+Fibrosis&draw=2&rank=1

2020 Author Index

2020 Author Index

2020 Author Index

2020 Referee Index

2020 Referee Index